THE UNIVERSITY
of EDINBURGH

Identifying Therapeutic Implications of Cancer Stem cells in Human and Canine Insulinoma

Ylenia Capodanno

Thesis submitted for the degree of Doctor of Philosophy (PhD)

The University of Edinburgh - 2018

THE UNIVERSITY *of* EDINBURGH

Doctor of Philosophy - The University of Edinburgh - 2018

Declaration

This thesis is submitted to the University of Edinburgh in accordance with the requirements for the degree of Doctor of Philosophy in the faculty of Medicine and Veterinary Medicine. The work presented is the work of the author except where stated otherwise by reference and/or acknowledgement. The candidate's contribution to the work in the publication is clearly stated in the manuscript. This work has not been submitted for award or degree at any other University.

Signed:

Ylenia Capodanno

Acknowledgements

"There's an end to every storm. Once all the trees have been uprooted. Once all the houses have been ripped apart. The wind will hush, the clouds will part, the rain will stop, the sky will clear in an instant. But only then, in those quiet moments after the storm, do we learn who was strong enough to survive it."

When a storm comes, it usually hits us unexpectedly. And once it is over, we often do not remember how we made it through; we only know that we are not the same person who walked in it. This PhD has felt like a "stormy" adventure. It has changed me, and I must admit, even if it was tough from time to time, it was an amazing journey and, today, I wanted to acknowledge the people that made it hard but enjoyable, memorable and most often crazy.

First of all I would like to thank my supervisors, Prof David Argyle and Dr Lisa Pang for the support throughout the PhD. Thank you for giving me this opportunity, I gained an invaluable experience that I will bring with me for the rest of my career. The most significant lesson I learnt in these years is the perseverance. The hardest the challenges get, the greatest will be the rewards that come from it. It hasn't been always easy but thanks to this experience I found a strength I did not know I had and, in the end, I am glad we have made it together to the other side.

I would like to thank our collaborators at the University of Utrecht, Dr Jan Mol and Prof Jolle Kirpensteijn and, in particular, to Dr Floryne Buishand. Thank you for hosting me in the Netherlands and for your kind help and suggestions throughout these years. Towards our collaboration, I learnt a lot. It was a pleasure to work with you, and I hope there will be many other chances in the future.

Thanks to the Morris Animal Foundation for believing in this project and giving me the opportunity to explore in-depth this very unique tumour that, even after three years, still extremely fascinates me.

A big thank you goes to my former supervisor, Dr Richard Elders, for believing in me in the first place. I will never forget your advice on all the kind of topics and I know now I gain not only a great collaborator for the future but first of all a friend.

To the people, present and past, in the Argyle's group for handling all this Italian craziness! Especially Breno, Karen and Rhona. You gave me always a different perspective and simply turned on the light when I could not see clear.

To the Roslin and the people who work here, I am honoured that I had the chance to meet so many brilliant scientists that kindly help me in experimental design, optimising procedures and sometimes even to write emails! To Liz, you are one of the strongest women I have ever met; I would not forget your precious advice and that you showed that you cared.

At the Roslin, there have been some people that held the pieces together in the everyday life and made this possible. First of all, Mark, my calm and my anchor in the heaviest of the storm; Sonsi, my science opposite always full of questions and new perspectives on every matter; and Paolo, the specular reflection of each and any of my thoughts, who told me "to behave" when I needed the most.

To the people that sit in my area for handling my endless talking and the constant mess on my desk!

To the "coffee breakers", the Roslin couldn't have been such an excellent place without you.

And now, Edinburgh. I have spent the last ten years of my life as a nomad, but since I came here, I felt at home. Thank you for embracing me in your cold but homely arms and for giving me so many wonderful (and less wonderful) people. Thanks to you now I have a place where I know I can feel safe.

Some of these people have made Edinburgh warm in the coldest of the nights. In particular, Irene and Roberta, you are the finest friends that Edinburgh could have ever given me. Thank you simply for being who you are.

To my soulmates, Alessia, Benedetta, Deborah, Giordana e Piero. You are the living's proof that friendship is thicker than blood. You were there for me no matter what and sometimes without even needing to ask. You are part of me, and so everything I have is as much mine as it is yours. The success of this PhD today is yours as much as it is mine.

And finally, my family, my roots, my blood, the fabric I have been made from. You believed in my dreams since I was a kid. If I could have a wish in my life would be

to bring you always with me wherever I go. Thank you for being always there. I would have been lost without you. To S., always with me, every step of the way.

Today, once more, I believe that everything is possible and no battles can be lost when you have wonderful people by your side. Once again I thank all of you for taking part in this journey and today make me able to stand up and go ahead to the next adventure of my life.

To you I dedicate this quote from one of my favourite writers cause you are within the most beautiful people I have ever known:

"The most beautiful people we have known are those who have known defeat, known suffering, known struggle, known loss, and have found their way out of the depths. These persons have an appreciation, a sensitivity, and an understanding of life that fills them with compassion, gentleness, and a deep loving concern. Beautiful people do not just happen."

E.Kubler Ross

Publications and presentations

The following paper has been published and includes work that has arisen from this thesis (Chapter 4 and Chapter 5):

- Capodanno Y, Buishand FO, Pang LY, Kirpensteijn J, Mol JA, Argyle DJ. (2017) Notch pathway inhibition targets chemoresistant insulinoma cancer stem cells, Endocr Relat Cancer. 2017 Nov 24. pii: ERC-17-0415. doi: 10.1530/ERC-17-0415.

Work from this thesis has been presented in the following conferences:

- Oral presentation at ESVONC conference (20th-22nd April 2017) in Lyon. "*Inhibition of the Notch pathway targets Cancer Stem Cells in Canine and Human Insulinoma."*
- Poster presentation at "7th International Notch meeting" (14th-16th of June) in Cyprus. *"A top NOTCH treatment to target Human and Canine Insulinoma Cancer Stem Cells."*

Table of contents

List of tables

List of figures

List of abbreviations

5-FU	5- Fluorouracil
ACTH	Adrenocorticotropic hormone
AKT	Protein kinase B
APS	Ammonium Persulphide
ATP	Adenosine triphosphate
BSA	Bovine serum albumin
CAM	Chick chorioallantoic membrane
cDNA	Complementary DNA
CSC	Cancer stem cell
CSL	C-terminal binding protein
DAPT	N-[N-(3,5-Difluorophenacetyl)-L-alanyl]-S-phenylglycine t-butyl ester
DMEM	Dulbecco's modified Eagle medium
DMSO	Dimethyl sulfoxide
DNA	Deoxyribonucleic acid
DTT	Dithiothreital
EGF	Epidermal growth factor
EGFR	Epidermal growth factor receptor
ELISA	Enzyme-linked immunosorbent assay

EMT	Epithelial to mesenchymal transition
ERK	Extracellular signal-regulated kinase
ES	Enrichment score
FACS	Fluorescent-activated cell sorting
FBS	Fetal bovine serum
FDR	False discovery rate
logFC	logarithm Fold change
GADPH	Glyceraldehyde 3-phosphate dehydrogenase
GH	Growth hormone
GHRF	Growth hormone-releasing factor
GSEA	Gene set enrichment analysis
GSI	Gamma secretase inhibitor
Hh	Hedgehog
HPF	High power field
HRP	Horse radish peroxidase
IGF	Insulin growth factor
IGFR	Insulin growth factor receptor
INS	Insulinoma
MACS	Magnetic cell sorting
MDS	Multidimensional scoring
mL	Millilitre

mM	Millimolar
mm	Millimitre
nM	Nanomolar
mRNA	messenger RNA
mTOR	mammalian target of rapamycin
MEN1	Multi-endocrine neoplasia 1
NET	Neuroendocrine tumours
NCID	Notch intracellular domain
PBS	Phosphate buffered saline
PDGF	Platelet-derived growth factor
PI3K	Phosphatidylinositol-4,5-bisphosphate 3-kinase
PNET	Pancreatic neuroendocrine tumours
PP	Pancreatic polypeptide
PTEN	Phosphatase and tensin homolog deleted on chromosome 10
QC	Quality control
RIN	RNA integrity number
RNA	Ribonucleic acid
RP	Ribosomial protein
RPS5	Ribosomial protein S5
RPMI	Roswell Park Memorial Institute
SDS	Sodium dodecyl sulphate

SDS-PAGE	Sodium dodecyl sulphate polyacrylamide gel electrophoresis
TBST	Tris-Phosphate buffered saline
TEMED	Tetramethyl ethylene-di-amine
TGF-alpha	Transforming growth factor alpha
TKIs	Tyrosine kinase inhibitors
TNM	Tumour, Node, Metastasis
VEGF	Vascular endothelial growth factor
VHL	Von-Hippel Lindau
VIP	Vasoactive intestinal polypeptide
WHO	World Health Organisation
μL	Microlitre
μM	Micromolar

Lay summary

Cancer arises when a group of cells within the body start growing in an abnormal manner destroying tissues and organs. Pancreatic neuroendocrine tumours (PNETs) are a type of cancer that occurs due to abnormal growth of hormone-producing cells in the pancreas. Insulinoma (INS) is the most commonly diagnosed PNET in humans and dogs. They mainly cause problems by secreting an excessive amount of insulin, the hormone that regulates sugar levels in the blood. An increased production of insulin can cause persistent low sugar levels in the blood that can be life-threatening if not properly treated.

INS are usually restricted to the pancreas and can be easily treated with surgery. Occasionally, INS may spread and develop secondary tumours beyond the pancreas, most often affecting the liver. These INS are known as malignant. In dogs, INS is more common and it is often malignant. Human and dog malignant INS share many features, thus, INS that naturally occurs in dogs can represent a valuable model for studying the natural progression of human malignant INS.

This project aimed to investigate a small group of cancer cells, called cancer stem cells (CSCs), considered responsible for promoting tumour growth. By characterising these cells the aim was to identify potential ways to target them. It is known that CSCs hijack biological pathways that are normally involved in cell growth and repair and use them to defend themselves against commonly used cancer therapy allowing them to resist treatment and continue to grow. Here, human and canine INS CSCs were isolated and studied to identify biological signalling pathways linked to the development of drug resistance. To understand the relevance of these mechanisms for patient treatment, we determined the active genes in canine INS samples to reveal a set of biological signalling pathways involved in the progression and spread of the disease. Results of this study showed that the Notch pathway is involved in the early stage of INS carcinogenesis and in promoting the growth of INS cancer cells. Interestingly, the Notch pathway has previously shown to have a key role in pancreatic development and as well in the spread of PNETs.

Using specific inhibitors, evidence was provided that inhibition of Notch signalling could reduce the growth of INS CSCs, and made them more susceptible to commonly used chemotherapy. In conclusion, these findings provided evidence that the Notch pathway might be an interesting drug target for improving, in the future, the outcome of patients diagnosed with malignant INS.

Abstract

Pancreatic neuroendocrine tumours (PNETs) are the most common neuroendocrine tumours diagnosed in humans and dogs. Due to the highly heterogeneous nature of these tumours, definitive data are still lacking over the molecular mechanisms involved in their cancerous behaviour.

This study focused on insulinoma (INS), as it is the most commonly diagnosed PNET in human and veterinary oncology. INS is an insulin-producing tumour that causes a hypoglycaemic syndrome related to the excessive insulin production. In humans, it is often a small benign neoplasm readily curable by surgical resection whereas, in dogs, INS is often malignant. Despite current treatment modalities, malignant canine and human INS have a poor prognosis as patients tend to develop metastases in liver and lymph nodes that do not respond to current therapies. From a comparative oncology perspective, the close resemblance

of canine and human malignant INS makes canine INS an interesting study model for human INS.

Cancer stem cells (CSCs) are critical for the engraftment and chemoresistance of many tumours. Although CSCs have been isolated from a range of solid tumours, a comprehensive characterisation of INS CSCs has not yet been reported. In this study, it was confirmed that INS CSCs can be enriched and are potential targets for novel INS therapies. Highly invasive and tumourigenic human and canine INS CSCs were successfully isolated and exhibited greater resistance to chemotherapy, which may play a significant role in the poor prognosis of this disease. To date, the mechanisms by which tumours spread and the clinical causes of chemoresistance remain only partially understood. Here, RNA-sequencing analysis was performed over a small set of canine INS tumour samples in order to identify mechanisms involved in INS carcinogenesis through different stages of the disease. Preliminary data showed that distinct gene profiles characterised early and late stage of canine INS. Interestingly, differential gene expression and gene pathways analysis, highlighted that sets of genes involved in pancreatic embryogenesis and insulin secretion were overexpressed in canine primary INS lesions compared with normal pancreas. The

Notch pathway is fundamental in pancreatic embryogenesis and it has been previously associated with carcinogenesis of neuroendocrine tumours and with the CSC phenotype. Protein analysis showed that the Notch pathway is activated in both human and canine INS CSCs, particularly when treated with chemotherapy, indicating that the Notch pathway may be involved in chemoresistance. Additionally, it was demonstrated that inhibition of the Notch pathway decreased INS CSCs' survival and chemoresistance, both *in vitro* and *in vivo*. These findings provide preclinical evidence that anti-Notch therapy may improve outcomes for patients with malignant INS.

1 Introduction

1.1 Background

Pancreatic neuroendocrine tumours (PNETs) comprise a heterogeneous group of endocrine tumours arising in the pancreas. They are among the most common neuroendocrine tumours (NETs) and are becoming increasingly important both clinically and from a research standpoint (Ehehalt *et al.*, 2009; Ito *et al.*, 2012; Ro *et al.*, 2013; Reid *et al.*, 2014).

In humans, PNETs comprise 1.3% to 2.8% of new pancreatic malignancies each year (Zhang *et al.*, 2013; Yu, 2016). According to various Asian and European population studies, they are uncommon neoplasms with an incidence lower than 1 per 100,000 persons per year (Halfdanarson *et al.*, 2008; Ehehalt *et al.*, 2009; Vandamme *et al.*, 2015). Generally, PNETs have a more indolent clinical course than do pancreatic ductal adenocarcinomas, which arise from the exocrine pancreas and comprise the majority of pancreatic cancer diagnoses (Lubeseder-martellato *et al.*, 2016). Remarkably, up to 40% of all PNETs are incidentally diagnosed, highlighting the number of clinically asymptomatic cases (Okabayashi *et al.*, 2013; Zhang *et al.*, 2013). In fact, the incidence is frequently higher in autopsy studies, ranging from 0.8% to 10% suggesting that these tumours frequently go unnoticed (Ehehalt *et al.*, 2009; Ito *et al.*, 2012; Ro *et al.*, 2013). The incidence of PNETs in veterinary oncology is unknown. However, they are still considered rare neoplasms (Finotello *et al.*, 2014).

Insulinomas (INS) are the most commonly diagnosed PNETs in human and canine patients (Buishand *et al.*, 2010; Okabayashi *et al.*, 2013). INS are insulin-producing tumours that can arise from beta-cells of the pancreas (Trifonidou *et al.*, 1998; Jonkers *et al.*, 2007; Polton *et al.*, 2007; Goutal *et al.*, 2012). Clinical signs of INS are usually related to the excessive production of insulin. The incidence of INS in humans is reported to be four cases per million of the population per year, and the peak age-specific incidence rate occurs in the fifth decade of life with a slight female predilection (Callacondo *et al.*, 2013). The incidence of canine INS seems higher

compared to humans. In fact, data collected at the Department of Clinical Sciences of Companion Animals of Utrecht University, have recorded at least 10 cases of canine INS each year, on a total population of 2 million dogs in the Netherlands (Buishand, unpublished data).

The principles of management of INS include the diagnosis and control of the functional hormonal syndrome and the potentially malignant tumour (Polton *et al.*, 2007; De Herder *et al.*, 2011). The treatment of choice for localised benign tumours is surgical resection (Bailey and Page, 2007; Vaidakis *et al.*, 2010; Wouters *et al.*, 2011). However, for malignant INS that require adjuvant therapy following surgery, the medical treatment options are rarely curative (Corroller *et al.*, 2008; Goutal *et al.*, 2012; Baudin *et al.*, 2014).

In dogs, previous reports in the literature describe average life expectancies for malignant INS of approximately one year for patients undergoing surgery and 6,5 months for medical management (Tobine *et al.*, 1999; Polton *et al.*, 2007; Goutal *et al.*, 2012). In humans, patients diagnosed with malignant INS have a survival rate within 30-60% at 5 years from diagnosis (Borson-Chazot *et al.*, 2013; Rossi *et al.*, 2014; Giuroiu and Reidy-Lagunes, 2015). Whereas, for patients treated with chemotherapy after surgery the survival time rise to 71% at five years (Corroller *et al.*, 2008).

Malignant INS can be hard to diagnose as they require diagnostic tools and treatment approaches different from those commonly used in human and veterinary oncology (Anlauf *et al.*, 2009; Goutal *et al.*, 2012). Therefore, molecular markers that predict INS behaviour and new treatment strategies are required to improve clinical decision-making in human and canine patients diagnosed with malignant INS. From a comparative oncology perspective, which aims to utilise spontaneous tumours in pet animals as natural models for the study of human cancer biology and therapy (Gordon *et al.*, 2009), the similarities of canine INS to human malignant INS, makes canine INS an interesting study model for human malignant INS.

1.2 Comparative anatomy of Canine and Human Pancreas

Before describing the biological and clinical aspects of human and canine PNETs and specifically of INS, the main anatomical and histological features of the pancreas in these two different species will be briefly outlined here.

The pancreas is a glandular lobulated organ. The embryonic pancreas in vertebrates develops from the endoderm as evaginations of the primitive gut. A dorsal and ventral protrusion grow, branch and then fuse to form the definitive pancreas (Edlund, 2002; Gittes, 2009; Tsuchitani *et al.,* 2016).

The pancreas is a composite gland that contains both exocrine and endocrine components. The precursor cells are called amphicrine cells, and they are developmentally plastic as they may differentiate into either endocrine or exocrine cells (Ordonez, 2001). The exocrine part constitutes the majority of the pancreas volume whereas the endocrine part constitutes just about 2% of it (Edlund, 2002; Tsuchitani *et al.,* 2016). The exocrine pancreas is constituted by acinar cells which secrete digestive enzymes in the small intestine through the pancreatic duct (Tsuchitani *et al.,* 2016). The exocrine pancreas has a basic common structure among mammals being composed of two epithelial cell types, acinar and ductal epithelial cells. The acinar epithelial cells make up the major portion of the pancreas, and the ductal system is composed of centroacinar cells, followed by the intercalated, intralobular, interlobular, and main ducts (Pandol *et al.* 2010; Longnecker, 2014). The acinar cells produce a variety of digestive enzymes, such as proteases, amylases and lipases (Kim *et al.*, 2010).

Endocrine pancreatic cells are organised in ‘Islets of Langerhans', These islets are located in different part of the pancreas and secretes various hormones that regulate glucose metabolism in the body (Tsuchitani et al., 2016) (Table 1.1).

Extra-insular endocrine cells are scattered randomly as single cells or as clusters. (Edlund, 2002; Tsuchitani *et al.,* 2016). The islet of Langerhans displays a remarkable variability in cellular composition and morphology producing insulin (β-cells), glucagon (α-cells), somatostatin (δ-cells), vasoactive intestinal polypeptide (VIP) (β-cells), pancreatic polypeptide (PP-cells) and substance P/serotonin

(enterochromaffin cells). Gastrin-producing G cells are present in foetal but not adult pancreatic islets (Lechner *et al.*, 2005; Lopez *et al.*, 2010; Fendrich *et al.*, 2012). The topographic distribution and number of islet endocrine cells differ between the lobes of the pancreas and species (Kim *et al.*, 2010; Steiner *et al.*, 2011). For instance, total β- cell mass increases proportionately to compensate the demand for insulin in the body (Kim *et al.*, 2010). Therefore this difference in the islet structure results from different metabolic requirements (Steiner *et al.*, 2011).

1.2.1 Canine pancreas

1.2.1.1 Gross anatomy

In dogs, the pancreas has got the form of an inverted-V, and it is divided into three parts: the right lobe, the body and the left lobe (Evans, 1993; Tsuchitani *et al.*, 2016). The right lobe is a thin structure whereas the left lobe is thicker and wider. They are united in the body, which lies caudomedial to the pylorus. The right lobe lies in the meso-duodenum extending caudally from the body along the duodenum. The left lobe extends caudo-sinistrally from the body to the hilum of the spleen (Evans, 1993; Tsuchitani *et al.*, 2016) (Figure 1.1 A).

1.2.1.2 Histology

The canine pancreatic islets are composed of a core of β-cells (>50% of the islet) surrounded by peripherally located α-cells (<30%) (Figure 1.2 A). The δ-cells, in this species, tend to be randomly distributed through the islet. The α-, β- and δ-cells tend to congregate in organised islets in the left lobe, whereas the right lobe contains small scattered islets (Steiner *et al.*, 2011). Flattem *et al.* (2001) showed that, in the canine pancreas, β-cells and α-cells collaborate very efficiently to respond even to minimal changes in plasma glucose (Flattem *et al.*, 2001).

1.2.2 Human Pancreas

1.2.2.1 Gross anatomy

The human pancreas is divided into four parts: head, neck, body, and tail. In humans, the pancreas has a J-shape and the head constitutes 50% of its volume (Longnecker, 2014). The human pancreas is a compact organ protected from severe trauma by lying close to the posterior abdominal wall in the upper abdomen. The tail of the pancreas and spleen are in the left upper quadrant of the abdomen, and the head of the pancreas is in the right upper quadrant just to the right of the midline. The head of the pancreas is surrounded by the duodenum in its concavity. The tail of the pancreas lies near the hilum of the spleen, and the body lies posterior to the distal portion of the stomach (Pandol *et al.* 2010; Longnecker, 2014) (Figure 1.1 B).

1.2.2.2 Histology

Human islets have a more "disorganised structure" where the α-, β- and δ-cells do not have a specific distribution throughout the islet. The adult human islet contains about ~50% β-cells, ~40% α-cells, 10% δ-cells and few PP-cells (Figure 1.2 B). This structure is functional for β-cell to respond to low concentrations of glucose (<1 mM) (Kim *et al.*, 2010).

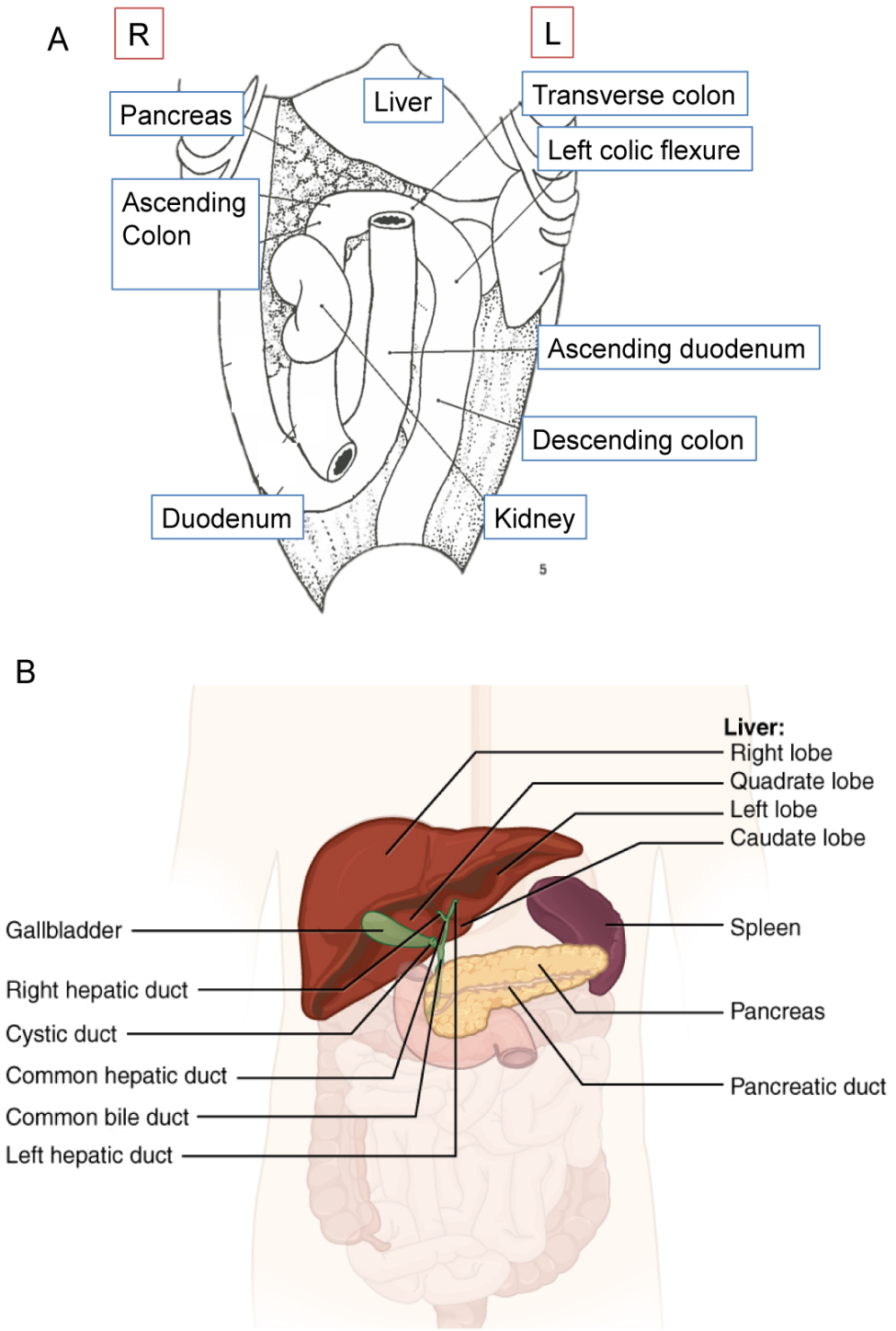

Figure 1.1 Gross anatomy of canine and human pancreas. A: Anatomical localisation of canine pancreas. R=right. L=left. (adapted from illustration of A. Gardiner & M. Raynor, The Dog Anatomy Workbook: A Guide to the Canine Body, J.A. Allen (London)). B: Anatomical localisation of human pancreas. (Illustration from Anatomy & Physiology, 2013, http://cnx.org/content/col11496/1.6; licensed under the Creative commons attribution 3.0).

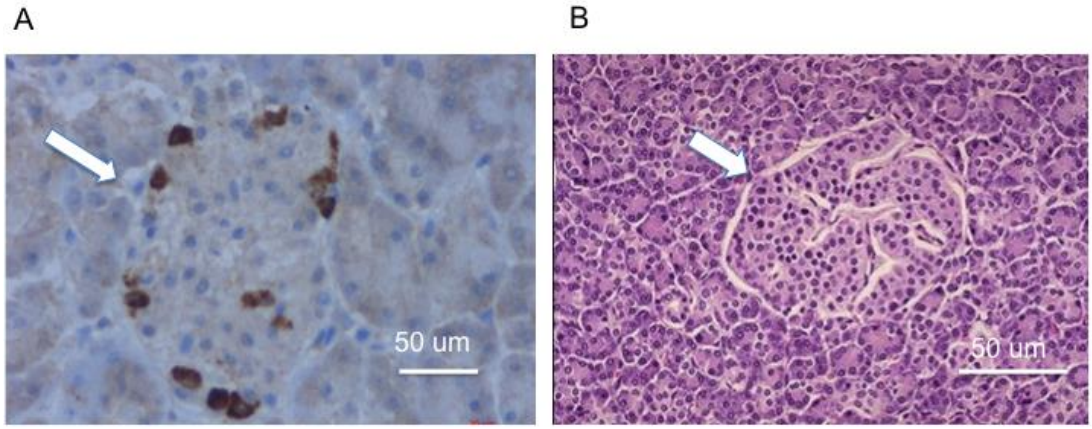

Figure 1.2 A: Histology of canine pancreatic islets. Immunoperoxidase staining with insulin of formalin-fixed, paraffin-embedded canine pancreatic islet. B: Histology of human pancreatic islets. Picture shows H&E staining of human pancreatic islet (adapted from binipatia.com, 2013; licensed under the Creative commons attribution 3.0).

Table 1.1. Hormones of the pancreas and their effects on regulating the glucose metabolism in the body (adapted from Tsuchitani et al., 2016).

Pancreatic hormones		
Hormones	**Cells**	**Effect**
Insulin	Beta cells	Reduce blood glucose levels
Glucagon	Alpha cells	Increase blood glucose levels
Somatostatin	Delta cells	Inhibits insulin and glucagon
Pancreatic polypeptide (PP)	PP cells	Role in appetite

1.3 Classification and clinical aspect of Pancreatic Neuroendocrine Tumours

1.3.1 Classification

PNETs typically occur sporadically in humans and dogs (O'Brien *et al.*, 1987; Bailey and Page, 2007; Ro *et al.*, 2013; Rossi *et al.*, 2014). In humans, they can also be components of familial syndromes such as multiple endocrine neoplasia syndrome type 1 (MEN1), von Hippel-Lindau disease (VHL), neurofibromatosis type 1 (von Recklinghausen disease), tuberous sclerosis, and Mahvash disease (due to inactivating glucagon receptor mutation) (Crabtree *et al.* 2016; Yu 2016). PNETs are frequently divided into two groups based on their capacity to produce, store, and secrete peptides or hormones that may induce clinical syndromes (Grande *et al.*, 2011). Functioning PNETs are the most common and they can be distinguished into: INS (the most common PNET in human and veterinary oncology), gastrinoma, and rare tumours such as vasoactive intestinal polypeptide (VIP)-oma, glucagonoma, carcinoids, somatostatinoma, and exceedingly rare neoplasms like pancreatic polypeptide (PP)-oma, adrenocorticotropic hormone (ACTH-oma), growth hormone-releasing factor (GHRF-oma), calcitonin-producing tumours, parathyroid hormone-related peptide-producing tumours and others (Höpfner *et al.*, 2003; Polton *et al.*, 2007; Okabayashi *et al.*, 2013; Finotello *et al.*, 2014; Rossi *et al.*, 2014; Crabtree *et al.*, 2016) (Table 1.2). Non-functioning PNETs cause non-specific signs related to the mass-effect of metastases, mainly in the liver, such as pain, anorexia, and weight loss, and are often an incidental findings (Jutting *et al.*, 1997; Ro *et al.*, 2013; Rossi *et al.*, 2014).

Table 1.2 Hormone-producing pancreatic neuroendocrine tumours (adapted from Höpfner et al., 2003; Polton et al., 2007). VIP, vasoactive intestinal polypeptide; PP, pancreatic polypeptide; ACTH, adrenocorticotropic hormone; GHRF, growth hormone-releasing factor

Tumour	Clinical signs	Hormone
Insulinoma	Hypoglycaemia	Pro-insulin, Insulin
Gastrinoma	Peptic ulcer and diarrhoea	Gastrin
VIPoma	Watery diarrhoea, hypokalaemia	VIP
Glucagoma	Anaemia, diabetes	Glucagon
Somatostatinoma	Diabetes, diarrhoea, steatorrhea	Somatostatin
GHFRoma	Acromegaly	GHRF
ACTHoma	Cushing's Syndrome	ACTH

1.3.2 Diagnosis, treatment and prognosis

Endocrine testing, imaging, and histological evidence are necessary to accurately diagnose PNETs. The diagnosis of PNETs rests upon confirming the neuroendocrine nature of the malignant cells and immunohistochemical stainings with markers such as chromogranin A, synaptophysin and neuron-specific enolase. Nevertheless, these tumours can have heterogeneous microscopic findings. Thus it can be difficult to assess the degree of malignancy of pancreatic endocrine tumours. Accepted histological criteria for malignancy, such as nuclear pleomorphism or infiltration of adjacent tissue, are unreliable in the evaluation of PNETs in humans and dogs (Ro *et al.*, 2013; Buishand *et al.*, 2014).

For human PNETs, the current World Health Organisation (WHO) classification provides guidance in that respect (Table 1.3). Using the TNM (tumour, node, and metastasis) system, PNETs are divided into four main stages of tumour advancement (Table 1.3). Using proliferative markers such as mitotic count and Ki67 index, PNETs are categorised as low- (G1), intermediate- (G2), or high-grade (G3) (Table 1.3) (Ito *et al.*, 2012; Reid *et al.*, 2014; Rossi *et al.*, 2014). PNETs grade and stage are the major determinants of prognosis in humans (Ito *et al.*, 2012). Therefore, before treatment a complete histological assessment of the tumour is usually required (Ro *et al.*, 2013; Zhang *et al.*, 2013).

This system has been adapted for staging canine PNETs (Table 1.4). Previous studies showed that in dogs, together with TNM stage, increased nuclear size, pleomorphism, Ki67 and DNA content are considered valuable histological features to predict the biological behaviour of PNETs (Jutting *et al.*, 1997; Buishand *et al.*, 2010). However, in both human and dogs, the presence of metastases, mainly located in the liver, represent the only definitive feature that characterises these tumours as malignant (Jutting *et al.*, 1997; Halfdanarson *et al.*, 2008; Ehehalt *et al.*, 2009; Buishand *et al.*, 2013; Baudin *et al.*, 2014).

Considering their high heterogeneity, treatment options for PNETs are highly variable. Small, benign neoplasms like benign INS are readily curable by surgical resection (Vaidakis *et al.*, 2010). Still, the majority of PNETs have a less favourable

prognosis depending on local invasiveness and liver metastases and often require adjuvant medical therapy (Corroller *et al.*, 2008; Ehehalt *et al.*, 2009; Fendrich *et al.*, 2012). The treatment of patients diagnosed with advanced metastatic, hormonally-active PNETs has two primary goals. First, to control the hormone oversecretion which can lead rapidly to complications and death. Secondly, to reduce the growth and spread the PNET itself (Ito *et al.*, 2012).

A supervised diet and somatostatin analogues constitute the major medical therapy for canine patients diagnosed with malignant PNETs (Jutting *et al.*, 1997; Goutal *et al.*, 2012). In dogs, chemotherapy has not been shown to be beneficial as adjuvant therapy post-resection of liver metastases due to the high level of toxicity and side effects (Jutting *et al.*, 1997; Northup *et al.* 2013). In dogs, Caywood *et al.* (1998) have shown that patients with distant metastasis with or without local lymph node involvement (stage III) had a significantly shorter survival time compared to dogs with localised pancreatic lesions (stage I and II). All stage III dogs died by 18 months post-surgically (Caywood *et al.*, 1998).

In humans, medical treatment of malignant PNETs often includes the use of chemotherapy (De Herder *et al.*, 2011; Ro *et al.*, 2013; Baudin *et al.*, 2014; Rossi *et al.*, 2014). However, complete responses are rare, and the median responses are short (6–20 months). For example, combinations of streptozotocin and 5-fluorouracil (5-FU), with or without doxorubicin, have shown an objective response rate of 20–45%. Moreover, streptozotocin-based treatments have considerable morbidity, with most of the patients developing side-effect, including nausea/vomiting and 15–40 % developing renal toxicity with long-term treatment (Ehehalt *et al.*, 2009; Ro *et al.*, 2013). (Ro *et al.*, 2013; Reid *et al.*, 2014). In humans, only 25% of the patients with advanced PNETs have up to 5-year survival time (Borson-Chazot *et al.*, 2013; Reid *et al.*, 2014).

Even though PNETs are considered uncommon in human and veterinary oncology, they still cause significant morbidity and mortality. Unique challenges facing PNETs studies include prolonged disease course, the difficult access to pancreatic tissue during surgery, and the heterogeneity of these tumours (Bernard *et al.*, 2013; Carter *et al.*, 2013; Wang *et al.*, 2013; Zhang *et al.*, 2013; Baratelli *et al.*, 2014; Reid *et al.*, 2014; Fujino *et al.*, 2015; Krampitz *et al.*, 2016). In this study will focus on the most

commonly diagnosed PNETs in human and veterinary oncology to design specific treatment therapy and improve the diagnosis of human and canine patients bearing INS.

Table 1.3 TNM classification and disease staging for pancreatic neuroendocrine tumours (PNETs) in humans. HPF, high power field (adapted from Ehehalt et al., 2009)

Stage and grade of PNETs in humans

T: Primary tumour			
TX	Primary tumour cannot be assessed		
T0	No evidence of primary tumour		
T1	Tumour limited to the pancreas and size>2cm		
T2	Tumour limited to the pancreas and size 2–4 cm		
T3	Tumour limited to the pancreas and size >4 cm		
T4	Tumour invading adjacent organs or the wall of large vessels		
N: regional lymph nodes			
NX	Regional lymph nodes cannot be assessed		
N0	No regional lymph node metastasis		
N1	Regional lymph node metastasis		
M: distant metastases			
MX	Distant metastases cannot be assessed		
M0	No distant metastases		
M1	Distant metastases		
Stage			
I	T1	N0	M0
IIa	T2	N0	M0
IIb	T3	N0	M0
IIIa	T4	N0	M0
IIIb	Any T	N1	M0
IV	Any T	Any N	M1
Grade	**Mitotic count (10HPF)**	**Ki-67 index (%)**	
1	< 2	<2	
2	2-20	3-20	
3	>20	>20	

Table 1.4 TNM classification and disease staging for pancreatic neuroendocrine tumours (PNETs) in dogs. HPF, high power field (adapted from Buishand et al., 2010)

Stage and grade of PNETs in dogs

T: Primary tumour			
TX	Primary tumour cannot be assessed		
T0	No evidence of primary tumour		
T1	Tumour limited to the pancreas and size>2cm		
T2	Tumour limited to the pancreas and size 2–4 cm		
N: regional lymph nodes			
NX	Regional lymph nodes cannot be assessed		
N0	No regional lymph node metastasis		
N1	Regional lymph node metastasis		
M: distant metastases			
MX	Distant metastases cannot be assessed		
M0	No distant metastases		
M1	Distant metastases		
Stage			
I	T1	N0	M0
II	T2	N0	M0
III	Any T	N1	M0
IV	Any T	Any N	M1
Grade	**Mitotic count (10HPF)**	**Ki-67 index (%)**	
1	< 2	<2	
2	2-20	3-20	

1.4 Canine and Human Insulinomas: comparative aspects of a well-defined tumour syndrome

1.4.1 Epidemiology

In dogs INS usually occur sporadically and it is often diagnosed in older dogs with no sex predilection (Trifonidou *et al.,* 1998; Polton *et al.,* 2007; Goutal *et al.,* 2012; Buishand *et al.,* 2013). Medium to large breeds including Labrador retrievers, golden retrievers, German shepherds, Irish setters and Boxer seems to be the most common breeds diagnosed with INS (Siddons, 1976; Goutal *et al.,* 2012). INS are considered rare neoplasms but the occurrence of metastases in dogs is as high as 95% of the cases compared with only 5% to 16% in humans (Polton *et al.,* 2007; De Herder *et al.,* 2011; Goutal *et al.,* 2012; Mathur *et al.,* 2012; Buishand *et al.,* 2014).
In humans, INS can occur sporadically (90%) or constitute a part of MEN-1 (16%) (Dotzenrath *et al.,* 2000; Jonkers *et al.,* 2006; Vaidakis *et al.,* 2010). INS associated with MEN-1 tends to broadly affect individuals at younger ages compared with sporadic INS (median age at presentation is 25 years or less) (Dotzenrath *et al.,* 2000; Fontanière *et al.,* 2006). The median age of diagnosis for sporadic INS is 60 years old (Giuroiu and Reidy-Lagunes, 2015).

1.4.2 Clinical findings

The clinical signs of INS result from excessive insulin secretion, which leads to an increased rate of transfer of glucose from the extracellular fluid to body tissues and thus to severe hypoglycemia (Okabayashi *et al.,* 2013). The malignant behaviour of INS is usually related to recurrence of clinical signs of hyperinsulinemia-induced hypoglycaemia after surgery due to the outgrowth of micrometastases in lymph nodes and liver (Anlauf *et al.,* 2009; Buishand *et al.,* 2012; Northrup *et al.,* 2013; Okabayashi *et al.,* 2013).

Clinical findings are similar for canine and human INS, and they are majorly related to the central nervous system (Table 1.4). The predominance of clinical signs relating to the central nervous system demonstrates the primary dependence of the brain on the metabolism of glucose for energy. When the brain is not supplied with glucose, cerebral oxidation decreases and manifestations of hypoxia appear (Mohseni, 2014). Neuroglycopenic symptoms include abnormal behaviour, seizures and coma. In addition, hypoglycemia can cause catecholamine release and adrenergic sympathetic nervous system activation (Table 1.4). Clinical signs are episodic and occur initially at widely spaced intervals and become more frequent and severe in the later stage of the disease (Jordan and Carithers, 1980; Lurye and Behrend, 2001; Jonkers, Ramaekers and Speel, 2007; Polton *et al.*, 2007; Okabayashi *et al.*, 2013). The lack of specificity of the clinical signs makes the diagnosis of INS quite difficult particularly at an early stage. Certain stimuli such as excitement, fasting or exercise, preceded the most onset of clinical signs (Jordan and Carithers, 1980; Lurye and Behrend, 2001; Jonkers *et al.*, 2007; Polton *et al.*, 2007; Okabayashi *et al.*, 2013). Administration of glucose rapidly alleviates the signs (Jordan and Carithers, 1980; Trifonidou *et al.*, 1998; Goutal *et al.*, 2012). If untreated, repeated episodes of prolonged and severe hypoglycemia may result in irreversible neuronal degeneration throughout the brain (Mohseni, 2014). Permanent neurologic disability probably accounts for the terminal coma, unresponsiveness to glucose, and eventual death of the patient (Corroller *et al.*, 2008; Goutal *et al.*, 2012).

Table 1.4 Clinical signs of insulinoma in dogs and humans (adapted from Jonkers et al., 2007; Polton et al., 2007; Goutal et al., 2012)

	Dog	**Human**
Neuroglycopenic	Fatigue	Diplopia
	Disorientation	Blurred vision
	Apparent blindness	Amnesia
	Change of temperament	Anxiety
	Ataxia	Confusion
	Collapse	Abnormal behaviour
	Seizures	Seizures
	Coma	Coma
Adrenergic	Muscular twitching	Hunger
	Weakness	Weakness
	Hunger	Sweating
	Trembling	Tremor
	Palpitations	Heart pounding
	Tachycardia	Tachycardia

1.4.3 Diagnosis

The diagnosis of INS is achieved on the combination of hyperinsulinemia, hypoglycaemia and the exclusion of alternative diagnoses such as exogenous insulin administration (Polton *et al.*, 2007; Druce *et al.*, 2010; Goutal *et al.*, 2012; Okabayashi *et al.*, 2013).

Diagnosis of INS was previously obtained by documenting Whipple's triad (Figure 1.3); however, it is now evident that many other disorders could respond similarly. For this reason, additional tests are often needed to confirm the diagnosis of INS-induced hypoglycaemia (Figure 1.3) (Jordan and Carithers, 1980; Jonkers *et al.*, 2007; Goutal *et al.* 2012).

In dogs, a blood glucose curve should be done when a history of periodic weakness, collapse, or seizures is recorded in an older dog. Blood analysis evaluating the amended insulin-to-glucose ratio may be warranted. This assay assesses the lack of response to physiologic negative feedback inhibitory loops that decreases insulin secretion following hypoglycemia. A positive insulin-to-glucose ratio demonstrates an inappropriately elevated insulin level in the setting of low glucose level. Insulin:glucose ratio greater than 4.2 is considered diagnostic (Thrall *et al.*, 2011).

In humans, with symptoms of neuroglycopenia or documented low blood glucose levels, the gold standard for biochemical diagnosis remains measurement of plasma glucose, insulin, C-peptide, and proinsulin during a 72-h fast (Okabayashi *et al.*, 2013). This test has the advantages of evaluating both the correlation between hypoglycaemia and the patient's symptoms, and the inadequately elevated insulin concentrations compared with the low blood glucose levels (Vaidakis *et al.*, 2010; Athanasopoulos *et al.*, 2011; Borson-Chazot *et al.*, 2013) (Figure 1.3).

1.4.3.1 Imaging

Imaging should be used as a complementary tool for diagnosing INS. In particular, imaging is usually used for preoperative localisation of INS. However, diagnosis and

location accuracy of INS remains challenging regardless of the imaging modality used in both humans and dogs (Druce *et al.*, 2010; Goutal *et al.*, 2012).

In dogs, abdominal ultrasound (US) represents the most common tool used to visualise masses in the pancreas. Ultrasound is often also a useful tool to detect metastatic lesions in different organs and lymph nodes (Goutal *et al.*, 2012). INS usually present either spherical or lobular shape and are hypoechoic compared with the surroundings tissues (Figure 1.4 A-B). Nonetheless, the sensitivity of US in detecting INS in dogs is reported to range from 28% to 75% and be highly operator-dependent (Fukushima *et al.*, 2015).

In humans, the sensitivity of transabdominal US for localising pancreatic insulinomas is 9–64% (Nakamura *et al.*, 2015). Computed tomography (CT) is commonly used in human medicine as a preoperative imaging technique as it is a more sensitive imaging examination than the non-contrast US, thus, being superior to the US for INS localisation and staging (Nakamura *et al.*, 2015). However, the cost and requirement for specialised equipment, as well as the need for anaesthesia, have currently limited routine use of these techniques in veterinary medicine (Figure 1.4 C) (Goutal *et al.*, 2012; Fukushima *et al.*, 2015).

1.4.3.2 Pathological and histopathological findings

INS usually appear as single, yellow to dark red, spherical, small (1–3 cm) nodules visible from the serosal surface of the pancreas and encapsulated in fibrous connective tissue that separates the neoplasm from the adjacent parenchyma. Occasionally INS appears as multiple nodules in the same or different lobes of the pancreas (Wouters *et al.*, 2011; Goutal *et al.*, 2012; Okabayashi *et al.*, 2013).

Definitive diagnosis of INS can be obtained only with histopathology that usually reveals tumour cells arranged in trabecular and glandular pattern separated by vascular stroma. The nuclei are usually highly pleomorphic, vesicular with 1-2 nucleoli (Srivastava and Hornick, 2009; Buishand *et al.*, 2010). Anaplastic features are often mild or inconsistent, even though INS are often malignant in dogs, thus the lack of anaplastic features should not be used to predict the biologic behaviour of INS (Goutal *et al.*, 2012; Buishand *et al.*, 2010; Zhu *et al.*, 2016).

Human INS presents a characteristic deposition of amyloid that can be visualised by immunohistochemistry together with insulin (Hawkins *et al.*, 1987; O'Brien *et al.*, 1994; Williams *et al.*, 1992), whereas in dog the deposition of amyloid is less common (O'Brien *et al.*, 1987). In both dogs and humans, immunohistochemically, INS stain positively for insulin, pro-insulin, chromogranin A, synaptophysin, neuron-specific enolase, cytokeratin and Ki-67 (O'Brien *et al.*, 1987; Heitz *et al.*, 1982; Buishand *et al.*, 2010; Buishand *et al.*, 2012).

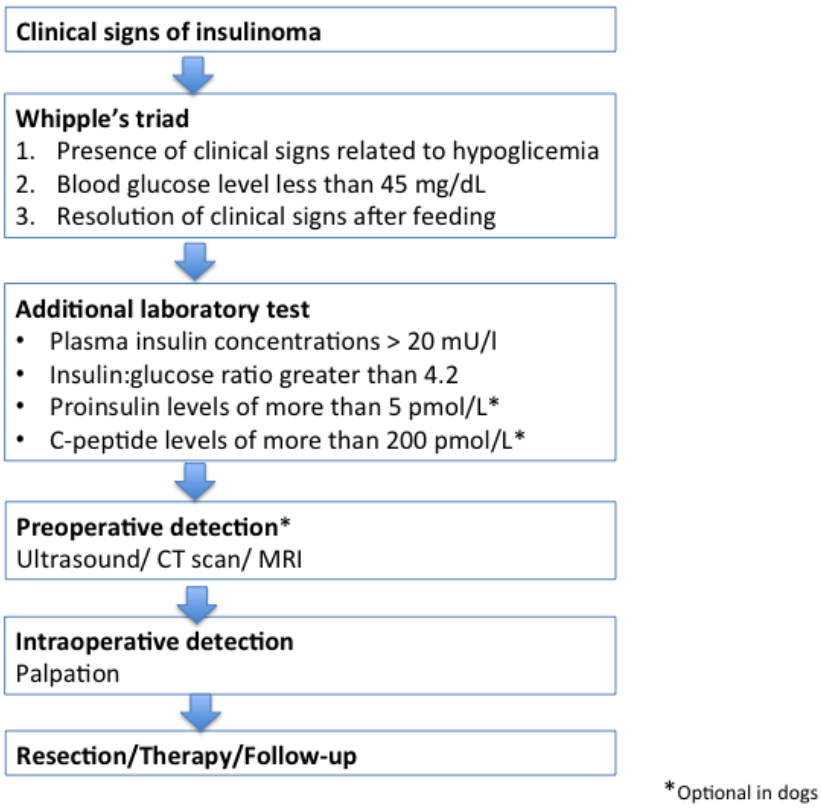

Figure 1.3 Flowchart outlining the diagnosis and the subsequent clinical tests for the detection of insulinomas in human and dogs.*indicates diagnostic tests optional in dogs (Jonkers et al. 2007; Goutal et al. 2012).

A

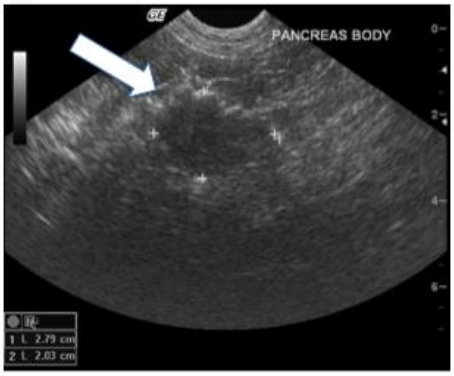

B

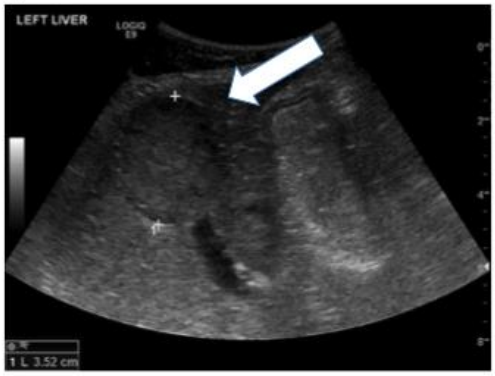

C

Arterial phase Portal phase Later phase

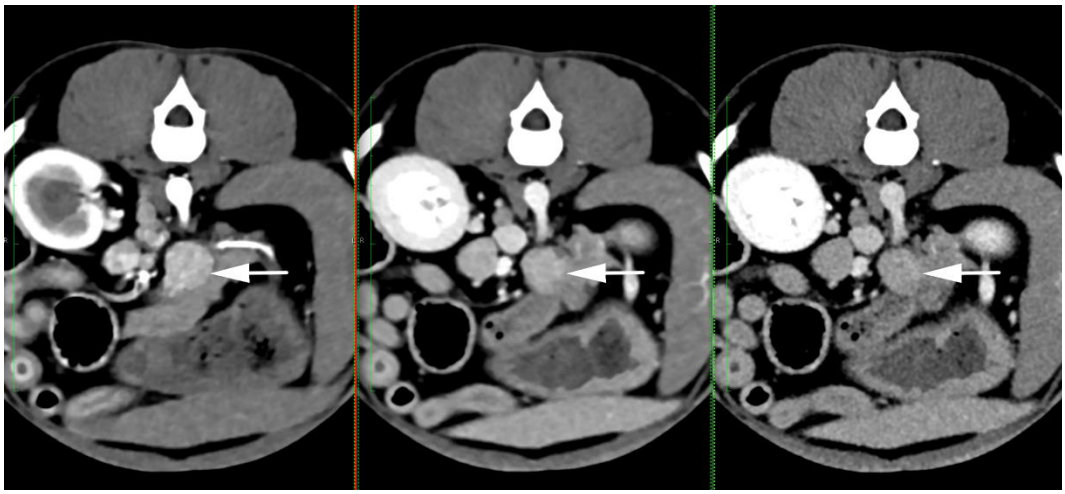

Figure 1.4 A-B: Pictures representing transabdominal ultrasound of canine insulinoma . A: Arrow indicates an irregularly shaped hypoechoic mass in pancreatic body approx. 2.7 x 2cm. Margins defined by hyperechoic peripancreatic fat surrounding the lesion. B: Arrow indicates a 3 cm hypoechoic lesion with irregular pattern and well-defined margins in the left lobe of the liver. C: Pictures representing triple-phase computer tomography of canine insulinoma. Arrows indicate a 1.6cm soft tissue nodule with hyperattenuation on arterial and portal phase images. It is possible to appreciate how insulinomas have a stronger contrast enhancement on the arterial phase and a hypoattenuation in later phase. Pictures are courtesy of the Hospital for small animals, Royal (Dick) Vet School, UK.

1.4.3.3 Differential diagnosis

For the differential diagnosis it is important to evaluate the duration and progression of signs, as INS usually have a history of prolonged seizures often associated with fasting periods and exercise both in humans and in dogs (Jordan and Carithers, 1980; Trifonidou, Kirpensteijn and Robben, 1998; Polton *et al.*, 2007; Goutal, Brugmann and Ryan, 2012; Okabayashi *et al.*, 2013; Giuroiu and Reidy-Lagunes, 2015).

Differential diagnoses for INS include other causes of hypoglycaemia that can be broadly classified into three main groups: (i) diseases associated with excess secretion of insulin or insulin-like factors, in which excessive production of insulin can be related to islet hyperplasia or extra-pancreatic paraneoplastic syndromes; (ii) differential diagnoses could include diseases where the metabolism of glucose is altered, such as hypoadrenocorticism, hunting dog hypoglycaemia, hepatic insufficiency, glycogen storage diseases, and sepsis; (iii) hypoglycaemia could be caused by iatrogenic insulin over-dose and toxic causes of insulin release like high dose of beta-blockers (Lurye and Behrend, 2001; Polton *et al.*, 2007; Vaidakis *et al.*, 2010; Goutal *et al.*, 2012; Okabayashi *et al.*, 2013; Vinik, 2017)(Table 1.).

A diagnosis of INS is also associated with other symptoms such as recurrent seizures. In case of seizures, several differential diagnoses must be included such as, idiopathic epilepsy, brain tumour, encephalitis, lead poisoning, hypoparathyroidism, and cardiovascular or respiratory diseases (as they could lead to cerebral ischemia and hypoglycaemia) (Jordan and Carithers, 1980; Polton *et al.*, 2007; Goutal *et al.*, 2012).

Table 1.6 Differential diagnosis associated with different causes of hypoglicaemia in human and dogs (Lurye and Behrend, 2001; Goutal et al., 2012; Vinik, 2017)

Causes of hypoglicaemia	Dog	Human
Excessive insulin production	Islet hyperplasia	Nesidioblastosis (islet hyperplasia)
	Extra-pancreatic tumours, particularly hepatic tumours and leiomyosarcoma	Extra-pancreatic tumours
Altered metabolism of glucose	Liver disease	Liver disease
	Hypoadrenocorticism (Idiopathic in working dogs)	Hypoadrenocorticism
		Hypothyroidism (severe)
	Congenital enzyme deficiencies (glycogen storage disease)	Specific enzymatic defects
	Growth hormone deficiency	Growth hormone and corticotropin deficiency
	Hunting dog hypoglycemia	Fanconi syndrome (renal loss of glucose)
Factitious	Excessive insulin administration	Excessive insulin administration
	Excessive administration of sulfonylurea, xylitol, aspirin, or b-blockers	Excessive sulfonylurea administration and pentamidine-induced hypoglycaemia
	Laboratory artefacts (incorrect anticoagulant/delayed separation of serum)	Laboratory artefacts (incorrect anticoagulant/delayed separation of serum)
Systemic disease	Severe polycythaemia	Severe polycythaemia
	Septicaemia or endotoxic shock	Septicaemia or endotoxic shock
	Malnutrition	Ethanol/malnutrition

1.4.4 Treatment approaches

The elective curative treatment for both human and canine INS is surgery (Jonkers *et al.,* 2007; Polton *et al.,* 2007; Buishand *et al.,* 2010). Optimally, control of the insulin secretion is achieved preoperatively to stabilise the patient's status before surgery, and surgical resection of the primary and metastatic lesions should be attained whenever feasible to improve the survival time (Jordan and Carithers, 1980; Vaidakis *et al.,* 2010). Depending on its location, INS enucleation they might require partial or distal pancreatectomy or a pancreatic-duodenectomy (Vaidakis *et al.,* 2010; Goutal *et al.,* 2012). Medical treatment palliates clinical signs, and it is mostly indicated for the preoperative control of blood glucose levels and non-surgical candidates (Trifonidou *et al.,* 1998; Steiner *et al.,* 2011; Buishand *et al.,* 2013; Baudin *et al.,* 2014).

The management of canine INS is usually based on frequent small feedings at least every 4–8 hr and food should contain high levels of proteins, fats, and complex carbohydrates. Glucocorticoids are also commonly used in conjunction with diet and exercise modifications as they stimulate hepatic gluconeogenesis and interfere with the insulin receptors for glucose (Trifonidou *et al.,* 1998; Polton *et al.,* 2007; Goutal *et al.,* 2012). Adjuvant therapy with diazoxide is also commonly recommended. Diazoxide promotes glycogenolysis and hepatic gluconeogenesis, and it effectively reduces hypoglycaemia directly suppressing insulin production by pancreatic beta-cells (Trifonidou, *et al.,* 1998; Polton *et al.,* 2007; Goutal *et al.,* 2012).

Chemotherapy does not represent the elective treatment in canine INS (Trifonidou *et al.,* 1998; Polton *et al.,* 2007; Goutal *et al.,* 2012). Previous studies reported that streptozocin (STZ) can be safely used to manage canine INS. Nonetheless, serious adverse effects such as diabetes mellitus were seen in 50% of the patients, resulting in euthanasia or death of the patients (Northrup *et al.,* 2013). Additionally, STZ is a known nephrotoxin and fatal nephrotoxicity has been reported in dogs due to necrosis of renal tubular epithelium (Bailey and Page, 2007; Northrup *et al.,* 2013).

Whereas, in humans, STZ, as a beta-cell-specific chemotherapeutic, represents the standard antitumor therapy for patients with metastatic or non-resectable INS. Toxicity is dose-related and cumulative (Vaidakis *et al.* 2010; Mathur *et al.* 2012).

Alternatively, combinations with 5-FU or doxorubicin are commonly used (Vaidakis *et al.,* 2010; Baudin *et al.,* 2014). In humans, adjuvant medical treatment to control hormone hypersecretion and clinical signs of INS includes somatostatin analogue such as octreotide. By inhibiting the production of insulin and growth hormone, octreotide has been shown to control hypoglycaemia efficiently in 35% to 50% of patients. Unfortunately, the decrease of insulin concentration is transient, and long-term therapy usually results as ineffective (Mathur *et al.,* 2012; Baudin *et al.,* 2014; Giuroiu and Reidy-Lagunes, 2015).

Additionally, in humans, continuous glucose monitoring and oral glucose intake after hypoglycaemia are considered an effective alternative to octreotide therapy to reduce hypoglycaemic episodes before they develop neuroglycopenic symptoms (Okabayashi *et al.,* 2013).

1.4.5 Prognosis

Prognosis for human and canine patients with benign INS is very favourable. They are anticipated to live a normal lifespan after a successful surgical resection. Conversely, regardless of the miscellaneous therapeutic modalities for patients with malignant metastatic INS prognosis is still poor (Anlauf *et al.,* 2009; Buishand *et al.,* 2014).

In dogs, at the time of diagnosis, metastases are usually present (Polton *et al.,* 2007; Buishand *et al.,* 2010). Due to the presence of (micro)metastases in lymph nodes and liver undetectable at the time of surgery patients diagnosed with malignant INS often show recrudescence of clinical signs (Trifonidou *et al.,* 1998; Buishand *et al.,* 2010; Wouters *et al.,* 2011; Buishand *et al.,* 2012; Goutal *et al.,* 2012). In dogs, the median survival time is 6-14 months after surgery, and the major cause of death is the recrudescence of clinical signs. When surgery is not performed the survival time is approximately of 2-3 months (Trifonidou *et al.,* 1998; Lurye and Behrend, 2001; Polton *et al.,* 2007).

Human INS are often curable by surgery as metastases are present in just 10% of all the cases (Jonkers *et al.,* 2007; Corroller *et al.,* 2008; Callacondo *et al.,* 2013). However, for patients diagnosed with malignant INS, the prognosis is highly variable

and often poor (30-60% overall survival) (Borson-Chazot *et al.*, 2013; Rossi *et al.*, 2014; Giuroiu and Reidy-Lagunes, 2015). As a treatment strategy, surgery on its own is not effective whereas aggressive multimodal therapy with a combination of chemotherapy and somatostatin analogues reported overall and symptom-free survival at five years of 71 and 24%, respectively (Corroller *et al.*, 2008).

1.5 Molecular pathogenesis and targeted therapy of insulinoma

In recent years, substantial progress has been made in the diagnosis and treatment of PNETs, especially in the pathogenesis and targeted therapy. Preclinical and clinical studies on the molecular biology of PNETs indicate unique PNET signalling events that are different from those in pancreatic ductal adenocarcinomas (Zhan *et al.*, 2012; Zhang *et al.*, 2013; Yu, 2016). Genetic syndromes account for 15–20% of PNETs, but the remaining 80–85% of PNETs are considered sporadic. Previous studies have shown that a set of somatic mutations in a number of genes involved in the mammalian target of rapamycin (mTOR) pathway, and, to a lesser extent, TP53 might be involved in sporadic PNET carcinogenesis (Crabtree *et al.* 2016). Using human PNET cell lines available including BON1, derived from a metastatic human carcinoid tumour of the pancreas (Lopez *et al.*, 2010), and CM, a cell line obtained from peritoneal ascites of a patient affected by a primary pancreatic INS (Gragnoli, 2008), some of the mechanisms involved in sporadic PNET carcinogenesis have been elucidated (Höpfner *et al.*, 2003; Buishand *et al.*, 2016). Various tyrosine kinase receptors were overexpressed in PNET cell lines and tumours; since then a number of inhibitors of growth factor cascades have been developed (Fazio *et al.*, 2010; Ito *et al.*, 2012; Ro *et al.*, 2013; Zhang *et al.*, 2013; Rossi *et al.*, 2014).

1.5.1 Molecular pathogenesis

INS are the most frequently detected functioning PNETs. They clearly differ from other PNET subtypes with respect to their clinical behaviour and low MEN1 mutation frequency (Jonkers *et al.*, 2006; Jonkers *et al.*, 2007). For instance, in dogs, INS usually occur sporadically whereas in humans less than 10% of the cases are related with MEN1 syndrome (Pelengaris and Khan, 2001; Fontanière *et al.*, 2006; Zhang *et al.*, 2013). MEN1 inactivation by mutation plays a minor role in human sporadic INS (Dotzenrath *et al.*, 2000). In dogs, mutations of MEN1 are not involved in the development of malignant INS (Goutal *et al.*, 2012).

One of the central signalling pathways involved in tumourigenesis of sporadic INS is the phosphatidyl-inositol-3 kinase (PI3K)/AKT/mTOR sequence, which is frequently over-activated in PNETs. In brief, PI3K-encoded by the PI3KCA gene is activated by different receptor tyrosine kinases such as insulin growth factor receptor (IGFR) and epidermal growth factor receptor (EGFR) and in turn activates AKT which leads to activation of mTORC1/p70S6K, cell proliferation and tumour growth (Figure 1.5) (Nölting *et al.*, 2017).

One of the growth factor receptors that seems to trigger the PI3K/Akt pathway is the IGF-R. Insulin-like growth factor (IGF) 1 and 2 binds to IGF-R type 1 or 2, respectively, and have been indicated to play a role in INS (Figure 1.5). In humans, IGF1 and IGF-1R were expressed in 70% (7/10) and 90% (9/10) of INS (Jonkers, *et l.*, 2007). Of interest, previous studies in canine INS showed an expression of IGF-1 in 90% (9/10) of primary INS (Buishand *et al.*, 2012). Moreover, Buishand *et al.* (2012) showed a higher expression of IGF-1 in canine INS metastases compared to primary lesions suggesting a role of IGF-1 in the growth advantage of metastases over primary canine INS (Buishand *et al.*, 2012). Increased expression of IGF-1 was also significantly correlated to higher expression of GH mRNA in canine INS metastases, suggesting the existence of a functional autocrine or paracrine GH/IGF-1 axis in metastasised INS cells related to metastatic spread of canine INS (Buishand *et al.*, 2012).

Cell cycle deregulation is one of the defining features of cancer (Zhan *et al.*, 2012; Zhang *et al.*, 2013). Cyclin-dependent kinase 4 (CDK4), together with its regulatory subunit cyclin D, governs cell cycle progression through the G1 phase. In particular, deregulation of the cyclin D/CDK4 complex has been observed in a variety of human cancers (Zhang *et al.*, 2013). Cyclin D1 was shown to be overexpressed in 36% of INS, when compared to normal pancreatic islets, suggesting that this oncogene is involved in the tumourigenesis of at least a subgroup of sporadic INS (Jonkers *et al.*, 2007). In INS, mTOR upregulates cyclin D1/ CDK4 showing an important role in cell proliferation and cell growth during tumorigenesis (Figure 1.5) (Fazio *et al.*, 2010; Zhan *et al.*, 2012). mTOR is a ubiquitous, highly conserved serine/threonine kinase that regulates cell survival, proliferation, and motility. In humans, previous data showed that mTOR and its downstream protein P70S6K were activated in 58%

(24/41) and 75% (31/41) of INS tissues, at a much higher level than in the islet tissues (Zhan *et al.*, 2012). The Akt1 gene has also been described to induce β-cell proliferation in a CDK4 dependent manner by increasing cyclin D1 and cyclin D2 levels (Figure 1.5) (Fatrai *et al.*, 2006). AKT, also known as protein kinase B, plays a key role in many cellular processes such as apoptosis, cell migration, and proliferation, as well as glucose metabolism. Its upregulation has been documented in multiple cancer types, including NETs (Ghayouri *et al.*, 2010; Fatrai *et al.*, 2006). In fact, previous studies showed that 61% to 76% of gastroenteropancreatic NETs have increased AKT activity (Ghayouri *et al.*, 2010). In PNET cell lines, inhibition of AKT signalling resulted in inhibition of PNET proliferation and a reduction in NET marker expression such as chromogranin A. *In* vivo, transgenic mice models overexpressing active Akt1, exhibited a striking increase in β-cell mass, proliferation, cell size, and malignant tumour formation thus providing evidence for the role of this kinase in islet physiology (Fatrai *et al.*, 2006).

PTEN (phosphatase with tensin homology) is a potent negative regulator of the PI3K/Akt signalling pathway (Figure 1.5). Previous *in vivo* studies have suggested that PTEN plays an integrative role in regulating growth and metabolism in normal pancreatic islets. PI3K activation and PTEN downregulation have been found in most PNETs (Krausch *et al.*, 2011). Microarray expression profiling of PNETs showed downregulation of PTEN in the majority of primary PNETs (Krausch *et al.*, 2011). Interestingly, loss of PTEN was associated with poorer disease-free time and overall survival in malignant human INS (Jonkers *et al.*, 2007).

Furthermore, immunohistochemical studies in benign and malignant INS suggested that activation of the proto-oncogenes, c-Myc and Ras, and overexpression of transforming growth factor (TGF-alfa), p53 tumour suppressor and anti-apoptotic Bcl-2 protein orchestrated the cell death/tumour growth and thus the malignant progression of human INS (Pelengaris and Khan, 2001).

Activation of Myc appears as an early event, being present at both the hyperplastic stage and in benign and malignant INS; whereas, Ras, TGF-alfa, and p53 proteins are undetectable in normal islets, but weak immunostaining is detected in benign INS, becoming strongly positive in malignant INS (Pelengaris and Khan, 2001). TGFα has previously been described to be associated with the development of INS. TGFα

secreted by tumour cells can bind to EGFR, leading to an autocrine activation of the Ras signalling pathway and, putatively, to its oncogenic activity (Figure 1.5) (Jonkers *et al.,* 2007).

The ability of tumour cell populations to expand is not only determined by the rate of cell proliferation but also by the rate of cell death. Acquired resistance toward programmed cell death (apoptosis) is a hallmark of most types of cancer including INS (Hager and Hanahan, 1999; Pelengaris and Khan, 2001). c-Myc often acts as an inducer of both cell proliferation and apoptosis *in vitro*. It has been previously demonstrated that the net balance of Myc-induced growth and death may be dictated by the presence of survival signals (Phesse *et al.,* 2014). In INS, for instance, the observed oncogenic synergy between Myc and Bcl-2 is fundamental during malignant progression as it induces beta-cell growth and decrease of apoptosis (Pelengaris and Khan, 2001). Bcl-2 blocks apoptosis without affecting cell proliferation and its expression leads to indolent tumour growth (Figure 1.5). An increased expression of the Bcl-2 protein in comparison with normal pancreatic tissue has been reported in one-third of human INS, suggesting that suppression of apoptosis may contribute to the initiation, progression, or both, of these tumours (Pelengaris and Khan, 2001). Survivin, a member of another family of apoptosis inhibitors, is usually upregulated in response to increased expression of Bcl-2 (Figure 1.5). Survivin acts as a bifunctional protein suppressing apoptosis and regulating cell division during INS tumourigenesis (Jonkers *et al.,* 2007). As a consequence of an increase in proliferation and a decrease in cell death the islets become significantly enlarged (Jonkers *et al.,* 2007).

Modulation of apoptosis is one of the biological activities of the p53 protein. Wild-type p53 is involved in the mediation of c-Myc induced apoptosis. When the wildtype *TP53* gene is inactivated (predominantly by deletion), the negative growth regulatory functions of p53 are abrogated. The *TP53* is mutated in more than 50% of all human neoplasms. Immunohistochemical detection of p53 is associated with the presence of a *TP53* mutation in most cases (Pelengaris and Khan, 2001; Subramanian *et al.,* 2005; Zlobec *et al.,* 2006). Controversy exists with respect to the p53 status in INS (Jonkers *et al.*2006). A decrease in p53-dependent beta-cell death might result from inactivating mutations leading to increased stability of the p53

protein, although previous studies have shown that mutation of p53 is exceedingly rare in INS (Jonkers *et al.*, 2006; Jonkers *et al.*, 2007). The role of p53 in INS carcinogenesis still remains to be elucidated. It has been previously shown a direct correlation between gene expression of p53 and c-Myc in tumorigenesis of pancreatic islets. For instance, overexpression of c-Myc in pancreatic islets alone does not induce tumorigenesis unless apoptosis is blocked, for example, by p53 loss, Bcl-2 overexpression (Phesse *et al.*, 2014).

It is possible that mutations of the check-point genes such as PTEN in PI3K/mTOR signaling and p53 contribute to constant cell progression, leading to overgrowth/hypertrophy that is escaped from the controls mediated by environmental cues such as nutrients/glucose levels and DNA damage (Zhang *et al.*, 2013).

In summary, several proteins, including Akt1, IGF-1, mTOR have been suggested to stimulate cell proliferation in INS. However, because of the overall low proliferation rate in INS, it is tempting to speculate that instead of increased proliferation, evasion of apoptosis is an important mechanism in INS progression (Figure 1.5). This can occur by activation of anti-apoptotic proteins, such as Bcl-2, or by inactivation of pro-apoptotic proteins, such as p53, although their roles in INS tumorigenesis remain elusive.

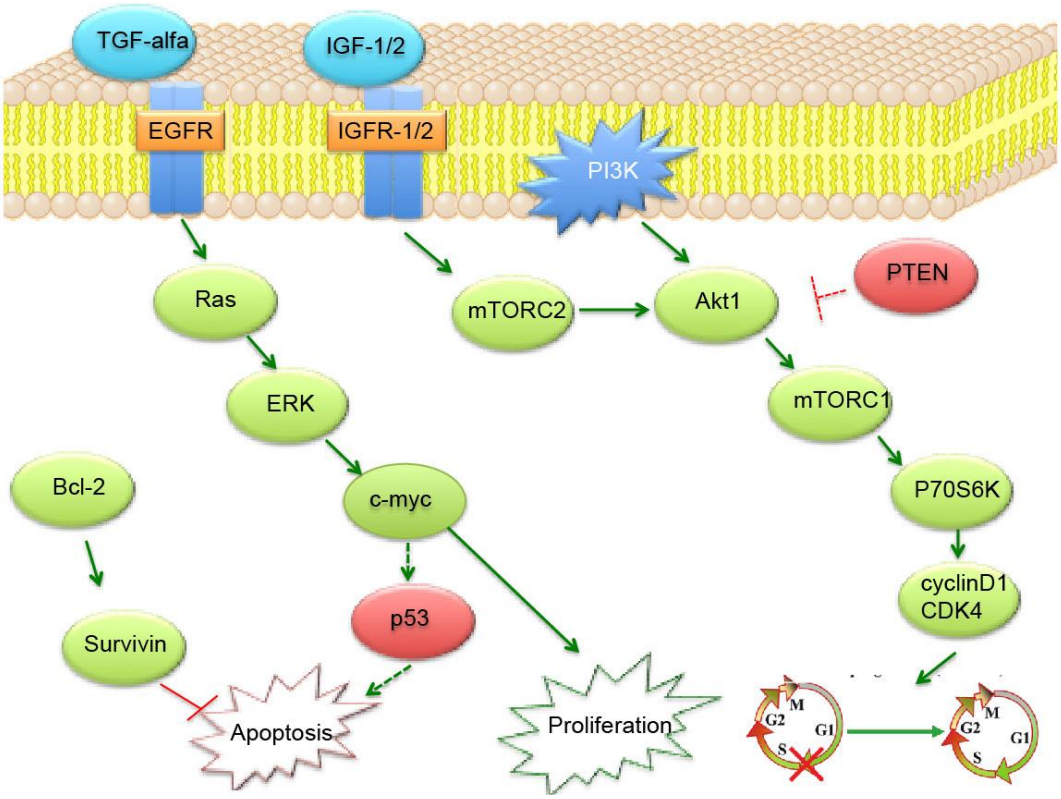

Figure 1.5 Schematic representation of the mechanisms of molecular pathogenesis of sporadic insulinoma (Pelengaris & Khan 2001; Jonkers et al., 2007; Zhan et al., 2012; Zhang et al., 2013. Green represents upregulated protein; red represents loss/mutated proteins. Solid line= active. Dotted line=inactive.

1.5.2 Targeted therapy

In humans, targeted therapy against multiple steps in the IGF-R1–activated PI3K/Akt/mTOR pathway has been developed for the treatment of PNETs including INS (Fazio *et al.*, 2010; Bernard *et al.*, 2013; Zhang *et al.*, 2013; Baudin *et al.*, 2014; Giuroiu and Reidy-Lagunes, 2015; Nölting *et al.*, 2017). In 2011, randomized phase III studies in PNETs led to clinical approval of two new agents for the treatment of progressive or metastatic PNETs, the multitargeted tyrosine kinase inhibitor sunitinib and the mTOR inhibitor everolimus (Ito *et al.*, 2012; Ro *et al.*, 2013; Reid *et al.*, 2014; Rossi *et al.*, 2014).

Everolimus (RAD001) is an orally active mTOR inhibitor that has been shown to have anti-growth effects in a number of studies involving PNETs (Figure 1.6) (Fazio *et al.*, 2010; Ito *et al.*, 2012; Stevenson *et al.*, 2013). In phase III clinical trials, overall survival in everolimus-treated patients (11 months) was longer than control patients (4.6 months). Successful control of PNET progression in everolimus-treated patients supports the notion that mTOR signalling plays a critical role in PNET tumourigenesis (Ito *et al.*, 2012; Zhang *et al.*, 2013) (Figure 1.6). As the activation of the PI3K/AKT/MTOR pathway is essential for inhibiting hepatic gluconeogenesis by insulin, hyperglycaemia is a frequent side effect of everolimus therapy, and this finding makes the drug appealing to manage INS (Figure 1.6) (Bernard *et al.*, 2013; Baratelli *et al.*, 2014; Baudin *et al.*, 2014). In INS, it has been shown that everolimus controlled the glucose level in spite of the high insulin level and disease progression (Baratelli *et al.*, 2014). Previous studies in patients diagnosed with metastatic INS recorded a median time to the first recurrence of symptomatic hypoglycaemia of 6.5 months (Bernard *et al.*, 2013; Baratelli *et al.*, 2014). However, drugs-related adverse effects have been reported mainly related to hyperglycaemia probably due to a decrease of insulin or everolimus-induced peripheral insulin resistance (De Herder *et al.*, 2011).

Due to the high vascularisation of PNETs trials of targeted therapy have been developed against pro-angiogenic molecules. Sunitinib malate is a multitargeted protein tyrosine kinase inhibitor that targets vascular endothelial growth factor (VEGF) receptors 2 and 3, platelet-derived growth factor receptors (PDGFRs) α and

β, and stem-cell factor receptor (c-kit) (Figure 1.6). Numerous *in vitro* and *in vivo* studies, as well as randomised phase III study, have demonstrated that sunitinib has anti-growth activity in PNETs, including INS (Figure 1.6) (Ito *et al.*, 2012; Bernard *et al.*, 2013; Baudin *et al.*, 2014; Giuroiu and Reidy-Lagunes, 2015). In 2011, the FDA approved sunitinib for the treatment of progressive, well-differentiated PNETs in patients with unresectable locally advanced or metastatic tumours (Ito *et al.*, 2012; Giuroiu and Reidy-Lagunes, 2015). Previous studies showed that sunitinib caused tumour shrinkage and prolonged progression-free survival from 5.5 to 11.4 months in patients with advanced PNETs. The success of this trial provided evidence that targeting distinctive tumour-related signalling pathways could improve clinical outcomes and should be the future approach to the development of therapeutic interventions for PNET. These include the possibility of overcoming resistance to the mTOR inhibitors that frequently emerges over time with continued treatment, in part due to the up-regulation of AKT via the IGF-1R/PI3K pathway (Ito *et al.*, 2012).

Although progression-free survival improved, objective response rates for everolimus and sunitinib in the treatment of advanced PNETs are less than 10% (Zhang *et al.*, 2013). Both sunitinib and everolimus have a potent effect on inhibition of angiogenesis, which may cause adaptive resistance, a phenomenon where cancer cells initially sensitive to the therapy, developed resistance mechanisms (Ito *et al.*, 2012; Zhang *et al.*, 2013; Reid *et al.*, 2014; Rossi *et al.*, 2014; Giuroiu and Reidy-Lagunes, 2015). Several preclinical studies have demonstrated that tumours develop adaptive resistance to antiangiogenic treatment. An increasing body of evidence also suggests that antiangiogenic agents alter the biology and the natural progression of tumours in an unfavourable manner increasing tumour invasion and metastatic behaviour (Zhang *et al.*, 2013).

Targeting angiogenesis and the PI3K/mTOR signal transduction delays progression-free and overall survival; however, no curative treatment has been yet designed for different subtypes of PNETs. In the future, thanks to an increased understanding of the molecular pathogenesis of PNETs, treatment approaches could be planned based on the different behaviour of these tumours (Ro *et al.*, 2013; Zhang *et al.*, 2013; Reid *et al.*, 2014).

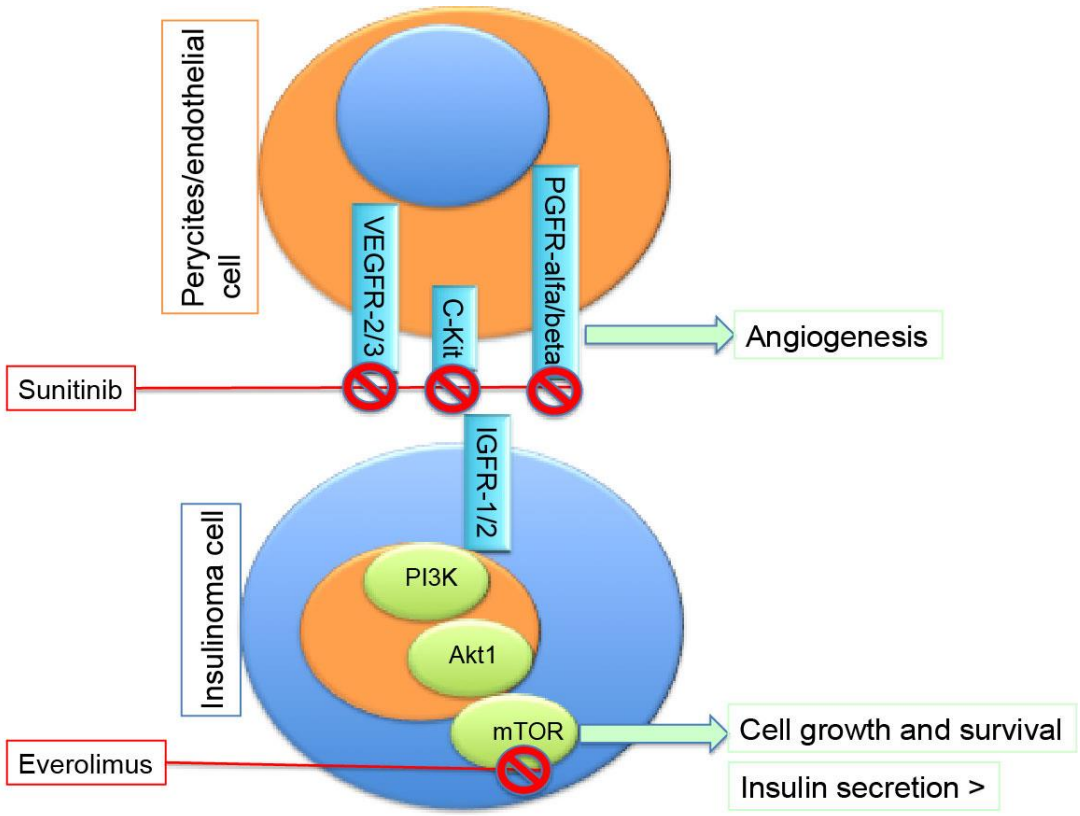

Figure 1.6 Small molecules inhibitors available for targeted therapy of insulinoma and their mechanisms of action: everolimus and sunitinib. VEGFR, vascular endothelial growth factor receptor; PDGRF, platelet-derived growth factor receptor; cKIT, stem-cell growth factor receptor; IGF-I R, insulin-like growth factor-1 receptor; sst, somatostatin receptor subtype; PI3K, phosphatidylinositol 3-kinase; mTOR, mammalian target of rapamycin (Adapted from Herder et al., 2011).

1.6 Cancer stem cells: future opportunities for the treatment of canine and human insulinoma

1.6.1 Origins of the cancer stem cell theory

The current treatment approaches to different cancer types are often designed based on the pathologic characterisation of the entire tumour. Unfortunately, currently available drugs often have only transient effects on the neoplasms resulting in recurrent and more malignant disease (Dean *et al.*, 2005; Wang *et al.*, 2011; Pang *et al.*, 2012; Franco *et al.*, 2016; Lu *et al.*, 2016). One reason for the failure of these treatments is the acquisition of drug resistance by the cancer cells as they evolve; another possibility is that existing therapies fail by selecting a more malignant subpopulation of cancer cells that are responsible for the tumour relapse (Reya *et al.* 2001; Dean *et al.* 2005; Guo *et al.* 2006; Alison *et al.* 2011; Rybicka *et al.* 2016). Therefore, we now understand that studying the molecular genetics of tumours can give a better view of the complexity of this disease. During the last few years, cancer research has been focused on the presence of malignant tumours of a rare population of cancer cells that are capable of regenerating new tumours *in vivo* with the same heterogeneity as primary ones (Guo *et al.*, 2006; Blacking *et al.*, 2007; Pang *et al.*, 2011, 2012; Pattabimaran *et al.*, 2014; Franco *et al.*, 2016). This type of cell has been identified as cancer stem cells (CSCs) (Mitra *et al.*, 2015). According to the CSC model, minimal residual disease and tumour recurrence would result from persistence of the therapy-resistant CSC fraction after treatment (Guo *et al.*, 2006; Reya *et al.*, 2001; Medema, 2013)(Figure 1.7).

The cellular hierarchy of CSCs was first identified in hematopoietic malignancies (Franco *et al.*, 2016). Post-therapeutic residual tumour cells were first isolated using specific stem cell surface markers in acute myeloid leukaemia and correlated with poor progression-free survival (Zhao, 2017). Then, CSCs were isolated from solid tumors of many cancer types including lung (Mao *et al.*, 2014), colon (Paschall *et al.*, 2016), brain (Zhu *et al.*, 2011), head and neck (Zhao *et al.*, 2016), and pancreatic cancers (Sakai *et al.*, 2017). Additionally, several research groups have isolated CSCs from a range of canine solid tumours, including osteosarcoma (Wilson *et al.*,

2008), squamous cell carcinoma (Pang *et al.* 2012), mammary carcinoma (Pang *et al.*, 2011; Rybicka *et al.*, 2016) and glioma (Stoica *et al.*, 2009; Pang *et al.*, 2017).

CSCs are clonogenic *in vitro* and *in vivo*. They typically represent only a small proportion of the tumour population (1%–5%), although some malignancies such as breast cancer (11%–35%) and glioblastoma (5%–30%) possess a larger population (Gaur *et al.*, 2011). CSCs undergo asymmetric and symmetric division resulting in both expansions of the stem cell pool and the production of morphologically and functionally distinct differentiated daughter cells (Medema, 2013). CSCs possess unrestrained proliferative abilities, resistance to apoptotic cues, and aptitude to establish tumours in immunodeficient mice (Franco *et al.*, 2016). They have an increased efficiency of DNA repair, changes in cell cycle parameters, and overexpression of anti-apoptotic proteins and/or drug transporters. These different pathways protect them from traditional chemotherapy and can contribute to minimal residual disease and cancer relapse (Zahreddine *et al.*, 2013).

There are two different theories regarding the origin of CSCs: (i) the "hierarchy model" states that only a subset of cancer cells have a tumour-initiating property and they derive from mutated adult stem cells; (ii) "the stochastic model" suggests that any differentiated cell can undergo a partial de-differentiation process, mainly through epithelial to mesenchymal transition (EMT) to obtain a CSC phenotype (Fendrich *et al.*, 2012; Mitra *et al.*, 2015) (Figure 1.8).

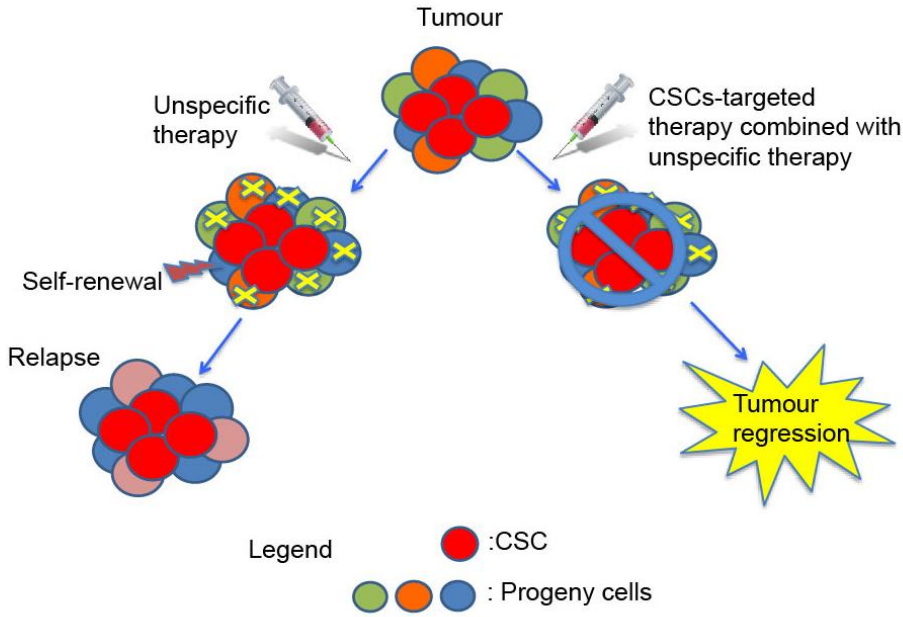

Figure 1.7 Diagram represents the cancer stem cell (CSC) model. CSCs represent a subset of the cancer cell population with self-renewal capability. Conventional chemotherapy selects for this population frequently causing tumour relapse. For this reason, a more CSC-targeted approach is necessary to have a proper tumour regression (adapted from Franco et al., 2016).

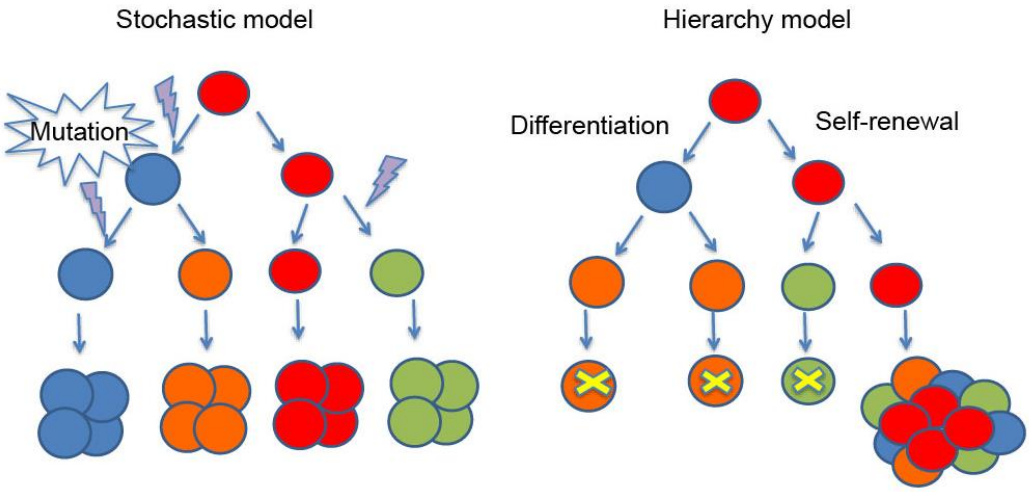

Figure 1.8 Diagram represents different cancer stem cell (CSC) model. Two CSC models have been postulated. The stochastic model states that all cells within the tumour can potentially have tumour-initiating properties. The hierarchy model states that only CSCs are tumourigenic (adapted from Chandler et al., 2010).

1.6.2 Isolation and enrichment of CSC

The identification of CSCs will likely be crucial for diagnosis and therapy, especially for future therapies targeting CSCs (Wang *et al.*, 2011; Borah *et al.*, 2015; Franco *et al.*, 2016; Lu *et al.*, 2016). Although identification of CSCs is a complicated process and it relies on different strategies, methods to isolate and identify CSCs have been developed in the last ten years using their characteristics to self-renew and to remain quiescent (Reya *et al.*, 2001; Dean *et al.*, 2005). According to the more recent literature, many approaches can be used to reach the CSC population *in vitro*. CSCs can be mainly isolated from cancer cell lines or primary tumours using methods based on the expression of specific surface markers or an intracellular enzyme activity and then assessed by specific anchorage-independent growth conditions (tumour sphere assays) and/or by their ability to initiate new tumour growth when xenotransplanted into immunocompromised mice (Yanagihara *et al.*, 2004; Fan *et al.*, 2006; Kreso *et al.*, 2014). Because tumour initiation is one of the defining features of CSCs, xenografting is considered the gold standard to isolate CSCs. In addition to the gold standard *in vivo* assay, CSCs have been isolated using specific stem cell surface markers (Wilson *et al.*, 2008; Pang *et al.*, 2012; Hou *et al.*, 2014; Mao *et al.*, 2014; Liu *et al.*, 2017). For instance, recent studies in pancreatic adenocarcinoma and glioblastoma have identified CD133 as a marker for CSCs (Fan *et al.*, 2010; Zhu *et al.*, 2011). Kreso *et al.* (2014) demonstrated that in pancreatic cancer three different stem cell markers represent CSC population: CD44, CD24 and CD133 (Kreso *et al.* 2014). Rybicka *et al.* (2016) showed that in canine mammary tumours enriched $CD44^{+}CD24^{-}$ cells are highly tumourigenic and associated with poor prognosis (Rybicka *et al.*, 2015). Still, depending on the cancer type the tumour stem cell markers may vary within human (Figure 1.9 A) and canine cancer (Figure 1.9 B) (Wilson *et al.*, 2008; Magee *et al.*, 2012; Hou *et al.*, 2014; Franco *et al.*, 2016).

Moreover, some proteins highly expressed in embryonic stem cells, like NANOG, OCT4, SOX9 and SOX2, are frequently present in poorly differentiated tumours with an adverse clinical outcome (Seymour *et al.*, 2007; Wilson *et al.*, 2008; Franco

et al., 2016). Therefore, expression of these embryonic stem cell markers is used to identify and select putative populations of CSCs (Wilson *et al.*, 2008; Pang *et al.*, 2011). Considering the heterogeneity of CSCs within cancer cell population, coupling the isolating/enriching methods together with xenografting techniques in immunodeficient mice is seen, so far, as the best way to analyse the complexity of CSCs (Yang *et al.*, 2007; Krampitz *et al.*, 2016).

A

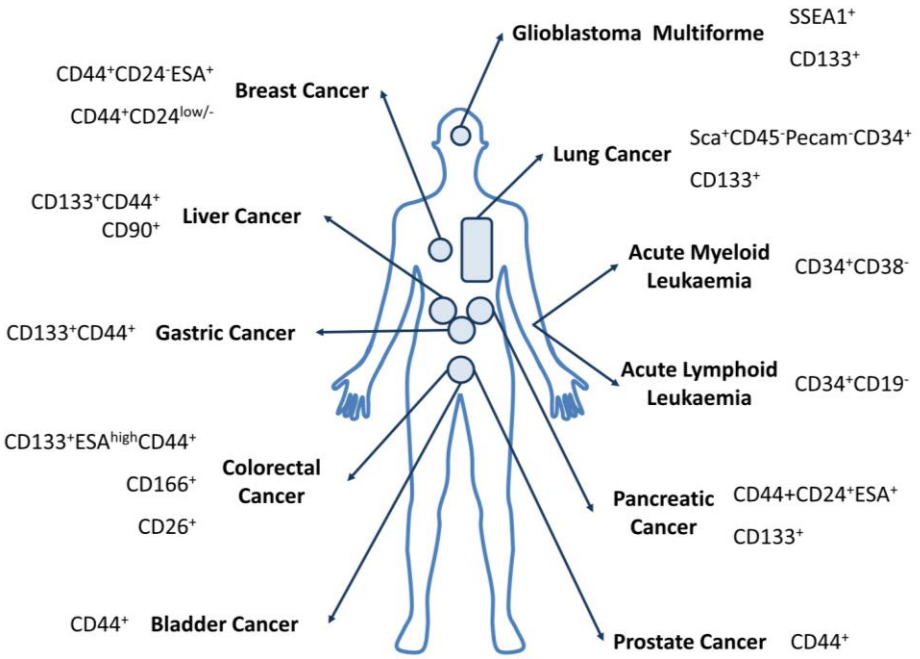

B

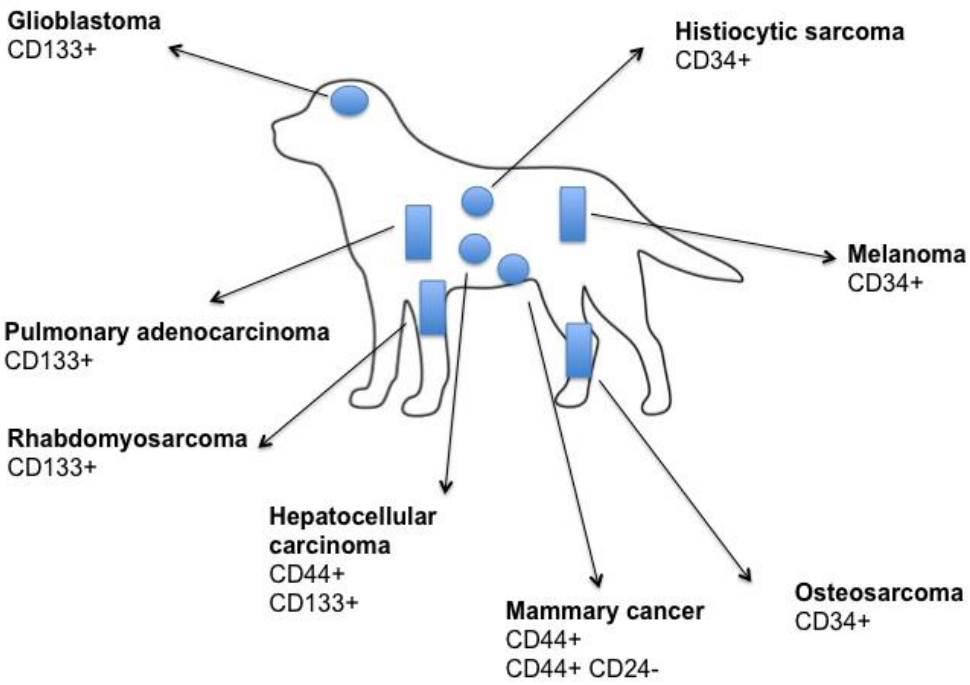

Figure 1.9 Diagram showing stem cell surface markers commonly associated with different tumour types in human (A) and canine (B) cancers (Stoica et al. 2009; Magee et

al. 2012; Pang et al., 2014; Pattabimaran et al., 2014; Franco et al. 2016; Rybicka et al., 2016; Itoh et al., 2017; Kishimoto et al., 2017; Sakai et al., 2017)

1.6.3 CSC-targeted therapy

The future of cancer therapy is projected to eliminate the pool of cancer cells that are intrinsically resistant to conventional therapies, the CSC, while a concomitantly administered traditional agent would reduce the non-CSCs, which are known to be susceptible to existing cytotoxic therapies (Blacking *et al.*, 2007; Borah *et al.*, 2015). Given the apparent close connection between stem cells and the CSC state, various signalling pathways involved in the development and the maintenance of stem cells have been studied for their role in solid organ malignancies Since then, novel targeted therapies against multiple self-renewal pathways have been tested in a variety of tumours (Table 1.7 Small molecule inhibitors in clinical trials (Pannuti et al., 2011; Schott et al., 2013; Richter et al., 2014; Abetov et al., 2015; Borah et al., 2015; Ran et al., 2017) (Wang, 2011; Borah *et al.*, 2015; Buishand *et al.*, 2016; Krampitz *et al.*, 2016; Lu *et al.*, 2016). For instance, LGK974, a Wnt inhibitor against Porcupine (an enzyme involved in the post-translational maturation of Wnt proteins) has shown effective results in patients with advanced melanoma, breast cancer, and pancreatic cancer in Phase I of clinical trials (Borah *et al.*, 2015; Takebe *et al.*, 2015). Wnt signalling is known to be fundamental for the balance of normal stem cells and also for the induction of the CSC state (Abetov *et al.*, 2015; Takebe *et al.*, 2015).

Several small molecules inhibitors against various nodes of the Hedgehog (Hh) and Notch pathways also came into prominence for their ability to target CSCs (Rizzo *et al.*, 2008; Ng & Curran, 2013). The first approved inhibitor of the Hh signalling pathway was cyclopamine. Unfortunately, due to limited oral bioavailability, low potency, rapid clearance, non-specific toxicity and chemical instability, novel inhibitors were developed and tested in clinical trials alone or in combination with chemotherapy (Ng & Curran, 2013; Borah *et al.*, 2015; Takebe *et al.*, 2015). IPI926, a derivative of cyclopamine, was recently tested in clinical trials for metastatic pancreatic cancer, in combination with 5-FU showing an increase of the cytotoxic action of 5-FU on the the tumour lesions (Ko, 2017). The first clinically approved

antagonist of Hh was vismodegib for the treatment of metastatic basal cell carcinomas (Pattabimaran and Weinberg, 2014; Takebe *et al.*, 2015). Vismodegib monotherapy has been explored also for the treatment of glioblastoma showing a significant decrease of tumour-derived CD133+ cells to form neurospheres (Sloan *et al.*, 2014). Unfortunately, resistance against currently used Hh signalling inhibitors has already been observed in basal cell carcinoma patients (Gonnissen *et al.*, 2015). Several more small molecules against Hh have been clinically tested such as, inhibitors of Gli transcription factor GANT-61 and arsenic trioxide (Ng & Curran, 2013; Franco *et al.*, 2016).

To block the Notch pathway small molecules inhibitors against the gamma-secretase have been developed. One of the most potent gamma-secretase inhibitors (GSIs) in clinical development is MK-0752. MK-0752 has shown to inhibit Notch signalling in human T-ALL and breast cancer (Brennan and Clarke, 2013; Schoot *et al.*, 2013). In Phase I clinical trial patients with advanced breast cancer a combination of MK-0752 and docetaxel showed a significant decrease of the tumour-derived CD44+/CD24- populations (Schoot *et al.*, 2013). Another GSIs previously tested in clinical trials is RO4929097. RO4929097 has been successfully used in combination with gemcitabine to treat patients in advanced stages of different type of solid tumours showing partial response in nasopharyngeal cancer and stable disease (>4 months) in pancreas, tracheal, and breast primary cancers (Richter *et al.*, 2014). However, recent studies have shown a high variability in the mechanisms and functional effects of the several GSIs in clinical development providing an important framework to evaluate results from ongoing and completed human trials with these compounds (Ran *et al.*, 2017).

Given the crosstalk between the different embryonic developmental signalling pathways, combinations of agents have been used in clinical trials to inhibit possible compensatory escape mechanisms of CSCs (Pannuti *et al.*, 2011; Richter *et al.*, 2014; Takebe *et al.*, 2015). For instance, phase I and phase Ib/II trials combining vismodegib to target the HH pathway and the GSI RO4929097 to inhibit Notch signalling were conducted in patients with breast cancer and sarcoma (Takebe *et al.*, 2015).

Targeting CSC via modification of the Wnt, HH and Notch embryonic signalling pathways holds the promise of preventing disease relapses. However, developing such agents is fraught with challenges. These inhibitors may either block the formation of new CSCs or also block mechanisms used by existing CSCs to maintain their quiescent state (Franco *et al.*, 2016). Still, considering the similarities within CSCs and stem cells the question that remains unanswered is whether these agents will in fact target more efficiently neoplastic CSCs than the normal stem cells. The main issues in the development of agents targeting CSCs include: choice of the most appropriate inhibitor for each patient; identification of biomarkers for pathway inhibition; selection of mechanism-based combination regimens; and patient stratification according to recognised efficacy biomarkers (Takebe *et al.*, 2015; Lu *et al.*, 2016; Ran *et al.*, 2017). In particular, more accurate preclinical models for testing CSC-targeted agents must be developed as the phenotype of tumour cells or CSCs is an output of the entire signalling network. Furthermore, molecular biomarkers that interrogate pathway activity and predict efficacy are fundamental for patient identification and stratification, and as biological correlatives of activity (Pannuti *et al.*, 2011).

In summary, the development of CSC-targeted therapy is still in its early stage, nonetheless, it holds promises to understand cell fate determination in tumours and target it therapeutically. Systems biology and personalised medicine will be essential to enable the design of a range of regimens in different subgroups of patients adapting treatment to clonal evolution within the tumour (Abetov *et al.*, 2015; Takebe *et al.*, 2015).

Table 1.7 Small molecule inhibitors in clinical trials (Pannuti et al., 2011; Schott et al., 2013; Richter et al., 2014; Abetov et al., 2015; Borah et al., 2015; Ran et al., 2017)

Stem signaling	Small molecule inhibitor	Tumours
Wnt	Phosphosulindac	Breast
Wnt	Salinomycin	Endometrial
Wnt	Acetaminophen	Breast
Wnt	Celecoxib	Colon
Wnt	Oximatrine	Breast
Wnt, hedgehog	Sulforaphane	Breast, pancreatic
Hedgehog	Cyclopamine	Glioblastoma
Hedgehog	Erismodegib	Prostate
Hedgehog	Vismodegib	Pancreatic, Glioblastoma
Hedgehog	GANT-61	Pancreatic
Notch	DAPT	Ovarian
Notch	MK-0752	Breast
Notch	Retinoic acid	Brain
Notch	RO4929097	Melanoma, pancreatic, breast, nasopharyngeal, tracheal

1.6.4 CSC: limitations, controversies and future aims

Despite extensive studies, there has been a long-lasting debate on the existence of CSCs and their roles in patients. The tumour environment is very heterogeneous, and the involvement of CSCs in tumour progression results from a plethora of stimuli (Reya *et al.*, 2001; Franco *et al.*, 2016). In the context of the CSC model, it has been recognised lately that extensive cellular variability exists within what was thought to be a uniform CSC population. This finding has substantial implications for therapeutic targeting as recent evidence has shown that CSCs are not static entities but can evolve over tumour development (Magee *et al.*, 2012; Hou *et al.*, 2014;

Kreso *et al.*, 2014; Pattabimaran *et al.*, 2014). As a result, more conservative terms (instead of CSC) have been used to name this population of cells such as, tumour-initiating cells, tumour-propagating cells, tumour-progenitor cells or tumour stem-like cells (Zhao, 2017). Nowadays, it is clear that tumours develop in a dynamic environment where many factors are involved. Mainly, when tumours progress and a number of mutations rise, more cells can acquire self-renewal capability and CSC properties. In this model, as cancers progress, tumour hierarchies become shallower, and it becomes difficult to divide the CSCs from the non-CSCs (Kreso *et al.*, 2014). For these reasons, it becomes difficult to evaluate which assay would be reliable to test this phenotypic and genetic tumour heterogeneity (Magee *et al.*, 2012; Kreso *et al.*, 2014).

Various hypotheses arose regarding the origins of CSCs including the malignant transformation of normal stem cells, mature cancer cell de-differentiation through EMT or induced pluripotent cancer cells (Zhao, 2017). Recent studies have suggested that the differentiation of CSCs into non-tumourigenic cells may be reversible (Chaffer *et al.*, 2011; Gupta *et al.*, 2017). As said previously, cells that undergo EMT can acquire the properties of CSCs. Mani *et al.*, (2008) showed that human mammary cancer epithelial cells after sustained expression of the transcription factors Snail or Twist, silencing of E-cadherin, or exposure to TGF-beta, acquire a $CD44^{+}CD24^{-}$ phenotype, as breast CSCs (Mani *et al.*, 2008).

According to these findings, it is not clear whether the CSC model would effectively describe the complexity of cancers. A tumour is not a static environment and for this reason elimination of the CSCs on its own may not suffice to induce an acceptable, durable clinical response, since new CSCs may be generated in CSC-depleted tumours via the spontaneous dedifferentiation of non-CSCs (Blacking *et al.*, 2007; Magee *et al.*, 2012). At the moment, a model that resembles this tumour heterogeneity does not exist as it becomes evident that xenograft models cannot faithfully reproduce the response of the patient to the drug targeted therapy (Kreso *et al.*, 2014). Furthermore, the CSC markers used so far have shown many difficulties in isolating CSCs in a number of solid cancers (Guo *et al.*, 2006; Blacking *et al.*, 2007; Zhao, 2017).

These results raise questions about whether we have overestimated the number of cancers that follow this model, underlining the importance of testing CSC markers in significant numbers of patients to appreciate the heterogeneity among individuals (Allison *et al.*, 2011; Magee *et al.*, 2012; Kreso *et al.*, 2014).

For these reasons, it is fundamental to understand the relevance of CSCs in tumour development. This way, we will be able to create drugs that specifically target this tumour environment improving in turn patients' outcome.

1.7 Comparative oncology and future opportunities for personalised cancer therapy in clinical trials

In 2012, an estimated 14.1 million new cases of cancer occurred worldwide, from which an estimate of 8.1 million people have died because of it. The four most common cancers occurring worldwide are lung, female breast, bowel and prostate cancer. In the UK in 2014 more than 350,000 people have been diagnosed with cancer with a survival rate of 50% at 5 years (data from Cancer research UK). The survival rate has doubled in the last 40 years, but there is still a huge variation between types of cancer. Less than 20% of people diagnosed with cancer types that are difficult to diagnose/treat survive for ten years or more. For example, just 1% of the patients diagnosed with pancreatic adenocarcinoma survive more than ten years, and no improvement has been achieved in the last 100 years (Pang *et al.*, 2017).

Murine cancer models have been handy for underpinning the basic biology behind cancer initiation, promotion, and progression (Gordon *et al.*, 2009). Unfortunately, due to differences in the physiology of these two species together with the artificial conditions of these cancer models, they frequently do not adequately represent many of the features that define cancer in humans, including long periods of latency, genomic instability, and the heterogeneity of both tumour cells and their surrounding microenvironment. Most importantly, murine models cannot reproduce the complex biology of cancer recurrence and metastasis, and therefore, it is not possible to evaluate the outcomes in human patients for the cancer drug development (Paoloni and Khanna, 2007).

Considering the long and expensive process that characterised the drug development and the continuous failure of drugs to pass clinical trials, a quest for new solutions is needed. In this setting, about 50 years ago the concept of comparative oncology was born. Comparative Oncology refers to the discipline that integrates the naturally occurring cancers seen in companion animals and compares them with their human counterparts to achieve more insight into cancer biology and therapy (Figure 1.10) (Gordon *et al.*, 2009).

A study in 2010 in the UK showed that almost 27% of purebred dogs have died of cancer (Dobson, 2013). As human cancer, canine cancer occurs in the context of an intact immune system and a tumour microenvironment and often shares similar features of pathophysiology and clinical presentation to the human counterpart. For this reason, the canine model could represent a more effective model compared with the murine induced one (Gordon *et al.*, 2009; Schiffman and Breen, 2015; Pang and Argyle, 2016).

As in humans, different type of cancer can occur in dogs, although, accurate studies about the incidence of cancer in dogs are very limited (Dobson, 2013). One study of insured dogs in the UK showed that cancer most commonly occurs in the skin and soft tissues with a standardised incidence rate of 1437 per 100,000 dogs/year, followed by mammary, urogenital, lymphoid, endocrine, alimentary, and oropharyngeal sites (Dobson, 2013).

Different types of cancer in dogs and humans has got some striking similarities and differences in their overall incidence. For instance, breast cancer is the most common malignancy in both women and bitches, and it is highly dependent on endogenous hormones in both species. In contrast, carcinomas of the prostate are a prevalent condition in men related to hormonal stimulation, whereas in dogs they are uncommon and occur more frequently in neutered dogs (Dobson, 2013). Interestingly, lung and large bowel are the most common sites of occurrence for human tumours but they rarely occur in dogs. Contrarily, soft tissue sarcomas, which are rare in humans, are relatively common in dogs (Dobson, 2013).

The great opportunities given by the comparative oncology approach have spurred to the recent completion of the canine genome sequence (Paoloni and Khanna, 2007). In 2005, the Canine Genome Project decoded 99% of the canine genome of about 2.5 billion base pairs. Results show that human and canine genomes are similar enough to apply findings of one species to the other with almost ~19,000 genes identified in the dog genome that has a similar or orthologous gene in the human genome (Paoloni and Khanna, 2007). On average, cancer rate in purebred dogs is estimated to be over ten times higher than in humans. This increase in cancer susceptibility is caused by the numerous genetic bottlenecks created during the phenotypic selection of purebred traits. Some specific purebreds are more susceptible to certain types of cancer. For

example, Bernese mountain dogs develop commonly histiocytic sarcoma, as much as Golden retrievers develop lymphomas. Scottish terriers have a high incidence of urothelial carcinoma, as well as Boxers with glioblastomas (Nunney *et al.* 2015).

Therefore, considering their features, natural-occurring tumours in companion animals can represent a better model for studying the natural progression of human cancer than induced murine models (Schiffman and Breen, 2015). Considering as well that clinical trials in pet dogs are not restrained to the strictness of the different phases trial design as in humans. Thus translational drug development studies in pet dogs with cancer could be the answer to fill the gap between conventional pre-clinical models and human clinical trials and benefit both human and canine patients diagnosed with cancer (Figure 1.10) (Paoloni and Khanna, 2007; Gordon *et al.*, 2009; Pang *et al.*, 2017).

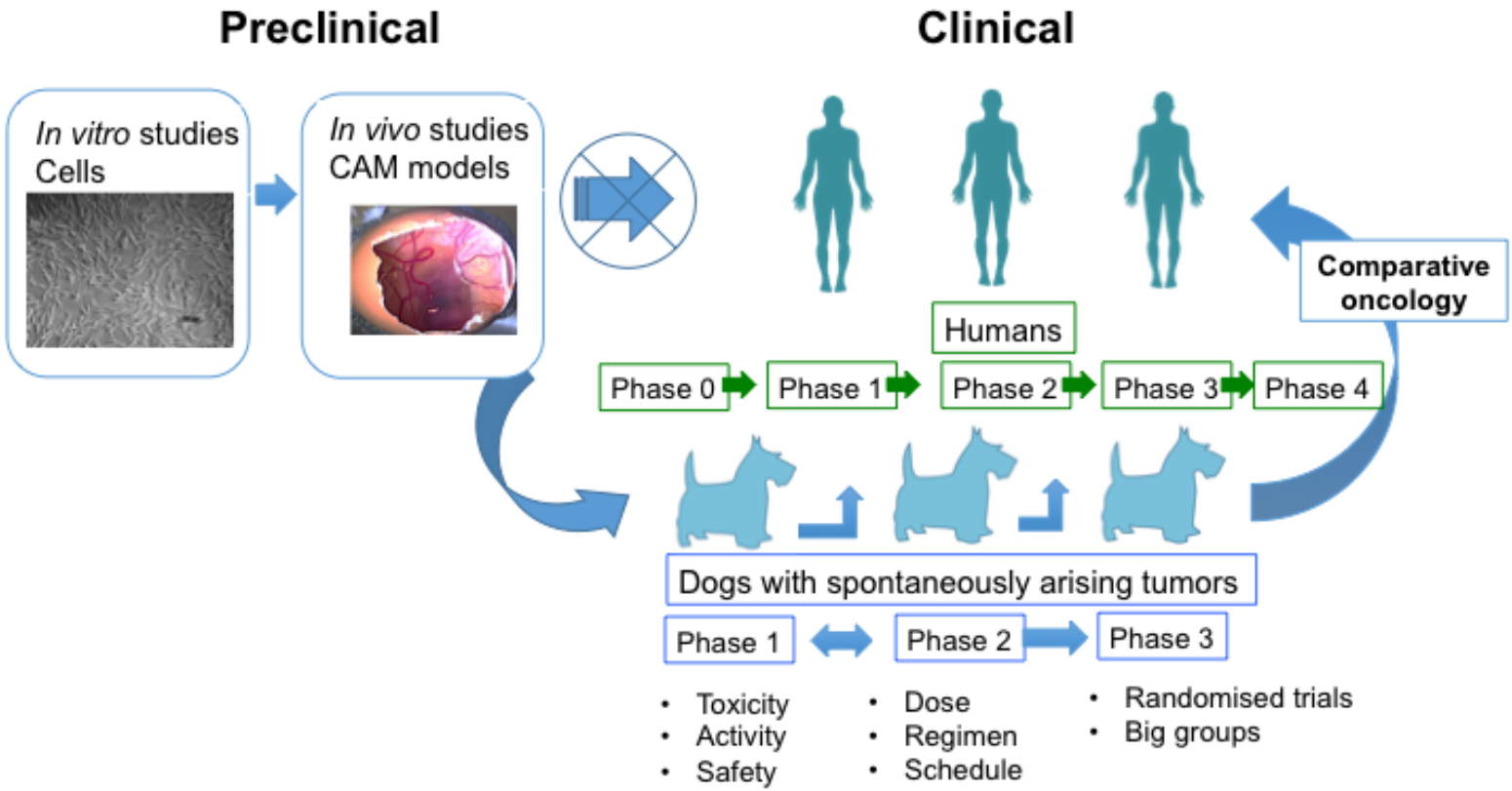

Figure 1.10 Flowchart showing process of clinical trials in human and animals.

1.8 Rationale of the study: Hypothesis, aims and objectives

Clinical challenges are often associated with definitive treatment of malignant INS in humans thus novel targeted therapy is required. Malignant INS is very common in dogs as metastases are present in 95% of the cases. Considering the similar clinical and pathological features of human and canine malignant INS, canine malignant INS could represent an appropriate model for studying the natural progression of human malignant INS.

Based on CSC theory, within a heterogeneous tumour population, a subpopulation of cancer cells drives tumour growth, with the abilities to self-renew, differentiate and resist chemotherapy and radiation therapy. The presence of this small subset of therapy-resistant tumour-initiating cells might explain the failure to current treatments to eradicate solid tumours including INS. Based on these findings this project hypothesised that a subpopulation of CSC might drive the malignant behaviour of canine and human INS driven by a subpopulation of CSC. Therefore, the aim was to isolate the INS CSCs and identifying potential promising targets for novel CSC-targeted therapies.

The specific objectives of this project were:

1. To determine gene expression profiles of canine INS progression through analysis of global changes in RNA expression from normal pancreatic canine tissues to metastatic stages of canine INS.
2. To isolate and characterise INS CSCs in both human and canine INS cell line using *in vitro* and *in vivo* techniques.
3. To identify and *in vitro* and *in vivo* targeting gene signalling pathways involved in maintaining the INS CSC subpopulation using small molecule inhibitors.

2 Materials and methods

2.1 Cell tissue culture

2.1.1 Cell lines

Two cell lines have been used for this study: CM, a human metastatic INS cell line and canINS, a recently established canine primary INS cell line, were provided by Dr Jan A. Mol and Dr Floryne Buishand, from the University of Utrecht (the Netherlands). (Details of the canine cell line validation and characterisation are included in section 8.1 and 8.2, respectively.)

CM is a previously characterised human cell line derived from the ascitic fluid of a patient with a liver metastasis from a malignant INS. It does not produce insulin, but it expresses GLUT2, a gene intimately associated with insulin expression (Baroni *et al.*, 1999). CM cells were successfully grown as monolayers, showing an epithelial morphology. The doubling time was approximately 48 hours. The human INS cell line CM was cultured in RPMI-1640 (Roswell Park Memorial Institute Media, Invitrogen, Paisley, UK) supplemented with 10% fetal bovine serum (FBS) (Invitrogen) and 1% penicillin-streptomycin and plasmid (Invitrogen).

The canine INS cell line canINS was derived from a primary canine INS, TNM stage II (Buishand *et al.* 2010), resected from a 6-year old male Flatcoated Retriever at the Faculty of Veterinary Medicine, Utrecht University (Buishand, unpublished data). canINS cells were successfully grown as monolayers, showing a fibroblast-like morphology. The doubling time was approximately 24 hours. Using an insulin radioimmunoassay (Cisbio, Codolet, France), it was determined that the first passage of canINS produced 305 μU/L insulin. However, insulin secretion was lost after the fourth passage (Buishand, unpublished data), like previously reported in the INS cell line (Labriola *et al.*, 2009). canINS was cultured in RPMI-1640 supplemented with

10% FBS, 1% penicillin-streptomycin, 200ng/mL growth hormone (GH) (Source Biosciences, Nottingham, UK).

2.1.2 Cell culture reagents and equipment

Cells were maintained in an incubator (HERA cell 150i, Thermo Scientific, USA) at 37^{o}C and 5% CO_2 in a humidified atmosphere. Unless stated otherwise, cells were grown in tissue culture treated disposable plates (Thermo Scientific, USA). Disposable plastic pipettes were used for cell culture (Corning, USA). Cell culture manipulations were performed within a BioMat 2 Class 2 Biological Safety cabinet (CAS). Media were stored at 4^{o}C and were warmed to 37^{o}C before use at room temperature.

Unless stated otherwise, 15 and 50 mL plastic tubes were from Greiner. Small (0.5 and 1.5 mL) tubes were from Eppendorf (Germany). Pipette tips were from Starlab (UK). In most instances, centrifugations of 0.5 and 1.5 mL tubes were done using the centrifuge 5415R (Eppendorf, Germany); 15 mL and 50 mL tubes were centrifuged using 5810R (Eppendorf, Germany).

2.1.3 Freezing and thawing cells

Cells were frozen by resuspending 2 x 10^6 cells in 500 µL of ice-cold FBS (Gibco, USA). A solution of FBS + DMSO (20%) was then added dropwise to the cells, to a final volume of 1 mL. Cells were placed in cryovials (Corning, USA) and placed on ice. The vials were frozen overnight in a –80^{o}C freezer, inside a Mr Frosty Freezing Container containing isopropanol (Thermo Scientific, USA). The following day the cells were transferred to a –150^{o}C freezer for prolonged stock.

To revive frozen cells, vials were thawed rapidly at 37^{o}C and the cells transferred to a 15 mL tube with warm media added dropwise (to 10 mL). The tube was centrifuged at 300 × g for 5 min, the supernatant was removed, and cells were plated in a T75 flask with 12 mL of media.

2.1.4 Passaging cells

Both cell lines were routinely passaged at 80-95% confluency every 3-4 days. To passage cells, medium was removed by pipetting, and the cells were washed once with PBS before incubation at 37°C in 0.25% trypsin-EDTA (Gibco, USA) until detached. Once cells had become detached, complete medium (T75: 5-10mL, T150: 10mL) was used to wash the cells from the base of the flask. Cells were split as required (1:10 to 1:20) and seeded directly into new culture vessels with fresh media.

2.1.5 Determination of cell viability

Detached cells were diluted 1:1 with Trypan blue dye (Gibco, USA). The mixture was visualized in a Neubauer counting chamber (SLS). The living cells (not stained by the Trypan dye) in the central 5 × 5 square were counted. Cell number was calculated by the following formula:
Cells/ml = Cells in central square X 2 (dilution factor) X 10^4

2.1.6 Primary insulinoma cell lines

Attempts to establish a new canine INS cell line were made using the protocol developed at Utrecht University for the canine cell line (Buishand, unpublished data).
After obtaining signed consent from the owners, samples were harvested during surgery from dogs with a definitive diagnosis of primary/metastatic INS. An 8 mm biopsy punch was harvested from the centre of the lesion. Half of the sample was stored in 10% formalin (Sigma-Aldrich, USA) to confirm the diagnose of INS. Half of the sample was harvested in cold, sterile Hank's Balanced Salt Solution (HBSS) and put on ice. Tissues were then washed three times in 10 cm Petri dishes (Corning, USA) and minced finely. Samples were then placed in a 50 mL Falcon tube and centrifuged for 3 min at 1000 rpm at 4^{o}C. A solution of 3mg/mL of collagenase IV (Gibco, USA) with 0.004% DNAse (Sigma-Aldrich, USA) in Dulbecco's modified

Eagle's medium (DMEM) containing Glutamax-I (Gibco, USA) + 10% FCS + 1% Penicillin/Streptomycin was added to the pellet and then incubated for 75 minutes at 37^{o}C on a Titramax 1000. The solution was then centrifuged and washed twice in HBBS. In case of cells were not entirely dissociated a step of homogenisation using Dounce tissue grinder set (Sigma-Aldrich, USA) was performed. Cells were then filtered through a 70µm cell strainer. After counting the cells, they were seeded at a density of $2x10^{6}$ in T75 Primaria flasks (Corning, USA) in RPMI1640 + 1% penicillin/streptomycin + 10% FBS + 200 ng/mL porcine GH + 1.25µg/mL of Fungizone (Gibco, USA).

After 48 hours, flasks were examined for adherent cells and checked for signs of bacterial contamination. If contamination was heavy, flasks were discarded. If the medium was cloudy and the cells were attached, the medium was changed. Medium was changed twice weekly and replaced with 50% fresh: 50% conditioned medium (growth medium from flasks centrifuged to remove debris) after gently washing adherent cells twice with PBS. At 80-90% confluence, cells were transferred to larger (T75) culture flasks after dissociation of the monolayer using 0.05% Trypsin-EDTA and then subcultured as necessary. Fifty percent conditioned medium was used for media changes and plating at subculture for up to 5-7 passages.

2.1.7 Sphere assay protocol

2.1.7.1 Tumorspheres culture

Cells in monolayer were trypsinized as described previously and centrifuged at 1200 rpm for 5 minutes. Cells were then counted and seeded at a density of 60,000 cells per well in 2 mL of N2 media in six-well low adhesion tissue culture plates (Corning, USA).

Cells were grown in serum-free conditioned medium, which contained DMEM/F12 supplemented with progesterone (20 nM), putrescine (100 µM), sodium selenite (30 nM), transferrin (25 µg/mL), and insulin (20 µg/mL) (Sigma Biochemicals, Dorset, UK). Every two days, human recombinant EGF (10 ng/mL) and human recombinant basic fibroblast growth factor (bFGF) (10ng/mL) (Peprotech, USA) were added. For

maintaining canINS spheres B27 serum-free supplement (Invitrogen, UK) was also added to the media every two days. All experiments were conducted in triplicate. Plates were maintained at 37 °C in a humidified CO2.

2.1.7.2 Tumorsphere passaging

To passage spheres, cells were collected by pipetting, and the wells were washed twice with PBS to maximise collection. Tumorspheres were washed gently (1000 rpm, 5 minutes) using at least an equal volume of PBS. 1 mL of 0.05% trypsin-EDTA was added to the cells and incubated at RT for 5 minutes. Three mL of FBS-free media were added to terminate trypsinisation and cells were collected by centrifugation at 1000 rpm for 5 minutes. The cell pellet was resuspended in 1 mL of PBS and counted as previously described and seeded at a density of 60,000 cells per well in 2 mL of N2 media.

Once the spheres were passaged at least five times, images were captured using Zeiss Axiovert 40 microscope (Carl Zeiss, Germany) equipped with a cooled CCD camera and Axiovision software.

2.1.8 Chemosensitivity Assays

Cells were assessed for their sensitivity to different chemotherapy drugs over a range of concentrations, including at doses that can be achieved in plasma *in vivo*. Cells were treated with 5-Fluorouracil (plasma concentration: 800 ng/mL-2000ng/mL, 5μM-15μM) (Danquechin-dorval and Gesta, 1996; Yamada, 2003; Blaschke *et al.*, 2012) (R&D, USA) (Yamada, 2003) over the indicated range of concentrations.

Cells were harvested, counted, resuspended in complete medium and plated in black 96-well culture plates at 50 μL / $5x10^3$ cells per well. Plates were incubated at 37°C, 5% CO_2. After 24 hours, drug dilutions were made in complete medium, and 50 μL of each dilution was added to triplicate wells. Fifty μL of medium only was added to triplicate wells as a control. Plates were incubated at 37°C, 5% CO_2 for another 48-72 hours.

The CellTiter-Glo® reagent was added to each well in 1:1 concentration with the media. The solutions were mixed on an orbital shaker for 2 minutes before being incubated at RT for 10 minutes. The luminescence was then recorded for 1 second per well using the Perkin Elmer 1420 Multilabel Counter Victor^{3}TM plate reader.

2.1.9 Colony formation assay

Cells were counted and seeded at a density of 250 to 500 cells per 10 cm plate containing ten mL of standard or chemotherapy supplemented medium. The medium was changed, and the plates were checked for colony formation biweekly. When visible colonies had formed after 10 to 15 days, the colonies were fixed. The medium was removed from each plate, and the cells were washed twice in PBS. Five mL of cold methanol was then added to each plate and left to stand at RT for 5 minutes. The methanol was removed, and ten mL of 10% Giemsa stain (Sigma-Aldrich, USA) was used to stain the colonies for 20 minutes. The plates were rinsed thoroughly in tap water before allowing drying. The colonies were then counted manually.

2.1.10 Chorioallantoic membrane assay

The chick chorioallantoic membrane **(**CAM) assay has long been used as an *in vivo* model for the study of tumour behaviour. The assay is conducted within the protected environment of a developing chick embryo and is particularly useful because of the ready availability of fertilised eggs and the ease of access to a fully functioning membrane. Rejection of the grafted cells is minimised due to the natural immunodeficiency of the chick embryo. Moreover, the CAM assay allows rapid vascularisation and development of grafted tumour cells in an *in vivo* microenvironment (Vargas *et al.*, 2007; Deryugina and Quigley, 2008; Lokman *et al.*, 2012; Pang *et al.*, 2013).

2.1.10.1 Eggs

Fertilised ISA Brown layer strain chicken eggs (Roslin Institute Poultry Unit, UK) were used to evaluate the capability of INS CSCs to invade and form tumours in an in vivo xenograft model. According to the UK Animals (Scientific Procedures) Act 1986 regulated by the Home Office, as chick embryo chorioallantoic membrane experimental protocols were conducted and concluded during the first two-thirds of the incubation of the embryonated eggs, we did not require a licence (Home Office, 2014).

2.1.10.2 Preparing eggs for xenografting

Chicken embryonated eggs were incubated until day 11 of incubation without the need for a licence. Briefly, chicken embryonated eggs were incubated rocking (Brinsea Octagon 40 OX incubator) at 37.5^{o}C until day 4 of development in a horizontal position. At this date, approximately two mL of egg albumin was removed with a syringe and a 24 gauge needle (Becton Dickinson), to detach the CAM from the shell and to disclose the underlying CAM vessels. A 1 cm × 1 cm window was opened on the shell with scissors, having the egg in the horizontal position. Two drops of penicillin/streptomycin (Gibco, USA) diluted 1:10 in PBS were added to the surface of the CAM to minimise the risk of infection. The shell window was sealed with microporous surgical tape and incubation at 37.5^{o}C (RCOM Maru Digital Incubator) was continued until day seven without turning.

2.1.10.3 Graft and incubation of cells

On day 7, single cell suspensions of trypsinised adherent cells or spheres (both CM and Nielson) were labelled with PKH26 (Sigma-Aldrich), a red fluorescent live cell membrane dye, according to manufacturers' instructions. Cells were suspended in a 1:1 mixture of serum-free media and Matrigel Phenol Red Free (Corning, USA), and 2x10^{5} cells inoculated directly onto the CAM. The shell windows were resealed and incubated without turning (Figure 2.1).

At day 11, pictures were taken using Axio ZoomV16 coupled with AxioCAM HRM camera (Zeiss). Images were processed using Zeiss pro image software and then the fluorescence was calculated using the software ImageJ 1.46 software (open source).

2.1.10.4 Harvesting and fixation of CAM

The embryos were sacrificed by decapitation. The area of CAM inoculated with the fluorescent cells was harvested and stored in 10% neutral buffered Formalin solution (Sigma-Aldrich, USA) for 48hrs. Then the excess of Formalin was removed and the CAM embedded in an agarose block by pouring the agarose into a small plastic weigh boat and then transfer the tissue from PBS to liquid agarose. Tissue was then embedded in fresh paraffin. Tissue blocks were then trimmed and 4μm sections were cut and mounted onto glass microscope slides.

2.1.10.5 Immunostaining

Sections were rinsed in PBS Tween 20 for 2x2 min then incubated with the primary antibody for 1 h at room temperature or overnight at 4oC with Monoclonal Mouse Anti-Human Cytokeratin (Clone MNF116) (1:50) (Dako, Denmark).

Sections were rinsed in PBS Tween 20 for 2x2 min then blocked with Dako REALTM Peroxidase-Blocking Solution (Dako) for 10min at room temperature.

Sections were rinsed with PBS Tween 20 for 3x2 min then incubated with the secondary antibody Dako REAL™ EnVision™/HRP Mouse (ENV) for 40 min at room temperature.

The cutting and staining with a cytokeratin pan antibody (MNF116) were performed by Neil MacIntyre and the R(D)SVS pathology laboratory. Images were taken using a Nikon Eclipse Ni Brightfield Microscope (Nikon) and after that processed with Zeiss pro image software (Zeiss).

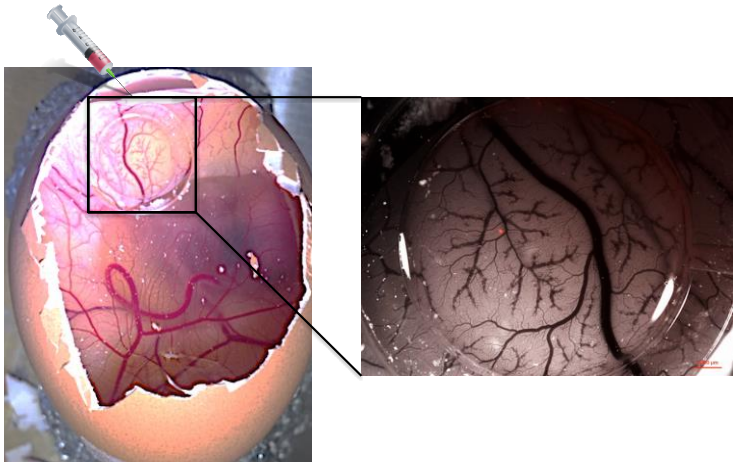

Figure 2.1 Pictures showing chorioallantoic membrane of chicken embryo. Cells have been labelled with red fluorescent marker and seeded on the membrane on a plastic ring.

2.2 Isolation and quantification of nucleic acids

2.2.1 RNA extraction, quantification and Reverse Transcription (RT)

The RNeasy mini kit (Qiagen, UK) was used according to the manufacturer's instructions.

Depending on whether the extraction was performed on tissues or cell pellets different protocols were used for lysation. Information regarding specific protocols will be detailed in each chapter. DNA digestion was performed using DNase I (Qiagen, UK) at the recommended point in the RNA extraction protocol. Total RNA was quantified, and purity checked using absorbance spectrophotometry at 260 and 289 nm (Nanodrop 1000, Thermo, UK).

RNA was converted to cDNA using the Omniscript reverse transcription kit (Qiagen, UK) according to the manufacturer's instructions. Omniscript RT was carried out by mixing the following reagents: 10 x Buffer RT; dNTP (to 0.5 mM of each dNTP, Promega); Specific primers (to 1 μM); Random nonamers (to 10 μM, Sigma); RNase inhibitor (10 units, Promega); Omniscript reverse transcriptase (4 units); template RNA (1 μg); water to 20 μL. Unless stated otherwise, the reaction was incubated for 60 min at 37°C.

2.2.2 Primer design and preparation

Where available, previously published primers were checked using NCBI Primer-blast (https://www.ncbi.nlm.nih.gov/tools/primer-blast). For primer design, the NCBI nucleotide database was used. In primer design, it was attempted to maintain the primer melting temperature similar to the pair (within 57-63 degrees) and to avoid primer hairpins, self-dimers and heterodimers that involved the 3'-end of the sequence. The parameters mentioned were quantified using the IDT OligoAnalyzer online program (https://www.idtdna.com/calc/analyzer). Primers were produced by Eurofins Genomics. All primers were diluted to 100 pmol/μL with nuclease-free

water and stored at -20 °C. A detailed list of the primers used is available in Appendix 8.6.

2.2.3 Polymerase Chain Reactions (PCR)

PCR reactions were set up using HotStarTaq® DNA polymerase (Qiagen, UK) PCR kits according to the manufacturer's instructions. To ensure consistency, all experiments were performed on the same thermal cycler (Labtech G-Storm GS-4822, France) following the cycling protocol as described in Table 2.1. To assess the consistency of sample loading and PCR conditions between separate experiments, primers that amplified cDNA of transcripts from the human and canine housekeeping gene glyceraldehyde 3-phosphate dehydrogenase (GAPDH) were included in separate reactions (Pang *et al.*, 2014).

Table 2.1 Optimised cycling protocol for HotStarTaq DNA Polymerase.

Initial activation step	**15 min**	**95°**
3 step cycling:		
Denaturation	1 min	94°
Annealing	1 min	50-68°
Extension	1 min	72°
Number of cycles	35	
Final extension	10 min	72°

2.2.4 Agarose gels

Gel concentrations between 1% and 2% were used depending on the size of the product to be resolved. Gels were made by dissolving agarose powder (UltraPure Agarose, Invitrogen) at the stated concentrations in TAE buffer (40 mM Tris, 20 mM acetic acid, and 1 mM EDTA). The mixture was heated in a microwave until the gel was completely dissolved. Gel Red (Biotium) was added in 1:1000 dilution. The gel was then poured into a mould and allowed to set. A volume of 12 μL of PCR product was added to 4 μL of 6 X Blue/Orange Loading Dye (Promega, UK). A 100 bp ladder or 1.5 Kb DNA (Promega, UK) was used to assess product size. Gels were run

for approximately 2 hours at 100-130V, and then the products were visualised using a BioRad Molecular Imager GelDoc.

2.2.5 Real-time polymerase chain reaction (qPCR)

The Platinum Sybr Green qPCR Kit (Invitrogen, UK) was used in all qPCR reactions. The master mix is outlined in Table 2.2. Reactions were performed on the Stratagene MX3000P (Agilent, UK). For primer optimisation, cDNA from CM and Nielson cell lines was diluted in ten-fold steps to 100,000, and 9 µL of this was added to each well. Primer efficiency, and dissociation curves were calculated using MXPro software (Agilent, UK), specificity was assessed by agarose gel electrophoresis. Relative gene expression was performed using cDNA, diluted 1:20 and 9 µL of this added to each well. Each reaction was performed in triplicate and three no-template controls were also included for each primer using 9 µL of nuclease-free water. Relative gene expression levels were obtained by normalisation to the expression levels of housekeeping gene *GADPH*. Calculations were made using the Delta Delta Ct Method (Pfaffl, 2004).

Table 2.2 qPCR master mix Reaction conditions were 2 minutes at 50°, 2 minutes at 95°C, then 40 cycles of 95° x 15secs and 60°C x 30secs. The final cycle was 95°C for 1 minute then cooling to 60°C before monitoring for dissociation to 95°C. The dissociation curve produced and lack of amplification of the no template controls were checked using MXPro Software (Agilent, UK).

Component	Volume (µL per reaction)
SYBR Green Mix	12.5
Forward primers	1
Reverse primers	1
ROX	0.5
Free nuclease water	1
Total	16

2.2.6 mRNA sequencing using Next Generation Sequencing (NGS)

2.2.6.1 Assessment of RNA quality

All sequencing was performed by The University of Edinburgh sequencing service (Edinburgh Genomics, Ashworth Laboratories, King's Buildings, Edinburgh). Samples were prepared in clearly labelled RNase free tubes. Samples were checked for quality by the 2100 Bioanalyzer (Agilent) with the Agilent RNA 6000 Nano kit or by the Agilent 2200 Tapestation with the RNA analysis screen tape (Agilent). These two methods provide an accurate and objective assessment of total RNA degradation the RNA integrity number (RIN) as measurement. The RIN is a software output that estimates the integrity of total RNA samples based on the entire electrophoretic trace of the RNA sample rather than just the ratio of the ribosomal bands, 28S and 18S. This includes the presence or absence of degradation products. The assigned RIN is independent of sample concentration, instrument and analyst, and therefore it is considered a de facto standard for RNA integrity (Griffin *et al.*, 2012). Samples sent for sequencing accomplished all the following requirements: RIN > 6; concentration >30ng/uL; A260:280 >1.9. Good quality of RNA is critical for obtaining optimal sequencing results.

A

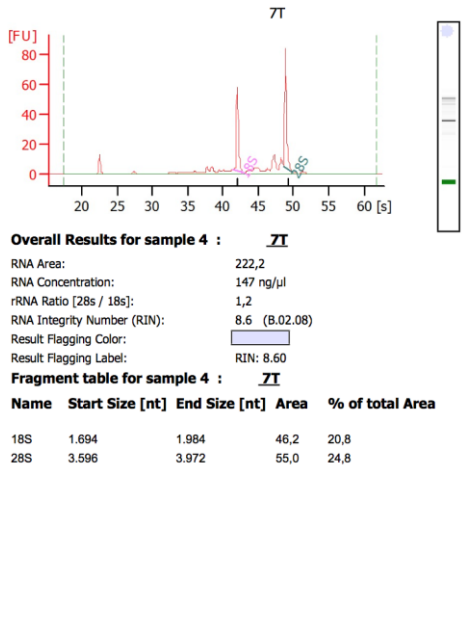

Overall Results for sample 4 : 7T

RNA Area:	222,2
RNA Concentration:	147 ng/µl
rRNA Ratio [28s / 18s]:	1,2
RNA Integrity Number (RIN):	8.6 (B.02.08)
Result Flagging Color:	
Result Flagging Label:	RIN: 8.60

Fragment table for sample 4 : 7T

Name	Start Size [nt]	End Size [nt]	Area	% of total Area
18S	1.694	1.984	46,2	20,8
28S	3.596	3.972	55,0	24,8

B

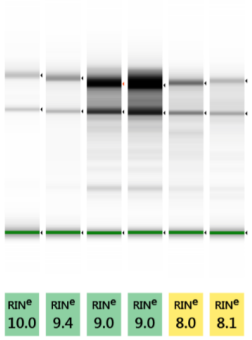

RIN^e	RIN^e	RIN^e	RIN^e	RIN^e	RIN^e
10.0	9.4	9.0	9.0	8.0	8.1

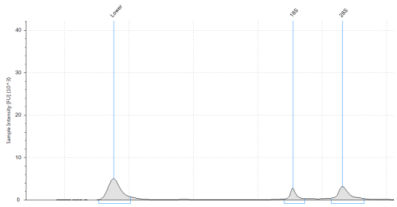

Sample Table

Well	RINe	28S/18S (Area)	Conc. [ng/µl]	Sample Description
A1	10.0	2.0	27.4	Nielson parental

Figure 2.2 Example of an RNA quality analysis report with 2100 Bioanalyzer (Agilent) (A) and 2200 Agilent Tapestation (B).

2.2.6.2 Library preparation for mRNA sequencing

Library preparation from mRNA before sequencing is necessary to obtain a clear view of the coding transcriptome with strand-specific information (Corney *et al.*, 2013).

The mRNA library was prepared by The University of Edinburgh sequencing service (Edinburgh Genomics, Ashworth Laboratories, King's Buildings, Edinburgh) using Tru Seq Stranded mRNA Library Prep Kit (Illumina). Library preparation consists of the following steps:

1. **RNA fragmentation.** mRNAs are typically fragmented to smaller pieces of RNA to enable sequencing.
2. **Reverse transcription.** First and second strand cDNA is reverse transcribed from fragmented RNA using random hexamers or oligo(dT) primers.

3. **Adapter ligation.** The 5' and 3' ends of cDNA are repaired, and adapters (containing sequences to allow hybridization to a flow cell) are ligated.
4. **Library clean-up and amplification.** Libraries are enriched for correctly ligated cDNA fragments and amplified by PCR to add any remaining sequencing primer sequences.
5. **Library quantification, quality control and sequencing.** Library concentration is assessed using qRT-PCR and Bioanalyzer and is ready for sequencing (Corney *et al.*, 2013).

2.2.6.3 Sequencing

At the moment, Illumina sequencing is the most commonly used RNA-sequencing method. It uses a "sequencing by synthesis" (SBS) approach (Metzer *et al.*, 2010).

After library preparation is completed, the libraries are denatured and undergo a process known as "bridge amplification" to create clonal clusters of single-stranded DNA molecules. Briefly, once the fragments attach on the flow cell, DNA is sequenced by adding polymerase resulting in a covalently bound full-length complementary copy of the cDNA fragment. The cDNA fragment obtained is subjected to several rounds of PCR amplification to produce clones that can be optically resolved during sequencing. Obtaining optimal cluster density is critical since it will determine the number of reads obtained. Therefore, the cDNA is labelled with dNTPs (nucleoside triphosphate). Each of the dNTPs is labelled with a specific fluorescent colour. After laser excitation, different emitted fluorescent waves are recorded for each cluster. Based on the fluorescence emission the base of each cluster is identified. Because the clusters contain identical DNA sequences, the entire cluster is read as one base. A camera records this base reads across the entire flow cell. This takes place between 50 and 100 cycles to create about 150-200 million 50bp to 100bp reads. When two separate read cycles occur in both directions, it is called paired-end reads. This kind of read will provide data about both sides of the fragment of interest (Metzer *et al.*, 2010).

For this study, we sequenced fragments of 75bp to a yield of at least 290milion paired-end reads using an Illumina HiSeq 4000 machine.

2.3 Bioinformatic NGS analysis

Bioinformatic analyses were performed by The University of Edinburgh sequencing service (Edinburgh Genomics, Ashworth Laboratories, King's Buildings, Edinburgh). The process of analysis is described as follows:

1. Raw reads were filtered for quality (Q30) and adapter using cutadapt (v1.8.3).
2. Trimmed reads were then aligned to Canis_lupus_familiaris_v3.1.84 using tophat2.
3. Read counts were obtained using HTSeq v.6.0.1 with mode 'union'.
4. Differential gene expression was then carried out using edgeR (version 3.12.0). Genes with less than 20 reads were discarded from this analysis. Further down, only genes with uncorrected *P*-value < 0.05 were retained.
5. Functional analysis (Gene set enrichment analysis) was conducted using GSEA2-2.2.2. Gene sets with a False Discovery Rate (FDR) <0.05 were considered as significantly enriched.

2.4 Recovery and detection of protein

2.4.1 Cell lysis

All manipulations were performed on ice. Cells, either growing as monolayer or as spheres, were harvested washing twice with cold PBS. After that, cells were centrifuged at 1200 rpm x 5 min. The pellet obtained was then frozen, and a volume of chilled urea buffer with protease inhibitor mix was added. The pellet was then mixed by pipetting until no cell clumps were visible and incubated for 10 minutes on ice. Then cells were transferred to 0.1 mL Bioruptor®Microtubes (Diagenode, Belgium) and sonicated using pre-chilled Bioruptor® Pico sonicator (Diagenode, Belgium) with the following settings:

Sonication cycle: 30 sec ON/30 sec OFF

Total sonication time: 3 - 5 cycles

Temperature: 4°C

The cell lysates were cleared by centrifugation at 4°C at 15,000 x g for 15 minutes, snap frozen on dry ice, and stored at -70°C.

2.4.2 Protein quantification

The Bradford assay was used for protein quantification. The sample proteins were added and mixed in a transparent 96-well plate in concentrations that were within the standard range. Subsequently, 200 μL of the ready-made reagent (QuickStart Bradford reagent, Bio-Rad, UK) were added to the samples prepared in triplicates. To create the standard curve, BSA was used in increasing concentrations, in triplicates: 0, 0.12, 0.25, 0.5, 1, 2 and 4 mg/mL. The wells were mixed to allow the development of the blue colour and left at RT for 5 min. The plate was then read in a Victor3 plate reader (Perkin Elmer, USA) at 595 nm.

2.4.3 Western blots and gel stains

Protein samples were resolved on denaturing SDS-polyacrylamide gels by electrophoresis. The SDS-polyacrylamide gels were prepared and assembled using the Bio-Rad Protean II minigel system. The gel was allowed to set at RT. Twelve percent resolving polyacrylamide gels were prepared (based on anticipated protein product size of 15-150kDa), along with 5% stacking gels, on the day of electrophoresis.

Gels were made using the protocol as follows: 30% acrylamide/0.8% bisacrylamide solution (National Diagnostics, USA); 1.5 M Tris-Cl with 0.4 % SDS, pH 8.8 (3.75 mL); distilled water to 15 mL; 10 % ammonium persulfate (50 μL, Bio-Rad, USA); TEMED (5 μL, Bio-Rad, USA). These were mixed and poured to 2/3 of the height of Mini-Protean glass plates of either 1 – 1.5 mm, depending on the sample volumes (Bio-Rad, USA). The gel was covered with distilled water and allowed to set. After setting, the water was removed and the stacking gel was added to the plates (30% acrylamide/0.8% bisacrylamide solution (0.65 mL), 0.5 M Tris- HCl with 0.4 % SDS, pH 6.8 (1.25 mL), distilled water (3.05 mL), 10% ammonium persulfate (50 μL), TEMED (5 μL)). The plastic comb was added into the poured stacking gel to shape the wells. The gel was allowed to set. The samples were prepared by the addition of 6 × sample buffer (Tris-Cl/SDS, pH 6.8 as above (7 mL), glycerol (3.8 g

or ~ 3 mL), SDS (1 g), DTT (0.93 g), bromphenol blue (1.2 mg), water (to 10 mL if needed)). Unless stated otherwise, samples were heated at 95°C for 5 min after the addition of the sample buffer. The samples were pipetted into the wells of the gel. The size standard used was Precision Plus Protein Dual Colour (5 µL, Bio-Rad). The gel was run at 120 V until the samples were resolved.

On completion of electrophoresis, the gel was removed from the glass plates, and the stacking gel was removed. The gel was then used to transfer proteins to a nitrocellulose membrane. The transfer cassette (Bio-Rad, USA) was assembled in the following order, from the anode (white) to the cathode (black) side: sponge, filter paper, nitrocellulose membrane (GE Healthcare), gel, filter paper, sponge. The cassette was placed in a transfer apparatus with transfer buffer (Tris base (18.2 g), glycine (86.5 g), methanol (1200 mL), distilled water (to 6 l)). The transfer was performed at 100 V for 1 h at 4^{o}C.

If necessary, the membrane was stained using Ponceau red (Ponceau S (Sigma-Aldrich, USA), 0.5 g dissolved in 1 mL glacial acetic acid. The staining solution was placed on the nitrocellulose membrane and incubated for 30 sec mixing. The stain was returned to the container for reuse. The membrane was washed with distilled water until the bands were visible.

Depending on the primary antibody used, the membrane was either blocked with Tris-Buffered Saline Tween20 (TBST; 10 mM Tris HCl, 150 mM NaCl, 0.1% (v/v) Tween 20) + skimmed milk (5 %) or with TBST + BSA (5%) for 1 hour at RT.

The membrane was then incubated at 4°C overnight with the primary antibody diluted in the specific blocking buffer. After incubation overnight, the membrane was washed in TBST/0.1%Tween20 three times (15 minutes each) and then probed with secondary antibody. Horseradish peroxidase- (HRP-) conjugated secondary antibodies were obtained from Dako (Goat anti-Rabbit-HRP; Rabbit anti-Mouse-HRP). The appropriate secondary antibody was diluted 1:1000 (Rabbit anti-Mouse-HRP) or 1:2000 (Goat anti-Rabbit-HRP) in blocking solution and applied to the membrane. After incubation at RT for 1 hour, blots were washed for 3 x 5 minutes in TBST/0.1%Tween20. Table 2.3 shows a list of the primary and secondary antibodies used. The following antibodies were optimised and validated for both human and canine INS cell lines.

2.4.4 Chemoluminescent detection

The enhanced chemoluminescence reagent (GE Healthcare) was prepared in a 1:1 dilution and applied to blots. After 1-2 minutes, excess reagent was drained, and blots were transferred to a Saran wrap folder secured within a film cassette. In a darkroom, radiographic film was loaded into the cassette and allowed to expose for 2-20 minutes depending on signal strength. After developing, the molecular weight marker sizes were labelled on to the radiographic film to allow determination of protein band size.

Table 2.3 Primary antibodies used for western blotting.

Antibodies	Clonality	Dilution	Blocking buffer	Manufacturer
Notch2 (D76A6)	Rabbit monoclonal	1:1000	TBST+5% BSA	New England Bio
Hes1 (EPR4226)	Rabbit Monoclonal	1:600	TBST+5% skimmed milk	Abcam
Beta-actin (AC-15)	Mouse monoclonal	1:5000	TBST+5% skimmed milk	Abcam
Sox9 (ab26414)	Rabbit Polyclonal	1:500	TBST+5% skimmed milk	Abcam
Oct4 (ab18976)	Rabbit polyclonal	1:1000	TBST+5% skimmed milk	Abcam

2.5 Flow cytometry and Fluorescence-activated cell sorting (FACS) sorting

Fluorochrome-conjugated antibodies have been used to label and then sort CM and canINS cell line using BD Fortessa or FACS-Aria flow customers (both BD Biosciences, USA). Specific protocols and antibodies are detailed in each chapter. Following a general protocol, cells were harvested, washed and adjusted to a concentration of 0.5-1x 10^6 cells per condition in ice cold PBS. Cells have been strained using 70µm cell strainers to avoid clumps that could block the flow cytometer. Cells were then stained in polystyrene round-bottom 12x75 mm. Control samples (cells incubated with equivalent concentration of isotype-matched control antibody / unstained cells) were evaluated for each experiment. A secondary antibody control was added as a negative control.

At least 100,000 events were acquired for analysis. The optimal concentration of the test antibody was determined for each cell line, such that the fluorescence of the concentration-matched isotype control sample was equivalent to that of the unstained aliquot. Doubling dilutions of test antibody and concentration-matched isotype control antibody were made in PBS, with the manufacturers' recommended concentration as the initial dilution. All stainings were performed at 4°C protected from light. Cells were then analysed in the flow cytometer by a laser at different wavelengths depending on the conjugated fluorochrome. Cells were gated by adjusting the size (forward scatter/FSC) and granularity or complexity (side scatter/SSC) of the cells to the middle of an FSC × SSC graph. Red fluorescent emission (Alexa Fluor 647) was excited by the 670nm laser line. Yellow-green fluorescent emission (Phycoerythrin-PE) was excited by the 586 nm laser line. Cell debris and dead cells were excluded from the analysis based on scatter signals and Sytox Blue (Invitrogen, UK) or Zombie Violet (Biolegend, UK) fluorescence. Both dead cell discriminators were excited by a violet laser at a wavelength of 450 nm. Post-acquisition analysis was performed using FlowJo (Treestar, USA). Results were analysed after setting the gate on the cellular population, eliminating debris. The percentage of positive cells was determined by comparison to the negative (secondary antibody or isotype) control level.

2.6 Statistical analysis

All experiments were repeated at least on two separate occasions. Quantitative analysis was based on a minimum of three replicates. Data were analysed using Minitab® 17 Statistical Software (Minitab Ltd., Coventry, UK) and all graphs and diagrams were generated using Microsoft Office 2011 software (Microsoft Corporation). *P*-values <0.05 were considered statistically significant. When data followed a normal distribution, two sample *t*-tests were used to compare differences between two samples, or one-sample *t*-tests to determine whether the sample mean was statistically different from a known or hypothesised mean. IC_{50} values were calculated using GraphPadPrism 6 (GraphPad Software, La Jolla, CA, USA). To assess combined treatment effects on the canINS and CM cell lines, the Bliss additive model was used (Buck *et al.*, 2006).

3 Investigating molecular mechanisms of canine insulinoma progression using transcriptome analysis

3.1 Abstract

Insulinomas (INS) are the most common functioning pancreatic neuroendocrine tumours (PNETs) in dogs. Although considered to be 'indolent' tumours, at the time of diagnosis approximately 95% of the cases in dogs develop micrometastases resistant to chemotherapy and there is no curative treatment for metastatic INS. Using RNA-sequencing technologies, differential gene expression and pathway analysis were combined to conduct a pilot study and gain new insight into the underlying molecular mechanisms of this disease. The hierarchical clustering analysis suggested that normal tissues had a different gene expression profile compared to primary and metastatic lesions. When comparing normal pancreas with primary INS, 1900 differentially expressed genes were identified ($P < 0.01$, FDR<0.05; logFC>2); whereas, comparison between primary INS and metastatic lesions revealed that only 164 were differentially expressed ($P < 0.01$, FDR<0.05; logFC>2). This study confirmed a number of identified genes previously implicated in the malignant subtypes of human INS, such as *INSM1* and *IAPP*, and also provided new findings. We revealed a gene signature that might be indicative of early carcinogenesis and that could aid in the identification of malignant subtypes of canine INS. For instance, genes related to pancreatic endocrine development and insulin secretion such as *PDX1, INS, PAX4, NKX2* and *NESTIN* were upregulated in primary INS when compared to normal pancreatic tissues. Using Gene set enrichment analysis and Reactome tool, we confirmed these data showing that significantly disrupted biological processes were mainly related to beta cell differentiation, pancreatic development and also to protein transcription and extracellular matrix. In this study, the combination of differential gene expression with pathway and network analyses represented a starting point into an in-depth

understanding of this poorly studied cancer. These integrative computational approaches could be the key to future effective early cancer diagnosis and treatment planning in canine patients diagnosed with malignant INS.

3.2 Introduction

INS are rare neoplasms that can arise from pancreatic beta cells in humans and dogs (Okabayashi *et al.,* 2013; Buishand *et al.*, 2014). In 10% of the cases, INS in humans occur as part of an autosomal dominant familial cancer syndrome, MEN 1, but the majority arise as sporadic lesions (Dotzenrath *et al.,* 2000); whereas, in dogs INS occur sporadically (Goutal *et al*., 2012).

Canine INS are more often malignant (95% of the cases metastasise to liver/lymph nodes) compared to human ones which are usually benign (5-16% of the cases metastasise to liver/lymph nodes) (Jonkers *et al*., 2007; Buishand *et al.,* 2010). If INS is detected early, it can be cured by surgical resection. Nevertheless, there is no curative treatment for metastatic disease (Goutal *et al.,* 2012; Okabayashi *et al.,* 2013).

Previous studies showed that in human INS, grading and TNM stage had prognostic significance for disease-free interval (DFI) and survival time (ST) in INS (De Herder *et al*., 2011; Zhu *et al*., 2016). Similarly, in dogs, previous studies demonstrated that tumour size, TNM stage, the Ki67 and necrosis are prognostic factors related both to DFI and ST (Buishand *et al*., 2010; Buishand *et al.*, 2014). In particular, stromal fibrosis is significantly predictive of survival, while tumour size, the Ki67 index, and TNM stage are significant prognostic marker of DFI and ST (Buishand *et al.,* 2010). These factors have also been reported as prognostic markers in human INS biopsies (La Rosa *et al.,* 2007, 2009). Additionally, tumour cell nuclear cytoplasm and nuclear density (number of nuclei per square millimetre) have been identified as discriminators between metastatic and non-metastatic tumours in both human and canine INS (Jutting *et al.,* 1997; Anlauf *et al*., 2009). Numerous studies have demonstrated the utility of several NE biomarkers, such as chromogranin A, synaptophysin, and CD56 to give a definitive diagnosis of INS (Jonkers *et al.,* 2006, 2007; Buishand *et al.,* 2014; Fujino *et al.,* 2015). In particular, a few biomarkers have been identified for their prognostic significance in human and canine INS. For instance, IGF 1 and 2 bind have been indicated to play a role in INS in both human and canine INS. In human INS, IGF1 and IGF1R were expressed in 70% and 90% of tumours, respectively (Jonkers *et al.,* 2007). These findings were confirmed in dogs

where expression of IGF1 was related to highly metastatic INS (Buishand *et al.*, 2010). Whereas IGF2 has been related with a more benign phenotype of PNETs in dogs (Finotello *et al.*, 2014).

Today it is clear that each type of tumours has a unique gene signature that promote tumour growth. Therefore, further investigations of the transcriptomic alterations and underlying molecular mechanisms are essential for early diagnosis and treatment (Höpfner *et al.*, 2003; Kuboki *et al.*, 2016; Liu and Chang, 2016). However, the molecular pathways underlying the development and progression of INS are yet poorly understood.

A novel approach in human oncology is the use of therapeutics that specifically target gene products that promote tumour growth and metastasis. Therefore, identifying potential biomarkers and novel targets can improve treatment and outcome of patients diagnosed with malignant INS (Fazio *et al.*, 2010; Rossi *et al.*, 2014; Giuroiu and Reidy-Lagunes, 2015). The study of spontaneously occurring tumours in the dog, a species that has a genetically stronger relationship to the human than mice, can potentially enrich the knowledge of rare human cancers. This could lead to more insight in the pathogenesis of the disease and facilitate the identification of therapeutic targets valuable for dogs and humans (Gordon *et al.* 2006).

In this chapter, the aim was to develop integrative computational approaches to identify differentially expressed genes and altered pathways to unravel the mechanisms of tumourigenesis of malignant INS. Considering the higher incidence of malignant INS in dogs compared to humans, we investigated the gene expression profiles of malignant INS in dogs as a model for studying tumour progression of the human malignant tumours. Conventional mRNA profiling tools, such as Northern blot, real-time PCR, and microarray, rely on the design of gene-specific primers (Higgins *et al.*, 2010; Boerkamp *et al.*, 2013; Buishand *et al.*, 2014); due to differences in length, GC content, and target regions of the primers, these mRNA profiling tools are not able to quantify and compare the real abundance of transcripts between genes (Cui *et al.*, 2012). RNA-Seq instead represents a highly sensitive and accurate device for measuring expression across the transcriptome (Soneson *et al.*, 2013). Compared to the previously used microarray it provides an increased dynamic

range of the differentially expressed genes and the ability to detect and quantify the expression of previously unknown transcripts and isoforms (Cui *et al.*, 2012; Soneson *et al.*, 2013; Conesa *et al.*, 2016). For these reasons, RNA-seq was chosen over microarrays for studying this poorly characterised tumour as it would offer a broader insight of the differential gene expression of INS compared to the previously used microarray (Buishand *et al.*, 2013). In particular, RNA-sequencing that uses next-generation sequencing (NGS) methods to quantify the messenger RNA (mRNA) provide a quantification of transcripts at high levels of sensitivity and accuracy and an unbiased detection of transcript variants (Cui *et al.*, 2012; Soneson *et al.*, 2013). For instance, this technology sequences cDNA from RNA samples to produces millions of short reads that are mapped to a reference genome and then analysed for differentially expressed genes between conditions (Soneson *et al.*, 2013). Since the canine genome sequence became available, RNA-seq has already proven its value in the research of various canine tumours but not yet in INS (Davis & Ostrander 2014; Hoeppner *et al.*, 2014).

Therefore, the purpose of this study was to quantify the mRNA abundance of differentially expressed genes in canine INS using a computational approach with edgeR. edgeR software is designed for finding changes between two or more groups when at least one of the groups has replicated measurements (Robinson *et al.*, 2010).

Despite the discoveries of differentially expressed genes and genetic mutations, the knowledge of biological pathways involved in the disease is limited. In general, pathway analysis in dogs has its constraints because pathway identification relies heavily on existing functional annotation, which is still limited for this species (Boerkamp *et al.*, 2013). However, pathway analysis provides an additional way to analyse expression data across species. In order to obtain improved data convergence and ensure a systematic insight into the pathways altered during INS pathogenesis, a combination of RNA-sequencing data, gene-set enrichment analysis (GSEA) and Reactome was used to categorise expression patterns on the differentially expressed genes (Subramanian *et al.*, 2005; Croft *et al.*, 2011). GSEA and Reactome pathway analysis revealed that differentially expressed genes were significantly enriched in a few biological pathways known to have a role in cancer, as well as previously unreported pathways, thus providing new insights into the regulatory mechanisms of

malignant INS. Through comprehensive differential gene expression, pathway and network analyses, this study improved our understanding of the functional processes involved in canine INS carcinogenesis.

3.3 Materials and methods

3.3.1 Clinical samples

RNA sequencing analysis was performed on 16 samples including controls (4 pancreas and 3 mediastinal lymph nodes) and tumour lesions (6 primary INS and 3 metastatic lymph nodes). Canine patients diagnosed with INS were staged according to the TNM notation system (Buishand *et al.*, 2010) (Control and samples outlined in Table 3.1 and Table 3.2).

3.3.2 RNA isolation

3.3.2.1 Normal pancreas

Pancreatic tissues were isolated from four dogs (Table 3.1). A protocol from Griffin *et al.* 2012 was optimised for isolating high-quality RNA from canine pancreatic tissue harvested during autopsy (Griffin *et al.*, 2012). Briefly, the pancreas was perfused with RNA later® (Qiagen) using a 5 ml syringe with a 26 gauge needle to obtain a homogeneous distribution of the RNA later® in the various acini of the pancreas. Tissues were then cut into small pieces, placed in cryovials, snap frozen in liquid nitrogen and stored at −80°C. Tissue homogenisation was performed using mortar and pestle, and RNA was extracted using Qiagen RNeasy Mini Kit (Qiagen, Germany). The optional DNase digestion step was done to prevent genomic DNA contamination (Griffin *et al.*, 2012). RNA concentrations were quantified by spectrophotometry (NanoDrop ND-1000, Isogen Life Sciences).

3.3.2.2 Normal lymph nodes

Mediastinal lymph nodes were isolated from 3 healthy dogs without breed or sex predilection. Briefly, lymphatic tissues were harvested and immersed into RNA later® for 24 hours at 4°C then placed in cryovials, snap frozen in liquid nitrogen and stored at −80°C. Tissues were then cut into small pieces and homogenised using mortar and pestle. Finally, RNA was extracted using Qiagen RNeasy Mini Kit (Qiagen, Germany). The optional DNase digestion step was performed to prevent genomic DNA contamination. RNA concentrations were quantified by spectrophotometry (NanoDrop ND-1000, Isogen Life Sciences).

3.3.2.3 Insulinomas and metastatic lymph nodes

All tumour samples were confirmed as being spontaneously occurring INS and were obtained from family-owned dogs with informed owner consent. Six primary canine INS and three metastatic lymph nodes were resected at the Faculty of Veterinary Medicine, Utrecht University, from 1993 to 2014 from FO Buishand and J Kirpensteijn (Table 3.2). Portions of tissue (5–15mm diameter) for RNA extraction were removed from the central portion of the tumours, placed in cryovials, snap frozen in liquid nitrogen and stored at −80°C. Tissue fragments were fixed in 10% neutral-buffered formalin for 24–36 h for histopathology to confirm the diagnosis of INS (Buishand *et al.*, 2012).

Tissue was homogenised using rotary homogeniser (#SHM2, Stuart) with an additional first step of beta-mercaptoethanol to denature the RNases and obtaining high-quality RNA. Total RNA was then isolated using the RNeasy Mini Kit (Qiagen). To prevent contamination of the samples with genomic DNA, an on-column DNase treatment was performed. RNA concentrations were quantified by spectrophotometry (NanoDrop ND-1000, Isogen Life Sciences).

3.3.3 RNA quality control

Following RNA extraction, RIN were obtained using Agilent 2100 bioanalyzer system and Agilent RNA screen tape (Agilent Technologies, Inc., Santa Clara, CA).

This system determines the integrity of RNA and automatically calculates RNA concentration in relation to the relative ratio of 18S and 28S ribosomal peaks. The RIN software uses a numbering system from 1 to 10, with 1 being the most degraded profile and 10 being the most intact RNA. RIN values above 6.5 were considered acceptable (Soneson *et al.*, 2013) (Figure 3.1) (Appendix 8.3).

Table 3.1 Clinical features and RNA-quality of control samples samples used in this study. RIN, RNA integrity numbers.

Breed	Age (years)	Sex	Type of sample	Type of tissue	RIN value	Concentration (ng/μl)	Abbreviation
Strattforshire	10	Female	Control	Pancreas	7.0	490	**NP4**
Strattforshire	2	Male	Control	Pancreas	7.8	185	**NP1**
				Mediastinal lymph node	7.5	386	**LN1**
West highland	9	Male	Control	Pancreas	7.7	225	**NP2**
				Mediastinic lymph node	9.7	318	**LN2**
Pitbull	2	Male	Control	Pancreas	7.5	240	**NP3**
				Mediastinal lymph node	9.2	354	**LN3**

Table 3.2 Clinical features and RNA-quality of insulinoma samples used in this study. RIN, RNA integrity numbers; DOD, death of disease.[1]

Breed	Age (years)	Sex	Glucose (mmol/L)	Insulin (mIU/L)	DOD	Type of sample	TNM stage	Type of tissue	RIN value	Concentration (ng/μl)	Abbreviation
German longhaired pointer	8	Male	1.0-3.3	Unknown	1	Tumour	I	Pancreas	7.9	130	**P3B**
Irish Soft-coated Wheaten Terrier	11	Male	3.3	31	0	Tumour	I	Pancreas	6.7	217	**BEN**
Flatcoated Retriever	7	Male	3.0	25	LTF	Tumour	II	Pancreas	6.7	100	**N17**
Boxer	7	Male	2.9	Unknown	1	Tumour	III	Pancreas	6.5	275	**H30**
Cocker Spaniel	10	Male	1.6-5.0	Unknown	1	Tumour	IV	Pancreas	6.7	445	**D35**
Scottish shepherd	10	Male	1.5-2.2	Unknown	1	Tumour	IV	Pancreas	7.3	100	**W36**
Boxer	8	Male	3.0	46	LTF	Metastatic	IV	Lymph	7.0	258	**B13**

[1] *Continue next page*

Breed	Age (years)	Sex	Glucose (mmol/L)	Insulin (mIU/L)	DOD	Type of sample	TNM stage	Type of tissue	RIN value	Concentration (ng/μl)	Abbreviation
						Lymph node		node			
Malinois	11	Male	2.2	Unknown	1	Metastatic Lymph node	IV	Lymph node	7.5	168	**SmM**
Crossbreed	9	Male	3.3	Unknown	LTF	Metastatic Lymph node	IV	Lymph node	6.6	144	**SnM**

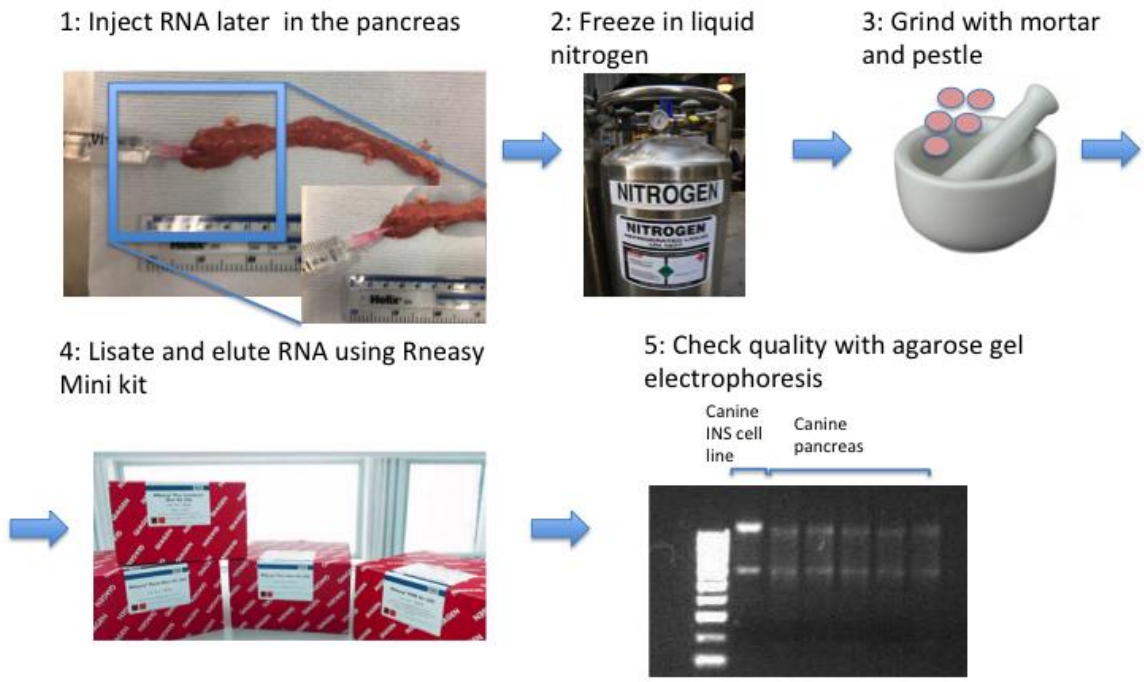

Figure 3.1 Flowchart outlining the pipeline for RNA extraction and quality check for normal pancreatic tissues.

3.3.4 RNA sequencing pipeline

After isolation of high quality RNA (RIN value > 6.5 and concentration >100 ng/µl), samples were processed for mRNA library preparation, sequencing, differential gene expression and functional analysis by Edinburgh Genomics (Edinburgh, UK) (Figure 3.2).

3.3.4.1 Library preparation and mRNA sequencing

Briefly, cDNA libraries were prepared from total RNA, using Tru-Seq Stranded mRNA Library Prep Kit (Illumina) following manufacturer's instructions and were subjected to 75-bp paired-end sequencing on an Illumina HiSeq40000 Platform (Illumina, San Diego, CA) from Edinburgh Genomics service (Edinburgh, UK).

The RNA-seq reads were generated in fastq format. After removing reads containing sequencing adapters and low-quality reads with more than five unknown bases by cutadapt v1.8.3, high-quality reads from the fastq files were mapped to the canine reference genome (CanFam 2.0) (Hoeppner *et al.*, 2014) resulting in around 95-99% sequences mapped using TopHat2 (v3.1.84) with default parameters (Kim *et al.*, 2013). The output files in the compressed binary version of the Sequence Alignment/Map (BAM) were then assembled and counted using HTSeq (v6.0.1) with mode "union" (Anders, Pyl and Huber, 2015).

3.3.4.2 Differential gene expression

Differential gene expression was then carried out using edgeR (version 3.12.0). edgeR estimates the genewise dispersions by conditional maximum likelihood, depending on the total count for that gene. An empirical Bayes procedure was used to shrink the dispersions towards a consensus value. Finally, differential expression was assessed for each gene using an exact test analogous to Fisher's exact test but adapted for overdispersed data. edgeR was chosen for this study as it is the only software that can account for biological variability with only one or two replicates per sample. (Robinson *et al.*, 2010). edgeR software was used for the identification of differences in gene expression of pairwise comparisons organised as follows: (i) normal pancreas against primary INS; (ii) primary INS against metastatic lymph nodes; (iii) normal lymph nodes against metastatic lymph nodes. Genes with less than 20 reads were discarded from the analysis. Genes were considered differentially expressed only at a P-value <0.05 and at FDR < 0.05. Genes with log2-fold changes of more than 2 or less than 2 were then selected to ensure that only robust changes were considered. Differentially expressed genes were identified by hierarchical clustering analysis. In hierarchical clustering, each cluster is subdivided into smaller clusters, forming a tree-shaped data structure or dendrogram. Agglomerative hierarchical clustering starts with the single-gene clusters and successively joins the closest clusters until all genes have been joined into the supercluster (D'haeseleer, 2005). Heatmaps were generated using the package called heatmap.2 in R which normalised counts were used for all differentially expressed genes (cpmall). By default, "heatmap.2" does hierarchical clustering using hclust which further uses euclidean distance matrix. The Euclidean distance is the square root of the sum of the

square differences and takes into consideration the differences between the expression values, considering the solid red gene to be the furthest, and the solid green to be the closest (Gibbons and Roth, 2002). The algorithm is initialised assigning each gene to the cluster to the nearest centroid, which is randomly set at the beginning. Next, the centroids are reset to the average of the genes in each cluster. This process is continued until no more genes change cluster (D'haeseleer, 2005).

3.3.4.3 Functional Annotation

To examine whether certain pathways are over- or under-represented in the gene list, all genes significantly differentially expressed between INS, metastatic lymph nodes and normal tissues, were introduced into GSEA (GSEA version 2.2.2). GSEA employs the (weighted) Kolmogorov-Smirnov (K-S) statistic to test whether genes contributing to the phenotype are 'enriched' in each gene-set (Boerkamp *et al.*, 2013). Thereby, GSEA evaluates how genes in queried pathways are distributed in the fold change ordered list generated by the data. This distribution is quantified by using the Enrichment Score (ES) that evaluates if the members of the pathway are randomly distributed or found at the extremes (top or bottom) of the list (Boerkamp *et al.*, 2013). For each gene set, GSEA looks if differentially expressed genes in a pathway rank are enriched at the top fold change list (up-regulated genes), then the ES will be close to 1. Conversely, if the ES=−1, then genes are enriched at the bottom of our fold change data (down-regulated genes) (Lowes *et al.*, 2010). Also, Reactome (http://www.reactome.org) was performed based on the dysregulated genes that were identified in the RNA-seq datasets.

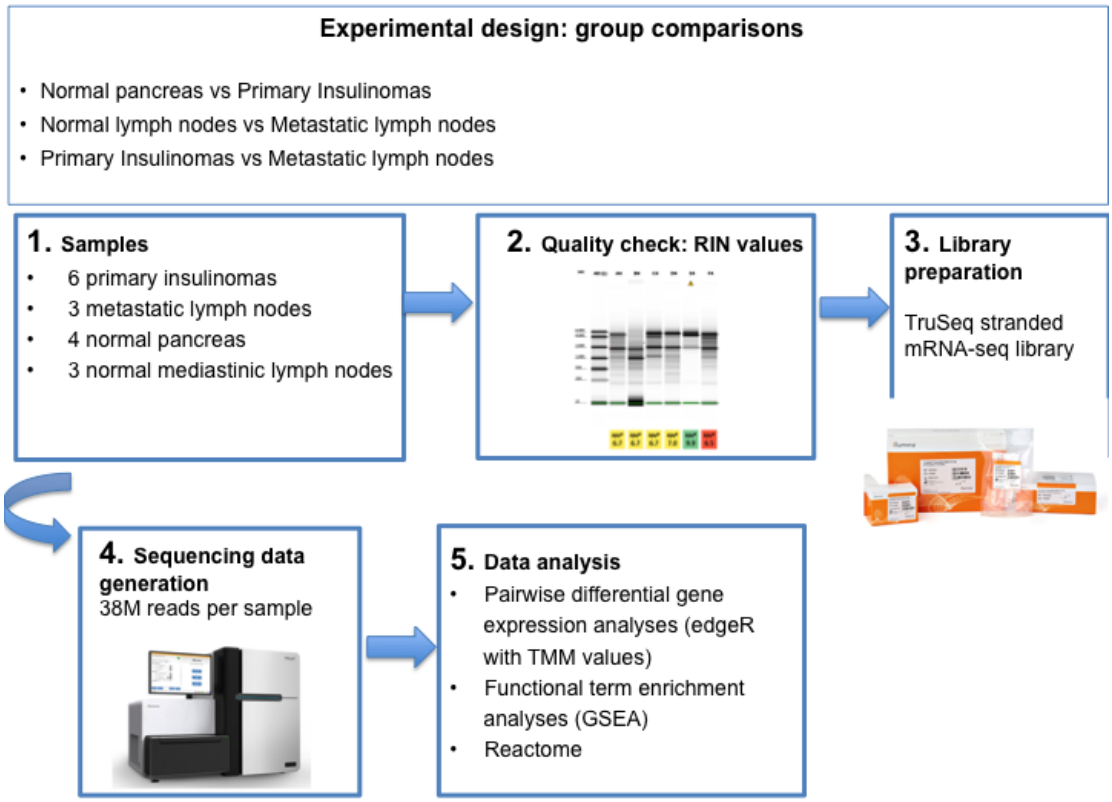

Figure 3.2 Flowchart showing experimental design of RNA sequencing analysis of canine insulinomas.

3.3.5 PCR and agarose gels

PCR reactions were set up using HotStarTaq® DNA polymerase PCR kits (Qiagen, UK) according to the manufacturer's instructions. To ensure consistency, all experiments were performed on the same thermal cycler (Labtech G-Storm GS-4822, France). To assess the consistency of sample loading and PCR conditions between separate experiments, primers that amplified cDNA of transcripts from the canine housekeeping gene glyceraldehyde 3-phosphate dehydrogenase (GAPDH) were included in different reactions. A volume of 12 µL of PCR product was added to 4 µL of 6 X Blue/Orange Loading Dye (Promega, UK). This was loaded into the cell of 1.5% agarose gel. Gels were made by dissolving agarose powder (UltraPure Agarose, Invitrogen) at the stated concentrations in TAE buffer (40 mM Tris, 20 mM

acetic acid, and 1 mM EDTA). A 1.5 Kb DNA ladder (Promega, UK) was used to assess product size. Gels were run for approximately 2 hours and then visualised using a BioRad Molecular Imager GelDoc (BioRad, UK).

3.3.6 Quantitative real-time PCR

Following the outcome of the RNA-sequencing profiling, 13 genes were selected. Selection of these genes was based on significantly differential expression; fold changes and potential biological function in relation to tumour development. (Primers are listed in Table 3.3).

The Platinum Sybr Green qPCR Kit (Invitrogen, UK) was used in all qPCR reactions according to manufacturer's instructions. Reactions were performed on the Stratagene MX3000P (Agilent, UK). Primer efficiency and dissociation curves were calculated using MXPro software (Agilent, UK), specificity was assessed by agarose gel electrophoresis. Each reaction was performed in triplicate and three no-template controls were also included for each primer using nine μL of nuclease-free water. Relative gene expression levels were obtained by normalisation to the expression levels of housekeeping genes (*RPS19* and *GADPH).* Calculations were made using the Delta Delta Ct Method (Pfaffl, 2004).

3.3.7 Statistical analysis

P-values were adjusted for multiple hypothesis corrections using the Benjamini-Hochberg approach, which controls the false discovery rate (FDR). Probesets with FDR<0.05 and log fold change >2 were considered differentially expressed. All analyses were carried out using R programming language (www.R-project.org). GSEA was conducted using GSEA software (http://software.broadinstitute.org/gsea/index.jsp). Power size calculation was made using RNASeqPS tool (https://cqs.mc.vanderbilt.edu/shiny/RnaSeqSampleSize/).

Table 3.3 List of primers for validation of RNA-sequencing data.

Gene symbol	Primer forward	Primer reverse
KRT19	F: GCCCAGCTGAGCGATGTGC	R:TGCTCCAGCCGTGACTTGATGT
HEY1	F: ACCTGAAAATGCTGCACACG	R:GCTGGGAGGCGTAGTTGTTA
SERPINA1	F:CAACGCCACCGCCTTCTTCATC	R:CCCATTTTGCTCAGGACGCTTTTC
PA	F: GGTTCAGATTTCTCCACCC	R: ACTCACAGCATTCCCACAC
PAX4	F:GGCACTGGAGAAAGAGTTCC	R: CTTGAGCTTCTCTTGCCGAC
PDX1	F: TCCCGTGGATGAAGTCTACC	R: CGTGGCCTCGAGATGTATTT
INS	F: CCTTCGTTAACCAGCACCTG	R:CCTTAGGCGTGTAGAAGAAGC
GADPH	F:TGTCCCCACCCCCAATGTATC	R:CTCCGATGCCTGCTTCACTACCT
PNLIP	F:TGTGTGGACTGGAAGAGTGGC	R: ACAAACTGGGCATCGCTGG
IAPP	F:GAGCTGGGAAAGGTGTGAAG	R:ATCCCAAATCTGCTCCTCCT
INSM1	F: TGCTAGTGTTCGCTGTGTCC	R:CCAGACTCCAGCAGTTCACA
RSP19	F: CCTTCCTCAAAAAGTCTGGG	R:GTTCTCATCGTAGGGAGCAAG
SOX17	F: CGACTCTGTTGTGAACCTCC	R:ATAGTTGCAGTAGTACACGGC
NESTIN	F:GGTCTCTTTTCTCTTCCGTCCTAA	R:GACCCACTGAGGATGGACAGA
NKX2	F: TTCAGTACTCCCTGCACG	R: ATTGTCCGGTGACTCGTC

3.4 Results

3.4.1 Quality analysis of RNA-sequencing data

RNA-Seq generated for each sample, between 50 and 110 million 75bp paired-end reads and around 95-99% of the reads were mapped to the canine genome by Tophat2 (Kim *et al.*, 2013).

Multidimensional scaling (MDS) was used as a type of unsupervised clustering to check the quality of RNA-seq data in the three pairwise comparisons. MDA is a plot of the RNA samples in which distances correspond to leading log-fold-changes between each pair of RNA samples (Yang *et al.*, 2014). MDS analysis of the expression profiles (normal pancreas vs primary INS; normal lymph nodes vs metastatic lymph nodes) revealed a separation of the control tissues from the tumour samples in dimension 1 (horizontal) (Figure 3.3). In dimension 2 (vertical) control tissues clustered together whereas tumour samples were heterogeneously distributed (Fig. 3.3). MDS analysis of the expression profiles of tumours and normal samples showed that the normal samples (both pancreas and lymph nodes) formed a homogenous cluster while the tumour samples (primary INS and metastases) were more heterogeneous (Figure 3.3). This observation is consistent with previous findings, thus suggesting that compared with normal tissues, tumours have expression hypervariability caused by DNA hypomethylation blocks (Hedegaard *et al.*, 2014).

3.4.2 Differential expression gene analysis

3.4.2.1 Normal pancreas and primary insulinomas

MDS analysis showed a separate gene profile between normal pancreas and the primary INS (Figure 3.3 A). The primary INS samples represented a heterogeneous group while the normal pancreatic tissues clustered together (Figure 3.3 A). Increased transcriptome heterogeneity among tumours samples compared to the normal tissue may have arisen from expression variability. Using edgeR, genes

showing increased expression variability were identified. P-values, FDR and fold changes were used as selection criteria. Paired statistical tests (P-value < 0.01; FDR<0.05) revealed 3212 genes to be differentially expressed between primary INS and normal pancreas (Appendix 8.4: Table 8.1). When only looking at 2-fold changes or larger, 1900 features remained (1590 upregulated genes and 310 downregulated genes). MA (log ratio versus abundance) plots can be created using the plotSmear function, allowing results to be displayed graphically and highlighting the set of altered genes (Figure 3.4 A). Next, hierarchical clustering analysis of the coding profiles was performed. According to the heat-map, two major clusters were generated between normal pancreatic tissue and primary INS. Interestingly, a trend of transition in the gene expression profiles was observed from the normal pancreatic tissues to the highly metastatic INS lesions (Figure 3.5). Hierarchical clustering showed that primary INS lesion in non-metastatic clinical stage (TNM 1) clustered together with normal pancreatic tissues, separate from primary lesions from patients with malignant metastatic disease (TNM 2,3,4) (Figure 3.5).

As we interrogated the details of the differentially expressed genes many of the upregulated genes are involved in beta cell differentiation [paired homeobox 4 (*PAX4*), NK-homeobox2 (*NKX2*), insulinoma-associated gene 1 (*INSM1*)] and insulin secretion [tetrapanin1 (*TSPAN1*), glucokinase (*GCK*)] or metabolism and transport of the glucose [glutathione peroxidase 3 **(***GPK3*), solute carrier 7 family 1 **(***SLC7A1*)] together with transmembrane proteins (*TMEM130, TMEM59L*) (Table 3.4) (Appendix 8.4: Figure 8.5).

This study showed that genes involved in the secretory pathway of insulin such as insulin (*INS*) and Nestin *(NESTIN)* were highly expressed in INS tissue. Furthermore, genes related to pancreatic development were upregulated such as with Hes-related family BHLH transcription factor 1 (*HEY1),* pancreatic duodenal homeobox 1 (*PDX1*) and SRY-Homeobox 17 *(SOX17)* (Table 3.4)(Appendix 8.4: Figure 8.5).

3.4.2.2 Normal lymph nodes and metastatic lymph nodes

MDS analysis revealed a clear separation in dimension 1 (horizontal) within normal lymph nodes and metastatic ones. On dimension 2 (vertical), normal lymph nodes

formed a homogenous cluster while the metastases were more heterogeneous (Figure 3.3 B). When comparing metastatic lymph nodes with normal lymph nodes, 6,349 features were differentially expressed. In this comparison, when only looking at 2-fold changes or larger, 3876 elements remained of which 2353 genes were upregulated and 1535 were downregulated. An MA plot displayed differentially expressed genes (Figure 3.4 B). According to the hierarchical clustering analysis mediastinal lymph nodes and metastatic lymph nodes formed two separate clusters with different gene expression patterns (Figure 3.6).

3.4.2.3 Primary insulinomas and metastatic lymph nodes

In the unsupervised clustering analysis, primary and metastatic INS did not separate into unique clades (Figure 3.3 C). For instance, primary lesions derived from patients with highly metastatic disease and metastatic lymph nodes had a similar gene profile (Figure 3.3 C). An MA plot graphically showed the differentially expressed genes (Figure 3.4 C). Hierarchical clustering analysis of the coding profiles was then performed confirming that primary lesions derived from patients with highly metastatic disease (TNM stage IV) clustered together with the metastatic lymph nodes (Figure 3.7), as previously seen in the literature (Buishand *et al.*, 2013). When comparing primary INS with metastatic lymph nodes, only 164 genes were differentially expressed with 2-fold changes or larger showing an increased genetic similarity between tumour samples compared to normal tissues (80 genes upregulated and 84 downregulated) (Appendix 8.4: Table 8.2). Relative expression variances showed that acinar-related genes were down-regulated in metastatic lesions including pancreatic lipase (*PNLIP*) chymotrypsinogen B2 (*CTRB2*), pancreatic amylase (*PA*), chymotrypsin-like (*CTRC*) together with epithelial genes [Cytocherathin 19 (*KRT19*)] and serin-peptidase genes [serine peptidase inhibitor, Kazal type 1 (*SPINK1*) and serpin peptidase inhibitor, clade I, member 2 (*SERPINA1*)] (Table 3.5) (Appendix 8.4: Figure 8.6). These results were consistent with previous data that showed that exocrine markers were downregulated in canine INS metastases (Buishand *et al.*, 2013). Furthermore, claudin 10 (*CLDN10*), claudin 19 (CLDN19), and gap junction protein beta 1 (GAPJB1), whose transcripts contribute to the formation of tight junctions, were downregulated in metastatic

lymph nodes (Table 3.5) (Appendix 8.4: Figure 8.6). Additionally, small cytokines previously related to tumourigenesis such as C-X-C motif chemokine receptor 5 (*CXCR5*), chemokine (C-X-C motif) ligand 13 (*CCL13*) and tumor necrosis factor receptor superfamily member 11b (*TNFRS11B*), were upregulated (Table 3.5) (Appendix 8.4: Figure 8.6).

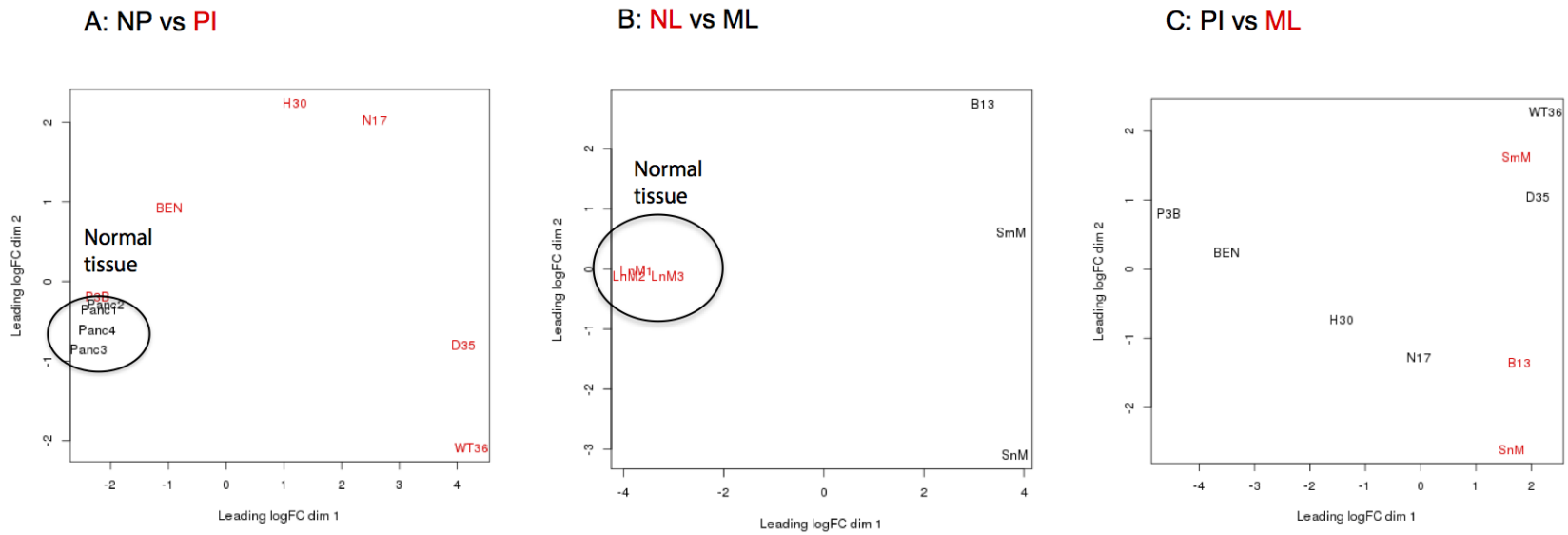

Figure 3.3 Multi-dimensional scaling (MDS) plot of RNA sequencing data of three pairwise comparisons. In MDS plots distances correspond to leading log-fold-changes between each pair of RNA samples. Dimension 1 is the direction that best separates the samples, without regarding whether they are treatments or replicates. Dimension 2 is the next best direction, uncorrelated with the previous one that separates the samples. NP, Normal pancreas: PI, primary insulinomas; NL, normal lymph nodes; ML, metastatic lymph nodes.

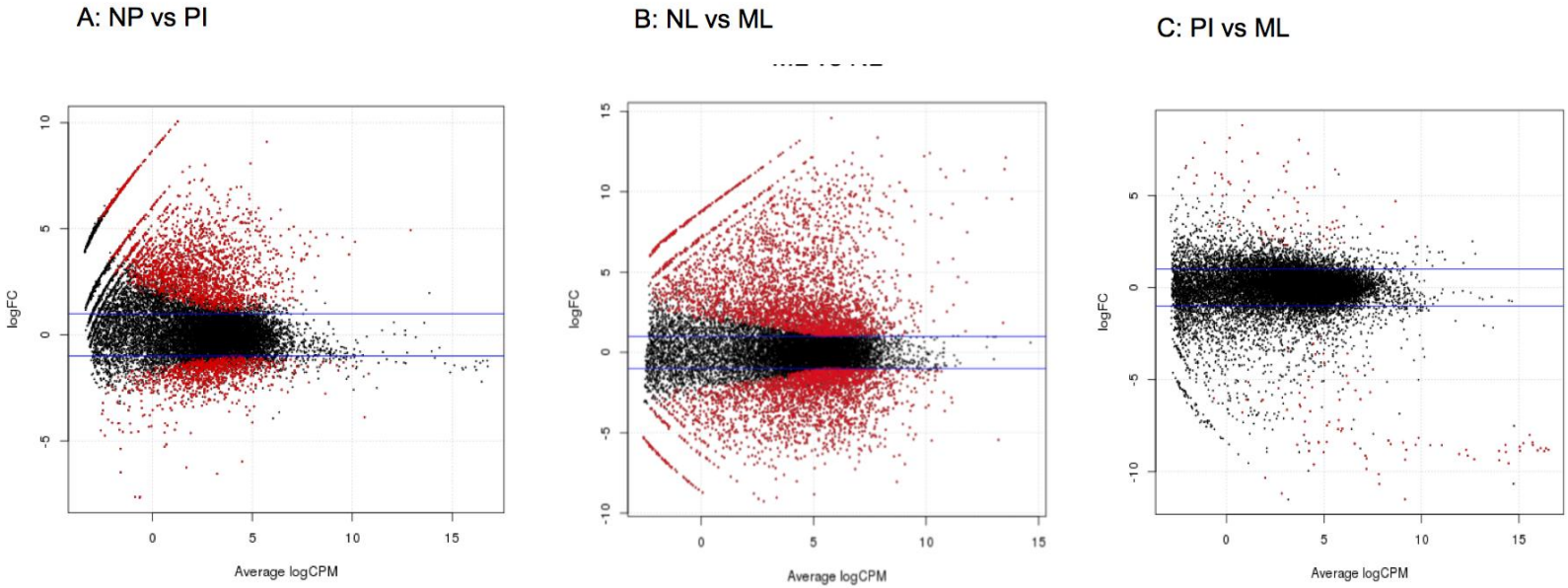

Figure 3.4 Smearplot of RNA sequencing data of three pairwise comparisons. Multidimensional Analysis plot where differential expressed genes results are displayed graphically. For instance, each red dot represents a gene differentially expressed in the comparison between control and sample. The axes of the plot correspond to the logarithm count per milion (logCPM) and Fold change (logFC) columns of the results. NP, Normal pancreas: PI, primary insulinomas; NL, normal lymph nodes; ML, metastatic lymph nodes.

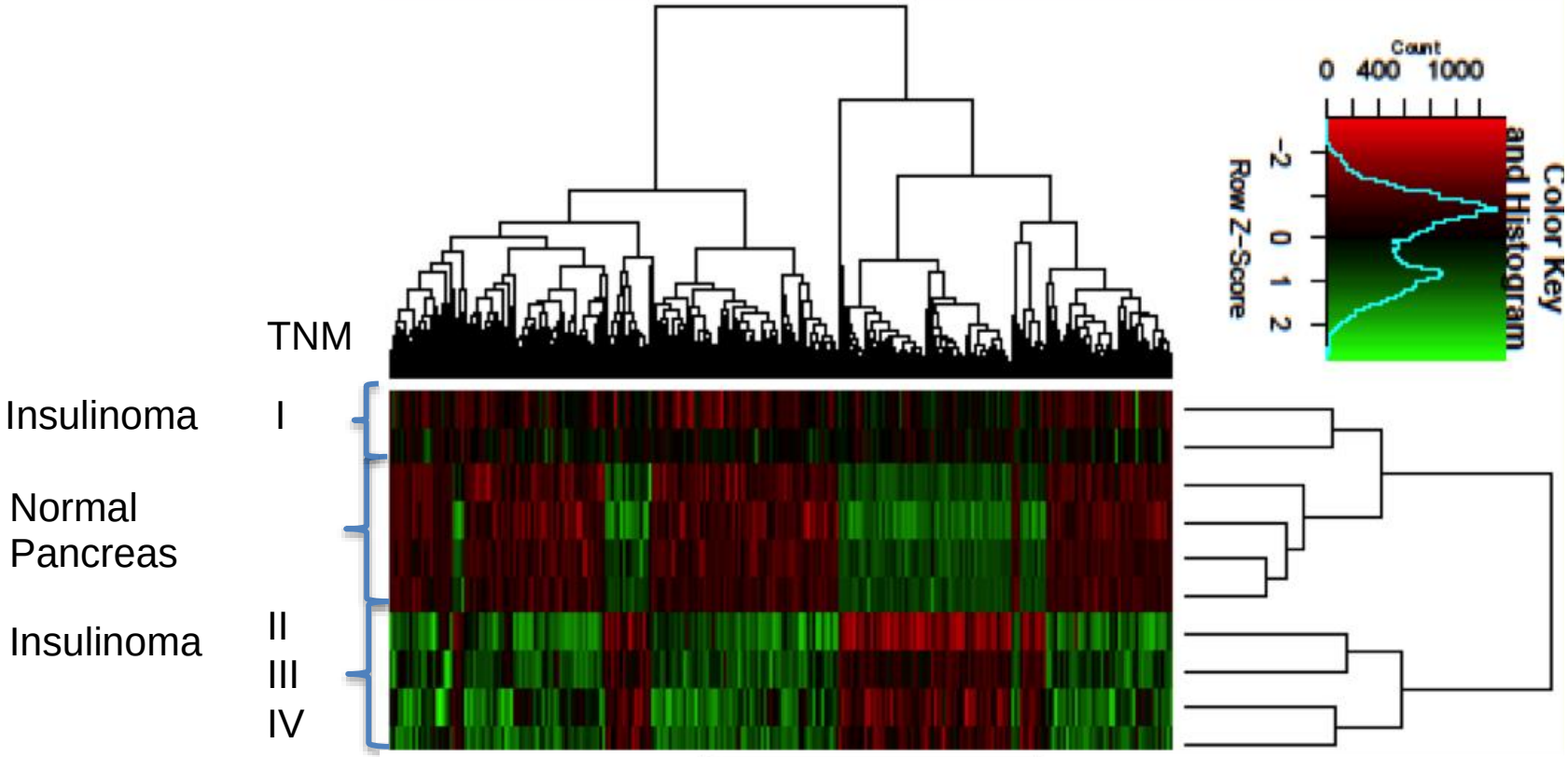

Figure 3.5 Gene heatmap generated using edgeR analysis showing clustering of six primary insulinoma vs four normal pancreas. TNM, Tumour, Node, Metastasis

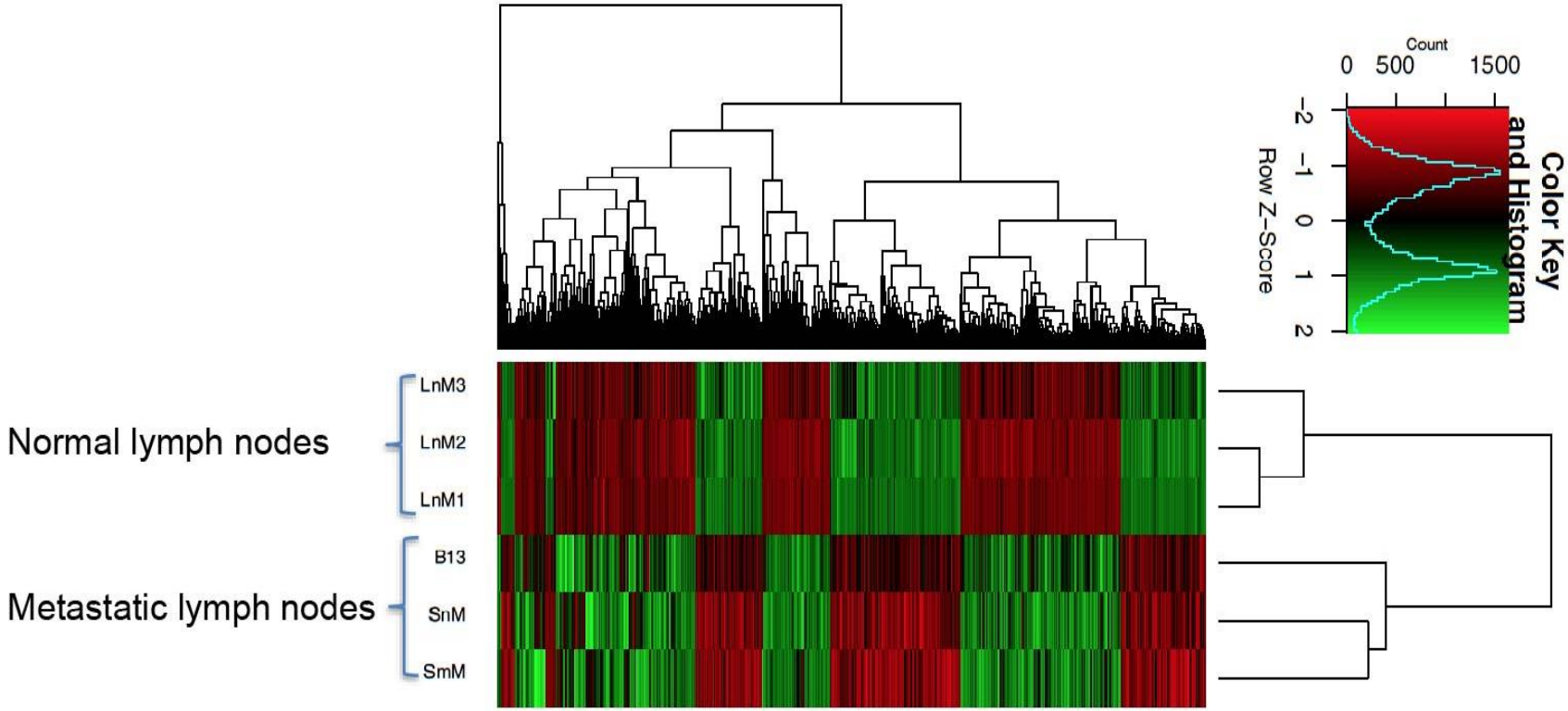

Figure 3.6 Gene heatmap generated using edgeR analysis showing clustering of three metastatic lymph node vs three normal lymph nodes.

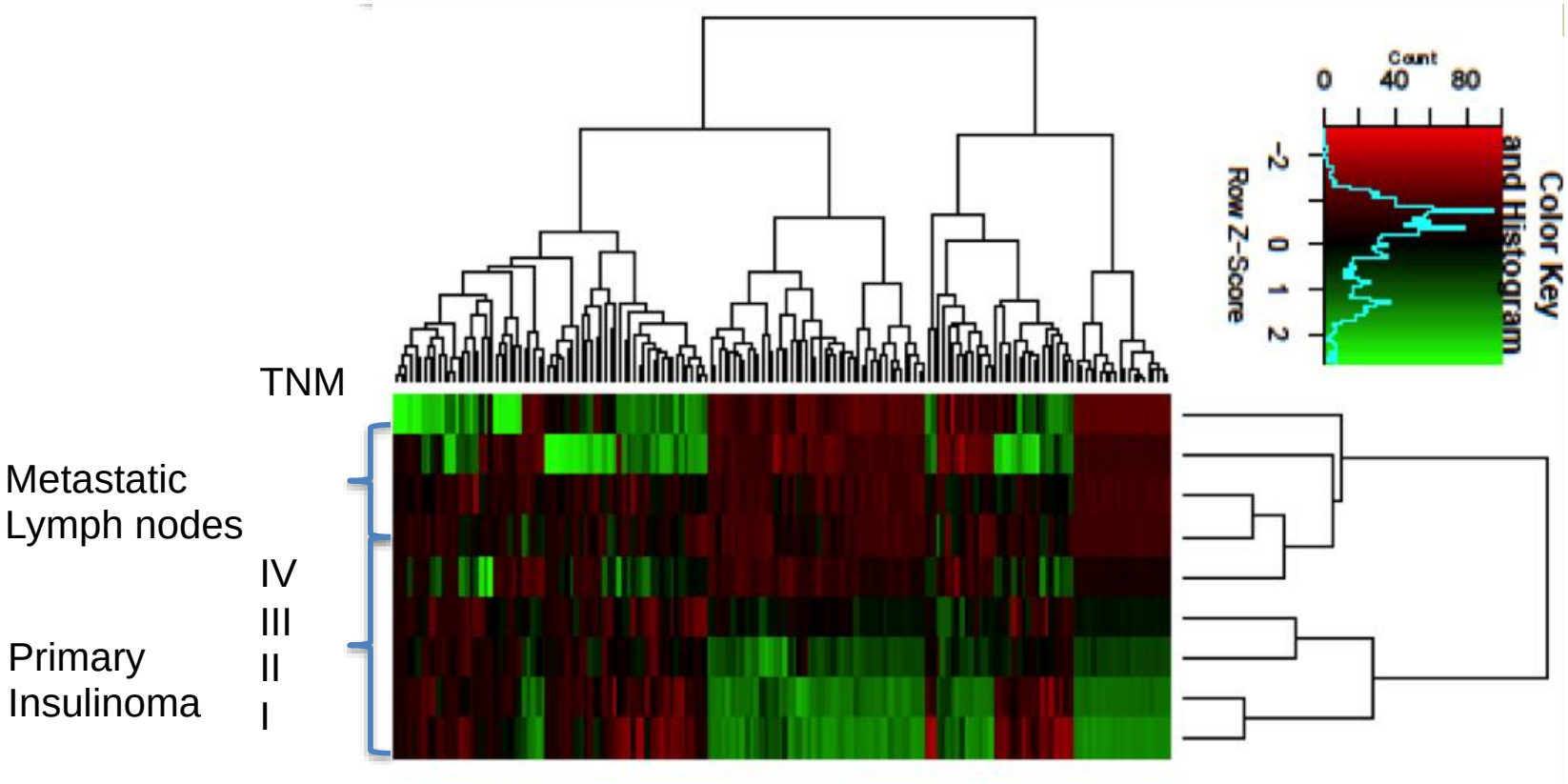

Figure 3.7 Gene heatmap generated using edgeR analysis showing clustering of three metastatic lymph nodes vs six primary insulinomas. TNM, Tumour, Node, Metastasis.

Table 3.4 Top differentially expressed genes in primary insulinoma vs normal pancreas. In bold genes used for validation with qRTPCR.[2]

Gene	Gene symbol	logFC	P-Value	FDR	Role
Pancreatic duodenal homeobox 1	PDX1	2.13	0.0001	0.003	Beta cell differentiation
Paired homeobox 4	PAX4	6.23	3.32E-09	3.92E-06	
Insulinoma associated 1	INSM1	5.021	3.40E-07	5.17E-05	
NK2 homeobox 2	NKX2	5.32	3.40E-09	3.92E-09	
Nestin	NES	2.53	0.0001	0.003	
Delta/notch-like EGF repeating containing ligand	DNER	4.41	3.05E-07	4.83E-05	Early pancreatic development
Notch 2	NOTCH2	3.19	5.17E-07	6.94E-05	
SRY-box 17	SOX17	2.20	0.009	0.04	
SRY-box 18	SOX18	2.89	0.003	0.02	
Hes-related family BHLH transcription factor 1	HEY1	2.46	0.0009	0.01	
RAB37, member RAS oncogene family	RAB37	7.92	6.71E-08	2.00E-05	Cell cycle
Cyclin-dependent kinase 5	CDK5	6.00	8.11E-08	2.16E-05	
Cyclin and CBS domain divalent metal cation transport mediator 1	CNNM1	5.11	6.71E-08	2.00E-05	
Glutathione peroxidase 3	GPX3	4.73	3.91E-08	1.42E-05	Metabolism of glucose

[2] *Continue page 100-102*

Gene	Gene symbol	logFC	P-Value	FDR	Role
Glucokinase	GCK	5.37	3.13E-08	1.23E-05	
Solute carrier 38 family 8	SCL38F8	9.65	9.63E-08	2.35E-08	Insulin secretion
Calcium bynding protein 1	CA1	5.09	1.66E-08	8.82E-06	
Potassium voltage-gated channel subfamily H member 2	KCNH2	5.47	7.40E-09	6.63E-06	
Otoferlin (calcium sensor)	OTOF	5.56	9.07E-08	2.32E-05	
Tetraspanin 1	TSPAN1	5.46	5.95E-08	1.97E-05	Insulin production
Insulin-degrading enzyme	IDE	-2.29	7.33E-06	0.0003	
Insulin growth factor receptor 2	IGF2	4.33	9.30E-06	0.0004	
Insulin like 6	INS	3.21	0.007	0.04	
Insulin receptor	INSR	-2.62	1.00E-07	2.35E-05	
Islet amyloyde polyptide	IAPP	4.37	2.32E-06	0.0001	Amyloid deposit
Prolactin releasing hormone receptor	PRHR	5.94	7.49E-08	2.12E-05	Stimulate insulin production
Transmembrane protein 130	TMEM130	5.46	3.76E-08	1.41E-05	Transmembrane proteins overexpressed in pancreatic cancer
Transmembrane protein 59 like	TMEM59L	4.89	6.88E-08	2.02E-05	
Chromogranin A	CHGB	4.58	1.33E-07	2.79E-05	Pancreatic neuroendocrine tumours markers
Secretogranin II	SCG2	4.97	1.11E-07	2.49E-05	
Synapsin I	SYN1	5.59	7.87E-09	6.68E-06	
Alpha amylase	AMY1A	-7.63	8.93E-09	6.88E-06	Pancreatic exocrine markers

Gene	Gene symbol	logFC	P-Value	FDR	Role
Nerve growth factor	NGR	5.89	6.24E-08	1.97E-05	Signalling molecule in neuroendocrine tissue
Pseudopodium-enriched atypical kinase 1	PEAK1	-3.09	6.10E-09	5.78E-06	Metabolism of glucose
Solute carrier 7 family 1	SLC7A1	-3.03	2.37E-07	4.13E-05	
RELT tumour necrosis factor	RELT	3.93	2.08E-07	3.87E-05	Tumour necrosis factors
C1q and tumour necrosis factor related protein 6	C1QTNF6	5.40	1.00E-07	2.35E-05	
Carbonic anydrase III	CA3	-7.63	3.54E-10	1.30E-06	Lipid metabolism
Integrin-alpha 2 (CD49b)	ITA2	-3.45	2.76E-08	1.17E-05	Cell adhesion

Table 3.5 Top differentially expressed genes in metastatic lymph nodes vs primary insulinomas. In bold genes used for validation with qRTPCR.[3]

Gene	Gene symbol	logFC	P-Value	FDR	Role
Chimotripsinogen 2	CTRB2	-8.72137	0.000178	0.033077	Exocrine markers
Pancreatic lipase	PNLIP	-8.54384	0.000343	0.04279	
Pancreatic amylase	PA	-4.79146	0.000451	0.047458	
Chymotrypsin-like	CTRC	-8.86682	0.000427	0.046186	
Cytocherathin 19	KRT19	-8.38703	0.000115	0.027504	Cell adhesion
matrix metallopeptidase 23B		-4.53596	0.000367	0.044113	
contactin associated protein-like 2		5.298697	8.31E-05	0.02421	
A-kinase anchoring protein 4		-9.34709	0.000102	0.026348	
Serpin peptidase inhibitor, clade I, member 2	SERPINA1	-8.809	0.00035	0.043207	Serine peptidase activity
Serine peptidase inhibitor, Kazal type 1	SPINK1	-8.55149	0.000344	0.04279	
Claudin 10	CLDN10	-7.19894	0.000195	0.034024	Cell junction
Claudin 19	CLDN19	-7.69326	2.40E-05	0.012854	
Gap junction protein beta 1	GAPJB1	5.41801	0.000178	0.033077	

[3] *Continue next page*

Gene	Gene symbol	logFC	P-Value	FDR	Role
adhesion G protein-coupled receptor F4		7.871758	0.000116	0.027504	
transmembrane protein 154		3.598028	2.64E-05	0.012854	
transmembrane protein 252		6.496054	0.000112	0.027179	
C-X-C motif chemokine receptor 5	CXCR5	3.178023	0.000205	0.03415	Inflammation
Chemokine (C-X-C motif) ligand 13	CCL13	4.853102	8.30E-05	0.02421	
Tumor necrosis factor receptor superfamily member 11b	TNFRS11B	3.551235	5.59E-06	0.005778	

3.4.3 RT-PCR Validation of the mRNA sequencing data

Determining the expression levels of 13 representative genes of interest validated the results from the RNA-seq data. Compared with the RNA-seq analysis, quantitative RT-PCR provides a much wider dynamic range (5-6 orders of magnitude) and thus a more accurate measurement of the relative gene expression values (Pfaffl, 2004). Changes in mRNA levels assessed by qRTPCR were concordant with those observed by RNA-seq analysis. When comparing primary INS with normal pancreatic tissues, there was a significant upregulation of genes involved in beta-cell differentiation including *PDX1, INSM1, PAX4, NKX2, SOX17* (Figure 3.8). Moreover, islet amyloid polypeptide (*IAPP*), *NESTIN* and *INS* were upregulated in primary INS compared to control pancreatic tissues (Figure 3.8). Significant down-regulation of acinar genes such as *PNLIP*, *CTRB2*, *PA* and epithelial genes such as *KRT19* was observed when comparing primary INS with metastatic lesions (Figure 3.8).

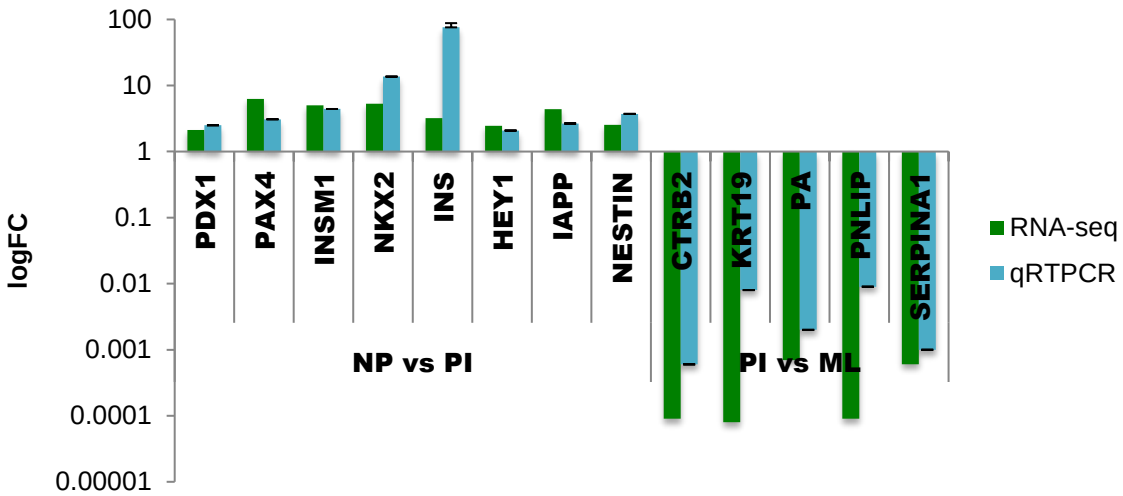

Figure 3.8 qRTPCR validation of RNA-sequencing data on 13 selected genes. NP, normal pancreas; PI, primary insulinoma; ML, metastatic lymph nodes.

3.4.4 Genes commonly differentially expressed between datasets

When merging the three datasets, we revealed that 12 genes were differentially expressed in all of them (Appendix 8.4:Table 8.3). Of interest, CCL13 and

TNFRS11B, were upregulated in both primary INS and metastatic lymph nodes. Moreover, genes involved in cell adhesion [von Willebrand factor A (VWA5A) and adhesion molecule with Ig like domain 2 (AMIGO2)] and extracellular matrix [Fibrilin 2 (FB2)] and genes related to insulin resistance [pappalysin 2 (PAPPA2) and glutamate decarboxylase 3 (GAD3)] and transport of glucose [solute carrier family4 (SCL4A8)] were also upregulated both in primary INS and metastatic lymph nodes (Appendix 8.4: Table8.3).

3.4.5 Functional analysis

3.4.5.1 Normal pancreas and primary insulinomas

To further consider the biological significance of these data, GSEA was used to identify pathways correlated with the malignant INS phenotype. Results of the GSEA revealed that 26 down- and 60 up-regulated pathways were present in this pairwise comparison.

Within the most upregulated pathways in canine primary INS compared to normal pancreatic tissues we identified pathways related to extracellular matrix organisation, cell growth and differentiation, negative regulation of cell apoptosis, beta cell signalling pathway and pancreatic endocrine development, insulin secretion and insulin growth factor (Figure 3.9). The majority of the downregulated pathways were associated with ribosome, transcription and translation of proteins while others were involved in gene regulation such as histone methylation and histone acetylation systems (Figure 3.10). Names of these pathways are listed in Table 8.4 and Table 8.5 in Appendix 8.5.

Reactome analysis confirmed these findings as pathways upregulated in primary INS (30 pathways) were related to four functional clusters: beta cell fate, cell signalling, cell cycle and extracellular matrix organisation (Appendix 8.5: Table 8.6). Of note, analysis with Reactome of the top 100 genes revealed that two major pathways were upregulated in primary INS (FDR<0.05): regulation of gene expression in endocrine-committed (NEUROG3+) progenitor cells (FDR=0.006); regulation of beta cell development (FDR=0.008). Additionally, 15 pathways were downregulated mainly related to protein translation and ribosomal activity (Appendix 8.5: Table 8.7).

3.4.5.2 Primary insulinoma and metastatic lymph nodes

Pathway analysis of the down- and up-regulated genes between primary INS and metastatic lymph nodes revealed significantly downregulated pathways majorly related to ribosome, translation and serine-peptidase activity (Appendix 8.5: Table 8.9). Using Reactome tool, 14 pathways were identified in the downregulated set majorly associated with translation, metabolism and transport of proteins. Interestingly, the only pathway upregulated in metastatic lymph nodes was related to gamma signalling through PI3K gamma. Of note, PI3K pathway has been identified as one of the primary pathway associated with human INS carcinogenesis (Zhan *et al.*, 2012) (Appendix 8.5: Table 8.10).

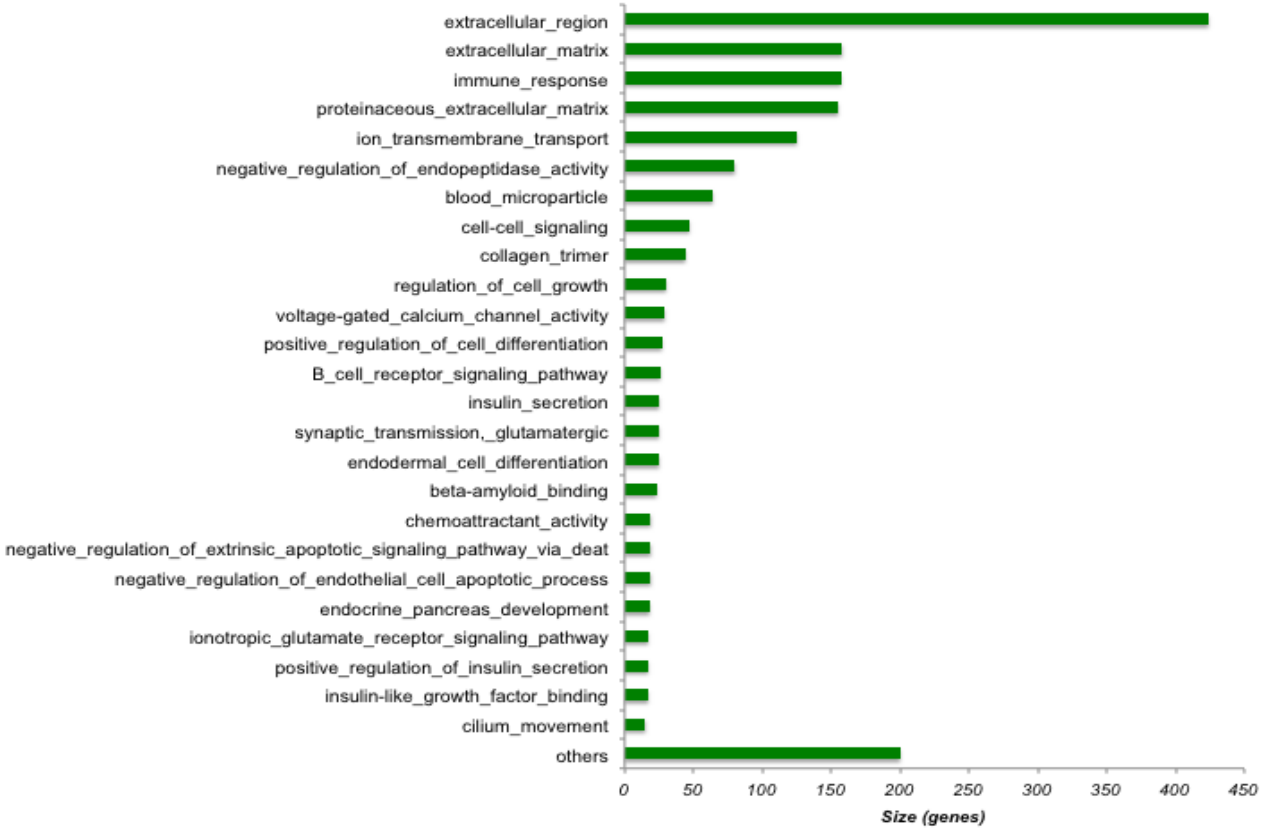

Figure 3.9 Graphs showing Gene set enrichment analysis of up-regulated functions between normal pancreatic tissues and primary insulinomas.

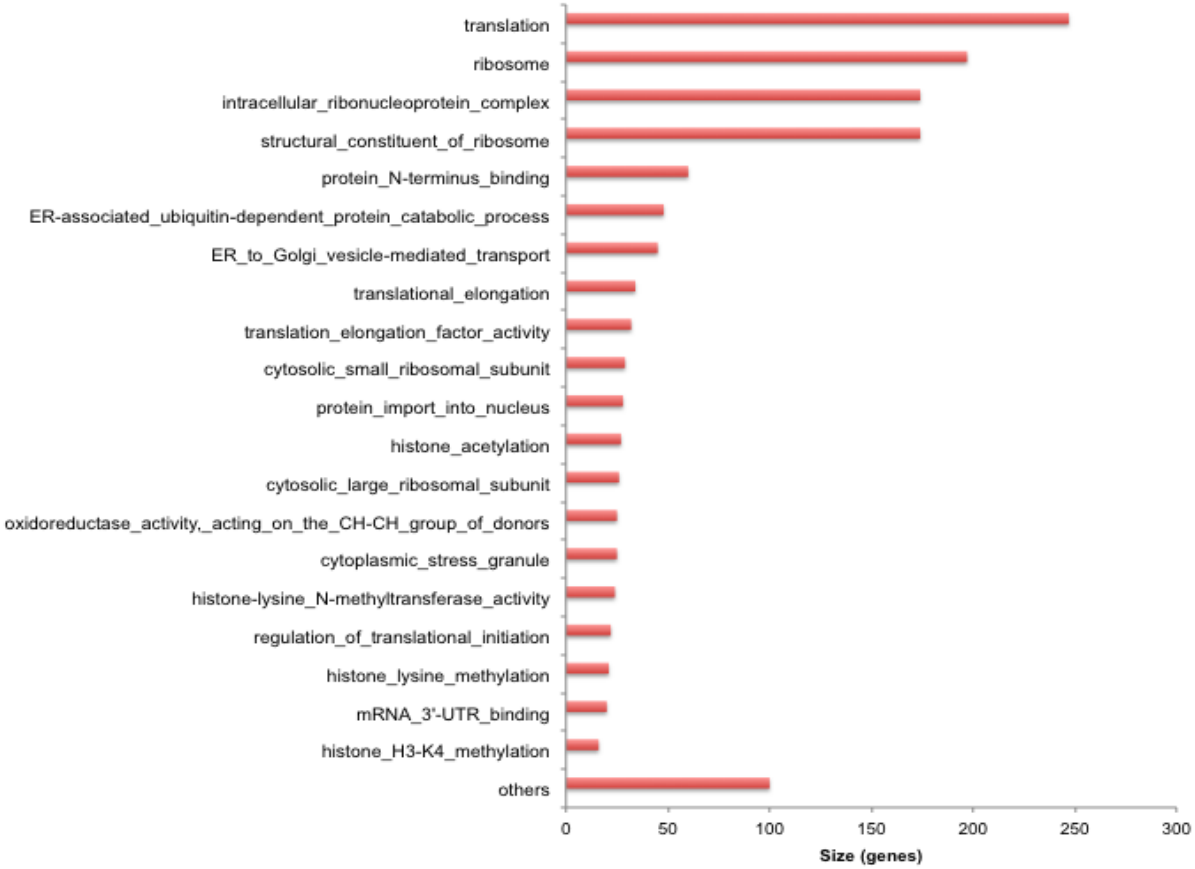

Figure 3.10 Graphs showing Gene set enrichment analysis of down-regulated functions between normal pancreatic tissues and primary insulinomas.

3.5 Discussion

The treatment of metastatic canine INS remains a significant challenge, thus more studies are required to reveal its pathogenesis (Polton *et al.*, 2007; Buishand *et al.*, 2012; Schermerhorn, 2013). Transcriptome analysis is an essential tool for characterisation and understanding the molecular basis of phenotypic variation in biology, including disease (Higgins *et al.,* 2010; Cui *et al.*, 2012; Hedegaard *et al.*, 2014; Lu *et al.,* 2015). Using microarrays, previous studies have identified altered expression of genes and deregulation of gene signalling pathways in primary canine INS and their corresponding metastases (Buishand *et al.,* 2013). However, no studies have yet analysed changes occurring in early stages of the disease. From the literature, significant changes linked to the development of neoplasms often occur in early stage of the disease (Kosari *et al.*, 2005; Tian *et al.,* 2014; Yang *et al.*, 2014; Zeng *et al.*, 2014; Slattery *et al.,* 2017; Zhang *et al.,* 2017). Thus, variations in gene expression was examined by comparing primary INS and metastatic lesions, from a previously characterised cohort of canine INS patients (Buishand *et al.*, 2012,2013), with normal control tissues, such as pancreas and lymph nodes.

Using mRNA profiling with NGS analysis, we identified a panel of differentially expressed genes between control tissues and primary and metastatic INS lesions that might be characteristic of early and late tumorigenesis. Thus, this analysis not only revealed potential therapeutic avenues for the patient in question but also highlighted biological processes of interest for this type of tumours.

Considering that progenitor pancreatic cells and epithelial cells have been involved in INS tumourigenesis (Jonkers *et al.,* 2007; Regitinig *et al.,* 2001; Vortmeyer *et al.,* 2004 Buishand *et al.,* 2013), the normal pancreas was chosen as control tissue instead of isolated beta cells. Previous studies showed that pancreatic islet tumours, including INS, arose not only from beta cells but also from both ductal and acinar cells (Regitinig *et al.,* 2001; Vortmeyer *et al.,* 2004). For instance, Regitinig *et al.,* 2001 described exocrine and ductal features in metastatic lesions of INS due to the presence of pluripotent cells (Regitinig *et al.,* 2001). Additionally, Vortmeyer *et al.,* (2004) demonstrated that initiation of neuroendocrine tumourigenesis in the ductal/acinar system rather than in pancreatic islets, raising the question of whether

analysing only the isolated beta cells would have given us the full complexity of the INS carcinogenesis. In normal pancreas, during embryogenesis, islet cell development appears to be initiated in from primary tubules of epithelial precursor cells (Vortmeyer *et al.,* 2004). Additionally, in the adult pancreas, after injury, islets can regenerate from ductal cells, suggesting that ductal epithelium retain totipotency even in the adult life. Of interest, a plethora of studies have shown that insulin-producing cells can be generated *in vitro* from both exocrine and ductal tissues in anchorage-independent growth conditions (Bayens *et al.,* 2005; Wang *et al.,* 2013; Seyedi *et al.,* 2015). Thus, we hypothesed that tumour initiating cells in INS might be of non-islet origin and might derive from ductal and acinar cells. Thus for this study, the whole pancreatic tissue was considered as a better control compared to the isolated beta cells for evaluating the complexity of the INS carcinogenesis.

Even though we did not use matched sets of samples for the identification of differentially expressed genes, unsupervised clustering of the RNA-seq data separated the tumour samples from non-neoplastic tissues, thus suggesting a good quality of our data. Using edgeR, we evaluated the expression levels of genes in the different pairwise comparisons. edgeR was used as it has the advantage of implementing the method based on negative binominal distribution, and model overdispersion for digital gene expression data even with small replicates (Robinson *et al.,* 2010).

In this study, data showed that between normal pancreas and primary lesions 1900 genes were differentially expressed ($P < 0.01$, and $|\log(FC)| > 2$ and FDR <0.05). These findings suggested that the majority of the changes in gene expression occurred in the early stages of INS carcinogenesis, as previously shown in a variety of human cancer such as, clear cell renal carcinoma (Yang *et al.,* 2014*;* Kosari *et al.,* 2015), pancreatic adenocarcinoma (Zhang *et al.,* 2017), breast cancer (Tian *et al.,* 2014), colon cancer (Slattery *et al.,* 2017). Moreover, the expression of 2300 genes was altered when comparing normal lymph nodes and metastatic lymph nodes, confirming that the metastatic lymph nodes had a gene signature that mostly resembled the neoplastic tissues rather than the normal lymph nodes. When comparing primary INS with metastatic lesions, only 164 genes were differentially

expressed. These findings suggested that primary INS lesions and metastases had a similar gene expression profile compared to non-neoplastic lesions. Previous microarray analyses have shown that primary canine INS lesions with high-metastatic potential cluster together with their correspondent lymph node and liver metastases identifying a homogeneous gene signature (Buishand *et al.*, 2013). These observations proposed that an altered gene expression resulting in metastatic potential in canine INS, might be already identified in the primary lesions.

When interrogating the single differential expressed genes between primary INS and normal pancreas, the upregulated genes were majorly involved in beta cell differentiation and insulin secretion such as *PDX1, INSM1,IAPP. INS, TSPAN1* and *PAX4*. Considering that the prominent characteristic of INS is hyperinsulinism (Goutal *et al.*, 2012), it is not surprising that the predominance of the genes participating in the insulin secretory pathway is upregulated in canine INS tissues. Therefore indicating that regulation of secretion may be a major mechanism by which insulin release is abnormally increased in patients with INS as previously shown in human INS (Wang *et al.*, 2004). Some of these genes, such as *INSM1* and *IAPP*, have been previously reported as negative prognosticator in human NET including PNETs (van Hulst *et al.*, 1999; Fujino *et al.*, 2015, 2017; Rosenbaum *et al.*, 2015). For instance, INSM1 mRNA expression has been previously correlated with metastatic disease in NET (Rosenbaum *et al.*, 2015). INSM1 is a transcription factor involved in the terminal steps of the pancreatic endocrine development. It acts as a transient negative feedback regulator during pancreatic development by regulating the expression of downstream genes, such as *PAX4* and *NKX2*, which are responsible for beta cell differentiation (Lan & Breslin 2009; Osipovich *et al.* 2014). One of the main features that makes INSM1 an interesting target is that it is absent in adult tissues and it is expressed at a high level only in NET and pancreatic progenitors (Lan and Breslin, 2009; Rosenbaum *et al.*, 2015; Fujino *et al.*, 2017). Despite the understanding of INSM1 in basic research, its relevance as a novel prognostic marker in INS remains mostly unclear (Rosenbaum *et al.*, 2015).

Islet Amyloid Polypeptide (IAPP), also named amylin, is the predominant protein component of amyloid deposits in human INS (van Hulst *et al.* 1999). In humans, IAPP is co-produced with insulin by islet beta cells; although, in INS, expression of

the IAPP and insulin are not coupled (van Hulst *et al.*, 1999). Immunohistochemical studies showed that, in dogs, amyloid deposition in INS lesions is uncommon (O'Brien *et al.*, 1987).

According to the data, large clusters of genes functioning in the pancreatic endocrine development were overexpressed. For instance, *PAX4* and *NKX2* were within the top upregulated genes in primary canine INS lesions. PAX4 and NKX2 are expressed in the early pancreas, but are later restricted to beta cells and not expressed in mature islets, suggesting an important role of these genes in differentiation and development of pancreatic islet (Edlund, 2002). Previous studies have already shown that PAX4 mRNA was highly expressed in human INS tissues compared to normal islets (Miyamoto *et al.*, 2001) and that *in vitro* PAX4 plays an essential role in INS cell survival (Brun and Gauthier, 2008) . Furthermore, in this study we identified that the transcript encoding gene necessary for insulin biosynthesis and embryologic pancreatic development, PDX-1, was highly expressed in primary INS tissue. PDX-1 is well known as an essential regulator of many pancreatic endocrine genes such as neurogenin3, insulin, glucokinase, islet amyloid polypeptide, glucose transporter type 2, pancreatic polypeptide and somatostatin, and thus plays a critical role in glucose homeostasis and islet maintenance in the adult pancreas (Baeyens *et al.*, 2005; Srivastava & Hornick 2009; Stevenson *et al.*, 2009; Liu *et al.*, 2012). Interestingly, PDX1 has been previously identified as a therapeutic target for human pancreatic adenocarcinoma and PNETs (Liu *et al.*, 2012).

When comparing primary INS and metastatic lymph nodes, our data showed that acinar exocrine pancreatic enzymes genes such as *PNLIP, PA, CTRC and CTRB2* were downregulated in the metastases, confirming the data previously published by Buishand *et al.*, (2013). Of note, Buishand *et al.*, (2013) speculated that the downregulation of acinar-related genes in metastatic tissues might be related to a decrease in the stem-like cells population in the metastases suggesting that these cells might not be able to migrate (Buishand *et al.*, 2013). Additionally, *KRT19* was downregulated. These findings are also consistent with the results previously shown by Buishand *et al.* 2013. *KRT19,* which encode for CK19 protein, has been proposed as a predictor of survival in human PNETs, including INS (Jonkers *et al.*, 2006). For instance, previous studies showed that CK19 immunoreactivity is useful for

predicting poor prognosis of INS (Sakai *et al.*, 2017). Considering that CK19 is widely expressed in (pre)malignant cells of epithelial origin and it is usually expressed in the exocrine ducts of the pancreas, we can speculate that CK19 may be involved in tumour growth during early stages but plays a minor role in the metastatic spread. Further studies are needed to confirm this hypothesis.

Additionally, tight junctions-related proteins such as claudins were downregulated in metastatic lymph nodes. According to the literature, downregulation of claudins causes loss of cell adhesion, which in cancer is an essential step towards metastatic spread (Zeng *et al.*, 2014). These findings suggest that this mechanism could be important in the development of metastatic disease in INS.

Furthermore, this study revealed that genes involved in the chemokine signalling pathway were overexpressed in metastatic lymph nodes. *CXCL13*, also known as B lymphocyte chemoattractant and its receptor *CXCR5*, were found to be upregulated in the metastatic lymph nodes. Interestingly, CXCL13-CXCR5 network has been already related to tumour growth, migration, and EMT in a variety of cancer such as of colon cancer (Zhu *et al.*, 2015) and breast cancer (Biswas *et al.*, 2014). Notably, targeted disruption of CXCL13 or its receptor CXCR5 in prostate cancer cells impaired their migratory and tumourigenic properties (Garg *et al.*, 2017). Therefore, the in-depth study of the adjustment mechanisms of CXCL13 expression might be beneficial in the development of novel treatments for metastatic canine INS.

On a final note, when we analysed the altered genes in common within the three pairwise comparisons, 15 genes were identified, related to insulin secretion, chemokine activity and cell adhesion. These findings might strengthen our previous speculations on the role of these mechanisms in canine INS carcinogenesis.

Genome analysis provides a large quantity of information concerning molecules that are involved in disease pathogenesis and may be used to interpret diseases (Soneson *et al.*, 2013). While it is not difficult to obtain the gene expression profiles, the extraction of biological insight from such information remains a major challenge. Pathway analysis is a frequently used analytical tool for a better detection of biological processes related to a wide distribution throughout the whole network of genes (Lowes *et al.*, 2010; Yang *et al.*, 2014; Zeng *et al.*, 2014). GSEA compared to

single-gene methods gives a better overwiew of the complex biological altered hubs such as metabolic pathways and transcriptional programmes. GSEA can capture the subtle but coordinated changes in a gene-set and has been commonly used to find important pathways or functions in various diseases and cell conditions from microarray data (Yoon *et al.*, 2016). Reactome is a peer-reviewed pathway database of human pathways that have additional types of annotations to support pathway curation including a variety of biological processes such as signalling, metabolism, transcriptional regulation, apoptosis and synaptic transmission (Croft *et al.*, 2011).

In this project, combined analysis with GSEA and Reactome tools revealed a set of mechanisms dysregulated in primary and metastatic canine INS lesions. For instance, when comparing normal pancreatic tissues and primary INS we identified that the majority of the upregulated pathways were involved in the extracellular matrix organisation, cell growth, beta cell development and insulin secretion.

The extracellular matrix represents a complex network of macromolecules with distinctive physical, biochemical, and biomechanical properties (Lu *et al.,* 2012). Extracellular matrix changes are often seen during cancer progression causing cell migration and metastasis. Importantly, extracellular matrix anomalies also deregulate behaviour of stromal cells, facilitating tumour-associated angiogenesis and inflammation, and thus lead to generation of a tumourigenic microenvironment (Lu *et al.,* 2012). These observations suggest that alterations of the extracellular matrix could potentially be an important mechanism of INS tumourigenesis. Besides, we identified that downregulated functions were mostly related to methylation, ribosome activity, translation and protein and mitochondrial transcription in both primary INS and metastatic lymph nodes. It should be noted that a deregulation in the protein synthesis machinery has been previously related with cancer (Kosari *et al.*, 2005; Yang *et al.*, 2014; Zeng *et al.*, 2014). Cell growth and division require first of all protein synthesis, and for having protein synthesis, the ribosome is necessary. Translation is one of the last steps of gene expression and later synthesis of proteins. A growing body of evidence indicates that the translation process *per se* plays a crucial role in tumorigenesis (Goudarzi and Lindström, 2016). In particular, ribosome plays a pivotal role in the maintenance of the efficiency and accuracy of the translation. It is known that the synthesis of ribosomes is a mechanism regulated

and balanced at multiple levels, and that ribosome proteins (RPs) produced in excess are rapidly degraded in the nucleus (Goudarzi & Lindström 2016; Wei Wang et al. 2016). One of the major mechanisms by which tumour cells alter ribosome biogenesis to drive selective translation of the cancer genome is through rRNA modifications, predominantly methylation on nucleotides in functionally important regions (Truitt & Ruggero, 2016). According to our data, these pathways were downregulated both in primary INS and metastatic lesions. Ribosome activity can have many roles in cancer including apoptosis, cell differentiation, DNA repair mechanisms and cell cycle control (Goudarzi & Lindström 2016; Wang *et al.*, 2016). In particular, it has been previously shown that RPs are necessary for p53 activation and signalling and loss or impairment of RPs may lead to disruption of this tumour suppressor pathway, ultimately leading to carcinogenesis (Wang *et al.*, 2016). Previously, Buishand *et al.*, 2013 demonstrated that the ATM/ATR pathway was downregulated in the high-metastatic group of INS and metastases; thus, they speculated a correlation to an aberrant expression of p53 protein (Buishand *et al.* 2013). According to our data, a decrease in apoptosis and an increase in cell cycle functions have been recorded in primary and metastatic INS. Considering the important role of the mTOR pathway and p53 in human INS tumourigenesis (Zlobec *et al.*, 2006; Zhan *et al.*, 2012), we can speculate that these mechanisms collaborate with an altered ribosome activity to potentially induce INS carcinogenesis in dogs.

Taken together, these findings suggest that downregulation of ribosome function in INS may contribute to ineffective cell cycle arrest and inadequate apoptotic responses after DNA damage. Thus, ribosome biogenesis could be exploited as a target in future INS anticancer therapy given that it can play a key role in INS carcinogenesis (Goudarzi and Lindström, 2016).

3.6 Conclusions, limitations and future directions

In summary, our experimental analyses identified a panel of altered gene expression profiling involved in early and metastatic stage of canine INS progression.

The selection of cases in our study included both staging of the patients and pathologic features. However, the main shortcomings of this study were the small

number of cases enrolled and the lack of matched control and tumour samples. Nonetheless, considering the good quality of the data obtained, this study provided useful guidelines for future analysis on larger-scale. For instance, considering that the total number of genes for testing was around 16000 and minimum average read counts among the prognostic genes in the control group is 150 (maximum dispersion 0.5), if the desired minimum fold change is 2, 35 subjects will have to be studied for each group (power= 0.8, FDR<0.05). Additionally, isolated beta cells could be added to the experimental design for confirming the findings of this study.

In conclusion, further analyses are required to determine the significance of the mechanisms highlighted from this project. Nevertheless, these data suggested that combining differential gene expression with pathway and network analyses could provide, in the future, efficient biomarkers for early cancer diagnosis and treatment planning of canine malignant INS.

4 Isolation and characterisation of insulinoma cancer stem cells in canine and human cell lines

4.1 Abstract

Insulinomas (INS) are the most common neuroendocrine pancreatic tumours in human and dogs. The long-term prognosis for malignant INS is still poor due to a low success rate of the current treatment modalities, particularly chemotherapy. A better understanding of the molecular processes underlying the development and progression of INS is required to develop novel targeted therapies. Cancer stem cells (CSCs) are thought to be critical for the engraftment and chemoresistance of a variety of tumours, including INS. The aim was to investigate isolated INS CSC with a view of developing new treatment strategy.

Highly invasive and tumourigenic human and canine INS CSC-like cells have been successfully isolated based upon their sphere-forming ability and the presence of specific stem cell surface marker (CD34; CD133; CD90; CD24). These cells express stem cell markers (OCT4, SOX9), and exhibit greater resistance to chemotherapeutics commonly used in human INS therapy. Importantly, these cells have a greater invasive and tumourigenic phenotype *in vivo* compared to non-CSCs. Results show that CSCs can be isolated from human and canine INS and they could be the drivers of the malignant behaviour of this tumour.

4.2 Introduction

INS is the most commonly diagnosed neuroendocrine pancreatic tumour in dogs and humans (Corroller *et al.*, 2008; Schermerhorn, 2013). In humans, INS are often benign and can be effectively treated by surgical excision (Anlauf *et al.*, 2009; Mathur *et al.*, 2012). However, a subset of human INS exhibits cellular characteristics and clinical behaviour consistent with malignancy and these are referred to as 'malignant INS' (Jonkers *et al.*, 2007; Baudin *et al.*, 2014). Because of the low incidence of human INS (four cases per million population per year), the availability of research material is limited, especially for malignant subtypes (Callacondo *et al.*, 2013). Therefore previously, investigators have analysed changes in gene expression of malignant INS mainly as part of broad studies on PNETs (Speel *et al.*, 1999; Zhao *et al.*, 2001; Sakai *et al.*, 2017). However, PNETs represent a heterogeneous group of tumours and therefore, the specific tumourigenesis of INS is still poorly understood. Canine INS are classified as malignant tumours in 95% of the cases due to the outgrowth of micrometastases in liver and lymph nodes (Buishand *et al.*, 2010). In the dog, the biological course of INS most often resembles that of malignant INS in humans (Buishand *et al.*, 2012; Goutal *et al.*, 2012; Schermerhorn, 2013). As in humans, canine patients with malignant INS often present relapse episodes of hyperinsulinaemia that can cause severe hypoglycaemia even after resection of the tumour (Jonkers *et al.*, 2007; Goutal *et al.*, 2012). Due to the recurrence of the hypoglycaemic symptoms, many clinical challenges are faced in the treatment of both human and canine malignant INS. For this reason, new therapeutic strategies are necessary to improve the prognosis of patients with this disease.

The hypothesis of this study is that the malignant behaviour of INS is driven by a subpopulation of CSCs. According to the CSC hypothesis, different cell populations reside within a tumour including cancer cells with more malignant features that can drive tumour growth and are able to form tumours in animal models (Abetov *et al.*, 2015). Growing evidence supports the notion that this small subset of treatment-resistant cells called CSCs are uniquely capable of resisting the effects of conventional chemotherapeutics and thereby survive for a long time, resulting in

tumour recurrence, metastasis and poor prognosis (Alison *et al.*, 2011; Pang *et al.*, 2012; Mitra *et al.*, 2015). Thus, eradication of these cells is necessary for the better treatment of patients diagnosed with cancer (Guo *et al.*, 2006; Stevenson *et al.*, 2013; Abetov *et al.*, 2015; Ran *et al.*, 2017). Despite the growing evidence to support the existence of CSCs in a wide array of solid tumours, a comprehensive characterisation of INS CSCs has not yet been reported. Previous immunohistochemical studies have identified a small population of cells with stem cell characteristics within human and canine INS (Ordonez, 2001; Buishand *et al.*, 2013). These cells are called amphicrine cells and are characterised by the co-localisation of both endocrine and exocrine markers (Ordonez, 2001). Previous studies have demonstrated that CSCs can be isolated using ALDH activity in GEP-NETs (Gaur *et al.*, 2011). Moreover, recent studies have identified CD90 as a potential marker for CSCs in human PNETs (Krampitz *et al.*, 2016) and specifically in human INS cell line (Buishand *et al.*, 2016). However, there are no consensus markers available to identify INS CSC-like cells and additionally, recent studies show that several CSC populations may reside within one tumour (Hou *et al.*, 2014; Krampitz *et al.*, 2016).

Considering the close resemblance of canine INS to human malignant INS, from a comparative oncology perspective, which aims to utilise spontaneous tumours in pet animals as natural models for the study of human cancer biology and therapy (Gordon *et al.*, 2009), canine INS represents an interesting study model for human malignant INS. Using a comparative oncology approach, the first goal of this study was to isolate human and canine enriched INS CSC populations and characterise their malignant behaviour and their role in INS carcinogenesis.

The ability to purify different populations of cells and assess their *in vitro* and *in vivo* behaviour presents unique challenges to obtaining a viable single cell suspension. As said previously, the hallmark traits of CSCs include their heterogeneity, interaction with microenvironments and plasticity (Zhao, 2016). The CSC model is a dynamic one with a functional subpopulation of cancer cells rather than a stable cell population responsible for tumour regeneration (Dean *et al*., 2005; Blacking *et al.*, 2007; Islam *et al.*, 2015). As such it is crucial to optimise each isolation step to maximize yields (Pastrana *et al.*, 2011). Therefore, in this chapter two separate *in vitro* methods will be used to isolate INS CSCs: 1) an enriching INS sphere forming

method, based on enrichment of a heterogeneous population of INS CSCs; 2) an isolation method, based on isolating a single well-defined population of CSCs.

4.2.1 Isolation of INS CSCs based on sphere forming ability

CSCs have been efficiently enriched using their sphere-forming ability in a plethora of studies (Michishita *et al.*, 2011; Pastrana *et al.*, 2011; Pang *et al.*, 2012; Gao *et al.*, 2014). The sphere-forming assay is an *in vitro* assay based on the assumption that only individual CSCs will survive serial passages under non-adherent conditions (Pastrana *et al.* 2011). Often stem-like cells are cultured in low-density anchorage-independent growth conditions, in media supplemented with EGF, hydrocortisone, insulin, progesterone, and/or heparin, in the absence of FBS (Franco *et al.*, 2016). Therefore, the sphere-forming assay is often used to evaluate the stem-like properties of cancer cells (Pastrana *et al.*, 2011; Franco *et al.*, 2016). It is estimated that approximately 1% of tumour cells give rise to tumorspheres (Blacking *et al.*, 2007; Pang *et al.*, 2012). In order to characterise whether tumorspheres actually represent a subpopulation of undifferentiated cells, the expression of embryonic stem cell markers is usually evaluated. OCT4 and NANOG are most widely used for this purpose, as they are transcriptional determinants essential for self-renewal and maintenance of the undifferentiated state (Wilson *et al.*, 2008). Members of the SOX transcription factors family, such as SOX2 and SOX9, are also commonly used as markers of a stem cell-like state (Seymour *et al.*, 2007; Fridriksdottir *et al.*, 2011). Highly invasive and tumourigenic INS CSCs were enriched from both canine and human INS cell line contributing to the evidence that these subset of cells might be involved in the malignant behaviour of canine and human malignant INS.

4.2.2 Isolation of INS CSCs based on stem cell surface markers

CSCs are a rare subset of tumour cells that bear properties of stem cells (Guo *et al.*, 2006; Alison *et al.*, 2011; Magee *et al.*, 2012; Lee *et al.*, 2017). Considering the close remsemblance within CSCs and stem cells, stem cell-associated surface markers are frequently used to isolate and analyse the functional behaviour of purified CSC

populations (Pastrana *et al.,* 2011). To date, researchers have identified a few surface markers that enrich various CSCs from a primary tumour for the majority of cancer types (Fan *et al.,* 2010; Hou *et al.,* 2014; Zhu *et al.,* 2014; Sukowati *et al.,* 2015; Lubeseder-martellato *et al.,* 2016). In some cases, these are well-established markers of normal stem and progenitor cells (for example, CD34 in the haematopoietic system)(Guo *et al.* 2006). For others (e.g. CD133, CD44) the situation is less clear (Zhao 2017). According to previous studies a set of stem cell surface markers have been most commonly associated with pancreatic stem cells, pancreatic tumours, NET and specifically PNETs, such as CD90, CD34, CD24 and CD133 (Stevenson *et al.,* 2009; Gaur *et al.,* 2011; Zhu *et al.,* 2014; Krampitz *et al*., 2016; Lubeseder-Martellato *et al.,* 2016; Lee *et al.,* 2017). Therefore, in this chapter, the potential of these stem cell surface markers will be explored as valuable tools to isolate human and canine INS CSCs.

CD90 is a glycophosphatidylinositol anchored cell surface protein. CD90 is a marker of human hematopoietic stem cells and a regulator of proliferation, metastasis, and therefore it is a potential candidate marker for CSCs (Kumar *et al.,* 2016). For instance, immunohistochemical studies on pancreatic adenocarcinoma revealed that CD90 is an important prognostic marker as its expression is related to highly metastatic cancers (Zhu *et al.,* 2014). Moreover, previous studies reveal that CD90 expression marks a subset of tumour-initiating cells within PNETs (Krampitz *et al.,* 2016). Interestingly, a recent study has shown that CD90 has a role also in human INS (Buishand *et al.,* 2016). Buishand *et al.,* (2016) demonstrated an increased tumour-initiating potential in athymic nude mice when CD90+ CM cells were injected (Buishand *et al.,* 2016). They demonstrated that anti-CD90 monoclonal antibodies decreased the viability and metastatic potential of injected cells in a zebrafish embryo INS xenograft model (Buishand *et al.,* 2016). However, very little is currently known about CD90 signalling capabilities, and potential ligands are poorly characterised. Furthermore, many controversies have arisen from the use of CD90 as a CSC marker, due to its lack of specificity in isolating CSCs and also its action as a tumour suppressor in different types of tumours (Kumar *et al.,* 2016).

CD34 is a cell surface sialomucin and the first CSC marker recognised in acute myeloid leukaemia (Alison *et al.,* 2011). The expression of CD34 is associated with pancreatic ductal progenitors (Stevenson *et al.,* 2009) and epithelial stem cells (Blanpain *et al.,* 2004). Although its function has not been fully elucidated the consensus view in haematological malignancies is that the CD34+CD38− signature does identify most CSCs in acute myeloid leukaemia (Alison *et al.,* 2011). Since then a range of malignant tumours has been associated to CD34-committed stem cell precursors including gastric cancer (Xu *et al.,* 2015), mammary tumours (Rybicka *et al.,* 2016) and osteosarcoma (Pang *et al.,* 2012). However, its role in cancer development remains unclear, yet it is of particular interest since CD34 expression serves as a CSC marker.

CD24 is a glycosylphosphatidylinositol-linked cell surface protein originally discovered in leucocytes (Lubeseder-martellato *et al.,* 2016). CD24 regulates cell motility and invasion and its expression is often related to haematopoietic cells and some neuronal and epithelial tissues (Lubeseder-martellato *et al.,* 2016). CD24 has been frequently used on its own or in combination with others to isolate CSCs in various type of cancer such as breast cancer (Ricardo *et al.,* 2011) and pancreatic adenocarcinoma (Skoda *et al.,* 2016). Pei *et al.,* (2016) have also shown that CD24 is upregulated in various stages of pancreatic intraepithelial neoplasia (Pei *et al.,* 2016)
.

CD133 (Prominin-1) is a pentaspan transmembrane glycoprotein. CD133 has been extensively associated in the literature with CSCs in a plethora of tumours, such as glioblastoma (Fan *et al.,* 2010), pancreatic adenocarcinoma (Hou *et al.,* 2014), prostate carcinoma (Kalantari *et al.,* 2017) and melanoma (Argaw-Denboba *et al.,* 2017). For instance, in pancreatic adenocarcinoma, the expression of CD133 was associated with a lower 5-year survival rate (Hou *et al.,* 2014). Sakai *et al.,* (2017) have recently shown that CD133 expression appeared significantly associated with unfavorable pathological features and shorter disease-free periods in a subset of well-differentiated PNETs, thus representing a valuable predictor for clinical outcomes (Sakai *et al.,* 2017).

Results from this study suggested that canine INS CSCs could be isolated using both isolation and enrichment methods. According to our data, both CD133 and CD34 represented valuable markers for isolating chemoresistant INS CSCs in canine INS cell line. Whereas, it was not possible to isolate chemoresistant INS CSCs from human INS cell line using the surface markers tested in this study.

4.3 Materials and methods

Basic methodological descriptions and brands not stated here are presented in Chapter 2. Specific materials and methods of this chapter are herebin described.

4.3.1 Sphere-formation assay

The sphere forming ability of human and canine INS cells was determined following the protocol described in section 2.1.7.

4.3.2 Drug treatment of cells

Cells were treated with 5-Fluorouracil (5-FU) (Tocris, R&D System, Canada) diluted in DMSO over the indicated range of concentrations. Equal volumes of the vehicles were used as control. The chemosensitivity of the cells was evaluated using cell profileration assays as described in section 2.1.8 and colony formation assays as described in section 2.1.9.

4.3.3 Magnetic cell sorting (MACS)

CD34 MicroBead Kit UltraPure, human (130-100-453) and CD133 MicroBead Kit, human–lyophilized (130-097-049) have been used to MACS sort the human and canine INS cell lines.

Cells were labelled with CD34 or CD133/1 microbeads and sorted using the Miltenyi Biotec CD133/CD34 cell isolation kit according to the manufacturer's protocol (Miltenyi Biotec, UK). Briefly, 1x 10^7 cells were resuspended in 300 μL of chilled separation buffer (PBS + 5% of BSA). One hundred μL of FcR blocking reagent and 100 μL of CD133 MicroBeads were added and the solution was incubated for 30 minutes at 4°C with rotation. The cells were washed by adding 5 mL of cold separation buffer and centrifuged at 300 x g for 10 minutes at 4°C before being resuspended in 1 mL of separation buffer and transferred to a pre-washed LS separation column mounted on the magnetic separator.

Thereafter, cells were added to a pre-washed magnetic separation (LS) column on the magnetic holder. The column was washed in order to collect the negative fraction. The column was removed from the magnetic holder and the positive fraction was collected. The column was washed three times to collect the negative fraction. The column was removed from the magnetic holder and the positive fraction was collected adding 5 mL of separation buffer. The labelled and unlabelled fractions were counted and seeded at required densities for cell culture, or fractions were pelleted and snap frozen for RNA or protein analysis.

4.3.4 Flow cytometry and Fluorescence-activated cell sorting (FACS)

Cells have been sorted using the protocol as described in section 2.5.

Briefly, CM and canINS were detached by trypsinisation, washed with PBS and subsequently incubated with labelled phycoerythrin (PE-Cy5)-conjugated CD90 monoclonal antibody at the dilutions indicated by the manufacturers at 4°C for 30 minutes in the dark. The antibodies used were anti-human CD90-PE-Cy5 (BD Biosciences, USA) and PE-Cy5-labeled isotype-matched immunoglobulin was used as a negative control (Appendix 8.7: Figure 8.9 and Appendix 8.8: Figure 8.15 and Figure 8.16).

A different protocol has been followed to stain cells with the cell surface marker CD34 (Appendix 8.7: Figure 8.10) and CD24 (Appendix 8.7: Figure 8.11; Appendix 8.8: Figure 8.15 and Figure 8.16). After fixation and washing with PBS, cells have been incubated with labelled phycoerythrin (PE)-conjugated monoclonal antibodies

at the dilutions indicated by the manufacturers at 4°C for 10 minutes in the dark. The antibodies used were anti-mouse IgG2a CD34-PE (Miltenyi Biotec, Surrey, UK) and anti-mouse IgG1k CD24-PE (Miltenyi Biotec, Surrey, UK). PE-labeled isotype-matched immunoglobulin was used as a negative control. An unstained sample of cells was used as a negative control for all the experiments. Sytox blue (Invitrogen, UK) was used as a dead cell discriminator and added at 1:1000 dilution before processing the samples in BD Fortessa or FACS-Aria flow cytometers (BD Biosciences).

4.3.5 RNA extraction and quantitative Real Time PCR

Basic methods for RNA extraction and qRT-PCR are described in section 2.2. Total cellular RNA was extracted using RNeasy® kit (Qiagen, CA, USA) and RNA quality was determined by A260 measurement. Total RNA was reverse transcribed using the Omniscript™ RT Kit (Qiagen, CA, USA) according to the manufacturer's instruction. qRT-PCR was performed with the primers listed in Table 8.11 and Table 8.12 (Appendix 8.6) using the Stratagene M63000p qRT-PCR system (Aligent, CA, USA), and the PlatinumH SYBRH Green qRT-PCR SuperMix-UDG (Invitrogen, CA, USA) according to manufacturer's instruction. Relative gene expression levels were obtained by normalisation to the expression levels of housekeeping genes (canINS: *Rps5* and *Gapdh*; CM: *HPRT* and *GAPDH).* Calculations were made using the Delta Delta Ct Method.

4.3.6 Chorioallantoic membrane assay (CAM)

The tumour forming and invasive ability *in vivo* of human and canine INS cells using CAM assay was determined following the protocol described in section 2.1.10.

4.3.7 Invasion assay

The invasive ability of cells was determined using the QCM™ collagen-based cell invasion assay kit (Millipore, MA, USA) according to the manufacturer's instructions. Briefly, cells were seeded into the upper inserts at 1×10^5 cells per insert in serum-free RPMI. Cells were incubated at 37 °C with 5% CO_2 for 48 hours. Non-invading cells were removed. Cells that migrated through the gel insert to the lower surface were stained and quantified by colorimetric measurement at 560 nm. Images were taken using a Nikon Eclipse Ni Brightfield Microscope and thereafter processed with Zeiss pro image software (Zeiss).

4.3.8 Insulin and C-peptide ELISA kit

CM and canINS cells were passaged up to 25 times for the adherent and 15 times for the spheres. Aliquots of medium were collected at several time points. Insulin released into the medium was measured by an ultrasensitive human/porcine/canine Insulin Quantikin ELISA kit (R&D System, Minneapolis, USA) according to the manufacturer's instructions. C-peptide released into the medium was measured by an ultrasensitive canine C-peptide ELISA kit (AMSBiotechnology, Abingdon, UK) according to manufacturer's instructions.

4.3.9 Statistical analysis

Statistical analysis was performed following the methodology described in section 2.6.

4.4 Results

4.4.1 CSCs are enriched in human and canine INS spheres

Tumorspheres have been cultured using an optimised protocol for both canine and human INS cell lines. Cells have been passaged for at least five times before testing into different assays as previously described (Pang *et al.*, 2011, 2014). Canine (canINS) (Figure 4.1 A) cells gave rise to wheel-shaped and well-rounded spheres (Figure 4.1 B-C), whereas human (CM) (Figure 4.1 D) spheres had an irregular shape and appeared like agglomerates of cells (Figure 4.1 E-F). canINS CSCs tended to cluster quite tightly and formed larger (up to 200μm of diameter) but fewer spheres (Figure 4.1 B-C) compared to CM, which presented small but numerous tumorspheres (Figure 4.1 E-F). It was possible to culture both human and canine tumorspheres for extended passages (up to 15 passages).

After isolation we characterised our INS CSC enriched tumorspheres on their multi-differentiation potential and the expression of stem cells markers such as *OCT4* and *SOX9*. *OCT4* was not only a transcription factor determinant of pluripotency of embryonic stem cells but it has also been associated specifically with pancreatic endocrine precursor cells (Wang *et al.*, 2009). *SOX9* was a specific pancreatic stem cell marker, responsible for the maintainance of pancreatic progenitor pool (Seymour *et al.*, 2007). Protein analysis showed that the expression of both markers was increased in canINS (Figure 4.1 G) and CM (Figure 4.1 H) tumorspheres compared to parental adherent cells.

Gene expression levels of a number of CSC-associated genes was evaluated including stemness markers (*OCT4, NANOG, STAT3, SOX2, SOX9),* stem cell surface related markers (*CD133, CD24, CD90, CD34, CD44),* epithelial-mesenchymal transition markers (*SNAIL, VIMENTIN*), growth factor receptors (*EGFR, LIFR, GHR, IGFR),* Notch signalling pathway receptors and target genes (*NOTCH1-4, JAG1-2, HEY1, HES1*), and pancreatic neuroendocrine and exocrine markers (*PA, PNLIP, PDX1, ISL1).* Pancreatic progenitors markers *OCT4, SOX2, SOX9* were upregulated in human and canine INS CSCs (Figure 4.2 A). Stem cell associated surface markers (*CD133, CD90, CD34, CD24*) were overexpressed in

human and canine INS (Figure 4.2 B). Pancreatic exocrine (*PNLIP*) and endocrine (*ISL1* and *INS*) markers were overexpressed at the RNA level in human and canine spheres (Figure 4.2 C). *NOTCH2 and HES1* were significantly upregulated in both human and canine INS tumorspheres compared with the adherent population. Additionally, target genes of the Notch pathway, such as *HEY1* and *SNAIL1*, demonstrated a trend of upregulation in both human and canine spheres. No significant differences in gene expression were recorded for *NOTCH1,* whereas *NOTCH3* and *NOTCH4* showed a trend to downregulation in canine and human INS spheres (Figure 4.2 D). No significant differences in gene expression were recorded for mesenchymal markers such as *VIMENTIN* and *CD44* in human spheres, whereas both markers were downregulated in canine spheres (Figure 4.2 E). (Additional data of tested markers with different relative gene expression patterns between canine and human tumorsphere are included in Appendix 8.9: Figure 8.19).

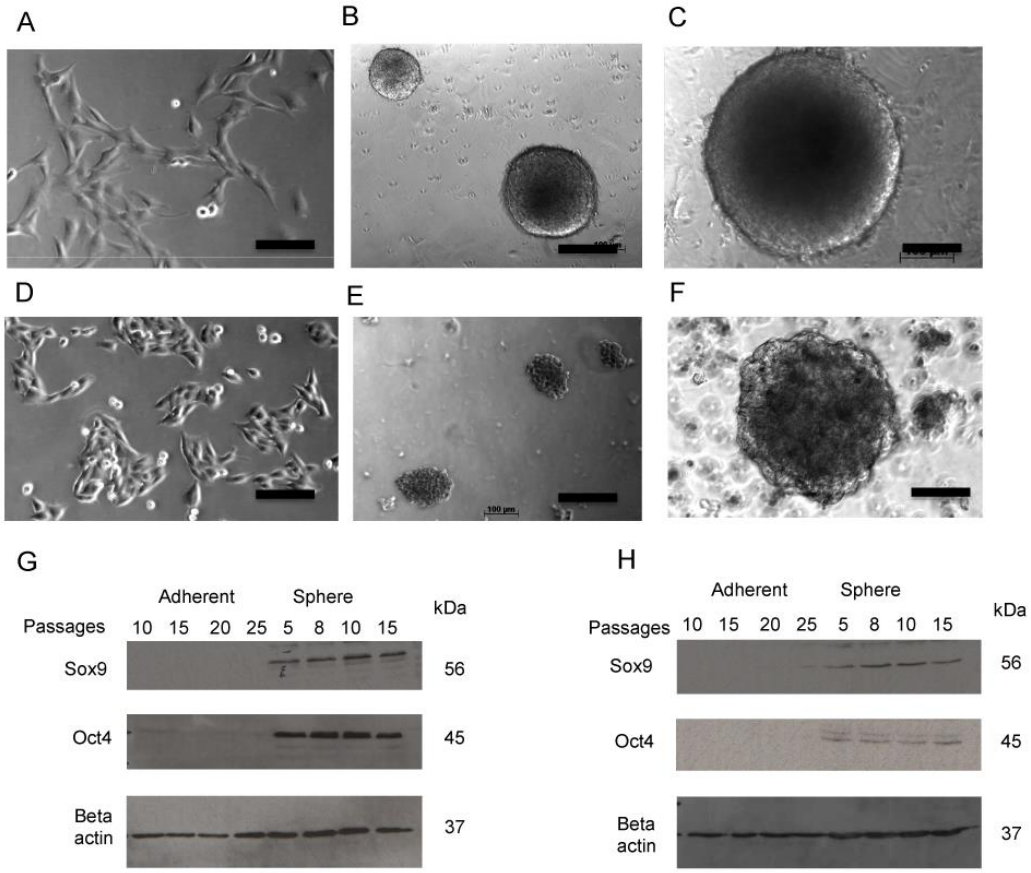

Figure 4.1 Isolation of canine (canINS) and human (CM) insulinoma cancer stem cells. A-C: canINS in adherent (A) and tumorsphere (B-C) culturing conditions at different magnifications (B:10x; C:20x) (scale bar: 100µm). D-F: CM in adherent (D) and in tumorsphere (E-F) culturing conditions at different magnifications (B:10x; C:20x) (scale bar: 100µm). G-H: Western blot analysis of caniNS (G) and CM (H) stem cell markers OCT4 and SOX9 and beta actin as loading control (adapted from Capodanno et al. 2017).

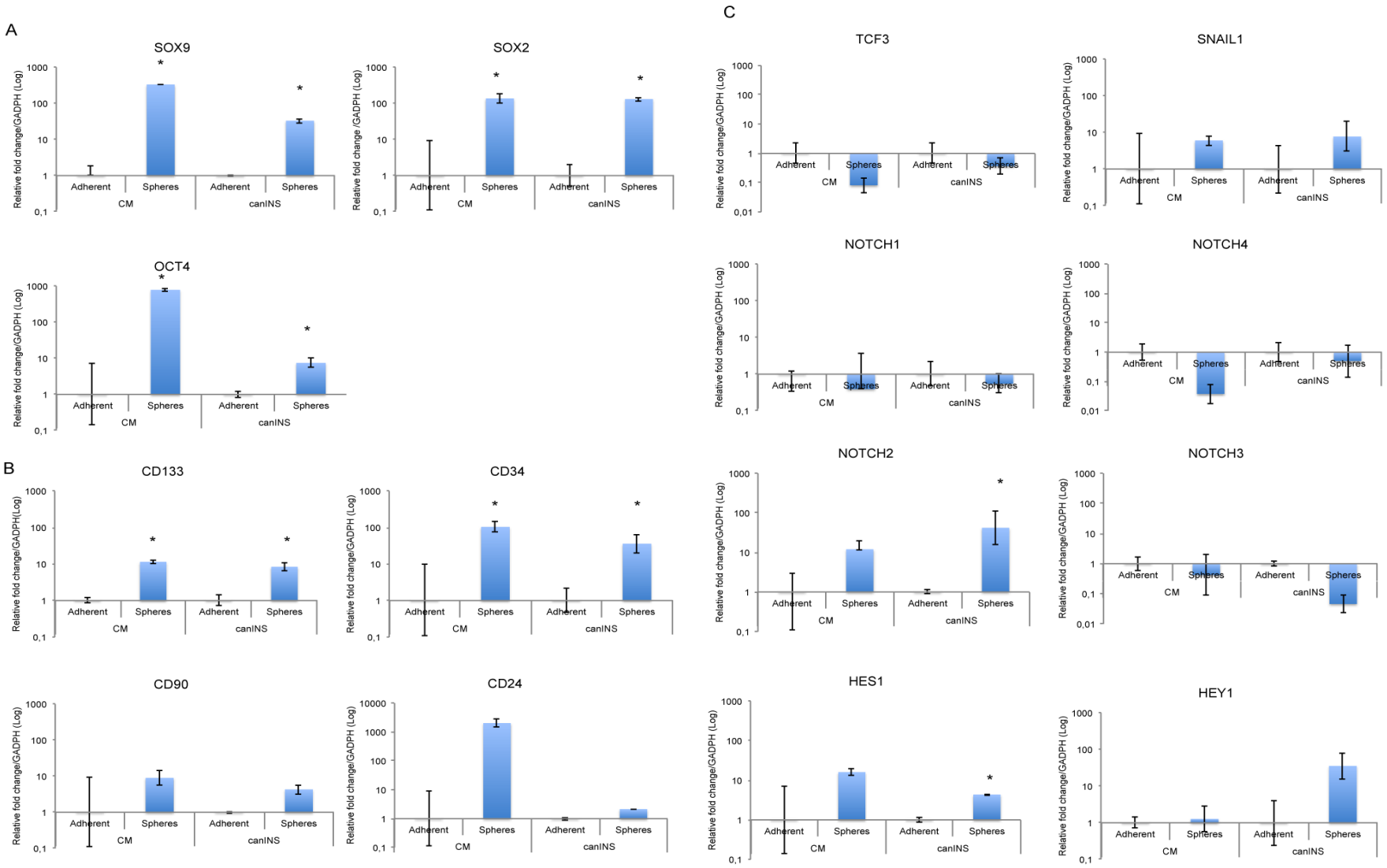

Continue next page

Continue next page

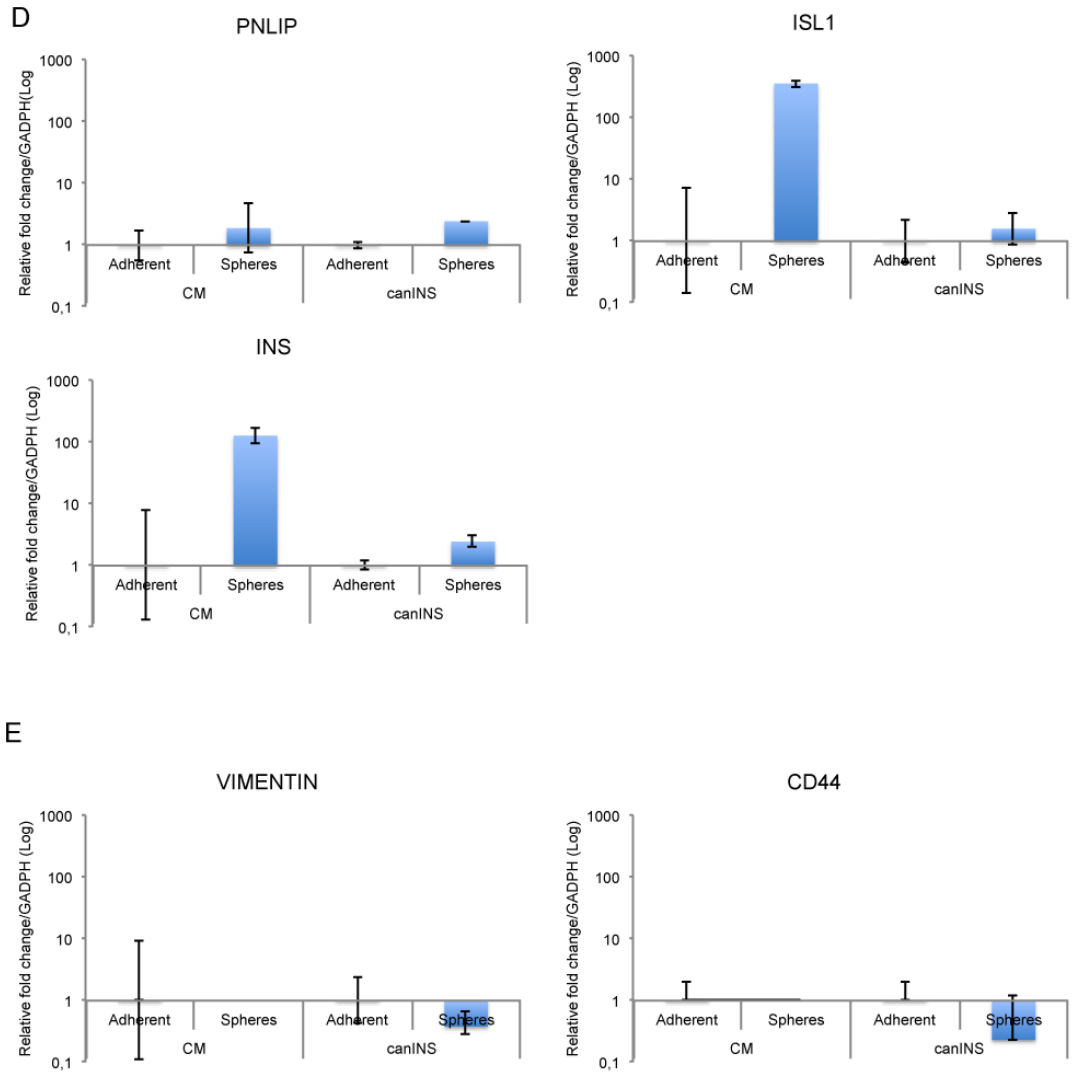

Figure 4.2 qRT-PCR of stem cell and self-renewal pathway related genes comparing CM and canINS in both adherent and sphere culturing conditions. The expression of embryonic stem cell genes (SOX9, OCT4, SOX2) (A) and stem cell associated surface markers (CD133, CD34, CD90, CD24)(B) RNA were upregulated. C: The expression of NOTCH receptor, (NOTCH1-4) and downstream target gene (HES1, HEY1, SNAIL1) and transcription factors (TCF3) was evaluated. NOTCH2 and HES1 were significantly overexpressed at the RNA level in canINS and CM spheres. HEY1 and SNAIL1 were also overexpressed. D: Markers of pancreatic progenitors cells (PDX1) as well as endocrine (ISL1, INS) and exocrine (PNLIP) cells were analysed. PNLIP, ISL1, INS were commonly overexpressed at the RNA level in canINS and CM spheres. E: No significant difference in relative gene expression of markers of mesenchymal cells (VIMENTIN and CD44)was recorded in human and canine INS CSCs. The P-values represent the

comparison with a stated hypothesis (values >1) using one samples t-test. *P-values <0.05 were considered statistically significant (adapted from Capodanno et al. 2017).

4.4.2 INS CSC-enriched tumorspheres exhibit greater resistance to chemotherapy compared with adherent cells

To validate these data, enriched INS CSCs were selected for functional assays of CSC behaviour using *in vitro* chemosensitivity assays. Human and canine parental cell lines were screened for a set of chemotherapeutics commonly used in the treatment of human INS (Table 4.1). There is little available information detailing expected serum concentrations of these drugs in dogs. Therefore, drug effects were assessed over a range of concentrations based initially on levels achieved at therapeutic doses in humans (TPC=Therapeutic Plasma Concentration).

According to the $IC_{50,}$ canine INS cells have the optimal response to 5-FU at 0.5µM whereas human INS cells show the optimal response to 5-FU at 5µM. According to the literature, both concentrations reside within the TPC of 5-FU (800ng/mL - 2000 ng/mL) (Danquechin-dorval and Gesta, 1996; Yamada, 2003; Blaschke *et al.*, 2012). 5-Fluorouracil (5-FU) is the second most commonly used chemotherapic in the treatment of human INS (after streptozocin) and present less toxicity effects at TPC (Blaschke *et al.*, 2012). Results showed that isolated canine INS CSC spheres are more resistant to 5-FU than the non-CSC population (Figure 4.3 A-B), the same applied to human INS CSC (Figure 4.3 C-D).

***Table 4.1** Calculated IC_{50} values of chemotherapy drugs for canine (canINS) and human (CM) insulinoma cell lines. All cell viability assays were performed at a density of $5x10^2$ cells. IC50 has been calculated using GraphPad Prism 5.*

Cell line	Drug	IC50
CM	5-fluorouracil	5 µM
	Doxorubicin	5 µM
	Gemcitabine	0.7 µM
canINS	5-fluorouracil	0.5 µM
	Doxorubicin	0.2 µM
	Gemcitabine	0.3 µM

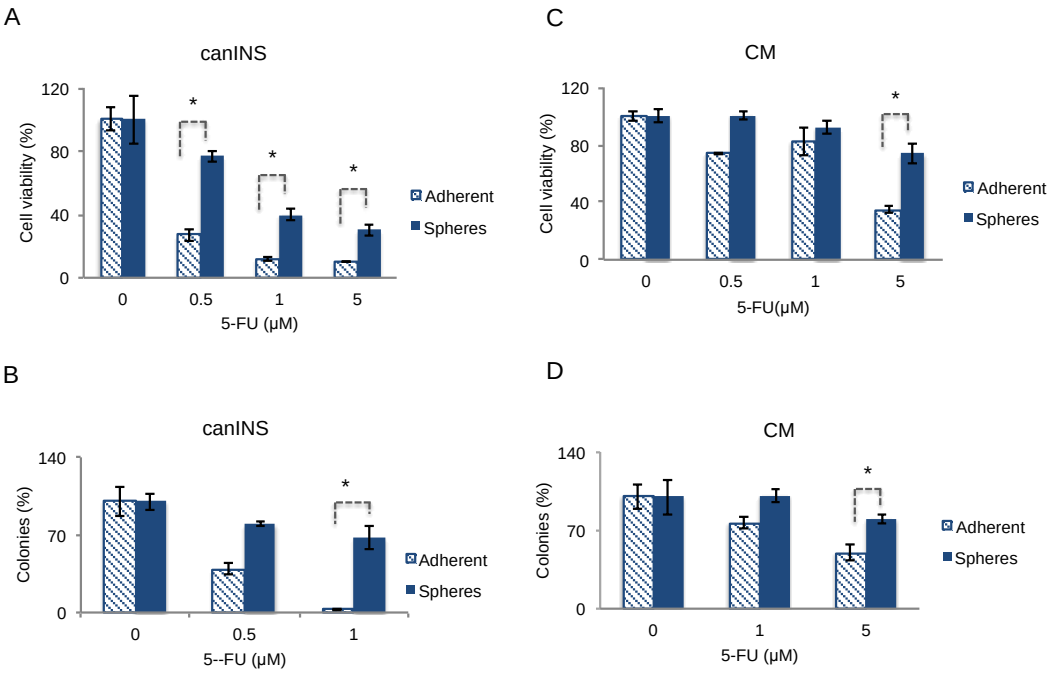

***Figure 4.3** Chemosensitivity and colony formation assays of canine (canINS) (A-B) and human (CM) (C-D) insulinoma cell lines. A-C: Chemosensitivity assay in canINS (A) and CM (C): cells were treated with increasing concentrations of 5-FU (from 0.5 to 5 µM) comparing the adherent population (dashed line) and the sphere population (continuous line). B-D: Colony formation assay canINS (B) and CM (D): Human and canine cells were treated with increasing concentrations of 5-FU (from 0.5 to 5 µM) comparing the adherent population (dashed) and the sphere population (solid). Values represent mean of triplicates ± SD. The P-values represent the comparison using 2 samples t-test within the adherent and the spheres. *P-value < 0.05 was considered statistically significant (adapted from Capodanno et al. 2017).*

4.4.3 INS CSC-enriched tumorspheres are highly invasive in vitro

The invasive capacity of cells was tested *in vitro* using a collagen-based invasion assay. CSC-enriched cells displayed a significantly greater invasive potential compared to the bulk of INS cells (Figure 4.4 A). When quantified both canine (Figure 4.4 B) and human (Figure 4.4 C) INS CSC-enriched cells presented a statistically significant increase in their ability to invade.

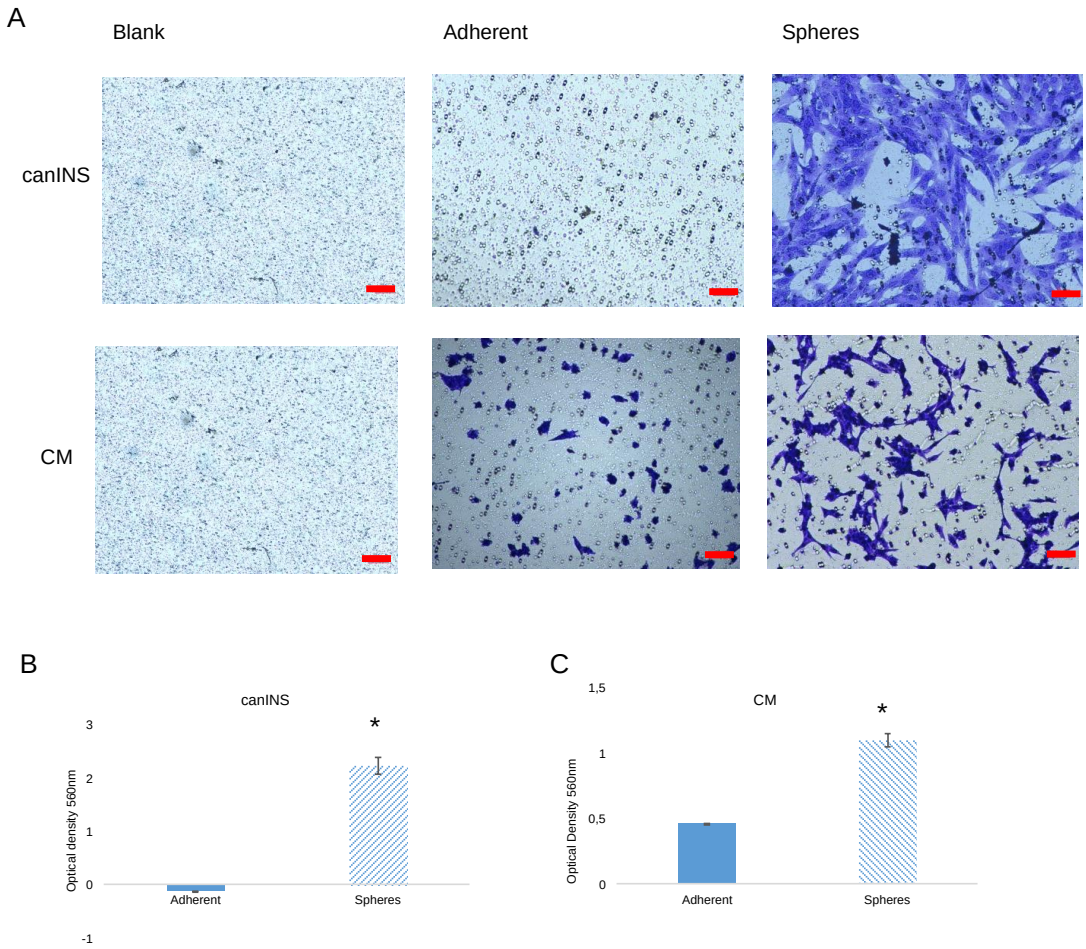

Figure 4.4 Invasive properties of insulinoma cancer stem cells in vitro. A: Representative images of invasive capacity of canine (top row) and human (bottom row) spheres against adherent cells using a collagen-based cell invasion assay kit. (scale bar: 20 µm) B-C: Canine (B) and human (C) invading cells were stained and quantified by colorimetric measurement at 560 nm Values are mean of 3 ± SEM. *P-value < 0.05 (adapted from Capodanno et al. 2017).

4.4.4 INS CSC-enriched tumorspheres have a more tumourigenic and invasive phenotype than adherent cells in vivo

The *in vivo* malignant behaviour of the INS CSC-enriched cells was assessed using the *in vivo* CAM assay model. The figures below represent a series of experiments conducted with both the adherent cells (Figure 4.5 A1-B1) and the cultured spheres, enriched in putative CSCs (Figure 4.5 A2-B2). The red fluorescence was recoded

and according to the results, the adherent population did not form tumours and did not migrate in this model (Figure 4.5 A1-B1), however the CSC population did migrate (Figure 4.5 A2-B2) and gave rise to substantial tumours (Figure 4.5 A3-B3). The red fluorescence was then quantified and a statistical significant difference was recorded between the canINS adherent and the enriched CSCs (Figure 4.5 C); whereas, no statistical difference was recorded in the human INS cell line (Fig. 4.5 D).

Immunohistochemical analysis showed that canINS and CM adherent cells (Figure 4.6 A-B) were less able to invade through the deep layers of the CAM compared to human and canine INS CSC-enriched cells (Figure 4.6 C-D). According to the results, INS CSCs had an invasive behaviour moving from the outer ectoderm CAM layer through the mesoderm towards the endoderm (Figure 4.6 E-F). These findings were consistent with our *in vitro* invasion data (Figure 4.4).

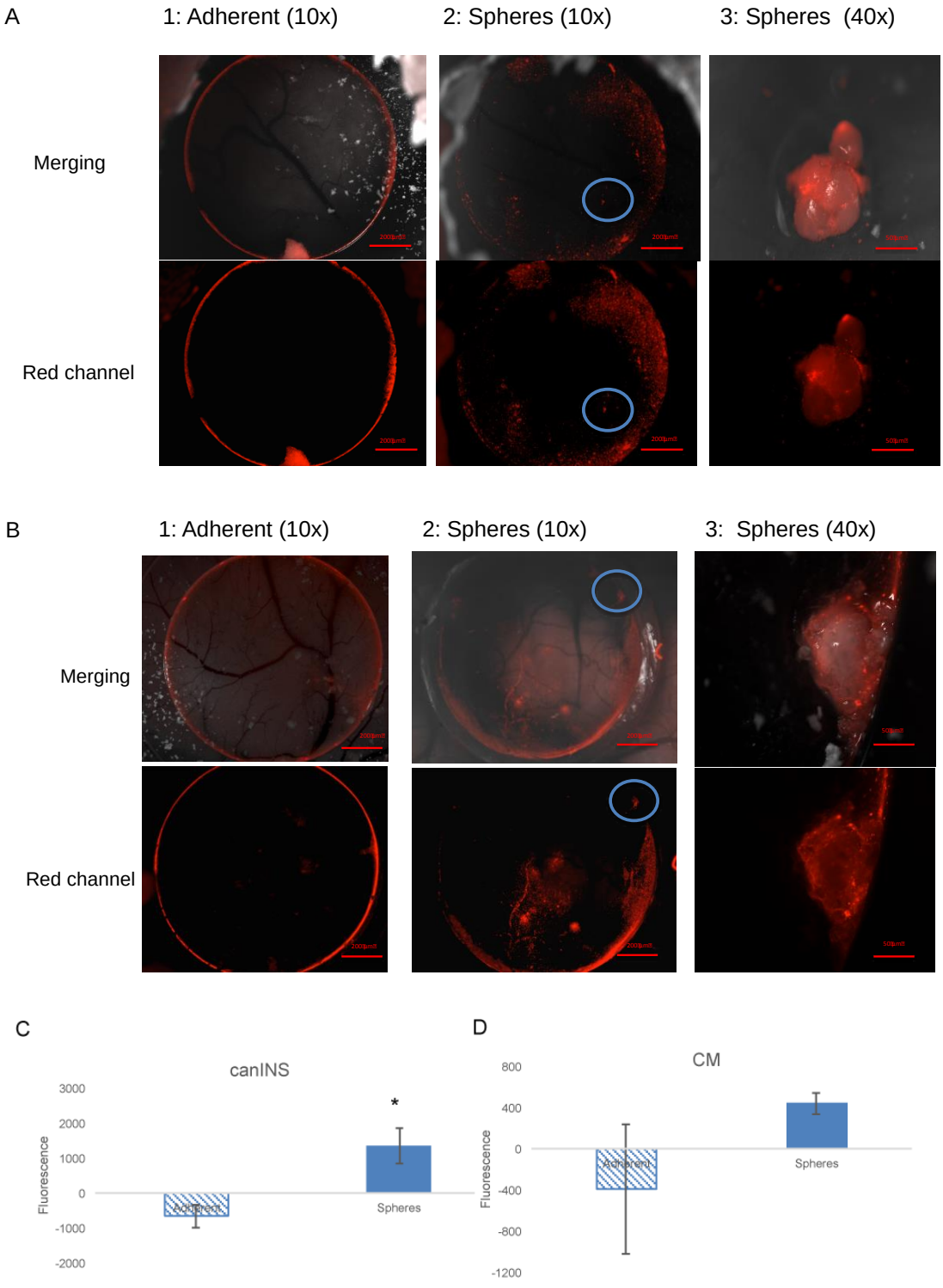

Figure 4.5 ***Representative photographs taken 11 days after seeding a chicken embryo chorioallantoic membrane with either canINS (A) and CM (B) adherent cells (A1-B1) or spheres (A2-B2) following red membrane labelling. Tumour growth was only demonstrated after seeding***

with spheres (A3; B3). A3 represents a magnified picture of the circles shown in A2. Magnification is specified on top of each picture. Pictures on the top row show merging of the brightfield channel; pictures on the bottom row show the red channel. C-D: Graph shows the differences in fluorescence between the canINS (C) and CM (D) adherent and spheres populations after quantification using ImageJ. Values are mean of 4 ± SEM. *p-value < 0.05 (adapted from Capodanno et al. 2017).

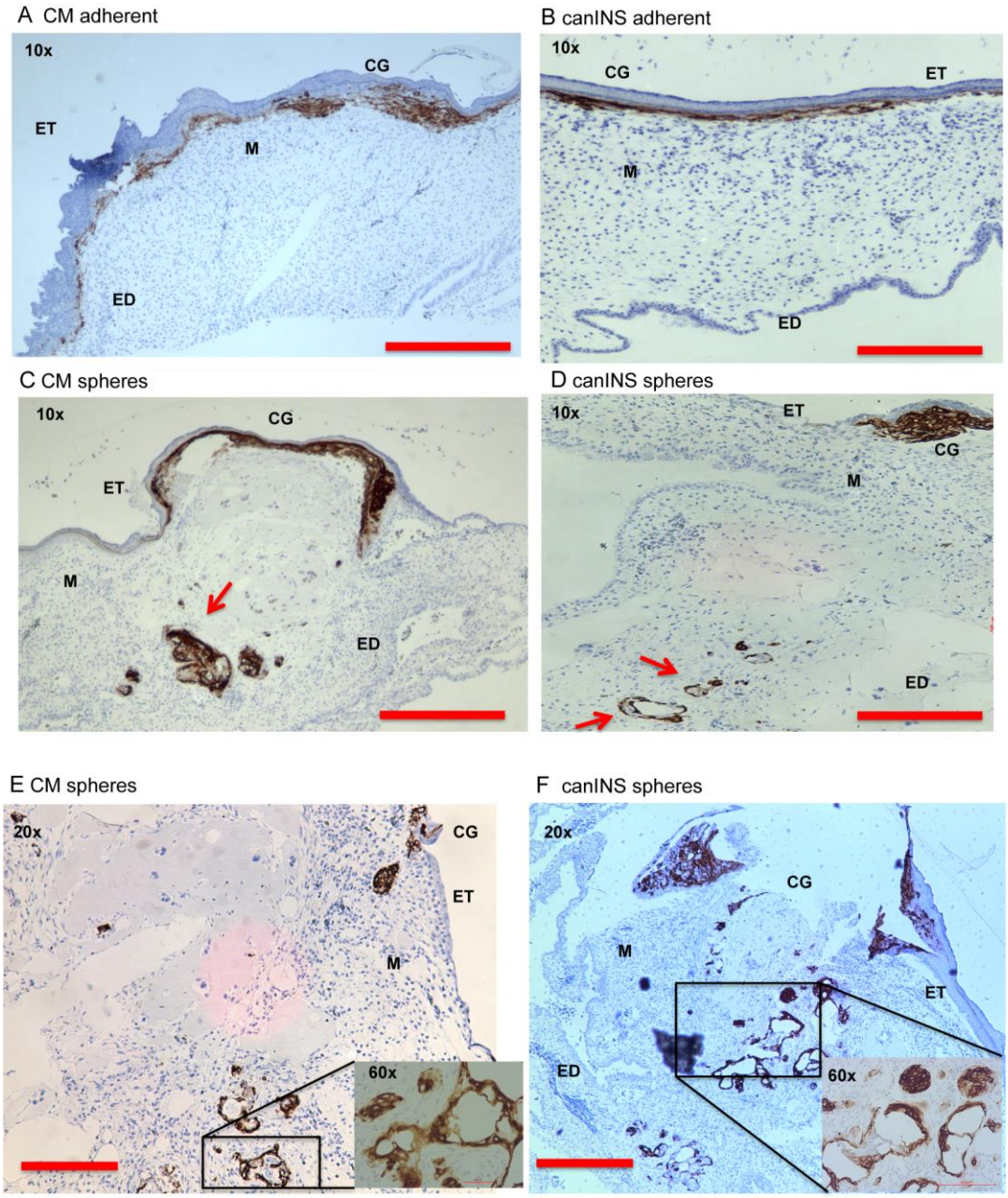

***Figure 4.6** Invasive properties of insulinoma cancer stem cells in vivo. A-F: Representative images of immunohistochemistry of CAM sections embedded in agar and stained with pan cytokeratin that stains only human and canine cells (brown). The structure of CAM layers is comprised by ectoderm (ET), mesoderm (M) and endoderm (ED). Cancer cell matrigel grafts (CG) were seeded on the CAM. Pictures show the migration of CM adherent (A) and canINS adherent (B) and CM sphere cells (C) and canINS sphere cells (D) in the inner part of the CAM 11 days after being seeded. Results show that the CM adherent (A) and the canINS adherent (B) migrate less through the different layers of the CAM compared with the CM sphere cells (C) and the canINS sphere cells (D). High magnifications (20x and 60x) shows in details how the CM (E) and canINS (F) sphere*

cells disrupt the CAM membrane and invade through the CAM layers. Magnification is specified on top of each picture (scale bar: 200 □m) (adapted from Capodanno et al. 2017).

4.4.5 Canine INS CSC-enriched tumorspheres can produce insulin

Clinical signs of INS are usually related to the endogenous hyperinsulinism that can cause a severe persistent hypoglycaemia in both humans and dogs (Anlauf *et al.*, 2009; Goutal *et al.*, 2012; Okabayashi *et al.*, 2013). Therefore, excessive insulin production is considered a feature of malignancy in INS (Jonkers *et al.*, 2007; Polton *et al.*, 2007). Considering that both the human and canine INS cell line in this study lost insulin production after early passages, after enrichment, CSCs were evaluated for insulin production.

According to the mRNA expression, pancreatic endocrine markers, such as insulin (*INS*) and islet1 *(ISL1),* were overexpressed in canINS and CM spheres (Figure 4.2 C). Results showed that when canINS cells were grown in non-adherent conditions the secretion of insulin and C-peptide, marker for insulin secretion, was reastablished (Figure 4.7 A-B), whereas for CM, it was not possible to reastablish insulin production (Figure 4.7 C-D).

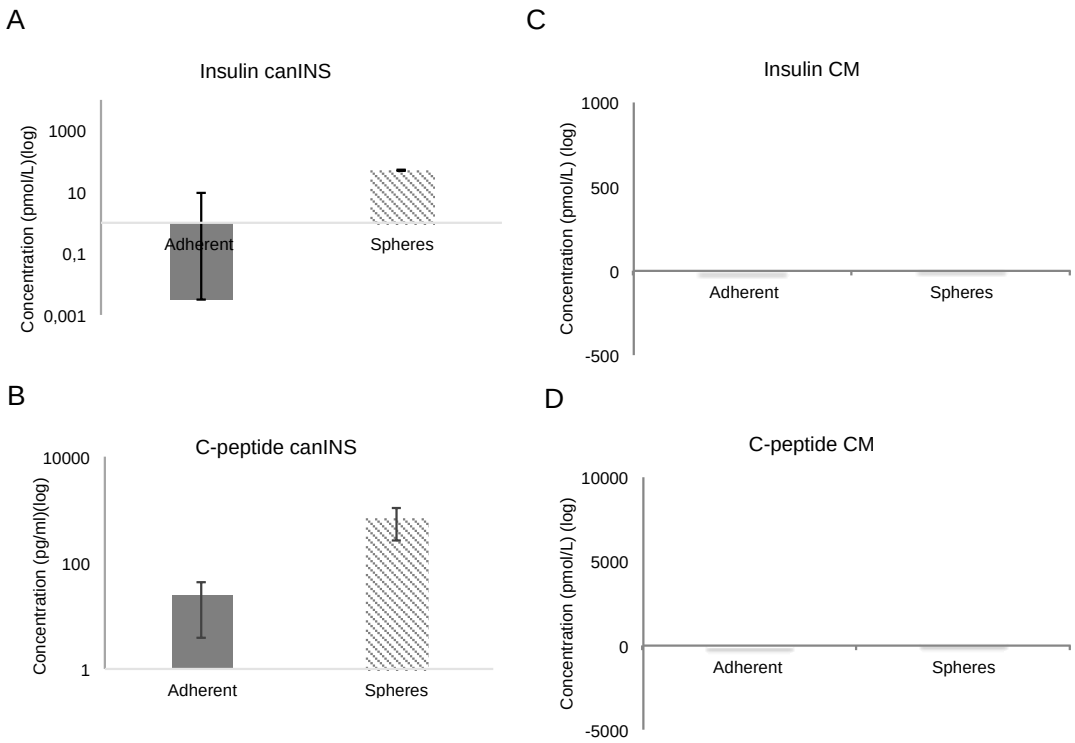

***Figure 4.7** Insulin secretion in canine and human cancer stem cells. ELISA insulin and C-peptide test of different passages of both adherent and spheres of canINS (A-B) and CM (C-D). Results show an increase in insulin active release from the canINS cells when growing in spheres condition. Values are mean of 3 different passages (passages: 10,15,25 for adherent and 5,10,15 for the spheres) ± SD (adapted from Capodanno et al. 2017).*

4.4.6 Canine and human INS CSCs can be isolated using stem cell-associated surface markers

As previously said, stem cell-associated surface markers were upregulated in putative canine and human INS CSCs compared with the adherent cells (Figure 4.2 B). Using flow cytometry, the protein expression of the following surface markers was assessed in both human and canine INS cancer cell lines: CD90, CD34, CD24 and CD133 (Figure 4.8 A). Results showed that the canine cell line has a high percentage of CD90+ (10%) and CD133+ (10%) cells. Whereas the human cell line has a high percentage of CD90 (30%) and CD24 (15%) positive cells (Figure 4.8 A). After treating canINS and CM sorted cells with different concentration of chemotherapy results showed that for canINS the CD133- and CD34- positive fraction had an increased resistance compared to the negative fraction of the population (Figure 4.8 B). Whereas, no differences was recorded between the positive and negative fractions of CM-sorted populations (Figure 4.8 C). Canine-sorted CD133 and CD34 population were tested for a range of doses of 5-FU. Results showed that canINS CD133+ and CD34+ cells were more resistant to 5-FU compared with the negative populations (Figure 4.8 D-E).

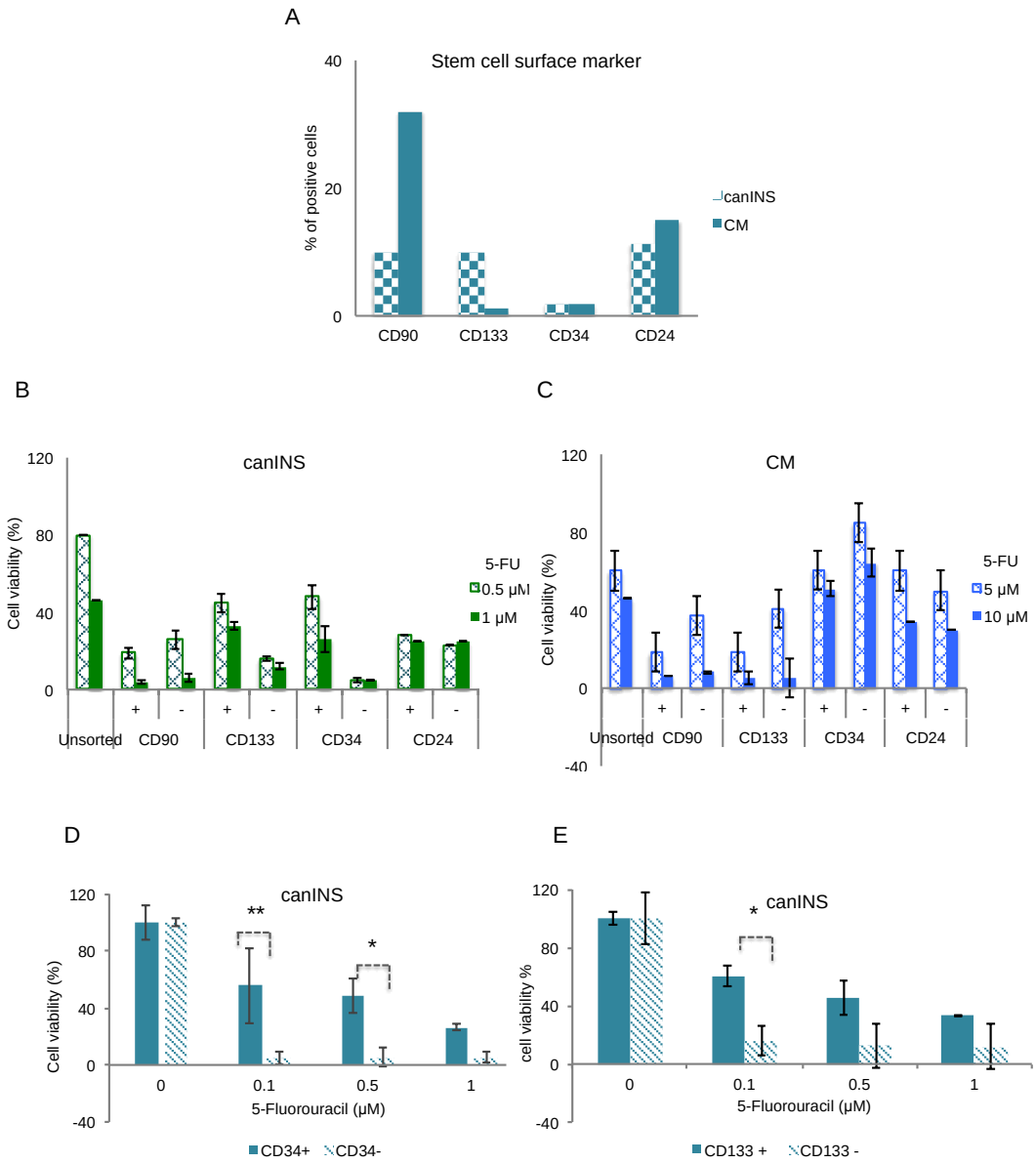

Figure 4.8 Screening of different stem cell-associated surface markers for canine (canINS) and human (CM) adherent cell line. A: Percentage of positive fraction of CD90, CD133, CD24, CD34 cells was assessed in canINS and CM using flow cytometry (BD Fortessa). B-C: Chemosensitivity assay for canINS and CM of FACS and MACS sorted populations. B: canINS cells have been sorted according to the previous mentioned stem cell-associated surface markers and subsequently treated with different concentrations of 5- Fluorouracil (5-FU) (0.5 µM and 1 µM). C: CM cells have been according to the previous mentioned stem cell-associated surface markers and subsequently treated with different concentrations of 5-FU (5 µM and 10 µM). D-E: Chemosensitivity assays for canINS CD34- and CD133- sorted cells. Cells have been treated with increasing

concentrations of 5-FU (from 0.01 µM to 1 µM) comparing the CD34- (D) and the CD133- (E) negative population (dashed) and the CD34- (D) and the CD133- (E) positive population (solid). All data were normalised against the appropriate vehicle control. Values represent mean of triplicates ± SD. *p value <0.05, **p value <0.01.

4.5 Discussion

According to the CSC theory, the malignant behaviour of tumours is driven by a subset of cancer cells inherently resistant to conventional therapies that might have the ability to repopulate the tumours after treatment. This population is referred as CSCs (Guo *et al.*, 2006; Pattabimaran *et al.*, 2014; Mitra *et al.*, 2015). In the last decade, CSCs have been identified and isolated in different type of human cancers (H. Wang *et al.*, 2009; Abel *et al.*, 2014; Gao *et al.*, 2014; Hou *et al.*, 2014). Several groups have been able to isolate CSCs from a range of canine solid tumours including osteosarcoma (Wilson *et al.*, 2008), rhabdomyosarcoma (Kishimoto *et al.*, 2017), hepatocellular carcinoma (Itoh *et al.*, 2017), mammary carcinoma (Rybicka *et al.*, 2016) and glioma (Pang *et al.*, 2017). Although, CSCs have not been yet characterised in malignant INS. Therefore, the aim in this chapter was to isolate INS CSCs and evaluate their role in INS carcinogenicity.

Results demonstrate that tumorspheres from both species have a statistically significant upregulation of stem cell-associated markers, such as *CD133, CD34, OCT4, SOX9,* and *SOX2.* Previously, *OCT4*, *SOX2*, *SOX9* and *CD133* have been identified as stem cell markers of pancreatic endocrine progenitor cells (Seymour *et al.*, 2007; Koblas *et al.*, 2008; H. Wang *et al.*, 2009; Venkatesan *et al.*, 2011). *CD133* has been previously studied as a valuable marker for a negative clinical outcome in PNETs (Sakai *et al.*, 2017). Furthermore, *PNLIP*, *INS* and *ISL1* genes are upregulated in human and canine enriched INS CSCs. Previous studies have demonstrated that a 10% of the cancer cell population within primary canine INS present both endocrine and exocrine markers (Buishand *et al.*, 2013). Additionally, ISL1 has also been described previously as a marker specific for human malignant INS (Hermann *et al.*, 2011).

This subpopulation of cancer cells are highly invasive and resistant to chemotherapy *in vitro*, similar to CSCs isolated in previous studies (Gaur *et al.*, 2011; Pang *et al.*, 2011; Gao *et al.*, 2014). Chemotherapy is not commonly adopted in the treatment of canine INS (Goutal *et al.*, 2012). Nevertheless, malignant human INS is commonly treated with a combination of different chemotherapeutics (Baudin *et al.*, 2014), and 5-FU represents the most commonly used one (Okabayashi *et al.*, 2013). 5-FU is an

antimetabolite chemotherapy and pyrimidin analogue that blocks DNA replication interfering with the enzyme, thymilidate synthase (Yamada, 2003). 5-FU is not commonly used in the veterinary practice, nonetheless previous studies reported an increased survival time in canine patients diagnosed with metastatic breast cancer and gastric adenocarcinoma (Karayaponolou *et al.*, 2001; Swann *et al.*, 2002). Therefore, in this study 5-FU has been used to test chemoresistance of INS CSC population. According to the results in this study, enriched INS CSCs are more resistant to 5-FU compared to the adherent cancer cells. This is consistent with the CSC model stating that despite the sensitivity of bulk tumour cells to chemotherapy, CSCs are resistant and lead ultimately to the failure of cytotoxic chemotherapy, increasing the need for new CSC-targeted therapies (Guo *et al.*, 2006). The aforementioned data suggest that a population of stem cell-like cells, resistant to chemotherapeutics, reside within the INS cancer cell population.

Results from the *in vivo* CAM model show that enriched INS CSCs cells display a greater invasive potential compared to the bulk of INS cells. Within 4 days not only do CSCs from INS tumorspheres develop visible tumours, but they also escape the primary inoculation site and reach the inner layers of the CAM. The *in vivo* CAM assay results are consistent with cancer cell proliferation and invasion observed in the *in vitro* assays. For instance, the invasive behaviour of INS CSCs in the CAM model with its highly vascularised structure, closely mimics the mode of INS metastasis which involves INS cancer cells invasion and spread through the abdominal lymphatic system to reach the site of metastasis in either lymph nodes or liver. The CAM model has previously shown to be an interesting model for metastatic behaviour in other types of cancer such as breast, bladder, prostate, ovarian cancer and head and neck cancers (Vargas *et al.*, 2007; Lokman *et al.*, 2012). These findings suggest CSCs may play a role in INS carcinogenesis and support the use of canine as an appropriate comparative model for studying the involvement of CSCs in INS oncogenesis.

As described previously, INS are insulin-secreting tumours, thus clinical signs are usually associated with excessive endogenous production of insulin (Okabayashi *et al.*, 2013). Due to the high insulin production, INS cell lines have been previously used as a model to study beta-cells and the function of endocrine pancreas (Labriola

et al., 2009). However, insulin production in these INS cell lines is often lost after early passages (Skelin *et al.*, 2010). For instance, in CM despite several beta-cell-specific characteristics of this cell line, like expression of beta cells genes (GLUT2, glucokinase and insulin), long-term passage resulted in loss of insulin secretion (Baroni *et al.*, 1999). Consistently with these findings, the newly isolated canINS cell line has also shown a loss of production of INS after early passages (Buishand, unpublished data). Previous studies have shown that insulin-producing cells can be generated from stem/progenitor cells (Sugiyama *et al.*, 2007; Xia *et al.*, 2009; Joglekar *et al.*, 2010). Therefore, insulin production was tested in canINS and CM enriched INS CSCs. Results show that pancreatic endocrine related genes (*INS* and *ISL1*) are overexpressed in both human and canine enriched INS CSCs and that insulin production can be reastablished in canine enriched INS CSCs. Considering that alteration of the glucose metabolism are fundamental for cancer growth and survival, accumulating evidences indicates a central role of insulin and IGF signalling in the induction/maintenance of EMT and cell stemness during cancer progression (Belfiore and Malaguarnera, 2011; Malaguarnera and Belfiore, 2014). For instance, increased insulin receptor overexpression together with autocrine production of its ligand IGF2 is emerging as an important mechanism of normal and cancer stem cell expansion and as a feature of several malignancies (Belfiore and Malaguarnera, 2011; Malaguarnera and Belfiore, 2014). According to these results, it is possible that insulin production might be functional to the tumour microenvironment of canine INS CSCs. Nevertheless, insulin production cannot be reastablished in human enriched INS CSCs due to a mutation of the chromosome 11, where the insulin gene is located (Gragnoli, 2008).

Tumorsphere culturing enriches for a heterogeneous cell population, containing stem cells, progenitors and more differentiated cells (Pastrana *et al.*, 2011). In order to isolate and study the behaviour of purified populations of CSCs, stem cell surface markers are usually used. After screening human and canine INS cell lines for the presence of stem cell-associated markers, *CD133* and *CD34* result as valuable markers for the isolation of canine INS CSC populations. Whereas in human INS cell line the stem cell surface markers used has not been efficient to isolate chemoresistant INS CSCs. Considering the different tumour staging and species of

these two cell lines, the different expression of stem cell surface marker might be related to their different origin. CSC state is not static and it develops during the different phases of the tumour (Blacking *et al.*, 2007), thus, particular care has to be taken when choosing the type of CSC marker. As shown before, some markers select for a heterogeneous population rather than isolate a specific CSC population. For instance in human INS, CD90 is a marker for both intratumoural fibroblasts and vascular endothelium (Buishand *et al.*, 2016). These results confirm what described before, that even though, in the last decade, substantial progress has been made in understanding genetic and epigenetic changes in CSCs, cancer cell populations are often heterogeneous and surface markers may not unequivocally enrich all CSCs (Blacking *et al.*, 2007).

4.6 Conclusions and future directions

In summary, INS CSC population can be enriched from both canine and human INS cell line. The data show that these cells not only express embryonic stem cell markers, but also have an invasive and tumourigenic phenotype and are more resistant to chemotherapy than the bulk of the tumour cells. Following a One Health approach, this study further contributes to the evidence that canine tumour model system can be used, alongside traditional rodent models, to study the equivalent human disease.

Significantly, results suggest that it is possible to isolate canine INS CSCs using both isolation and enrichment methods. Whereas, for human INS CSCs the enriching method is the only one that in this study showed consistency. These results show that within INS reside different CSCs population unravelling heterogeneity within INS cancer cells. In the future, a combination of several enrichment methods coupling human and canine cell lines from different stages of the disease could be the key for isolating INS CSC different populations. Nonetheless, this study provide evidence that the carcinogenic behaviour of malignant INS could be driven by INS CSCs. We identified a set of genes involved in the INS CSC phenotype, thus opening new opportunities for INS CSCs targeted therapy.

5 Targeting the Notch pathway to decrease chemoresistance of insulinoma cancer stem cell population

5.1 Abstract

5-Fluorouracil (5-FU) chemotherapy is used as adjuvant treatment for metastatic recurrent human insulinoma (INS), but drug resistance limits its efficacy. Emerging evidence suggests that the existence of cancer stem cells (CSCs) contributes to chemoresistance. The aim of the present study was to identify whether 5-FU treatment could generate residual cells with CSC-like properties in INS and target mechanisms that might contribute to chemoresistance of INS CSCs. Protein analysis showed that NOTCH2 and HES1 were activated in INS cancer cell lines, especially when treated with chemotherapy. Inhibition of the Notch pathway, using a gamma secretase inhibitor (GSI), significantly affected the viability of INS CSC. When used in combination GSI and cancer chemotherapy, the clonogenicity *in vitro* and the tumourigenicity *in vivo* of INS CSC were significantly reduced.

These data provided molecular evidence that the Notch pathway plays an important role in INS CSC survival and chemoresistance. In particular, enhanced NOTCH2 and HES1 expression was correlated to an INS chemoresistant phenotype and thus might serve as a potential therapeutic target to reverse chemoresistance in INS patients.

5.2 Introduction

Cancer chemotherapeutic agents kill rapidly dividing cancer cells mainly inducing apoptosis by DNA damage and/or inhibited mitotic division (Abdullah and Chow, 2013). Despite being one of the main anticancer treatments available at the moment, patients often develop resistance to chemotherapy and, thus, tumour relapse (Zhao, 2017). Unfortunately, slowly dividing and non-dividing cancer cells are less sensitive to chemotherapy particularly when reduced doses are given to avoid side effects on rapidly dividing normal cells (Abdullah *et al.,* 2013). The insensitivity of these cancer cells causes chemoresistance and plays a significant role in poor prognosis of cancer (Dean *et al.,* 2005; Mitra *et al.,* 2015). Some of the cancer cells possess an intrinsic resistance to chemotherapy. Whereas, other cancer cells are initially sensitive but acquire resistance during treatment (Dean *et al.,* 2005). Regardless of the resistance mechanisms, the chemoresistant cancer cells are the major cause of tumour recurrence or relapse and have garnered the most attention clinically (Dean *et al.,* 2005; Mitra *et al.,* 2015). Despite the intensive studies, the processes by which tumours become chemoresistant and the causes of chemoresistance remain only partially understood (Wang *et al.,* 2009; Acharyya *et al.,* 2012; Abdullah and Chow, 2013; Zhao, 2017). Growing evidence supports a critical role of CSCs in the chemoresistance mechanisms in many types of cancer including gliomas and glioblastoma (Irshad *et al.,* 2015), breast (Pang *et al.,* 2011), colorectal (Zhao *et al.,* 2016), osteosarcoma (Pang *et al.,* 2014), pancreatic (Wang *et al.,* 2011) and ovarian cancer (Mao *et al.,* 2014). Chemoresistance of CSCs can contribute to tumour initiation as well as continued tumour progression following treatment (Acharyya *et al.,* 2012; Zhao, 2017). In particular, previous studies have shown an association between chemoresistance and acquisition of a CSC-like phenotype in some types of cancers (Wang *et al.,* 2009; Xu *et al.,* 2015; Zhao *et al.,* 2016). For instance, in colon cancer and gastric cancer it has been previously reported that 5-FU treatment selectively enriches for a subset of CD133+ cancer cells with stem cell-like properties *in vitro* (Xu *et al.,* 2015; Paschall *et al.,* 2016). Consequently, CSCs investigation can be a powerful tool for the development of therapies for patients for whom traditional cancer chemotherapies and radiation treatments have poor clinical

outcomes (Lu *et al.*, 2016). CSCs hold great promise for redefining cancer therapy in advanced-stage cases. However, the mechanisms behind the apparent inherent resistance to therapy harboured by CSCs are unknown but it is likely that CSCs use active mechanisms to evade cytotoxic drugs or radiation treatment (Mitra *et al.*, 2015). Because of their highly heterogeneous nature and the repeated refinement of the CSCs by new markers, it is difficult to categorise the specific or overlapping populations responsible for promoting the processes of dissemination, intravasation, dormancy, and relapse (Zhao *et al.*, 2016). Therefore, the malignant behaviour of CSCs must be captured and characterised in different types of cancer, focusing particularly on drug-resistance and the identification of aberrant pathways in CSCs (Guo *et al.*, 2006; Borah *et al.*, 2015; Takebe *et al.*, 2015). Evidence shows that many properties that are classically associated with stem cells are also characteristics of CSCs (Mitra *et al.*, 2015). There are a number of signalling pathways functioning in normal stem cells, which have assigned roles in the early embryogenesis-like cell proliferation, cell differentiation, cell fate, and, particularly, self-renewal (Abetov *et al.*, 2015). Although as genetic and epigenetic changes might have a role in the unrestrained growth, invasion and acquired resistance in cancer cells, deregulation of these pathways could be involved in maintaining the CSC phenotype (Borah *et al.*, 2015). Our increasing understanding of the molecular biology and aberrantly activated cellular pathways of CSCs has revealed some novel targets for therapeutic strategies that have successfully reduced CSCs both *in vitro* and in preclinical models (Wang *et al.*, 2011; Lu *et al.*, 2016). Of note, extensive experimental evidence has revealed Hedgehog, Wnt, Notch and TGF-beta pathways to be the key players in maintaining the proliferating capacity of CSCs and are activated in most of the solid tumors, including NET (Pannuti *et al.*, 2011; Carter *et al.*, 2013; Abetov *et al.*, 2015; Borah *et al.*, 2015). As discussed in the section 1.6.3, CSC-targeted therapies have been recently tested in clinical trials against the aforementioned pathways in a variety of tumours.

In chapter 4 INS CSCs were successfully enriched from human and canine INS cell lines. Data demonstrated that the Notch pathway was associated with a stem cell-like phenotype in INS (Figure 4.2). The Notch signalling pathway is fundamental in pancreatic embryogenesis and plays an essential role in suppressing differentiation

and maintaining the pluripotency of embryonic stem cells (Edlund 2002; Wang *et al.*, 2011) (Figure 5.1). Briefly, Notch signalling is activated by the interaction of Jagged1&2 and Delta-like1,3&4 transmembrane ligands with Notch receptors (1–4) on adjacent cells. This leads to the endocytosis of ligands into the signal-sending cell and causes a conformational change of the extracellular domain of the Notch protein in the signal-receiving cell. This exposes a cleavage site in the signal-receiving cell for the ADAM proteins Kuzbanian (ADAM10) and TACE (ADAM17) and leads to the generation of a signalling intermediate known as NEXT (Notch extracellular truncation) in the signal-receiving cell. γ-secretase cleaves NEXT twice within the transmembrane domain to release the Notch intracellular domain (NICD) that translocate to the nucleus. Within the nucleus, NICD interacts with members of the CSL family of DNA-binding proteins, displacing transcriptional corepressors associated with the CSL proteins and recruiting members of the Mastermind-like (MAML) family of transcriptional co-activator. The genes transcribed differ significantly between tissues. However, members of the Hes/Hey family of transcriptional corepressors are commonly induced (Angelis *et al.*, 1999; Roy, Pear and Aster, 2007; Brennan and Clarke, 2013) (Figure 5.1).

Previous studies have analysed the key role of the Notch pathway in a number of processes including tumour initiation (Gao *et al.*, 2014), self-renewal (Chiron *et al.*, 2012), and chemoresistance (Liu *et al.*, 2013) of CSCs. The role of the Notch pathway has been previously described in various types of NETs (Grande *et al.*, 2011; Carter *et al.*, 2013; Crabtree *et al.*, 2016). However, to our knowledge, this is the first study to evaluate the role of the Notch pathway in INS tumourigenicity and in particular, its role in chemoresistance of INS CSCs. Our data showed that enriched INS CSCs did not only posess self-renewal and tumour-initiating capability but they were also resistant to therapeutic plasma dose range of 5-FU. Therefore, in this chapter the Notch pathway was investigated *in vitro* and *in vivo* to evaluate its role in INS CSC chemoresistant phenotype.

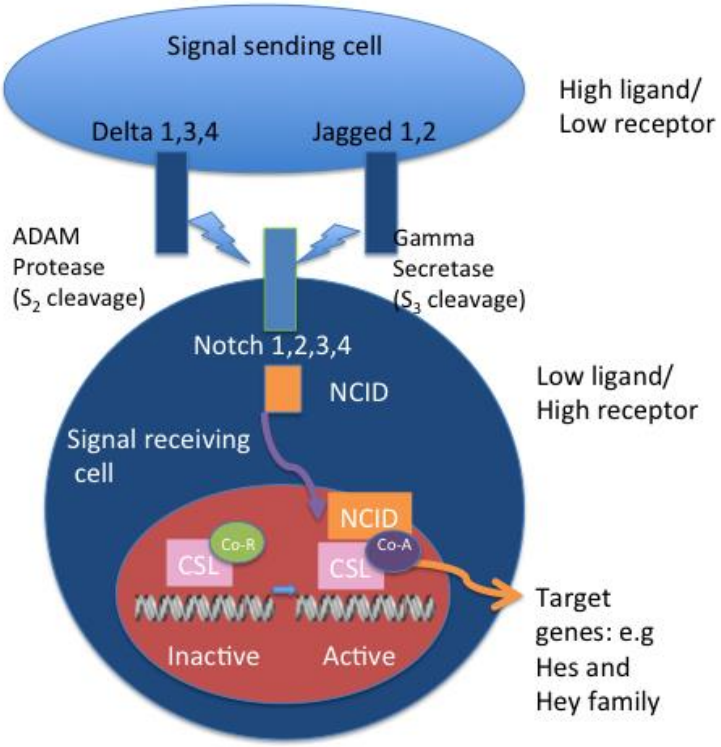

Figure 5.1 Schematic representation of the Notch pathway signalling. The Notch pathway includes two families of ligands: the Jagged and Delta-like ligands. After binding there are four types of receptors that can be activated termed Notch1-4. These receptors undergo a two-step proteolytic cleavage, first by ADAM10, then by gamma-secretase. After proteolytic release, Notch intracellular domain translocates to the nucleus, interacts with CSL transcription factors (CBF1/RBP-Jκ, Su(H), Lag-1) which activate and promote transcription of downstream genes involved in various differentiation programmes (HES1, HEY1, etc.) (Adapted from Roy et al. 2007;Abel et al. 2014; Lim et al. 2015).

5.3 Materials and methods

Basic methodological descriptions and brands not stated here are presented in Chapter 2. Specific materials and methods of the following chapter are described as follows.

5.3.1 Sphere-formation assay

The sphere forming ability of human and canine INS cells was determined following the protocol described in section 2.1.7.

5.3.2 Drug treatment of cells

Cells were treated with gamma-secretase inhibitor N-[N-(3,5-Difluorophenacetyl)-L-alanyl]-S-phenylglycine t-butyl ester (DAPT) (Sigma-Aldrich) diluted in DMSO over the indicated range of concentrations. Equal volumes of the vehicles were used as control. The sensitivity of the cells to DAPT was evaluated using cell proliferation assays as described in Chapter 2.1.8 and colony formation assays as described in Chapter 2.1.9.

5.3.3 Flow cytometry

CM and canINS were detached by trypsinisation, washed with PBS and stained with Zombie Violet Fixable Viability Kit (BioLegend Inc., USA) to detect dead cells. Next, cells were washed again with PBS and fixed in paraformaldehyde at 1% for 10 min at 37°C and then chilled for one minute on ice. A batch of cells was also permeabilised by adding ice-cold 90% methanol slowly to pre-chilled cells, while gently vortexing. Cells were incubated for 30 min on ice, washed in incubation buffer (PBS 0.5% BSA) twice and resuspended in 100 μL of the diluted primary antibody at 1:800 dilution. After incubation with the primary antibody, cells were washed and incubated with a fluorochrome-conjugated secondary antibody for 30 minutes. After washing with incubation buffer, cells were resuspended in PBS and analysed using BD Fortessa (BD

Biosciences, USA). The primary antibody used was monoclonal anti-rabbit Notch2 (D76A6) XP® with anti-rabbit IgG (H+L) $F(ab^{I})_2$ Fragment Alexa Fluor® 647 Conjugate (NewEnglandBio) as a secondary antibody. As a negative control Rabbit (DA1E) mAb IgG XP® Isotype control Alexa Fluor® 647 Conjugate has been used (NewEnglandBio) (Appendix 8.7: Figure 8.13 and Figure 8.14).

5.3.4 Chorioallantoic membrane assay (CAM)

The tumour forming and invasive ability *in vivo* of human and canine INS cells using CAM assay was determined following the protocol described in Chapter 2.1.10.

5.3.5 Statistical analysis

Statistical analysis was performed following the methodology described in Chapter 2.6.

5.4 Results

5.4.1 The Notch pathway is overexpressed and active in 5-FU resistant INS cells

Previous analysis of gene expression in human and canine INS CSCs had revealed that Notch pathway related receptor, NOTCH2, and its target gene, HES1 were significantly upregulated in both CM and canINS spheres (Figure 4.2). Using flow cytometry, evidence was provided that the NOTCH2 receptor is constitutively activated as present in both its inactive form (extracellular level) and active form (intracellular level) in INS cells (Figure 5.2 A-B). Protein analysis showed that both CM and canINS sphere cells demonstrated an intrinsic higher expression of NOTCH2 and HES1 compared to the adherent INS cells (Figure 5.2 C-D). After testing a set of chemotherapeutics commonly used in the treatment of human INS, 5-FU was identified as the most suitable drug to study INS cancer cells' chemoresistance (Table 4.1). Both CM and canINS

tumourspheres were more resistant to 5-FU treatment compared to adherent cells in cell viability and clonogenicity assays as shown in Figure 4.3.

To evaluate the role of the Notch pathway in INS chemoresistance, cells were treated with increasing doses of 5-FU. Results showed that 5-FU residual cells demonstrated an increased expression of both the inactive and active form of the NOTCH2 receptor in canINS (Figure 5.2 C) and CM cells (Figure 5.2 D). In response to an increase in active NOTCH2 expression, its downstream target gene HES1 was also overexpressed in cells resistant to 5-FU (Figure 5.2 C-D).

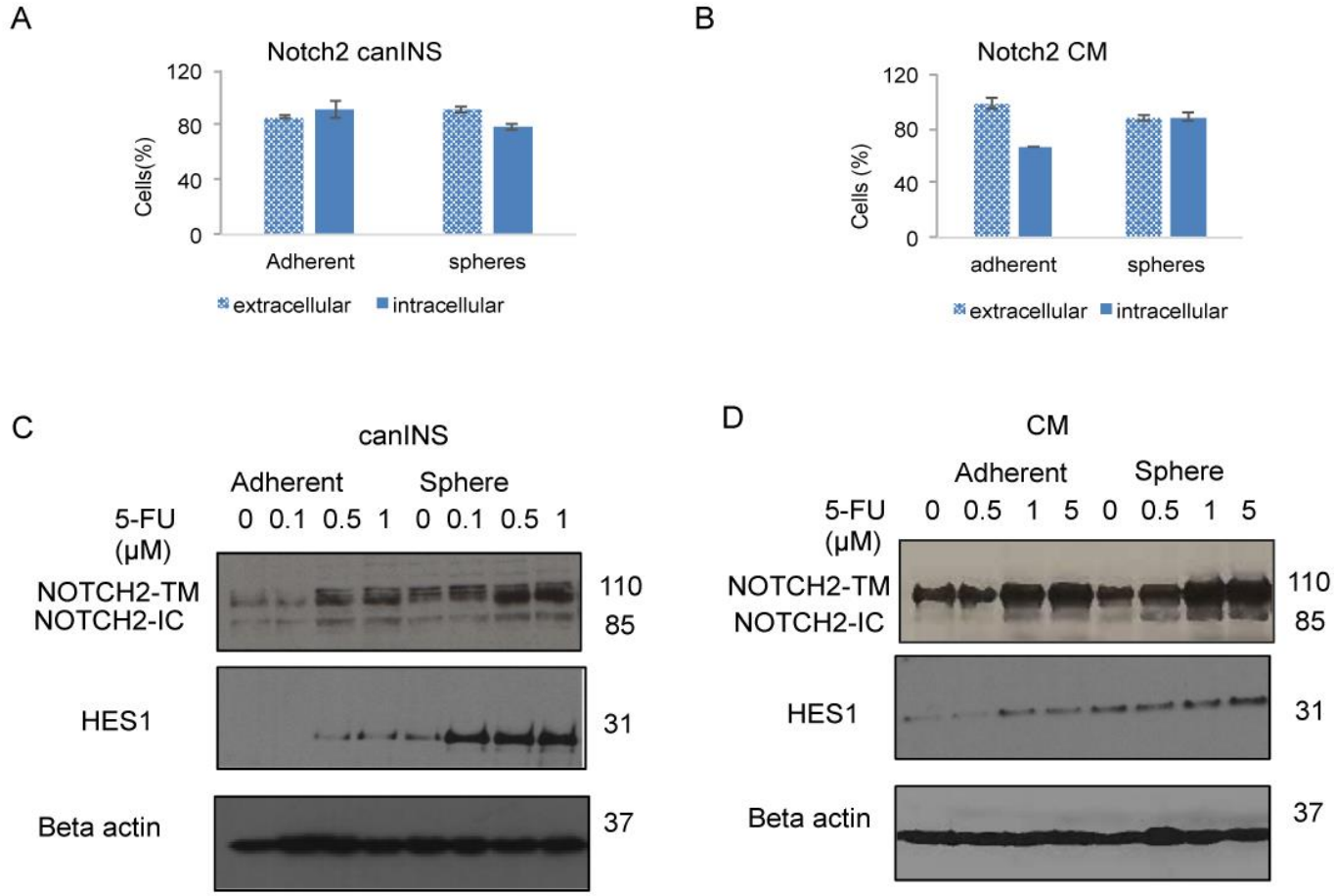

Figure 5.2 Analysis of Notch pathway protein expression and activation in human and canine insulinoma (INS) cells. A-B: Graph showing the percentage of cells positive to NOTCH2 antibody using flow cytometry in canine (A) and human (B) INS cell lines. C-D: Western blot analysis of

NOTCH2 in its inactive transmembrane form (NOTCH2-TM) and in its active intracellular form (NOTCH2-IC), and HES1 with beta actin as a loading control in canine (C) and human (D) INS cell lines, treated with increasing doses of 5-Fluorouracil (5-FU) (adapted from Capodanno et al. 2017).

5.4.2 Inhibition of Notch signalling decreases viability and 5-FU resistance in INS CSC-enriched tumorspheres

INS spheres were more resistant to 5-FU treatment compared to adherent cells (Figure 4.3) and 5-FU resistant INS cells demonstrated a higher expression of active NOTCH2 compared to the untreated adherent cells (Figure 5.2). Therefore, in the following section, the effect of Notch inhibition on INS cells was evaluated. A GSI, DAPT, was used to evaluate the response of INS cells to Notch blockade. Data showed that CM and canINS spheres were more sensitive to the Notch blockade compared to the adherent cells (Figure 5.4 A-B). Cell viability of canINS spheres was decreased at lower doses of DAPT (Figure 5.4 A) compared to CM spheres (Figure 5.4 B). Protein analysis was performed to show whether DAPT effectively blocked the Notch signalling pathway in INS cells (Figure 5.4 C-D). According to these data, treatment with DAPT effectively reduced NOTCH2 active form (NOTCH2-IC), and thus the transcription of HES1 in both canINS and CM spheres (Figure 5.4 C-D). Of note, in canINS spheres the blockade of the Notch signalling occured at lower doses of DAPT (Figure 5.4 C) compared to CM spheres (Figure 5.4 D). Finally, when used in combination DAPT and 5-FU, the clonogenicity of CM and canINS spheres was significantly reduced, better than either drug alone (Figure 5.4 A-B). The synergistic effect of the combination of 5-FU and DAPT was evaluated using the Bliss independence model (Figure 5.4 C-D).

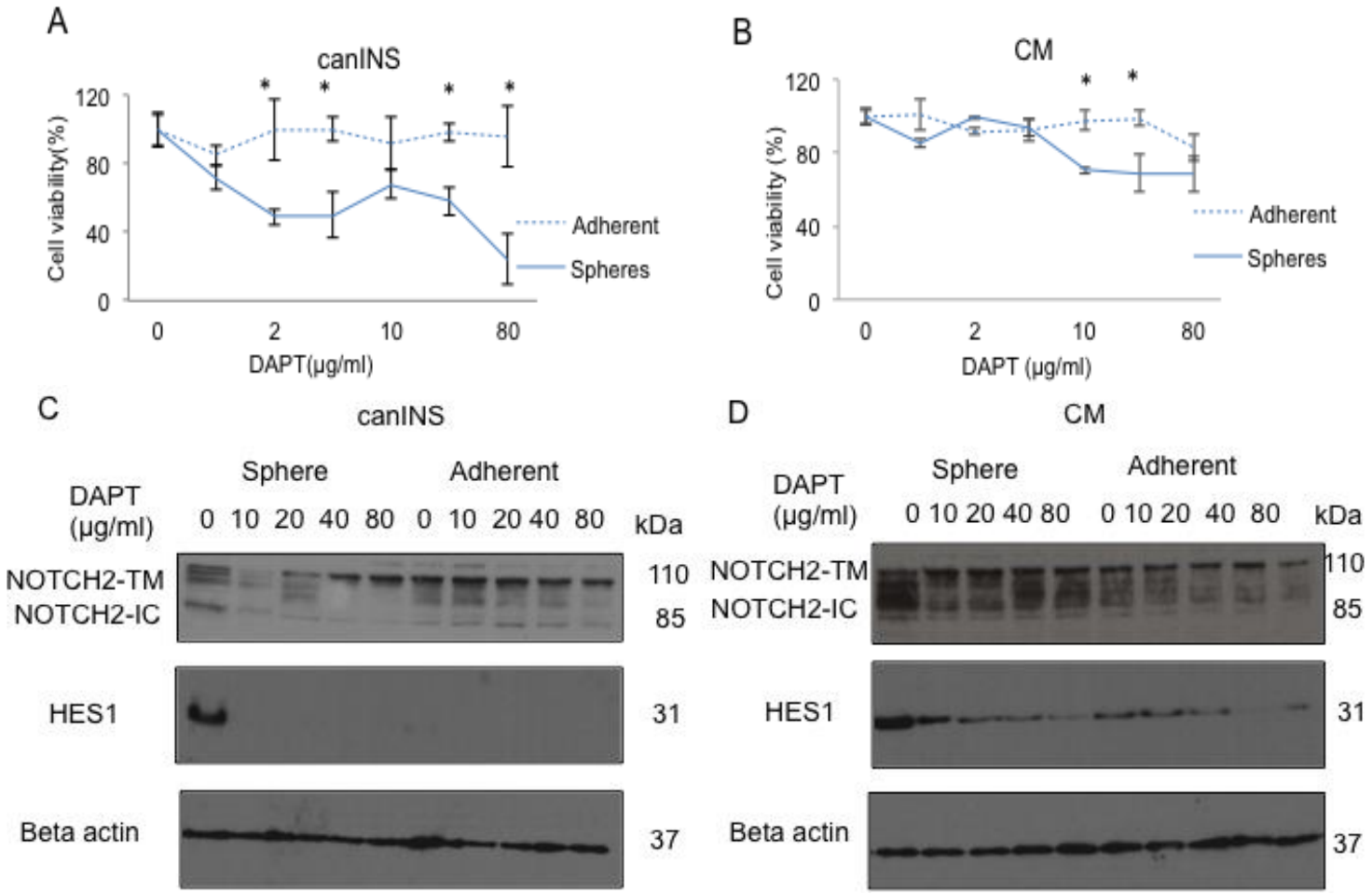

Figure 5.3 Function of the Notch pathway in canine and human insulinoma (INS) cancer stem cells (CSC). A-B: Cell viability assay of canine (A) and human (B) INS cell lines using increasing concentrations of comparing adherent cells (dashed line) against spheres (solid line). C-D: Western

blot analysis of NOTCH2 in its inactive transmembrane form (NOTCH2-TM) and in its active intracellular form (NOTCH2-IC), and HES1, with beta actin as a loading control in canine (C) and human (D) INS cell lines treated with increasing doses of gamma secretase inhibitor DAPT (adapted from Capodanno et al. 2017).

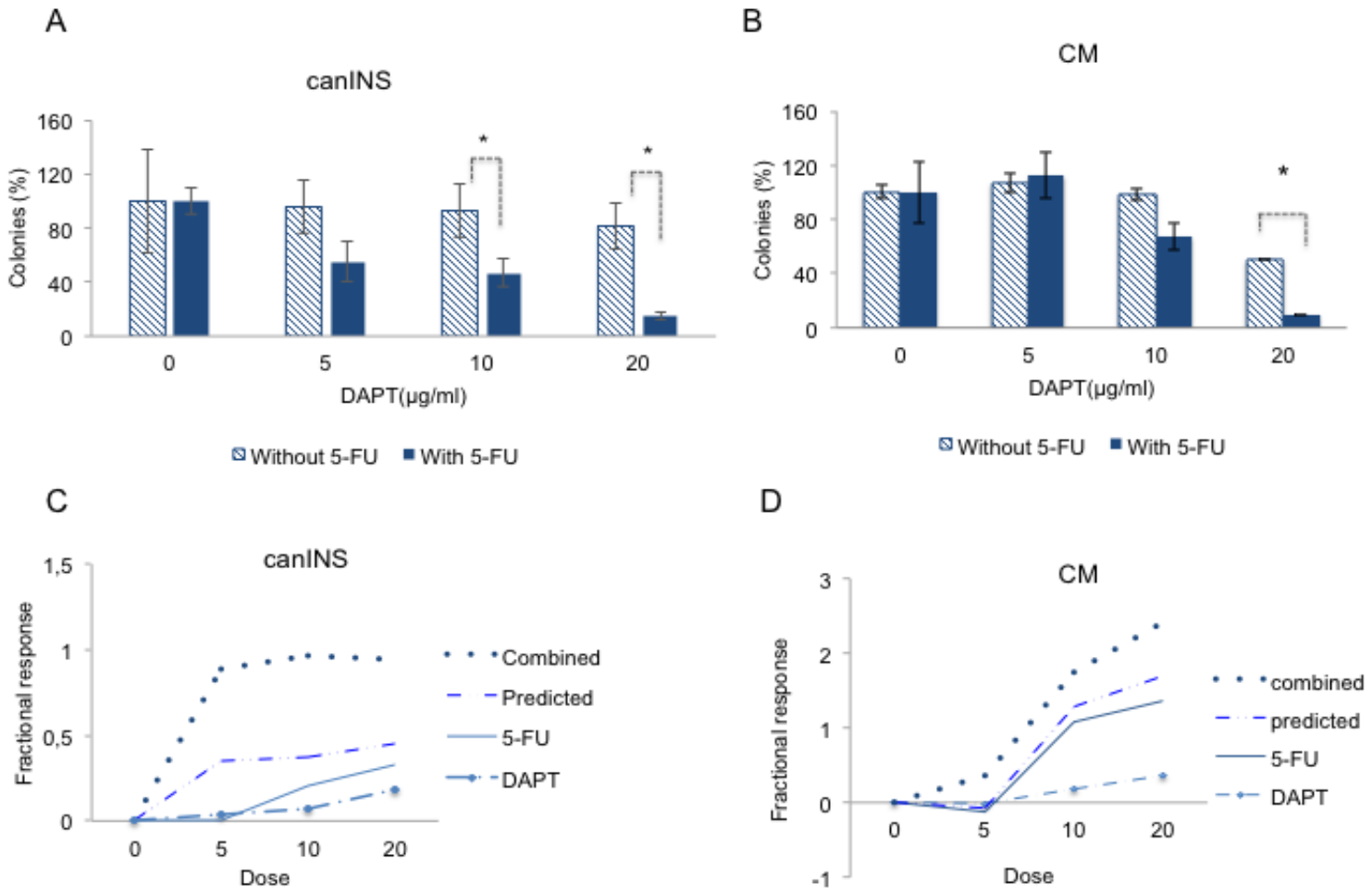

Figure 5.4 Combined treatment in vitro of canine (canINS) and human (CM) insulinoma cancer stem cells. A-B: Colony formation assay of canine (A) and human (B) INS cell lines using a combination of DAPT and 5-fluorouracil (5-FU). Values represent the mean of triplicates ± SD. The P-

values represent the comparison using 2 samples t-test within the adherent and the spheres. *P-value < 0.05. C-D: Calculation of the synergistic effect of the DAPT and 5-FU using e-bliss calculation in canINS (C) and CM (D). The method compares the observed combined response with the predicted combined response. The combined effect is synergistic as it is greater than the predicted one (adapted from Capodanno et al. 2017).

5.4.3 Notch inhibition enhances chemosensitivity to 5-FU treatment of INS CSC-enriched tumourspheres in vivo

To validate the results obtained with the *in vitro* experiments, the *in vivo* CAM model was used to test the role of the Notch pathway in the tumour-initiation properties of enriched INS CSCs. Treatment with either 5-FU, DAPT, or their combination, in the CAM model demonstrated that the canine (Figure 5.5) and human (Figure 5.6) INS CSC populations were not able to proliferate when treated with a combination of 5-FU and DAPT. The amount of fluorescence in the triplicate CAMs for the different conditions was recorded. Results shown that the combination regimen of 5-FU and DAPT significantly decreased the INS CSC-like cells proliferation, while neither treatment with DAPT, or 5-FU alone led to a significant reduction in cell proliferation (Figure 5.7).

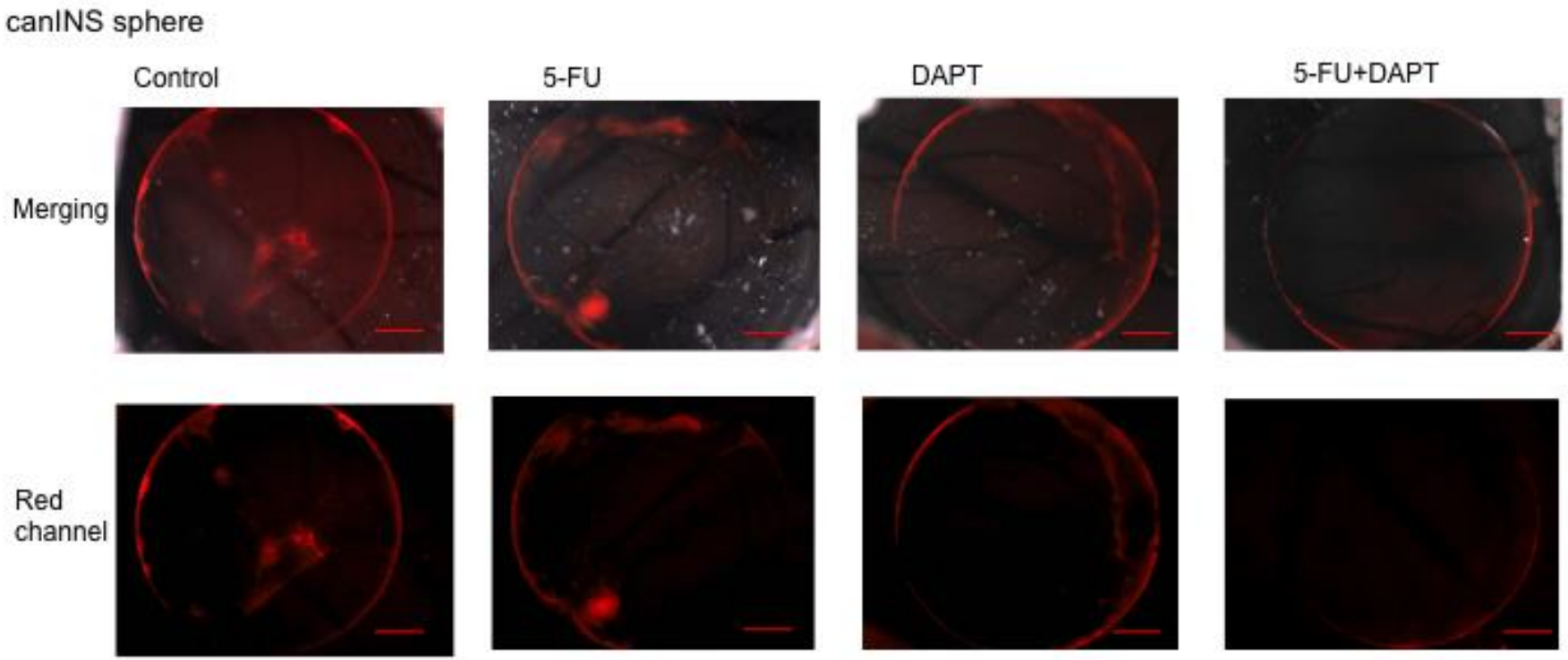

Figure 5.5 Representative photographs of the CAM 11 days after inoculation with canINS spheres following red membrane labelling. Cells have been treated with 5-FU (0.5 µM) and DAPT (20 µg/ml). Pictures on the top row show the merging of the brightfield channel; pictures on the bottom row show the red channel (scale bar: 100µm) (adapted from Capodanno et al. 2017).

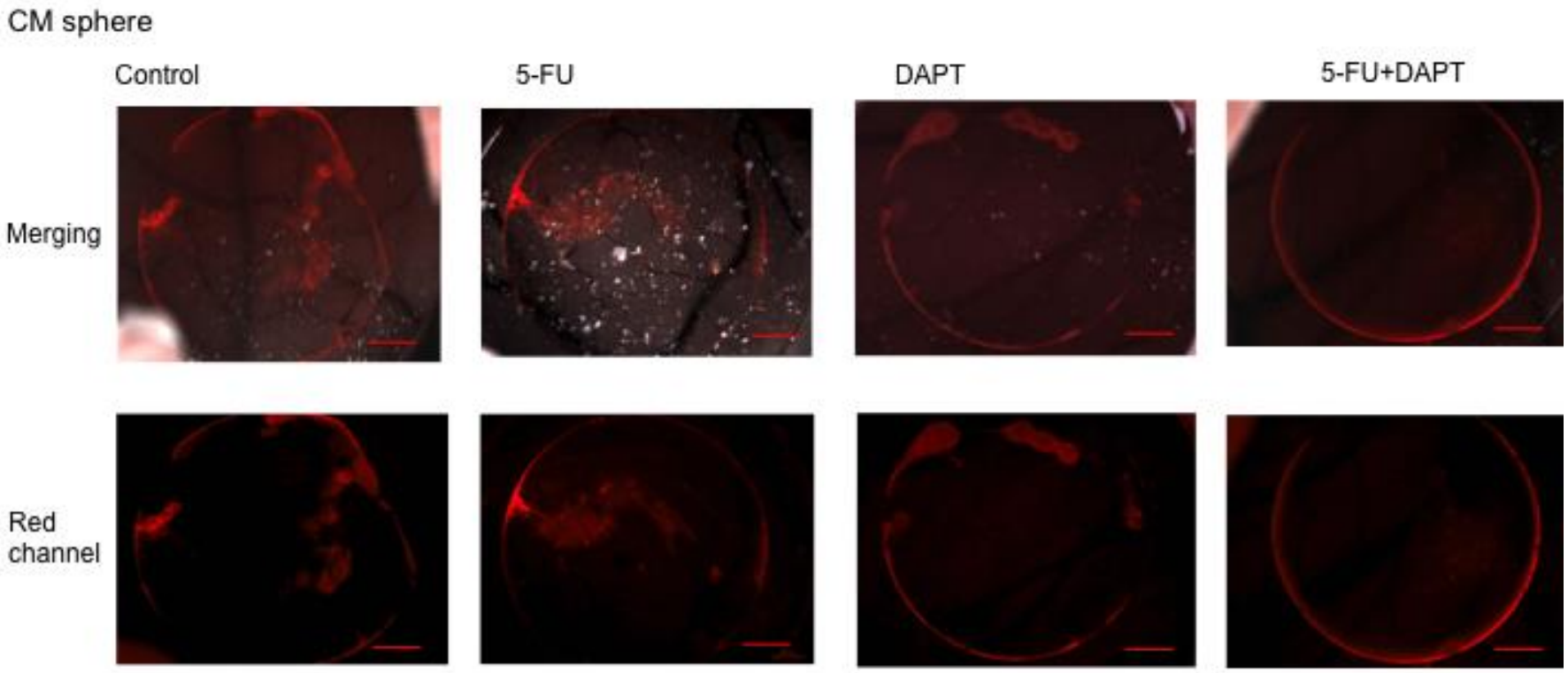

Figure 5.6 Representative photographs of the CAM 11 days after inoculation with CM spheres following red membrane labelling. Cells have been treated with 5-FU (5 µM) and DAPT (20 µg/ml). Pictures on the top row show the merging of the bright field channel; pictures on the bottom row show the red channel (scale bar: 100µm) (adapted from Capodanno et al. 2017).

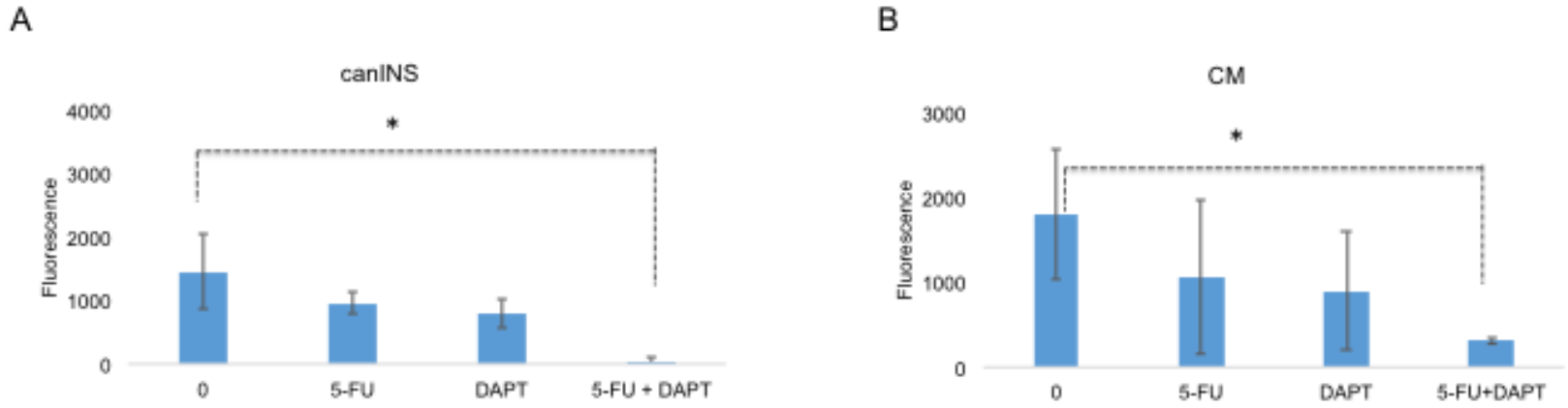

Figure 5.7 Combined 5-Fluorouracil (5-FU) and DAPT treatment decreases human and canine insulinoma cancer stem cells tumourigenic potential in the in vivo chorioallantoic membrane (CAM) model. A-B: Graphs show the differences in fluorescence between the different conditions after quantification using ImageJ of canINS (A) and CM (B) spheres. Values are mean of 3 ± SEM. *P-value < 0.05 (adapted from Capodanno et al. 2017).

5.5 Discussion

In chapter 4 it was demonstrated that CSCs could be enriched through tumorspheres culturing from both human and canine INS cell lines (Figure 4.1 A-B). INS CSCs were not only clonal *in vitro* and *in vivo* (Figure 4.5) but they were also resistant to cytotoxic chemotherapy (Figure 4.3). According to the CSC model, despite the sensitivity of bulk tumour cells to chemotherapy, CSCs are more resistant and lead ultimately to the failure of cytotoxic chemotherapy, increasing the need for new CSC-targeted therapies (Guo *et al.,* 2006). Understanding the mechanisms by which CSCs can contribute to chemotherapy and tumour relapse is essential as it provides valuable clues to better addressing cancer therapy and more specifically, cancer therapy that accounts for the unique biology of CSCs (Abdullah *et al.,* 2013). Therefore, potential targets involved in INS CSC chemoresistance have been investigated for targeted therapy. After isolating INS CSCs, the Notch pathway was identified as a potential target for INS CSC targeted therapy. Notch proteins are also oncoproteins, and deregulated Notch signalling has been demonstrated in many solid tumours, as well as NETs (Fan *et al.*, 2006; Rasul *et al.*, 2009; Dailey *et al.*, 2013; Abel *et al.*, 2014; Mao *et al.*, 2014; Irshad *et al.*, 2015). Results in this study showed that *NOTCH2* and its target gene *HES1* were overexpressed in the enriched CSC population (Figure 4.2). *NOTCH2* is the only Notch receptor that have demonstrated overexpression in both human and canine INS suggesting that *NOTCH2* is a crucial Notch receptor through which signalling in INS CSCs is mediated. The relatively few studies published in NETs to date have focused primarily on the expression and function of Notch1. Previous studies have identified Notch1 as a tumour suppressor in the majority of NET (Grande *et al.*, 2011; Carter *et al.*, 2013; Crabtree, Singleton and Miele, 2016). Although it was demonstrated that depending on the activated Notch receptors, Notch signalling can play tumour suppressive roles in some cancer types and oncogenic functions in others (Xu *et al.*, 2013; Liu *et al.*, 2017). Of note, different responses to Notch1 and Notch2 activation have been also seen within NETs. For instance, in small cell lung carcinoma, Notch1 activation inhibits tumor growth, whereas Notch2 signalling is involved in tumour promotion in small cell

lung carcinoma xenograft mice. These findings suggest that different receptor could have various functions during tumourigenesis of NET (Carter *et al.,* 2013; Crabtree *et al.,* 2016). According to our results, NOTCH2 was constitutively active in human and canine INS cells, both adherent and enriched spheres. This data showed that the Notch pathway is not only present but also active in the whole bulk of the INS cells, demonstrating the importance of cell-cell communication during tumorigenesis. Of note, the Notch pathway was upregulated in 5-FU chemoresistant INS cells. The enhanced Notch signalling may reflect selective enrichment of the INS 5-FU resistant cells; thus strengthening the hypothesis of a Notch-mediated INS chemoresistant phenotype. Previous studies have already shown the involvement of the Notch pathway in chemoresistance of a variety of tumours (Meng *et al.,* 2009; Candy *et al.,* 2013; Liu *et al.,* 2013; Mei *et al.,* 2015). For instance, overexpression of HES1 has been related to an increased resistance to 5-FU in colon cancer (Candy *et al.,* 2013) and oesophageal squamous cell carcinoma (Liu *et al.,* 2013).

Additionally, the rationale of considering the Notch pathway as a pathway triggering CSC has been already shown in various types of cancer (Fan *et al.,* 2006, 2010; Dailey *et al.,* 2013; Mao *et al.,* 2014; Irshad *et al.,* 2015). For instance, recent reviews have shown that the Hes-1/achaete–scute complex-like 1 network impacts on the tumourigenesis of NETs via Notch signalling (Crabtree *et al.,* 2016). Therefore, the effects of Notch blockade were tested in human and canine INS cells. A major class of agents targeting the Notch pathway is the γ-secretase inhibitors (GSIs). GSIs are the first class of pan-Notch inhibitors to reach clinical development in oncology (Ran *et al.,* 2017). GSIs prevent the final proteolytic cleavage of Notch receptors that releases the active intracellular fragment (Figure 5.1). In particular, we chose DAPT as it has been widely tested for its efficacy as a pan Notch inhibitor in a plethora of *in vitro* studies (Wu *et al.,* 2010; Mao *et al.,* 2014; Wang *et al.,* 2014; Lee *et al.,* 2015). Recently, it was also described its efficacy on inhibiting NOTCH2 receptor amongst all the Notch receptors (Ran *et al.,* 2017). Our results showed that DAPT, significantly decreased the survival of INS CSCs. Several studies have underlined the value of Notch targeting to reduce tumorsphere formation, prevent *in vivo* tumour formation and decrease chemoresistance in CSCs (Rizzo *et al.,* 2008; Pannuti *et al.,* 2011; Abel *et al.,* 2014). Nonetheless, due to their lack of specificity, pan-Notch

inhibitors can be more effective when used in combination with current therapies (Brennan and Clarke, 2013; Ran *et al.*, 2017). Therefore, a combined regimen of DAPT and 5-FU was used to deplete the INS CSC population both *in vitro* and *in vivo*. Data showed that treatment with DAPT alone did not inhibit CSC clonogenicity *in vitro*. However, when used in combination, DAPT and 5-FU significantly inhibited the colony-forming ability of enriched INS CSCs to a higher degree than either therapy alone. These findings were confirmed in the *in vivo* CAM assay highlighting a significant decrease in tumour formation after treatment with DAPT and 5-FU. According to our results, 5-FU-chemoresistant cells highly express NOTCH2 receptor and HES1 target gene, thus the Notch pathway is used as a mechanism of chemoresistance from INS cells. In particular, in enriched INS CSC the NOTCH pathway through NOTCH2/HES1 cascade is correlated to INS cells' stemness. Therefore, we can speculate that inhibiting the Notch pathway might cause a change in the INS CSC from quiescence to differentiation, making them sensitive to the effect of the 5-FU. The mechanism of synergy of these two drugs needs further investigations. Nonetheless, preclinical studies have already shown that inhibition of Notch using DAPT enhances the cytotoxic effects of chemotherapy in various type of cancers (Meng *et al*., 2009; Lee *et al*., 2015; Li *et al*., 2015). For example, in metastatic colon cancer, oxaliplatin-induced activation of Notch1 signalling is reduced by simultaneous GSI treatment, increasing tumour sensitivity to oxaliplatin (Meng *et al.*, 2009). In breast cancer, combined GSI and doxorubicin treatment results in synergistic cytotoxicity in triple negative breast cancer cell lines and decreased tumourigenicity in mouse xenograft models (Li *et al.*, 2015). In gastric cancer and ovarian cancer, Notch blockade increments cytotoxic effects of 5-FU and cisplatin, respectively (Wang *et al.*, 2014; Lee *et al.*, 2015).

5.6 Conclusions and future directions

In summary, the Notch pathway plays an important role in INS CSC survival and chemoresistance. In particular, treatment with 5-FU directly activates the Notch signalling pathway, through a Notch2/Hes1 cascade. The increased activation of Notch in response to chemotherapy may be clinically significant because it will

identify INS patients who would benefit from GSI treatment based on these molecular changes. Targeting the Notch pathway has shown a significant increment in the cytotoxic effects of 5-FU on the INS CSC population; although, the underlying mechanism of this process requires further studies. However, based on these results, GSI treatment could be a useful method to sensitise INS cancer cells to chemotherapy as previously reported for advances stages of solid tumours in phase I clinical trials (Richter *et al.*, 2014). Demonstrating that inhibition of the Notch pathway has functional consequences thus provides further evidence that this pathway is not only differentially expressed but it is also involved in INS tumour growth. Translationally, modulatory or inhibitory drugs targeting the Notch pathway may be applied in the treatment of INS, but its role needs to be more clearly elucidated. Since GSIs, including DAPT, inhibit cleavage of all Notch receptor families, these results may not be due to exclusive Notch2 signalling effects. Therefore, future studies will clarify the significance of specifically targeting either NOTCH2 or HES1 to develop novel therapies. Nonetheless, in the following study the Notch pathway demonstrated to be an attractive target for innovative treatment strategies to deplete the INS CSC population.

6 General discussion

6.1 Summary of findings

PNETs are neuroendocrine tumours of the duodenal-pancreatic region that often present many challenging problems in diagnosis and treatment (Ito *et al.*, 2012; Reid *et al.*, 2014; Rossi *et al.*, 2014; Giuroiu and Reidy-Lagunes, 2015). The behaviours of these tumours are highly variable and range from nearly benign to extremely aggressive. It has been recently appreciated that they are frequently more malignant than previously thought and can be a source of considerable morbidity as many patients have a protracted course (Rossi *et al.*, 2014). They also require treatment approaches that differ from those used for most common pancreatic adenocarcinoma (Ito *et al.*, 2012; Rossi *et al.*, 2014; Giuroiu & Reidy-Lagunes 2015).

In the last decade, thanks to improvements in diagnosis and case finding, PNETs have gained increased attention due to the rise of their incidence (Ro *et al.*, 2013). For instance, the development of standardised classification systems for pathological reporting and novel target medical treatments, such as everolimus and sunitinib, have increased our understanding of PNETs. Since then, numerous consensus guidelines for PNET management/ treatment of locally invasive and metastatic disease, have been developed by the European Neuroendocrine Tumour Society and the North American Neuroendocrine Tumour Society (Ito *et al.*, 2012; Baudin *et al.*, 2014; Reid *et al.*, 2014; Rossi *et al.*, 2014). Due to high heterogeneity of these tumours, so far, very few studies have specifically addressed the behaviour of the different PNET subtypes. INS are the most commonly diagnosed functioning PNETs in humans (around 30% of total PNETs) (Jonkers *et al.*, 2007). Although the optimal clinical management of INS involves a multidisciplinary approach, surgery remains the only curative treatment for early-stage disease. In advanced stages, alternative therapeutic approaches, including chemotherapy, antiangiogenic therapy, and selective internal radiotherapy, have failed to demonstrate a long-term survival benefit (Reid *et al.*, 2014).

The overall aim of this project was to improve our understanding of the complex functional biology of INS to develop novel therapeutic options for patients diagnosed with this disease. Considering the similar clinicopathologic features, canine INS was studied as a model of human INS carcinogenesis.

The first objective was to identify the mechanisms responsible for canine INS carcinogenesis using integrative computational approaches. The strategy of RNA sequencing for establishing gene expression profiles has been widely accepted in human research (Soneson *et al.*, 2013), and thanks to the recently whole canine genome characterisation (Hoeppner *et al.*, 2014), novel studies are developing to study this fascinating natural model of carcinogenesis for a variety of cancers (Davis and Ostrander, 2014).

According to the global gene expression analysis, different gene profiles characterised early and late stage of canine INS (Figure 6.1). Of interest, the majority of changes in gene expression occurred in the early stages of canine INS tumourigenesis and were majorly related to activation of beta cell differentiation mechanisms and increased insulin secretion (Figure 6.1). For instance, a large cluster of genes involved in the insulin secretory pathway such as PDX1, NESTIN, IGF2 were overexpressed in canine INS tissues compared with the control pancreatic tissues. Considering that hyperinsulinism is characteristic of INS, the predominance of the genes participating in the insulin secretory pathway suggested that an altered secretion might be a significant mechanism to increase insulin production in canine INS patients. Also, genes related with pancreatic beta cell differentiation such as PAX4, NKX2, INSM1, SOX17 were upregulated in primary canine INS lesions. For instance, INSM1 has been previously related to human INS carcinogenesis (Wang *et al.*, 2004) and studied as a negative prognosticator in human PNETs (Fujino *et al.*, 2015, 2017). Thus, we could speculate that an unbalanced pancreatic beta cell differentiation might cause an abnormal islet development and represent an early set of mutations and lead to formation of primary canine INS lesions.

In contrast, primary INS lesions and metastatic lymph nodes had a similar genetic profile, consistently with data previously published (Buishand *et al.*, 2013). According to our data, tight-junctions related genes, such as claudins, were

downregulated, and chemokine signalling-related genes were upregulated in metastatic tissues. According to the literature, downregulation of claudins-related genes causes loss of cell adhesion, which in cancer is an essential step towards metastatic spread (Zeng *et al.*, 2014). Of interest, loss of claudins expression, it has been related to EMT in the generation of stem cells from human islets (Gershengorn *et al.*, 2004). These findings highlighted that inflammation and loss of cell adhesion could be critical mechanisms during metastatic spread of canine INS (Figure 6.1). Through functional analysis we investigated the altered hubs in malignant canine INS progression. Extracellular matrix and ribosome activity were significant functions altered during early and late stage of canine INS (Figure 6.1). Ribosome activity plays a pivotal role during translation and protein synthesis. Although it is known that ribosome activity is often altered in cancer and affects the protein synthesis machinery (Goudarzi and Lindström, 2016), the role of RPs as tumour suppressors, or in certain cases, as tumour-causing or promoting genes is unknown. As discussed in section 3.5, an unbalanced ribosome assembly pathway leads to impaired protein synthesis, and as such, the level of critical tumour suppressors may be decreased below a threshold level (Goudarzi and Lindström, 2016; Wang *et al.*, 2016). This mechanism may lead to the INS cell to compensate a ribosome deficit by activation of pathways that boost ribosome production, e.g. the mTOR pathway. Considering that the mTOR signalling plays a key role in INS carcinogenesis (Zhan *et al.*, 2012), we could speculate that a loss or downregulation of RPs might alter the protein machinery in canine INS causing an uncontrolled cell growth through the mTOR pathway. This situation may create pressure to mutate components in the cell that restrains the mTOR pathway, such as PTEN and p53, which can ultimately cause uncontrolled cell growth and malignant transformation (Wang *et al.*, 2016).
In conclusion, in this project, preliminary data were collected over the global molecular biology of canine INS opening new insights on the carcinogenesis of this poorly studied tumours.

After obtaining a broad vision of the altered gene expression patterns during canine INS carcinogenesis, the second objective was to analyse functional and mechanistic behaviours of canine INS compared with the human malignant form. For this scope,

cell lines remain an invaluable source for developing techniques and assays, especially when trying to analyse behaviours that could not be tested on patients or on primary tissues, which may be available on a limited basis. Nevertheless, one key difficulty in investigating the mechanisms of INS tumourigenesis is the limited number of appropriate INS models. In this study, we characterised and compared *in vitro* and *in vivo* a primary canine INS cell line and a metastatic human INS cell line to identify mechanisms involved in resistance to conventional therapy and metastatic spread of this disease. Extensive cancer research in the past few decades has recognised the existence of a rare subpopulation of stem cells in the niche of cancer cells, the CSC. Current treatment strategies are often unspecific, and CSCs' inherent resistance to conventional chemotherapy results in many cases in tumour recurrence (Mitra *et al.,* 2015). Despite the growing evidence to support the existence of CSCs in a wide array of solid tumours, a comprehensive characterisation of a PNET CSCs has not yet been reported. In the last few years, there is an increasing interest in the isolation of CSCs from a range of human and canine solid tumours (Stoica *et al.,* 2009; Pang *et al.,* 2012, 2014; Rybicka *et al.,* 2016). Thus, suggesting that CSCs are essential in a variety of cancers and supports the use of canines as an appropriate comparative model for studying the involvement of CSCs in oncogenesis. However, little is known about the molecular mechanism of pathogenesis of INS due to lack of research materials and the high heterogeneity within the PNETs. Therefore, more studies are needed to define the presence of a subpopulation of INS CSC.

In this thesis, a subset of highly invasive cells has been isolated and characterised by human and canine INS cancer cell lines. These subpopulations of cancer cells result positive for stem cell markers and resistant to chemotherapy, similar to CSCs isolated in previous studies (Stoica *et al.,* 2009; Pang *et al.,* 2012, 2014; Rybicka *et al.,* 2016). In this PhD project, it was shown that tumorsphere culture represents a potential mean of enriching putative INS CSC. Many studies in our lab have reported the use of this assay to successfully isolate candidate CSC populations from cancer cell lines (Pang *et al.,* 2011, 2013, 2014; Pang *et al.,* 2017).

Based on selection using stem-cell surface markers, INS CSC populations were isolated in both human and canine cell lines. Thanks to gene and protein analysis, a few markers representative of human and canine INS CSC were identified such as

CD24, CD34, CD133 and CD90. Even though, CD133 and CD34 were valuable surface markers for isolating chemoresistant canine INS CSCs, these stem cell-associated surface markers were not efficient to isolate human INS CSCs. Considering the extensive heterogeneity even in a single tumour, it is it is possible that different CSCs may coexist within the human INS CSC subpopulation. It should be noted that so far no universal marker for CSCs has been identified. All of the currently described CSC markers can be detected not only on CSCs but also, to a certain extent, on normal stem cells or normal cancer cells or even normal tissues (Blacking *et al.,* 2007). Nonetheless, the lack of CSC surface marker candidate commonly expressed in both human and canine INS showed that while CSC markers might be informative to understand the cancer cell population, they alone cannot define CSCs.

Given the current lack of specificity and instability of the CSC population, the reliability of any system of CSC isolation and enrichment has to be tested experimentally through the in vivo tumour-initiating assay, as self-renewal capacity is one of the principal cellular characteristics of CSCs (Guo *et al.,* 2006). The *in vivo* CAM assay was used for this purpose demonstrating that tumorsphere-enriched CSCs are clonal and able to form tumours *in vivo*.

In summary, this part of the study revealed that, even though the existence of CSC remains a controversial topic, human and canine INS present such a cellular hierarchy, as previously shown in a variety of cancers (Gaur *et al.*, 2011; Wang *et al.*, 2011; Pang *et al.*, 2013; Hou *et al.*, 2014).

After isolating INS CSCs, the third objective of this study was to identify potential targets for novel INS CSC targeted therapy. CSCs are best characterized by enhanced drug-resistance, which could be derived either directly from their previous generations or through accumulation of the constant genomic and epigenetic mutations (Mitra *et al.*, 2015). The mechanisms behind CSCs chemoresistance have not been fully elucidated yet thus, in this study, molecules or pathways directly related to drug resistance and active survival pathways of CSCs in INS have been explored. Our results show that the expression of the Notch related-genes is increased in the enriched CSC population. In particular, NOTCH2 and its target gene

HES1 are overexpressed in both human and canine enriched INS CSC populations. Following protein analysis, we confirmed that the Notch pathway, through Notch2/Hes1 cascade, is constitutively activated in human and canine INS CSCs. The role of Notch pathway has been previously studied in various types of NET (Grande *et al.*, 2011; Carter *et al.*, 2013; Crabtree *et al.*, 2016). Although, to our knowledge, this is the first study that evaluated the importance of the Notch pathway in INS tumourigenicity and its function in INS CSC survival and chemoresistance. Given a large number of disease settings in which aberrant Notch signalling is involved, improved understanding of this pathway as a rational target is a pressing need. Results showed that Notch blockade significantly decreased cell viability of both human and canine enriched INS CSC (Figure 5.4). Moreover, treatment with 5-FU chemotherapy selected a chemoresistant Notch-active cancer cell population providing a rationale to study the Notch pathway as a mechanism of chemoresistance in INS CSCs. Furthermore, it was demonstrated that the lack of the Notch pathway sensitised INS CSCs to the effects of chemotherapeutics; thus this pathway could not only disrupt the maintenance of CSCs but also reduce their chemoresistance. These results were validated *in vivo* using the CAM model. The efficacy of the CAM assay was demonstrated as an *in vivo* model for screening of potential novel therapeutics in INS and evidence was provided that modulating Notch signalling pathway may be of great potential to eliminate CSC populations in INS.

In summary, this section of the study showed that treatment with 5-FU activated the Notch signalling pathway, through a Notch2/Hes1 cascade, and that combined treatment with Notch inhibitors and chemotherapy synergistically attenuated chemotherapy-enriched CSC population. Previous studies showed that the Notch pathway through HES1 cascade functions as an upstream regulator of the mTOR pathway, activating Akt signalling pathway, silencing PTEN (Gutierrez and Look, 2007) and controlling p53 activity through cMyc signalling (Wong *et al.*, 2012) (Figure 6.2). As discussed in section 1.5.1, mTOR and p53 collaborate during INS carcinogenesis (Pelengaris and Khan, 2001). Targeting the PI3K/mTOR signal transduction using everolimus (section 1.5.2) has shown to delay progression-free and overall survival in INS (Zhan *et al.*, 2012). Therefore, we could speculate that

the Notch pathway through a Notch2/Hes1 cascade acts as an oncogene in INS tumorigenesis promoting CSC survival and chemoresistance via mTOR activation and p53 aberration (Figure 6.2). In future studies, specifically targeting either NOTCH2 and/or HES1 could validate this hypothesis unravelling the downstream mechanisms involved in a putative Notch-driven INS carcinogenesis. Nonetheless, in this study we provided evidence that blockade of the Notch pathway decreased survival and chemoresistance of highly malignant INS cells thus providing a rationale for further investigation of this therapeutic strategy that might prevent the cascade of carcinogenic events that lead to the formation of INS.

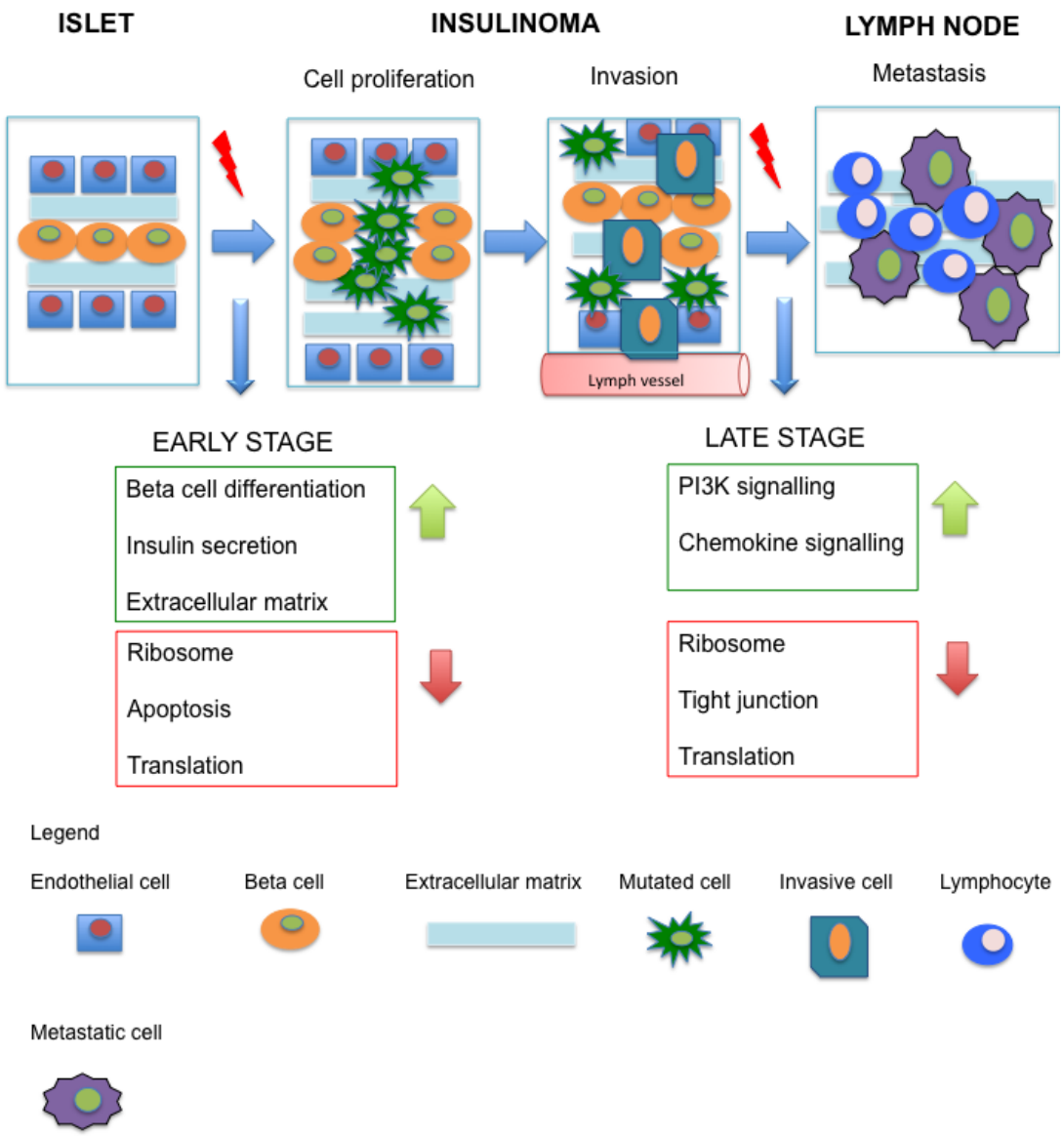

Figure 6.1 A two-stage model of canine insulinomas' carcinogenesis. Early stage: upregulation of beta cell differentiation and downregulation of apoptosis increase cell proliferation in the normal islets. Increased numbers of islet cells can elevate insulin secretion and induce a stressful microenvironment where cells mutate their ribosome activity, and the protein machinery is altered. In this condition, cell-cell interactions diminish and cells acquire invasive capability. Late stage: cell growth in the absence of cell-cell interaction causes loss of their cell adhesion and cells start to migrate towards the lymph vessel. An increased cell survival mechanism (PI3K signalling) and an increased inflammation (chemokine signalling) push the cells to disrupt the lymph vessel and metastasise to the adjacent lymph nodes. These mechanisms together might be responsible for highjacking the metastatic spread in INS.

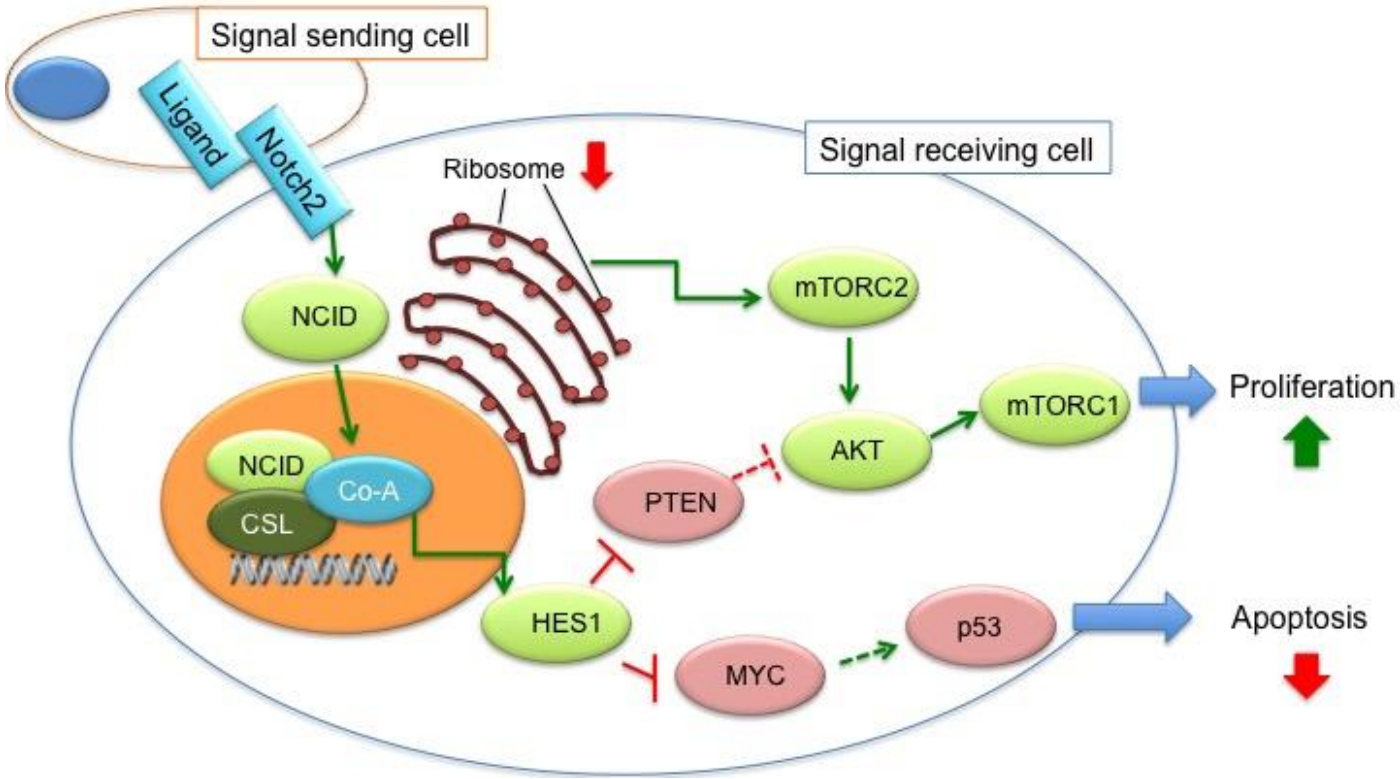

Figure 6.2 Diagram showing the model of molecular mechanisms involved in insulinoma (INS) carcinogenesis. The downregulation of the activity of ribosome proteins contributes to an increase of the mTOR signalling and thus, increasing cell proliferation. Notch activation, through a Notch2/Hes1cascade, upregulates Akt signalling and downregulates p53 pathway. HES1, via repression of PTEN and c-Myc, acts as a critical mediator of the Notch function increasing proliferation and decreasing apoptosis in INS cells. Solid line: active. Dotted line: inactive. Red: downregulated. Green: upregulated.

6.2 Limitations, controversies and recommendations for future research

One of the main shortcomings of this study was the shortage of tumour samples for the RNA-seq analysis. Due to the rarity of these tumours and the difficulties on isolating samples with high-quality RNA, significant challenges were faced during sample selection for this study. Furthermore, considering the control tissues were not matched to the tumour samples additional bias might have been introduced within this study. Therefore, despite the efforts made in selecting the samples and in the experimental design, the high inter- and intra- samples variability might have affected the validity of the data on differential gene patterns, including bias caused by the selection of normal pancreas as control tissues rather than isolated beta cells. Nevertheless, great quality of the controls was demonstrated thanks to the high homogeneity of their gene expression profiles. These observations represented an excellent starting-point for our comparisons. Moreover, RNA-Seq data analysis and functional analysis of tumour samples and metastases showed a set of altered gene patterns consistent with previously published data (Buishand *et al.*, 2013). To improve the power of the study, we recommend, in the future, increasing the number of samples and adding purified beta cells to the control tissues. Nonetheless, the overall consistency of the results obtained in this project gave some useful guidelines for the development of future RNA analysis of canine INS on a large scale.

The second part of the study was predominantly focused on the characterisation and functional analysis of a canine and human immortalised INS cell lines. Even though the use of cell lines have proven to be very useful for studying changes during carcinogenesis, limitations arise from continuous *in vitro* passaging related to mutations in the genome. This approach might lead to underestimating the scale of both mutations and differential responses within tumours and immortalised cell lines. Considering the paucity of INS models and difficulties in immortalising INS cell lines, experiments were performed on a canine primary INS cell line and a human metastatic INS cell line. Thus, some inconsistency might have been recorded due to

the different origin and species of the two cell lines used. In the future, the use of human and canine INS cell lines derived from both primary and metastatic lesions would clarify the efficacy of the present findings. Still, data comparing human and canine INS cell lines were overall consistent and confirmed our hypothesis that canine INS could represent a good model for studying human INS carcinogenesis.

Finally, the CSC hypothesis is possibly the most controversial topic in current biomedical research. Although CSCs have been well characterised in numerous malignancies, controversies have arisen on the CSC nature mainly related to the origin and frequency of CSCs and their phenotypic and functional properties (Wang *et al.*, 2015). It is reasonable considering that our knowledge of CSCs is still not complete and based on the understanding of normal stem cells. For these reasons, in the last decade, various names such as CSC, stem cell-like cancer cell, tumour-initiating cell and tumour-propagating cell have been suggested by different research groups (Fan *et al.*, 2006; Yang *et al.*, 2007; Pang *et al.*, 2012; Mei *et al.*, 2015).
Recent studies suggest that the state of CSCs is plastic and that CSCs can have different origins, including progenitor or normal cancer cell with acquired self-renewal capabilities through mutation and/or epigenetic change (Mitra *et al.*, 2015). A foundation of the CSC theory is that the CSC and non-CSC populations are biologically distinct, with different inherent properties. Thus, this observed plasticity of CSCs has majorly challenged another primary hypothesis of CSC theory over the unidirectional development. This opens a new debate line about the existence of a clear separation within CSCs and non-CSCs (Guo *et al.*, 2006).
Another fundamental paradox regarding CSC theory is that CSCs have to be dormant to be resistant to therapy and yet have to proliferate together with normal cancer cells to maintain a certain proportion size in tumours. To elucidate this contradiction the concept of "cancer stemloids" has been introduced (Wang *et al.*, 2015). According to this theory, a part of CSCs are dormant and shielded from selective pressure thus unable to drive tumour progression, whereas cancer stemloids are proliferating self-renewing cells that during clonal evolution accumulate mutations and eventually drive tumour progression. This explanation is theoretically important as it provides a basis to design therapies to selectively kill CSCs and spare normal resting stem cells.

For instance, a combination of stem-cell specific antibodies and anticancer drugs that are toxic only to cycling cells could allow targeting proliferating self-renewing CSCs (Wang *et al.*, 2015).

In summary, the current CSC hypothesis is contentious and the controversies may remain in the next few years. However, increasing understanding of the fundamental biology of CSCs could provide us with a promising opportunity to target tumour cells resistant to conventional therapies, as it has been already evidenced in recent CSC-related clinical trials (Pannuti *et al.*, 2011; Borah *et al.*, 2015; Takebe *et al.*, 2015). Nonetheless, in this study, we demonstrated that a CSC population with malignant features can be enriched in canine and human INS providing a rationale for future targeted INS CSC therapy.

6.3 Conclusions and future perspectives

Human and canine malignant INS have similar clinical and pathological features, therefore, canine INS was successfully used in this project as a model to study in-depth human INS carcinogenesis. Using integrative computational approaches, we have identified gene signatures characteristic of early and late tumourigenesis of malignant canine INS. As a result, novel markers have been investigated for future INS target therapy.

Following a comparative approach, a subpopulation of highly malignant cells has been enriched and characterised as CSCs in both human and canine INS. *In vitro* and *in vivo* data demonstrated that the Notch pathway could be fundamental for maintaining the survival and increasing chemoresistance of the CSC pool in malignant human and canine INS. In particular, NOTCH2 and HES1 were investigated as markers of INS CSC populations. These markers may have a clinical significance and help identify INS patients who would benefit from treatment with Notch inhibitors based on the change of these molecular levels. However, considering the lack of specificity of the Notch inhibitor currently tested, future studies should focus on defining the significance of explicitly targeting either NOTCH2 or HES1. Nevertheless, targeting the Notch pathway has exhibited great

potential to be an improved treatment for INS and reduce tumour relapse in what is currently a poorly treatable cancer.

7 References

Abdullah, L. N. and Chow, E. K. (2013) 'Mechanisms of chemoresistance in cancer stem cells', *Clinical and translational medicine*, 2(3), pp. 1–9. doi: http://www.clintransmed.com/content/2/1/3.

Abel, E. V., Kim, E. J., Wu, J., Hynes, M., Bednar, F., Proctor, E., Wang, L., Dziubinski, M. L. and Simeone, D. M. (2014) 'The notch pathway is important in maintaining the cancer stem cell population in pancreatic cancer', *PLoS ONE*, 9(3), pp. 1–13. doi: 10.1371/journal.pone.0091983.

Abetov, D., Mustapova, Z., Saliev, T., Bulanin, D., Batyrbekov, K. and Gilman, C. P. (2015) 'Novel Small Molecule Inhibitors of Cancer Stem Cell Signaling Pathways', *Stem Cell Reviews and Reports*, 11(6), pp. 909–918. doi: 10.1007/s12015-015-9612-x.

Acharyya, S., Oskarsson, T., Vanharanta, S., Malladi, S., Kim, J., Morris, P. G., Manova-Todorova, K., Leversha, M., Hogg, N., Seshan, V. E., Norton, L., Brogi, E. and Massagué, J. (2012) 'A CXCL1 paracrine network links cancer chemoresistance and metastasis', *Cell*, 150(1), pp. 165–178. doi: 10.1016/j.cell.2012.04.042.

Alison, M. R., Lim, S. M. L. and Nicholson, L. J. (2011) 'Cancer stem cells : problems for therapy ?', *Journal of Pathology*, pp. 147–161.

Anders, S., Pyl, P. T. and Huber, W. (2015) 'Genome analysis HTSeq — a Python framework to work with high-throughput sequencing data', *Bioinformatics*, 31(2), pp. 166–169. doi: 10.1093/bioinformatics/btu638.

Angelis, D., Lendahl, U., Hrabe, M. and Edlund, H. (1999) 'Notch signalling controls pancreatic cell differentiation', *Nature*, 400(August), pp. 14–16.

Anlauf, M., Bauersfeld, J., Raffel, A., Koch, C. a, Henopp, T., Alkatout, I., Schmitt, A., Weber, A., Kruse, M. L., Braunstein, S., Kaserer, K., Brauckhoff, M., Dralle, H., Moch, H., Heitz, P. U., Komminoth, P., Knoefel, W. T., Perren, A. and Klöppel, G. (2009) 'Insulinomatosis: a multicentric insulinoma disease that frequently causes early recurrent hyperinsulinemic hypoglycemia.', *The American journal of surgical pathology*, 33(3), pp. 339–46. doi: 10.1097/PAS.0b013e3181874eca.

Argaw-Denboba, A., Balestrieri, E., Serafino, A., Cipriani, C., Bucci, I., Sorrentino, R., Sciamanna, I., Gambacurta, A., Sinibaldi-Vallebona, P. and Matteucci, C. (2017) 'HERV-K activation is strictly required to sustain CD133+ melanoma cells with stemness features', *Journal of Experimental & Clinical Cancer Research : CR*. London: BioMed Central, 36, p. 20. doi: 10.1186/s13046-016-0485-x.

Athanasopoulos, P. G., Polymeneas, G., Dellaportas, D., Mastorakos, G., Kairi, E. and Voros, D. (2011) 'Concurrent insulinoma and pancreatic adenocarcinoma: report of a rare case and review of the literature.', *World journal of surgical oncology*. BioMed Central Ltd, 9(1), p. 7. doi: 10.1186/1477-7819-9-7.

Baeyens, L., De Breuck, S., Lardon, J., Mfopou, J. K., Rooman, I. and Bouwens, L. (2005) 'In vitro generation of insulin-producing beta cells from adult exocrine pancreatic cells.', *Diabetologia*, 48(1), pp. 49–57. doi: 10.1007/s00125-004-1606-1.

Bailey, D. B. and Page, R. L. (2007) *Withrow & MacEwen's Small Animal Clinical Oncology*. Fourth Edi, *Withrow & MacEwen's Small Animal Clinical Oncology*. Fourth Edi. Elsevier Inc. doi: 10.1016/B978-072160558-6.50027-7.

Baratelli, C., Brizzi, M. P., Tampellini, M., Scagliotti, G. V., Priola, A., Terzolo, M., Pia, A. and Berruti, A. (2014) 'Intermittent everolimus administration for malignant insulinoma.', *Endocrinology, diabetes & metabolism case reports*, 2014(September), p. 140047. doi: 10.1530/EDM-14-0047.

Baroni, M. G., Cavallo, M. G., Mark, M., Monetini, L., Stoehrer, B. and Pozzilli, P. (1999) 'Beta-cell gene expression and functional characterisation of the human insulinoma cell line CM', *Journal of Endocrinology*, (11 mM), pp. 59–68.

Baudin, E., Caron, P., Lombard-Bohas, C., Tabarin, A., Mitry, E., Reznick, Y., Taieb, D., Pattou, F., Goudet, P., Vezzosi, D., Scoazec, J.-Y., Cadiot, G., Borson-Chazot, F. and Do Cao, C. (2014) '[Malignant insulinoma: recommendations for workup and treatment].', *Presse médicale (Paris, France : 1983)*. Elsevier Masson SAS, 43(6 Pt 1), pp. 645–59. doi: 10.1016/j.lpm.2013.08.007.

Belfiore, A. and Malaguarnera, R. (2011) 'Insulin receptor and cancer', *Endocrine-Related Cancer*, 18(4), pp. 125–147. doi: 10.1530/ERC-11-0074.

Bernard, V., Lombard-Bohas, C., Taquet, M. C., Caroli-Bosc, F. X., Ruszniewski, P., Niccoli, P., Guimbaud, R., Chougnet, C. N., Goichot, B., Rohmer, V., Borson-Chazot, F. and Baudin, E. (2013) 'Efficacy of everolimus in patients with metastatic insulinoma and refractory hypoglycemia', *European Journal of Endocrinology*, 168(5), pp. 665–674. doi: 10.1530/EJE-12-1101.

Blacking, T. M., Wilson, H. and Argyle, D. J. (2007) 'Is cancer a stem cell disease? Theory, evidence and implications', *Veterinary and Comparative Oncology*, 5(2), pp. 76–89. doi: 10.1111/j.1476-5829.2007.00127.x.

Blanpain, C., Lowry, W. E., Geoghegan, A., Polak, L. and Fuchs, E. (2004) 'Existence of Two Cell Populations within an Epithelial Stem Cell Niche', *Cell*, 118, pp. 635–648.

Blaschke, M., Blumberg, J., Wegner, U., Nischwitz, M., Ramadori, G. and Cameron, S. (2012) 'Measurements of 5-FU Plasma Concentrations in Patients with Gastrointestinal Cancer: 5-FU Levels Reflect the 5-FU Dose Applied', *Journal of Cancer Therapy*, 3(1), pp. 28–36. doi: 10.4236/jct.2012.31004.

Boerkamp, K. M., van der Kooij, M., van Steenbeek, F. G., van Wolferen, M. E., Groot Koerkamp, M. J. a, van Leenen, D., Grinwis, G. C. M., Penning, L. C., Wiemer, E. a C. and Rutteman, G. R. (2013) 'Gene expression profiling of histiocytic sarcomas in a canine model: the predisposed flatcoated retriever dog.', *PloS one*, 8(8), p. e71094. doi: 10.1371/journal.pone.0071094.

Borah, a, Raveendran, S., Rochani, a, Maekawa, T. and Kumar, D. S. (2015) 'Targeting self-renewal pathways in cancer stem cells: clinical implications for cancer therapy.', *Oncogenesis*. Nature Publishing Group, 4(11), p. e177. doi: 10.1038/oncsis.2015.35.

Borson-Chazot, F., Cardot-Bauters, C., Mirallie, É. and Pattou, F. (2013) 'Insulinoma of genetic aetiology', *Annales d'Endocrinologie*, 74(3), pp. 200–202. doi: 10.1016/j.ando.2013.05.006.

Brennan, K. and Clarke, R. B. (2013) 'Combining Notch inhibition with current therapies for breast cancer treatment', *Therapeutic Advances in Medical Oncology*, 5(1), pp. 17–24. doi: 10.1177/1758834012457437.

Brun, T. and Gauthier, B. R. (2008) 'A focus on the role of Pax4 in mature pancreatic islet β-cell expansion and survival in health and disease', *Journal of Molecular Endocrinology* , 40(2), pp. 37–45. doi: 10.1677/JME-07-0134.

Buck E, Eyzaguirre A, Brown E, Petti F, McCormack S, Haley JD, Iwata KK, Gibson NW & Griffin G. 2006. Rapamycin synergizes with the epidermal growth factor receptor inhibitor erlotinib in non-small-cell lung, pancreatic, colon, and breast tumors. *Mol Cancer Ther* 5 2676-2684.

Buishand, F. O., Arkesteijn, G. J. A., Feenstra, L. R., Oorsprong, C. W. D., Mestemaker, M., Starke, A., Speel, E. J. M., Kirpensteijn, J. and Mol, J. A. (2016) 'Identification of CD90 as Putative Cancer Stem Cell Marker and Therapeutic Target in Insulinomas', *Stem Cells and Development*, 25(11), pp. 826–835. doi: 10.1089/scd.2016.0032.

Buishand, F. O., van Erp, M. G. M., Groenveld, H. a, Mol, J. a, Kik, M., Robben, J. H., Kooistra, H. S. and Kirpensteijn, J. (2012) 'Expression of insulin-like growth factor-1 by canine insulinomas and their metastases.', *Veterinary journal (London, England : 1997)*. Elsevier Ltd, 191(3), pp. 334–40. doi: 10.1016/j.tvjl.2011.03.014.

Buishand, F. O., Kik, M. and Kirpensteijn, J. (2010) 'Evaluation of clinico-pathological criteria and the Ki67 index as prognostic indicators in canine insulinoma', *The Veterinary Journal*. Elsevier Ltd, 185(1), pp. 62–67. doi: 10.1016/j.tvjl.2010.04.015.

Buishand, F. O., Kirpensteijn, J., Jaarsma, A. a, Speel, E.-J. M., Kik, M. and Mol, J. a (2013) 'Gene expression profiling of primary canine insulinomas and their metastases.', *Veterinary journal (London, England : 1997)*. Elsevier Ltd, 197(2), pp. 192–7. doi: 10.1016/j.tvjl.2013.01.021.

Buishand, F. O., Visser, J., Kik, M., Gröne, A., Keesler, R. I., Briaire-de Bruijn, I. H. and Kirpensteijn, J. (2014) 'Evaluation of prognostic indicators using validated canine insulinoma tissue microarrays.', *Veterinary journal (London, England : 1997)*. Elsevier Ltd, 201(1), pp. 57–63. doi: 10.1016/j.tvjl.2014.05.004.

Callacondo, D., Arenas, J. L., Ganoza, A. J., Rojas-Camayo, J., Quesada-Olarte, J. and Robledo, H. (2013) 'Giant insulinoma: a report of 3 cases and review of the literature.', *Pancreas*, 42(8), pp. 1323–1332. doi: 10.1097/MPA.0b013e318292006a.

Candy, P. a, Phillips, M. R., Redfern, a D., Colley, S. M., Davidson, J. a, Stuart, L. M., Wood, B. a, Zeps, N. and Leedman, P. J. (2013) 'Notch-induced transcription factors are predictive of survival and 5-fluorouracil response in colorectal cancer patients.', *British journal of cancer*. Nature Publishing Group, 109(4), pp. 1023–30. doi: 10.1038/bjc.2013.431.

Capodanno Y, Buishand FO, Pang LY, Kirpensteijn J, Mol JA, Argyle DJ. (2017) Notch pathway inhibition targets chemoresistant insulinoma cancer stem cells, Endocr Relat Cancer. 2017 Nov 24. pii: ERC-17-0415. doi: 10.1530/ERC-17-0415.

Carter, Y., Jaskula-sztul, R., Chen, H. and Mazeh, H. (2013) 'Signaling pathways as specific pharmacologic targets for neuroendocrine tumor therapy: RET, PI3K, MEK, growth factors, and Notch', *Neuroendocrinology*, 97(1), pp. 57–66. doi: 10.1159/000335136.Signaling.

Caywood, D.D., Klausner, J.S., O'Leary T.P., Withrow SJ, Richardson RC, et al. 1988. Pancreatic insulin-secreting neoplasms; clinical, diagnostic, and prognostic features in 73 dogs. J Am Anim Hosp Assoc 24: 577-584.

Chaffer, C. L., Brueckmann, I., Scheel, C., Kaestli, A. J., Wiggins, P. A., Rodrigues, L. O., Brooks, M., Reinhardt, F., Su, Y., Polyak, K., Arendt, L. M., Kuperwasser, C., Bierie, B. and Weinberg, R. A. (2011) 'Normal and neoplastic nonstem cells can spontaneously convert to a stem-like state', *Proceedings of the National Academy of Sciences of the United States of America*. National Academy of Sciences, 108(19), pp. 7950–7955. doi: 10.1073/pnas.1102454108.

Chiron, D., Maïga, S., Descamps, G., Moreau, P., Le Gouill, S., Marionneau, S., Ouiller, T., Moreaux, J., Klein, B., Bataille, R., Amiot, M. and Pellat-Deceunynck, C. (2012) 'Critical role of the NOTCH ligand JAG2 in self-renewal of myeloma cells.', *Blood cells, molecules & diseases*. Elsevier Inc.,

48(4), pp. 247–53. doi: 10.1016/j.bcmd.2012.01.006.

Conesa, A., Madrigal, P., Tarazona, S., Gomez-Cabrero, D., Cervera, A., McPherson, A., Szcześniak, M. W., Gaffney, D. J., Elo, L. L., Zhang, X. and Mortazavi, A. (2016) 'A survey of best practices for RNA-seq data analysis', *Genome Biology*, 17(1), p. 13. doi: 10.1186/s13059-016-0881-8.

Corney DC, Basturea GN (2013) RNA-sequencing. *Mater Methods* 3:203. doi: http://dx.doi.org/10.13070/mm.en.3.203.

Corroller, A. B., Valéro, R., Moutardier, V., Henry, J., Treut, Y. Le, Gueydan, M., Micco, C. De, Sierra, M., Conte-devolx, B., Oliver, C. and Raccah, D. (2008) 'Aggressive multimodal therapy of sporadic malignant insulinoma can improve survival : A retrospective 35-year study of 12 patients', *Diabetes & Metabolism*, 34, pp. 343–348. doi: 10.1016/j.diabet.2008.01.013.

Crabtree, J. S., Singleton, C. S. and Miele, L. (2016) 'Notch Signaling in Neuroendocrine Tumors.', *Frontiers in oncology*, 6(April), p. 94. doi: 10.3389/fonc.2016.00094.

Croft, D., Kelly, G. O., Wu, G., Haw, R., Gillespie, M., Matthews, L., Caudy, M., Garapati, P., Gopinath, G., Jassal, B., Jupe, S., Kalatskaya, I., Mahajan, S., May, B., Ndegwa, N., Schmidt, E., Shamovsky, V., Yung, C., Birney, E., Hermjakob, H., Eustachio, P. D. and Stein, L. (2011) 'Reactome : a database of reactions , pathways and biological processes', 39(November 2010), pp. 691–697. doi: 10.1093/nar/gkq1018.

Cui, J. Y., Gunewardena, S. S., Yoo, B., Liu, J., Renaud, H. J., Lu, H., Zhong, X. and Klaassen, C. D. (2012) 'RNA-Seq Reveals Different mRNA Abundance of Transporters and Their Alternative Transcript Isoforms During Liver Development', 127(2), pp. 592–608. doi: 10.1093/toxsci/kfs107.

D'haeseleer, P. (2005) 'How does gene expression clustering work?', *Nature Biotechnology*, 23(12), pp. 1499–1501. doi: 10.1038/nbt1205-1499.

Dailey, D. D., Anfinsen, K. P., Pfaff, L. E., Ehrhart, E. J., Charles, J. B., Bønsdorff, T. B., Thamm, D. H., Powers, B. E., Jonasdottir, T. J. and Duval, D. L. (2013) 'HES1, a target of Notch signaling, is elevated in canine osteosarcoma, but reduced in the most aggressive tumors.', *BMC veterinary research*, 9, p. 130. doi: 10.1186/1746-6148-9-130.

Danquechin-dorval, E. M. and Gesta, P. H. (1996) 'Intensity and Therapeutic Response in Patients with Advanced Colorectal Cancer Receiving lnfusional Therapy Containing 5-FU', *Cancer*, 77, pp. 441–451.

Davis, B. W. and Ostrander, E. A. (2014) 'Domestic dogs and cancer research: A breed-based genomics approach', *ILAR Journal*, 55(1), pp. 59–68. doi: 10.1093/ilar/ilu017.

Dean, M., Fojo, T. and Bates, S. (2005) 'Tumour stem cells and drug resistance.',

Nature reviews. Cancer, 5(4), pp. 275–84. doi: 10.1038/nrc1590.

Deng, W., Vanderbilt, D. B., Lin, C.-C., Martin, K. H., Brundage, K. M. and Ruppert, J. M. (2015) 'SOX9 inhibits β-TrCP-mediated protein degradation to promote nuclear GLI1 expression and cancer stem cell properties.', *Journal of cell science*, 128(6), pp. 1123–38. doi: 10.1242/jcs.162164.

Deryugina, E. I. and Quigley, J. P. (2008) 'Chick embryo chorioallantoic membrane model systems to study and visualize human tumor cell metastasis.', *Histochemistry and cell biology*, 130(6), pp. 1119–30. doi: 10.1007/s00418-008-0536-2.

Dobson, J. M. (2013) 'Breed-predispositions to cancer in pedigree dogs.', *ISRN veterinary science*, 2013, p. 941275. doi: 10.1155/2013/941275.

Dotzenrath, C., Simon, D., Berndt, I., Ro, H. D. and Goretzki, P. E. (2000) 'Lack of MEN1 gene mutations in 27 sporadic insulinomas', pp. 325–329.

Druce, M. R., Muthuppalaniappan, V. M., Leary, B. O., Chew, S. L., Drake, W. M., Monson, J. P., Akker, S. A., Besser, M., Sahdev, A., Rockall, A., Vyas, S., Bhattacharya, S., Matson, M., Berney, D. and Grossman, A. B. (2010) 'Diagnosis and localisation of insulinoma : the value of modern magnetic resonance imaging in conjunction with calcium stimulation catheterisation', pp. 6–8. doi: 10.1530/EJE-10-0056.

Edlund, H. (2002) 'Pancreatic organogenesis--developmental mechanisms and implications for therapy.', *Nature reviews. Genetics*, 3(7), pp. 524–32. doi: 10.1038/nrg841.

Ehehalt, F., Saeger, H. D., Schmidt, C. M., Tzmann, R. G. and Grützmann, R. (2009) 'Neuroendocrine Tumors of the Pancreas LEARNING OBJECTIVES', *The Oncologist*, 140014, pp. 456–467. doi: 10.1634/theoncolo-gist.2008-0259.

Eskandani, M., Abdolalizadeh, J. and Hamishehkar, H. (2015) 'Fitoterapia Galbanic acid inhibits HIF-1 α expression via EGFR / HIF-1 α pathway in cancer cells', *Fitoterapia*. Elsevier B.V., 101, pp. 1–11. doi: 10.1016/j.fitote.2014.12.003.

Evans HE, 1993. Chapter 7: the digestive apparatus and abdomen: the pancreas. In: *Miller's anatomy of the dog.* Evans HE and Evans SA,eds. Saunders, Philadelphia: 458-460

Fan, X., Khaki, L., Zhu, T. and Soules, M. (2010) 'NOTCH Pathway Blockade Depletes CD133- Positive Glioblastoma Cells and Inhibits Growth of Tumor Neurospheres and Xenografts', *Stem*, 28(1), pp. 5–16. doi: 10.1002/stem.254.NOTCH.

Fan, X., Matsui, W., Khaki, L., Stearns, D., Chun, J., Li, Y. M. and Eberhart, C. G. (2006) 'Notch pathway inhibition depletes stem-like cells and blocks

engraftment in embryonal brain tumors', *Cancer Research*, 66, pp. 7445–7452. doi: 10.1158/0008-5472.CAN-06-0858.

Fatrai S, Elghazi L, Balcazar N, Cras-Méneur C, Krits I, Kiyokawa H, Bernal-Mizrachi E. 2006. Akt induces beta-cell proliferation by regulating cyclin D1, cyclin D2, and p21 levels and cyclin-dependent kinase-4 activity. *Diabetes* 55(2):318-25.

Fazio, N., Cinieri, S., Lorizzo, K., Squadroni, M., Orlando, L., Spada, F., Maiello, E., Bodei, L., Paganelli, G., Delle Fave, G. and De Braud, F. (2010) 'Biological targeted therapies in patients with advanced enteropancreatic neuroendocrine carcinomas', *Cancer Treatment Reviews*. Elsevier Ltd, 36(SUPPL. 3), pp. S87–S94. doi: 10.1016/S0305-7372(10)70026-8.

Fendrich, V., Maschuw, K., Waldmann, J., Buchholz, M., Rehm, J., Gress, T. M., Bartsch, D. K. and König, A. (2012) 'Epithelial-mesenchymal transition is a critical step in tumorgenesis of pancreatic neuroendocrine tumors', *Cancers*, 4, pp. 281–294. doi: 10.3390/cancers4010281.

Finotello, R., Ressel, L., Arvigo, M., Baroni, G., Marchetti, V., Romanelli, G., Burrow, R., Mignacca, D. and Blackwood, L. (2014) 'Canine pancreatic islet cell tumours secreting insulin-like growth factor type 2: A rare entity', *Veterinary and Comparative Oncology*, pp. 170–180. doi: 10.1111/vco.12085.

Flattem, N., Igawa, K., Shiota, M., Emshwiller, M. G., Neal, D. W. and Cherrington, A. D. (2001) ' - and -Cell Responses to Small Changes in Plasma Glucose in the Conscious Dog', *Diabetes*, 50(2), pp. 367–375. doi: 10.2337/diabetes.50.2.367.

Fontanière, S., Tost, J., Wierinckx, a, Lachuer, J., Lu, J., Hussein, N., Busato, F., Gut, I., Wang, Z.-Q. and Zhang, C.-X. (2006) 'Gene expression profiling in insulinomas of Men1 beta-cell mutant mice reveals early genetic and epigenetic events involved in pancreatic beta-cell tumorigenesis.', *Endocrine-related cancer*, 13(4), pp. 1223–36. doi: 10.1677/erc.1.01294.

Franco, S. S., Szczesna, K., Iliou, M. S., Al-qahtani, M., Mobasheri, A., Kobolák, J. and Dinnyés, A. (2016) 'In vitro models of cancer stem cells and clinical applications', *BMC Cancer*. BMC Cancer, 16(Suppl 2). doi: 10.1186/s12885-016-2774-3.

Fridriksdottir, a J., Petersen, O. W. and Ronnov-Jessen, L. (2011) 'Mammary gland stem cells: current status and future challenges', *Int J Dev Biol*, 55(November), pp. 719–729. doi: 10.1387/ijdb.

Fujino, K., Motooka, Y., Hassan, W. A., Ali Abdalla, M. O., Sato, Y., Kudoh, S., Hasegawa, K., Niimori-Kita, K., Kobayashi, H., Kubota, I., Wakimoto, J., Suzuki, M. and Ito, T. (2015) 'Insulinoma-associated protein 1 is a crucial regulator of neuroendocrine differentiation in lung cancer', *American Journal*

of Pathology. American Society for Investigative Pathology, 185(12), pp. 3164–3177. doi: 10.1016/j.ajpath.2015.08.018.

Fujino, K., Yasufuku, K., Kudoh, S., Motooka, Y., Sato, Y. and Wakimoto, J. (2017) 'INSM1 is the best marker for the diagnosis of neuroendocrine tumors : comparison with CGA , SYP and CD56', 10(5), pp. 5393–5405.

Fukushima, K., Fujiwara, R., Yamamoto, K., Kanemoto, H., Ohno, K., Tsuboi, M., Uchida, K., Matsuki, N., Nishimura, R. and Tsujimoto, H. (2015) 'Characterization of triple-phase computed tomography in dogs with pancreatic insulinoma', *J. Vet. Med. Sci*, 77(12), pp. 1549–1553. doi: 10.1292/jvms.15-0077.

Gao, F., Zhang, Y., Wang, S., Liu, Y., Zheng, L., Yang, J., Huang, W., Ye, Y., Luo, W. and Xiao, D. (2014) 'Hes1 is involved in the self-renewal and tumourigenicity of stem-like cancer cells in colon cancer.', *Scientific reports*, 4, p. 3963. doi: 10.1038/srep03963.

Garg, R., Blando, J. M., Perez, C. J., Abba, M. C., Benavides, F. and Kazanietz, M. G. (2017) 'Protein Kinase C Epsilon Cooperates with Pten Loss for Prostate Tumorigenesis Through the Cxcl13-Cxcr5 Pathway', *Cell reports*, 19(2), pp. 375–388. doi: 10.1016/j.celrep.2017.03.042.

Gaur, P., Sceusi, E. L., Samuel, S., Xia, L., Fan, F., Zhou, Y., Lu, J., Tozzi, F., Lopez-Berestein, G., Vivas-Mejia, P., Rashid, A., Fleming, J. B., Abdalla, E. K., Curley, S. a., Vauthey, J. N., Sood, A. K., Yao, J. C. and Ellis, L. M. (2011) 'Identification of cancer stem cells in human gastrointestinal carcinoid and neuroendocrine tumors', *Gastroenterology*, 141(5), pp. 1728–1737. doi: 10.1053/j.gastro.2011.07.037.

Ghayouri M, Boulware D, Nasir A, Strosberg J, Kvols L, Coppola D. 2010. Activation of the serine/theronine protein kinase Akt in enteropancreatic neuroendocrine tumors. *Anticancer Res* 30(12):5063-7.

Gibbons, F. D. and Roth, F. P. (2002) 'Judging the quality of gene expression-based clustering methods using gene annotation', *Genome Research*, 12(10), pp. 1574–1581. doi: 10.1101/gr.397002.

Gittes GK, 2009. Developmental biology of the pancreas: a comprehensive review. *Dev Biol* 326:4-35.

Giuroiu, I. and Reidy-Lagunes, D. (2015) 'Metastatic insulinoma: Current molecular and cytotoxic therapeutic approaches for metastatic well-differentiated panNETs', *JNCCN Journal of the National Comprehensive Cancer Network*, pp. 139–144.

Gonnissen, A., Isebaert, S. and Haustermans, K. (2015) 'Targeting the Hedgehog signaling pathway in cancer: beyond Smoothened.', *Oncotarget*, 6(16), pp. 13899–913. doi: 10.18632/oncotarget.4224.

Gordon, I., Paoloni, M., Mazcko, C. and Khanna, C. (2009) 'The comparative oncology trials consortium: Using spontaneously occurring cancers in dogs to inform the cancer drug development pathway', *PLoS Medicine*, 6(10), pp. 2–6. doi: 10.1371/journal.pmed.1000161.

Goudarzi, K. M. and Lindström, M. S. (2016) 'Role of ribosomal protein mutations in tumor development (Review)', *International Journal of Oncology*, 48(4), pp. 1313–1324. doi: 10.3892/ijo.2016.3387.

Goutal, C. M., Brugmann, B. L. and Ryan, K. a (2012) 'Insulinoma in dogs: a review.', *Journal of the American Animal Hospital Association*, 48(3), pp. 151–63. doi: 10.5326/JAAHA-MS-5745.

Gragnoli, C. (2008) 'The CM cell line derived from liver metastasis of malignant human insulinoma is not a valid beta cell model for in vitro studies', *Journal of Cellular Physiology*, 216(2), pp. 569–570. doi: 10.1002/jcp.21453.

Grande, E., Capdevila, J., Barriuso, J., Antón-Aparicio, L. and Castellano, D. (2011) 'Gastroenteropancreatic neuroendocrine tumor cancer stem cells: do they exist?', *Cancer and Metastasis Reviews*, 31(1–2), pp. 47–53. doi: 10.1007/s10555-011-9328-6.

Griffin, M., Abu-El-Haija, M., Abu-El-Haija, M., Rokhlina, T. and Uc, A. (2012) 'A Simplified and Versatile Method for Obtaining High Quality Rna From Pancreas', *Biotechniques*, 52(5), pp. 332–334. doi: 10.2144/0000113862.A.

Guo, W., Lasky, J. L. and Wu, H. (2006) 'Cancer stem cells.', *Pediatric research*, 59(4 Pt 2), p. 59R–64R. doi: 10.1203/01.pdr.0000203592.04530.06.

Gupta, P. B., Fillmore, C. M., Jiang, G., Shapira, S. D., Tao, K., Kuperwasser, C. and Lander, E. S. (2017) 'Stochastic State Transitions Give Rise to Phenotypic Equilibrium in Populations of Cancer Cells', *Cell*. Elsevier, 146(4), pp. 633–644. doi: 10.1016/j.cell.2011.07.026.

Gutierrez, A. and Look, A. T. (2007) 'NOTCH and PI3K-AKT Pathways Intertwined', *Cancer Cell*, 12(5), pp. 411–413. doi: 10.1016/j.ccr.2007.10.027.

Hager, J. H. and Hanahan, D. (1999) 'Tumor cells utilize multiple pathways to down-modulate apoptosis. Lessons from a mouse model of islet cell carcinogenesis', *Ann N Y Acad Sci*, 887, pp. 150–163. doi: 10.1111/j.1749-6632.1999.tb07929.x.

Halfdanarson, T. R., Rubin, J., Farnell, M. B., Grant, C. S. and Petersen, G. M. (2008) 'Pancreatic endocrine neoplasms: Epidemiology and prognosis of pancreatic endocrine tumors', *Endocrine-Related Cancer*, 15(2), pp. 409–427. doi: 10.1677/ERC-07-0221.

Hawkins KL, Summers BA, Kuhajda FP, Msith CA. 1987. Immunocytochemistry of non-pancreatic islets and spontaneous islet cell tumours in dogs. *Vet Pathol*

24:170-179.

Hedegaard, J., Thorsen, K., Lund, M. K., Hein, A. M. K., Hamilton-Dutoit, S. J., Vang, S., Nordentoft, I., Birkenkamp-Demtröder, K., Kruhøffer, M., Hager, H., Knudsen, B., Andersen, C. L., Sørensen, K. D., Pedersen, J. S., Ørntoft, T. F. and Dyrskjøt, L. (2014) 'Next-generation sequencing of RNA and DNA isolated from paired fresh-frozen and formalin-fixed paraffin-embedded samples of human cancer and normal tissue', *PLoS ONE*, 9(5). doi: 10.1371/journal.pone.0098187.

Heitz PU, Kasper M, Polak JM, Kloppel JL. 1982. Pancreatic neuroendocrine tumours: immunocytochemical analysis of 125 tumours. *Hum Pathol* 13:263.

De Herder, W. W., Van Schaik, E., Kwekkeboom, D. and Feelders, R. A. (2011) 'New therapeutic options for metastatic malignant insulinomas', *Clinical Endocrinology*, 75(3), pp. 277–284. doi: 10.1111/j.1365-2265.2011.04145.x.

Hermann, G., Konukiewitz, B., Schmitt, A., Perren, A. and Klöppel, G. (2011) 'Hormonally defined pancreatic and duodenal neuroendocrine tumors differ in their transcription factor signatures: Expression of ISL1, PDX1, NGN3, and CDX2', *Virchows Archiv*, 459, pp. 147–154. doi: 10.1007/s00428-011-1118-6.

Higgins, R. J., Dickinson, P. J., Lecouteur, R. A., Bollen, A. W., Wang, H., Wang, H., Corely, L. J., Moore, L. M., Zang, W. and Fuller, G. N. (2010) 'Spontaneous canine gliomas: Overexpression of EGFR, PDGFRα and IGFBP2 demonstrated by tissue microarray immunophenotyping', *Journal of Neuro-Oncology*, 98(1), pp. 49–55. doi: 10.1007/s11060-009-0072-5.

Hodgkiss-Geere, H. M., Argyle, D. J., Corcoran, B. M., Whitelaw, B., Milne, E., Bennett, D. B. and Argyle, S. a. (2012) 'Characterisation and differentiation potential of bone marrow derived canine mesenchymal stem cells', *The Veterinary Journal*. Elsevier Ltd, 194(3), pp. 361–368. doi: 10.1016/j.tvjl.2012.05.011.

Hoeppner, M. P., Lundquist, A., Pirun, M., Meadows, J. R. S., Zamani, N., Johnson, J., Sundstrm, G., Cook, A., FitzGerald, M. G., Swofford, R., Mauceli, E., Moghadam, B. T., Greka, A., Alfldi, J., Abouelleil, A., Aftuck, L., Bessette, D., Berlin, A., Brown, A., Gearin, G., Lui, A., Macdonald, J. P., Priest, M., Shea, T., Turner-Maier, J., Zimmer, A., Lander, E. S., Di Palma, F., Lindblad-Toh, K. and Grabherr, M. G. (2014) 'An improved canine genome and a comprehensive catalogue of coding genes and non-coding transcripts', *PLoS ONE*, 9(3). doi: 10.1371/journal.pone.0091172.

Home Office (2014) *Guidance on the operation of the Animals (Scientific Procedures) Act 1986, Publications GOV.UK*. doi: ISBN 1474100287-9781474100281.

Höpfner, M., Sutter, a P., Gerst, B., Zeitz, M. and Scherübl, H. (2003) 'A novel

approach in the treatment of neuroendocrine gastrointestinal tumours. Targeting the epidermal growth factor receptor by gefitinib (ZD1839).', *British journal of cancer*, 89(9), pp. 1766–75. doi: 10.1038/sj.bjc.6601346.

Hou, Y.-C., Chao, Y.-J., Tung, H.-L., Wang, H.-C. and Shan, Y.-S. (2014) 'Coexpression of CD44-positive/CD133-positive cancer stem cells and CD204-positive tumor-associated macrophages is a predictor of survival in pancreatic ductal adenocarcinoma.', *Cancer*, 120(17), pp. 2766–77. doi: 10.1002/cncr.28774.

van Hulst, K. L., Oosterwijk, C., Born, W., Vroom, T. M., Nieuwenhuis, M. G., Blankenstein, M. a, Lips, C. J., Fischer, J. a and Höppener, J. W. (1999) 'Islet amyloid polypeptide/amylin messenger RNA and protein expression in human insulinomas in relation to amyloid formation.', *European journal of endocrinology / European Federation of Endocrine Societies*, 140(1), pp. 69–78. doi: 10.1530/eje.0.1400069.

Irshad, K., Mohapatra, S. K., Srivastava, C., Garg, H., Mishra, S., Dikshit, B., Sarkar, C., Gupta, D., Chandra, P. S., Chattopadhyay, P., Sinha, S. and Chosdol, K. (2015) 'A combined gene signature of hypoxia and notch pathway in human glioblastoma and its prognostic relevance.', *PloS one*, 10(3), p. e0118201. doi: 10.1371/journal.pone.0118201.

Islam, F., Qiao, B., Smith, R. A., Gopalan, V. and Lam, A. K. (2015) 'Cancer stem cell : Fundamental experimental pathological concepts and updates', *Experimental and Molecular Pathology*. Elsevier Inc., 98(2), pp. 184–191. doi: 10.1016/j.yexmp.2015.02.002.

Ito, T., Igarashi, H. and Jense, R. T. (2012) 'Therapy of metastatic pancreatic neuroendocrine tumors (pNETs): recent insights and advances', 47(9), pp. 941–960. doi: 10.1007/s11103-011-9767-z.Plastid.

Itoh, H., Nishikawa, S., Haraguchi, T., Arikawa, Y., Hiyama, M., Iseri, T., Itoh, Y., Nakaichi, M., Taura, Y., Tani, K. and Itamoto, K. (2017) 'Identification of rhodamine 123-positive stem cell subpopulations in canine hepatocellular carcinoma cells', *Biomedical Reports*, pp. 73–78. doi: 10.3892/br.2017.925.

Joglekar, M. V. and Hardikar, A. a. (2010) 'Epithelial-to-mesenchymal transition in pancreatic islet beta cells', *Cell Cycle*, 9(May 2015), pp. 4077–4079. doi: 10.4161/cc.9.20.13590.

Jonkers, Y. M. H., Claessen, S. M. H., Veltman, J. A., Geurts Van Kessel, A., Dinjens, W. N. M., Skogseid, B., Ramaekers, F. C. S. and Speel, E. J. M. (2006) 'Molecular parameters associated with insulinoma progression: Chromosomal instability versus p53 and CK19 status', *Cytogenetic and Genome Research*, 115(3–4), pp. 289–297. doi: 10.1159/000095926.

Jonkers, Y. M. H., Ramaekers, F. C. S. and Speel, E. J. M. (2007) 'Molecular alterations during insulinoma tumorigenesis.', *Biochimica et biophysica acta,*

1775(2), pp. 313–32. doi: 10.1016/j.bbcan.2007.05.004.

Jordan, D. and Carithers, R. W. (1980) 'Canine insulinoma', *Iowa State Vet*, 2(2), pp. 70–73.

Jutting, U., Aubele, M., Rodenacker, K., Gais, I., Breuer, W. and Hermanns, W. (1997) 'Canine Neuroendocrine Tumors of the Pancreas : Image Analysis Techniques for the Discrimination Versus Nonmetastatic Tumors of Metastatic', *Veterinary Pathology*, 145, pp. 138–145.

Kalantari, E., Asgari, M., Nikpanah, S. et al. Pathol. Oncol. Res. (2017) 23: 793. https://doi.org/10.1007/s12253-016-0169-z

Karayannopoulou, M., Kaldrymidou, E., Constantinidis, T. C. and Dessiris, A. (2001) 'Adjuvant Post-operative Chemotherapy in Bitches with Mammary Cancer', *Journal of Veterinary Medicine Series A: Physiology Pathology Clinical Medicine*, 48(2), pp. 85–96. doi: 10.1046/j.1439-0442.2001.00336.

Kim, A., Miller, K., Jo, J., Kilimnik, G. and Wojcik, P. (2010) 'NIH Public Access', 1(2), pp. 129–136. doi: 10.4161/isl.1.2.9480.

Kim, D., Pertea, G., Trapnell, C., Pimentel, H., Kelley, R. and Salzberg, S. L. (2013) 'TopHat2 : accurate alignment of transcriptomes in the presence of insertions , deletions and gene fusions', *Genome biology*, 4(R36), pp. 1–13.

Kishimoto, TE, Yashima S, Nakahira R., Onozawa E., Azakami D., Ujike M., Ochiaia K., Ishiwata T., Takahashi K. and Michishita M. (2017) 'Identification of tumor-initiating cells derived from two canine rhabdomyosarcoma cell lines', *Journal of Veterinary Medical Science*, 79(7), pp. 1155–1162. doi: 10.1292/jvms.16-0412.

Ko, A. H. (2017) 'Raising the bar for the adjuvant treatment of pancreatic cancer', *The Lancet*. Elsevier, 388(10041), pp. 214–215. doi: 10.1016/S0140-6736(16)30680-8.

Koblas, T., Pektorova, L., Zacharovova, K., Berkova, Z., Girman, P., Dovolilova, E., Karasova, L. and Saudek, F. (2008) 'Differentiation of CD133-Positive Pancreatic Cells Into Insulin-Producing Islet-Like Cell Clusters', *Transplantation Proceedings*, 40, pp. 415–418. doi: 10.1016/j.transproceed.2008.02.017.

Kosari, F., Parker, A. S., Kube, D. M., Lohse, C. M., Leibovich, B. C., Blute, M. L. and Cheville, J. C. (2005) 'Clear Cell Renal Cell Carcinoma : Gene Expression Analyses Identify a Potential Signature for Tumor Aggressiveness', 11(14), pp. 5128–5140.

Krampitz, G. W., George, B. M., Willingham, S. B., Volkmer, J.-P., Weiskopf, K., Jahchan, N., Newman, A. M., Sahoo, D., Zemek, A. J., Yanovsky, R. L., Nguyen, J. K., Schnorr, P. J., Mazur, P. K., Sage, J., Longacre, T. a, Visser, B. C., Poultsides, G. a, Norton, J. a and Weissman, I. L. (2016) 'Identification

of tumorigenic cells and therapeutic targets in pancreatic neuroendocrine tumors.', *Proceedings of the National Academy of Sciences of the United States of America*, 113(16), pp. 4464–9. doi: 10.1073/pnas.1600007113.

Krausch M, Raffel A, Anlauf M, et al. 2011 Loss of PTEN expression in neuroendocrine pancreatic tumors. Horm Metab Res;43(12):865–871.

Kreso, A. and Dick, J. E. (2014) 'Review Evolution of the Cancer Stem Cell Model', *Stem Cell*. Elsevier Inc., 14(3), pp. 275–291. doi: 10.1016/j.stem.2014.02.006.

Kruitwagen, H. S., Spee, B., Viebahn, C. S., Venema, H. B., Penning, L. C., Grinwis, G. C. M., Favier, R. P., van den Ingh, T. S. G. a M., Rothuizen, J. and Schotanus, B. a (2014) 'The canine hepatic progenitor cell niche: molecular characterisation in health and disease.', *Veterinary journal (London, England : 1997)*. Elsevier Ltd, 201(3), pp. 345–52. doi: 10.1016/j.tvjl.2014.05.024.

Kuboki, Y., Yamashita, S., Niwa, T., Ushijima, T., Nagatsuma, A., Kuwata, T., Yoshino, T., Doi, T., Ochiai, A. and Ohtsu, A. (2016) 'Comprehensive analyses using next-generation sequencing and immunohistochemistry enable precise treatment in advanced gastric cancer', *Annals of Oncology*, 27(1), pp. 127–133. doi: 10.1093/annonc/mdv508.

Kumar, A., Bhanja, A., Bhattacharyya, J. et al. Tumor Biol. (2016) 37: 11611. https://doi.org/10.1007/s13277-016-5112-0.

La Rosa, S., Rigoli, E., Uccella, S., Novario, R., Capella, C., 2007. Prognostic and biological significance of cytokeratin 19 in pancreatic endocrine tumours. Histopathology 50, 597–606.

La Rosa, S., Klersy, C., Uccella, S., Dainese, L., Albarello, L., Sonzogni, A., Doglioni, C., Capella, C., Solcia, E., 2009. Improved histologic and clinicopathologic criteria for prognostic evaluation of pancreatic endocrine tumors. Human Pathology 40, 30–40.

Labriola, L., Peters, M. G., Krogh, K., Stigliano, I., Terra, L. F., Buchanan, C., Machado, M. C. C., Bal de Kier Joffé, E., Puricelli, L. and Sogayar, M. C. (2009) 'Generation and characterization of human insulin-releasing cell lines.', *BMC cell biology*, 10, p. 49. doi: 10.1186/1471-2121-10-49.

Lan, M. S. and Breslin, M. B. (2009) 'Structure, expression, and biological function of INSM1 transcription factor in neuroendocrine differentiation.', *The FASEB journal : official publication of the Federation of American Societies for Experimental Biology*, 23(7), pp. 2024–2033. doi: 10.1096/fj.08-125971.

Lechner, A., Nolan, A. L., Blacken, R. a and Habener, J. F. (2005) 'Redifferentiation of insulin-secreting cells after in vitro expansion of adult human pancreatic islet tissue.', *Biochemical and biophysical research communications*, 327(2),

pp. 581–8. doi: 10.1016/j.bbrc.2004.12.043.

Lee, C. J., Dosch, J. and Simeone, D. M. (2017) Pancreatic Cancer Stem Cells. '*Journal of clinical Oncology*', 26(17). doi: 10.1200/JCO.2008.16.6702.

Lee, H. W., Kim, S. J., Choi, I. J., Song, J. and Chun, K. H. (2015) 'Targeting Notch signaling by γ-secretase inhibitor I enhances the cytotoxic effect of 5-FU in gastric cancer', *Clinical and Experimental Metastasis*. Springer Netherlands, 32(6), pp. 593–603. doi: 10.1007/s10585-015-9730-5.

Li, Z.-L., Chen, C., Yang, Y., Wang, C., Yang, T., Yang, X. and Liu, S.-C. (2015) 'Gamma secretase inhibitor enhances sensitivity to doxorubicin in MDA-MB-231 cells.', *International journal of clinical and experimental pathology*, 8(5), pp. 4378–87. Available at: http://www.pubmedcentral.nih.gov/articlerender.fcgi?artid=4503001&tool=pmcentrez&rendertype=abstract.

Liu, H., Zhou, P., Lan, H., Chen, J. and Zhang, Y. (2017) 'Comparative analysis of Notch1 and Notch2 binding sites in the genome of BxPC3 pancreatic cancer cells', *Journal of Cancer*, 8(1), pp. 65–73. doi: 10.7150/jca.16739.

Liu, J., Fan, H., Ma, Y., Liang, D., Huang, R., Wang, J., Zhou, F., Kan, Q., Ming, L., Li, H., Giercksky, K. E., Nesland, J. M. and Suo, Z. (2013) 'Notch1 Is a 5-Fluorouracil Resistant and Poor Survival Marker in Human Esophagus Squamous Cell Carcinomas', *PLoS ONE*, 8(2). doi: 10.1371/journal.pone.0056141.

Liu, S. H., Rao, D. D., Nemunaitis, J., Senzer, N., Zhou, G., Dawson, D., Gingras, M. C., Wang, Z., Gibbs, R., Norman, M., Templeton, N. S., DeMayo, F. J., O'Malley, B., Sanchez, R., Fisher, W. E. and Brunicardi, F. C. (2012) 'PDX-1 is a therapeutic target for pancreatic cancer, insulinoma and islet neoplasia using a novel RNA interference platform', *PLoS ONE*, 7(8). doi: 10.1371/journal.pone.0040452.

Liu, X. and Chang, X. (2016) 'Identifying module biomarkers from gastric cancer by differential correlation network', *OncoTargets and Therapy*, 9, pp. 5701–5711. doi: 10.2147/OTT.S113281.

Lokman, N. A., Elder, A. S. F., Ricciardelli, C. and Oehler, M. K. (2012) 'Chick chorioallantoic membrane (CAM) assay as an in vivo model to study the effect of newly identified molecules on ovarian cancer invasion and metastasis', *International Journal of Molecular Sciences*, 13(8), pp. 9959–9970. doi: 10.3390/ijms13089959.

Longnecker, Daniel, 2014. Anatomy and Histology of the Pancreas. *Pancreapedia*. DOI: 10.3998/panc.2014.3.

Lopez, J. R., Claessen, S. M. H., Macville, M. V. E., Albrechts, J. C. M., Skogseid, B. and Speel, E.-J. M. (2010) 'Spectral karyotypic and comparative genomic

analysis of the endocrine pancreatic tumor cell line BON-1.', *Neuroendocrinology*, 91(2), pp. 131–41. doi: 10.1159/000254483.

Lowes, M. A., Zaba, L. C., Krueger, J. G. and Sua, M. (2010) 'Evaluation of the Psoriasis Transcriptome across Different Studies by Gene Set Enrichment Analysis (GSEA)', 5(4). doi: 10.1371/journal.pone.0010247.

Lu, B., Huang, X., Mo, J. and Zhao, W. (2016) 'Drug Delivery Using Nanoparticles for Cancer Stem-Like Cell Targeting', *Frontiers in Pharmacology*, 7(April), pp. 1–12. doi: 10.3389/fphar.2016.00084.

Lu, C.-C., Liu, M.-M., Culshaw, G., Clinton, M., Argyle, D. a. and Corcoran, B. M. (2015) 'Gene network and canonical pathway analysis in canine myxomatous mitral valve disease: a microarray study', *The Veterinary Journal*, 204, pp. 23–31. doi: 10.1016/j.tvjl.2015.02.021.

Lu, P., Weaver, V. M. and Werb, Z. (2012) 'The extracellular matrix: A dynamic niche in cancer progression', *Journal of Cell Biology*, 196(4), pp. 395–406. doi: 10.1083/jcb.201102147.

Lubeseder-martellato, C., Hidalgo-sastre, A., Hartmann, C., Kamyabi-moghaddam, Z., Sipos, B., Wirth, M., Reichert, M., Heid, I., Schneider, G., Braren, R., Schmid, R. and Siveke, J. T. (2016) 'Membranous CD24 drives the epithelial phenotype of pancreatic cancer', *Oncotarget*, 7(31). doi: 10.18632/oncotarget.9402.

Lurye, J. C. and Behrend, E. N. (2001) 'Endocrine Tumors', *Veterinary Clinics of North America: Small Animal Practice*. Elsevier Masson SAS, 31(5), pp. 1083–1110. doi: 10.1016/S0195-5616(01)50014-5.

Magee, J. a., Piskounova, E. and Morrison, S. J. (2012) 'Cancer Stem Cells: Impact, Heterogeneity, and Uncertainty', *Cancer Cell*. Elsevier Inc., 21(3), pp. 283–296. doi: 10.1016/j.ccr.2012.03.003.

Malaguarnera, R. and Belfiore, A. (2014) 'The emerging role of insulin and insulin-like growth factor signaling in cancer stem cells', *Frontiers in Endocrinology*, 5(FEB), pp. 1–15. doi: 10.3389/fendo.2014.00010.

Mani, S. A., Guo, W., Liao, M.-J., Eaton, E. N., Ayyanan, A., Zhou, A. Y., Brooks, M., Reinhard, F., Zhang, C. C., Shipitsin, M., Campbell, L. L., Polyak, K., Brisken, C., Yang, J. and Weinberg, R. A. (2008) 'The epithelial-mesenchymal transition generates cells with properties of stem cells', *Cell*, 133(4), pp. 704–715. doi: 10.1016/j.cell.2008.03.027.

Mao, Z., Liu, J., Mao, Z., Huang, J., Xie, S. and Liu, T. (2014) 'Blocking the NOTCH pathway can inhibit the growth of CD133-positive A549 cells and sensitize to chemotherapy', *Biochemical and Biophysical Research Communications*. Elsevier Inc., 444(4), pp. 670–675. doi: 10.1016/j.bbrc.2014.01.164.

Mathur, A., Gorden, P. and Libutti, S. (2012) 'Insulinoma', 89(5), pp. 1105–1121. doi: 10.1016/j.suc.2009.06.009.

Mei, H., Yu, L., Ji, P., Yang, J., Fang, S., Guo, W., Liu, Y. and Chen, X. (2015) 'Doxorubicin activates the Notch signaling pathway in osteosarcoma', *Oncology Letters*, 9(6), pp. 2905–2909. doi: 10.3892/ol.2015.3135.

Meng, R. D., Shelton, C. C., Li, Y. M., Qin, L. X., Notterman, D., Paty, P. B. and Schwartz, G. K. (2009) 'gamma-secretase inhibitors abrogate oxaliplatin-induced activation of the Notch-1 signaling pathway in colon cancer cells resulting in enhanced chemosensitivity', *Cancer Research*, 69(2), pp. 573–582. doi: 10.1158/0008-5472.CAN-08-2088.

Metzker ML (2010) Sequencing technologies - the next generation. *Nat Rev Genet* 11(1):31-46. doi: 10.1038/nrg2626.

Michishita, M., Akiyoshi, R., Yoshimura, H., Katsumoto, T. and Ichikawa, H. (2011) 'Research in Veterinary Science Characterization of spheres derived from canine mammary gland adenocarcinoma cell lines', *Research in Veterinary Science*. Elsevier Ltd, 91(2), pp. 254–260. doi: 10.1016/j.rvsc.2010.11.016.

Mitra, A., Mishra, L. and Li, S. (2015) 'EMT , CTCs and CSCs in tumor relapse and drug-resistance', *Oncotarget*, 6(13), pp. 10697–10711.

Miyamoto, T., Kakizawa, T., Ichikawa, K., Nishio, S., Kajikawa, S. and Hashizume, K. (2001) 'Expression of dominant negative form of PAX4 in human insulinoma.', *Biochemical and biophysical research communications*, 282(1), pp. 34–40. doi: 10.1006/bbrc.2001.4552.

Mohseni, S. (2014) 'Neurologic damage in hypoglycemia', *Handbook of Clinical Neurology*, 126. doi: 10.1016/B978-0-444-53480-4.00036-9.

Nakamura, K., Lim, S. Y., Ochiai, K., Yamasaki, M., Ohta, H., Morishita, K., Takagi, S. and Takiguchi, M. (2015) 'Contrast-enhanced ultrasonographic findings in three dogs with pancreatic insulinoma', *Veterinary Radiology and Ultrasound*, 56(1), pp. 55–62. doi: 10.1111/vru.12177.

Ng, J. M. Y. and Curran, T. (2013) 'The hedgehog ' s tale : developing strategies for targeting cancer', *Nat Rev Cancer*, 11(7), pp. 493–501. doi: 10.1038/nrc3079.The.

Nölting, S., Rentsch, J., Freitag, H., Detjen, K., Briest, F., Möbs, M., Weissmann, V., Siegmund, B., Auernhammer, C. J., Aristizabal Prada, E. T., Lauseker, M., Grossman, A., Exner, S., Fischer, C., Grötzinger, C., Schrader, J. and Grabowski, P. (2017) 'The selective PI3Kα inhibitor BYL719 as a novel therapeutic option for neuroendocrine tumors: Results from multiple cell line models', *PLoS ONE*, 12(8), pp. 1–29. doi: 10.1371/journal.pone.0182852.

Northrup, N. C., Rassnick, K. M., Gieger, T. L., Kosarek, C. E., Mcfadden, C. W. and Rosenberg, M. P. (2013) 'Prospective evaluation of biweekly

streptozotocin in 19 dogs with insulinoma', *Journal of Veterinary Internal Medicine*, 27(3), pp. 483–490. doi: 10.1111/jvim.12086.

O'Brien, T. D., Hayden, D. W., O'Leary, T. P., Caywood, D. D. and Johnson, K. H. (1987) 'Canine Pancreatic Endocrine Tumors: Immunohistochemical Analysis of Hormone Content and Amyloid', *Veterinary Pathology*, 24, pp. 308–314. doi: 10.1177/030098588702400404.

O'Brien TD, Butler AE, Roche PC, Johnson KH, Butler PC. 1994. Islet amyloid polypeptide in human insulinomas. Evidence for intracellular amyloidogenesis. *Diabetes* 43(2):329-36.

Okabayashi, T., Shima, Y., Sumiyoshi, T., Kozuki, A., Ito, S., Ogawa, Y., Kobayashi, M. and Hanazaki, K. (2013) 'Diagnosis and management of insulinoma', *World Journal of Gastroenterology*, 19(6), pp. 829–837. doi: 10.3748/wjg.v19.i6.829.

Ordóñez NG, 2001 Insulinoma with fibrillar inclusions and acinar cell elements. *Ultrastructural Pathology* 25 485–495.

Osipovich, A. B., Long, Q., Manduchi, E., Gangula, R., Hipkens, S. B., Schneider, J., Okubo, T., Stoeckert, C. J., Takada, S. and Magnuson, M. A. (2014) 'Insm1 promotes endocrine cell differentiation by modulating the expression of a network of genes that includes Neurog3 and Ripply3', *Development*, 141(15), pp. 2939–2949. doi: 10.1242/dev.104810.

Pandol SJ, 2010. The exocrine pancreas. Morgan & Claypol lifesciences. PMID: 21634067. DOI: 10.4199/C00026ED1V01Y201102ISP01.

Pang, L. Y. and Argyle, D. J. (2016) 'Veterinary oncology: biology, big data and precision medicine', *The Veterinary Journal*. Elsevier Ltd, 213, pp. 38–45. doi: 10.1016/j.tvjl.2016.03.009.

Pang, L. Y., Bergkvist, G. T., Cervantes-Arias, a, Yool, D. a, Muirhead, R. and Argyle, D. J. (2012) 'Identification of tumour initiating cells in feline head and neck squamous cell carcinoma and evidence for gefitinib induced epithelial to mesenchymal transition.', *Veterinary journal (London, England : 1997)*. Elsevier Ltd, 193(1), pp. 46–52. doi: 10.1016/j.tvjl.2012.01.009.

Pang, L. Y., Blacking, T. M., Else, R. W., Sherman, A., Sang, H. M., Whitelaw, B. A., Hupp, T. R. and Argyle, D. J. (2013) 'Feline mammary carcinoma stem cells are tumorigenic, radioresistant, chemoresistant and defective in activation of the ATM/p53 DNA damage pathway', *Veterinary Journal*, 196(3), pp. 414–423. doi: 10.1016/j.tvjl.2012.10.021.

Pang, L. Y., Cervantes-Arias, A., Else, R. W. and Argyle, D. J. (2011) 'Canine Mammary Cancer Stem Cells are Radio- and Chemo- Resistant and Exhibit an Epithelial-Mesenchymal Transition Phenotype.', *Cancers*, 3(2), pp. 1744–62. doi: 10.3390/cancers3021744.

Pang, L. Y., Gatenby, E. L., Kamida, A., Whitelaw, B. a, Hupp, T. R. and Argyle, D. J. (2014) 'Global gene expression analysis of canine osteosarcoma stem cells reveals a novel role for COX-2 in tumour initiation.', *PloS one*, 9(1), p. e83144. doi: 10.1371/journal.pone.0083144.

Pang, L. Y., Saunders, L. and Argyle, D. J. (2017) 'Epidermal Growth Factor Receptor activity is elevated in glioma cancer stem cells and is required to maintain chemotherapy and radiation resistance', *Oncotarget*.

Pannuti, A., Foreman, K., Rizzo, P., Osipo, C., Golde, T. and Miele, L. (2011) 'Targeting Cancer Stem Cells through Notch Signaling', 16(12), pp. 3141–3152. doi: 10.1158/1078-0432.CCR-09-2823.

Paoloni, M. C. and Khanna, C. (2007) 'NIH Public Access', *October*, 454(1), pp. 42–54. doi: 10.1097/OPX.0b013e3182540562.

Paschall, A. V, Yang, D., Lu, C., Redd, P. S., Choi, J. and Christopher, M. (2016) 'CD133 + CD24 lo defines a 5-Fluorouracil-resistant colon cancer stem cell-like phenotype', 7(48). doi: 10.18632/oncotarget.12168.

Pastrana, E., Silva-Vargas, V. and Doetsch, F. (2011) 'Eyes Wide Open: A Critical Review of Sphere-Formation as an Assay For Stem Cells', *Cell Stem Cell.*, 8(5), pp. 486–498. doi: 10.1016/j.stem.2011.04.007.

Pattabimaran, D. R. and Weinberg, R. A. (2014) 'Tackling the cancer stem cells – what challenges do they pose?', 13(7), pp. 497–512. doi: 10.1038/nrd4253.

Pei, X., Zhu, J., Yang, R., Tan, Z., An, M., Shi, J. and Lubman, D. M. (2016) 'CD90 and CD24 Co-Expression Is Associated with Pancreatic Intraepithelial Neoplasias', *PLoS ONE*. Edited by P. K. Singh. San Francisco, CA USA: Public Library of Science, 11(6), p. e0158021. doi: 10.1371/journal.pone.0158021.

Pelengaris, S. and Khan, M. (2001) 'Oncogenic co-operation in beta-cell tumorigenesis.', *Endocrine-related cancer*, 8(4), pp. 307–314. Available at: http://ovidsp.ovid.com/ovidweb.cgi?T=JS&PAGE=reference&D=med4&NEWS=N&AN=11733227.

Pfaffl, M. W. (2004) 'Relative quantification', *Real-time PCR*, pp. 63–82. doi: 10.1186/1756-6614-3-5.

Phesse, T. J., Myant, K. B., Cole, A. M., Ridgway, R. A., Pearson, H., Muncan, V., van den Brink, G. R., Vousden, K. H., Sears, R., Vassilev, L. T., Clarke, A. R. and Sansom, O. J. (2014) 'Endogenous c-Myc is essential for p53-induced apoptosis in response to DNA damage in vivo', *Cell Death and Differentiation*. Nature Publishing Group, 21(6), pp. 956–966. doi: 10.1038/cdd.2014.15.

Polton, G. a, White, R. N., Brearley, M. J. and Eastwood, J. M. (2007) 'Improved survival in a retrospective cohort of 28 dogs with insulinoma.', *The Journal*

of small animal practice, 48(3), pp. 151–6. doi: 10.1111/j.1748-5827.2006.00187.

Ran, Y., Hossain, F., Pannuti, A., Lessard, C. B., Ladd, G. Z., Jung, J. I., Minter, L. M., Osborne, B. A., Miele, L. and Golde, T. E. (2017) 'γ- Secretase inhibitors in cancer clinical trials are pharmacologically and functionally distinct', *EMBO Molecular Medicine*, 9(7), p. 950 LP-966. doi: 10.15252/emmm.201607265.

Rasul, S., Balasubramanian, R., Filipović, a, Slade, M. J., Yagüe, E. and Coombes, R. C. (2009) 'Inhibition of gamma-secretase induces G2/M arrest and triggers apoptosis in breast cancer cells.', *British journal of cancer*, 100(12), pp. 1879–88. doi: 10.1038/sj.bjc.6605034.

Reid, M. D., Balci, S., Saka, B. and Adsay, N. V. (2014) 'Neuroendocrine tumors of the pancreas: Current concepts and controversies', *Endocrine Pathology*, 25(1), pp. 65–79. doi: 10.1007/s12022-013-9295-2.

Regitnig, P., Spuller, E. and Denk, H. (2001) 'Insulinoma of the pancreas with insular–ductular differentiation in its liver metastasis – indication of a common stem-cell origin of the exocrine and endocrine components', *Virchows Archiv*, 438(6), pp. 624–628. doi: 10.1007/s004280100406.

Reya, T., Morrison, S. J., Clarke, M. F. and L., W. I. (2001) 'S t em c e ll s , c a n c e r , a nd c a n c e r s t em c e ll s', pp. 105–111.

Ricardo, S., Vieira, A. F., Gerhard, R., Leitão, D., Pinto, R., Cameselle-Teijeiro, J. F., Milanezi, F., Schmitt, F. and Paredes, J. (2011) 'Breast cancer stem cell markers CD44, CD24 and ALDH1: expression distribution within intrinsic molecular subtype', *Journal of Clinical Pathology*, 64(11), p. 937 LP-946. Available at: http://jcp.bmj.com/content/64/11/937.

Richter, S., Bedard, P. L., Chen, E. X., Clarke, B. a., Tran, B., Hotte, S. J., Stathis, A., Hirte, H. W., Razak, A. R. a, Reedijk, M., Chen, Z., Cohen, B., Zhang, W. J., Wang, L., Ivy, S. P., Moore, M. J., Oza, A. M., Siu, L. L. and McWhirter, E. (2014) 'A phase i study of the oral gamma secretase inhibitor R04929097 in combination with gemcitabine in patients with advanced solid tumors (PHL-078/CTEP 8575)', *Investigational New Drugs*, 32(2), pp. 243–249. doi: 10.1007/s10637-013-9965-4.

van Rijn, S. J., Riemers, F. M., van den Heuvel, D., Wolfswinkel, J., Hofland, L., Meij, B. P. and Penning, L. C. (2014) 'Expression stability of reference genes for quantitative RT-PCR of healthy and diseased pituitary tissue samples varies between humans, mice, and dogs.', *Molecular neurobiology*, 49(2), pp. 893–9. doi: 10.1007/s12035-013-8567-7.

Rizzo, P., Osipo, C., Foreman, K., Golde, T., Osborne, B. and Miele, L. (2008) 'Rational targeting of Notch signaling in cancer', *Oncogene*, 27(38), pp. 5124–5131. doi: 10.1038/onc.2008.226.

Ro, C., Chai, W., Yu, V. E. and Yu, R. (2013) 'Pancreatic neuroendocrine tumors: biology, diagnosis,and treatment.', *Chin J Cancer*, 32(6), pp. 312–324. doi: 10.5732/cjc.012.10295.

Robinson, M. D., Mccarthy, D. J. and Smyth, G. K. (2010) 'edgeR : a Bioconductor package for differential expression analysis of digital gene expression data', 26(1), pp. 139–140. doi: 10.1093/bioinformatics/btp616.

Rosenbaum, J. N., Guo, Z., Baus, R. M., Werner, H., Rehrauer, W. M. and Lloyd, R. V. (2015) 'A novel immunohistochemical and molecular marker for neuroendocrine and neuroepithelial neoplasms', *American Journal of Clinical Pathology*, 144(4), pp. 579–591. doi: 10.1309/AJCPGZWXXBSNL4VD.

Rossi, R. E., Massironi, S., Conte, D. and Peracchi, M. (2014) 'Therapy for metastatic pancreatic neuroendocrine tumors.', *Annals of translational medicine*, 2(1), p. 8. doi: 10.3978/j.issn.2305-5839.2013.03.01.

Roy, M., Pear, W. S. and Aster, J. C. (2007) 'The multifaceted role of Notch in cancer.', *Current opinion in genetics & development*, 17(1), pp. 52–9. doi: 10.1016/j.gde.2006.12.001.

Rybicka, A. and Król, M. (2016) 'Identification and characterization of cancer stem cells in canine mammary tumors', *Acta Veterinaria Scandinavica*, 58(1), p. 86. doi: 10.1186/s13028-016-0268-6.

Rybicka, A., Mucha, J., Majchrzak, K., Taciak, B., Hellmen, E., Motyl, T. and Krol, M. (2015) 'Analysis of MicroRNA expression in canine mammary cancer stem-like cells indicates epigenetic regulation of transforming growth factor-beta signaling', *Journal of Physiology and Pharmacology*, 66 (1), pp. 29–37.

Sakai, Y., Hong, S.-M., An, S., Kim, J. Y., Corbeil, D., Karbanová, J., Otani, K., Fujikura, K., Song, K.-B., Kim, S. C., Akita, M., Nanno, Y., Toyama, H., Fukumoto, T., Ku, Y., Hirose, T., Itoh, T. and Zen, Y. (2017) 'CD133 expression in well-differentiated pancreatic neuroendocrine tumors: a potential predictor of progressive clinical courses', *Human Pathology*. Elsevier Inc., 61, pp. 148–157. doi: 10.1016/j.humpath.2016.10.022.

Schermerhorn, T. (2013) 'Canine insulinoma as a model for studying molecular genetics of tumorigenesis and metastasis.', *Veterinary journal (London, England : 1997)*, 197(2), pp. 126–7. doi: 10.1016/j.tvjl.2013.04.017.

Schiffman, J. D. and Breen, M. (2015) 'Comparative oncology: what dogs and other species can teach us about humans with cancer', *Philosophical Transactions of the Royal Society B: Biological Sciences*, 370(1673), pp. 20140231–20140231. doi: 10.1098/rstb.2014.0231.

Schoot, A., Landis, M., Dontu, G., Griffith, K. and Al., E. (2013) 'Preclinical and Clinical Studies of Gamma Secretase Inhibitors with Docetaxel on Human Breast Tumors', *Clinical Cancer Research*, 19(6), pp. 1512–1524. doi:

10.1111/j.1747-0285.2012.01428.

Schotanus, B. a, Kruitwagen, H. S., van den Ingh, T. S., van Wolferen, M. E., Rothuizen, J., Penning, L. C. and Spee, B. (2014) 'Enhanced Wnt/β-catenin and Notch signalling in the activated canine hepatic progenitor cell niche', *BMC Veterinary Research*, 10, pp. 1–9. doi: 10.1186/s12917-014-0309-1.

Seyedi, F., Farsinejad, A., Moshrefi, M. and Nematollahi-Mahani, S. N. (2015) 'In vitro evaluation of different protocols for the induction of mesenchymal stem cells to insulin-producing cells.', *In vitro cellular & developmental biology. Animal*. doi: 10.1007/s11626-015-9890-2.

Seymour, P. a, Freude, K. K., Tran, M. N., Mayes, E. E., Jensen, J., Kist, R., Scherer, G. and Sander, M. (2007) 'SOX9 is required for maintenance of the pancreatic progenitor cell pool.', *Proceedings of the National Academy of Sciences of the United States of America*, 104(12), pp. 1865–1870. doi: 10.1073/pnas.0609217104.

Siddons, E. B., Carters W. (1976) 'Canine Insulinoma', *Iowa State* University, 38(2).

Skelin, M., Rupnik, M. and Cencic, A. (2010) 'Pancreatic beta cell lines and their applications in diabetes mellitus research.', *Altex*, 27(2), pp. 105–113. doi: 20686743.

Skoda, J., Hermanova, M., Loja, T., Nemec, P., Neradil, J., Karasek, P. and Veselska, R. (2016) 'Co-Expression of Cancer Stem Cell Markers Corresponds to a Pro-Tumorigenic Expression Profile in Pancreatic Adenocarcinoma', *PLoS ONE*. Edited by D. Nie. San Francisco, CA USA: Public Library of Science, 11(7), p. e0159255. doi: 10.1371/journal.pone.0159255.

Slattery, M. L., Pellatt, D. F., Mullany, L. E., Wolff, R. K. and Herrick, J. S. (2015), Gene expression in colon cancer: A focus on tumor site and molecular phenotype. Genes Chromosomes Cancer, 54: 527–541. doi:10.1002/gcc.22265

Sloan, A. E., Nock, C. J., Supko, J., Ye, X., Takebe, N., Rich, J., Prados, M. and Grossman, S. (2014) 'TARGETING GLIOMA INITIATING CELLS IN GBM: ABTC-0904, A RANDOMIZED PHASE 0/II STUDY TARGETING THE SONIC HEDGEHOG-SIGNALING PATHWAY', *Neuro-Oncology*. Oxford University Press, 16(Suppl 3), p. iii46-iii46. doi: 10.1093/neuonc/nou209.17.

Soneson, C. and Delorenzi, M. (2013) 'A comparison of methods for differential expression analysis of RNA-seq data.', *BMC bioinformatics*. BMC Bioinformatics, 14(1), p. 91. doi: 10.1186/1471-2105-14-91.

Speel EJM, Richter J, Moch H, Egenter C, Saremaslani P, Rütimann K, Zhao J, Barg-Horn A, Roth J, Heitz PU, Komminoth P 1999 Genetic differences in

endocrine pancreatic tumor subtypes detected by comparative genomic hybridization. *American Journal of Pathology* 155 1787-1794.

Srivastava, A. and Hornick, J. L. (2009) 'Immunohistochemical Staining for CDX-2, PDX-1, NESP-55, and TTF-1 Can Help Distinguish Gastrointestinal Carcinoid Tumors From Pancreatic Endocrine and Pulmonary Carcinoid Tumors', *American journal of surgical pathology*, 33(4), pp. 626–632.

Steiner, D. J., Kim, A., Miller, K. and Hara, M. (2011) 'architecture and composition', 2(3), pp. 135–145.

Stevenson, R., Libutti, S. K. and Saif, M. W. (2013) 'Novel Agents in Gastroenteropancreatic Neuroendocrine Tumors', 14(2), pp. 152–154.

Stoica, G., Lungu, G., Martini-Stoica, H., Waghela, S., Levine, J. and Smith, R. (2009) 'Identification of cancer stem cells in dog glioblastoma.', *Veterinary pathology*, 46(3), pp. 391–406. doi: 10.1354/vp.08-VP-0218-S-FL.

Subramanian, A., Tamayo, P., Mootha, V. K., Mukherjee, S., Ebert, B. L., Gillette, M. a, Paulovich, A., Pomeroy, S. L., Golub, T. R., Lander, E. S. and Mesirov, J. P. (2005) 'Gene set enrichment analysis: a knowledge-based approach for interpreting genome-wide expression profiles.', *Proceedings of the National Academy of Sciences of the United States of America*, 102(43), pp. 15545–50. doi: 10.1073/pnas.0506580102.

Sugiyama, T., Rodriguez, R. T., McLean, G. W. and Kim, S. K. (2007) 'Conserved markers of fetal pancreatic epithelium permit prospective isolation of islet progenitor cells by FACS.', *Proceedings of the National Academy of Sciences of the United States of America*, 104(1), pp. 175–80. doi: 10.1073/pnas.0609490104.

Sukowati, C. H. C., Anfuso, B., Crocé, L. S. and Tiribelli, C. (2015) 'The role of multipotent cancer associated fibroblasts in hepatocarcinogenesis.', *BMC cancer*, 15, p. 188. doi: 10.1186/s12885-015-1196-y.

Swann, H. M. and Holt, D. E. (2002) 'Canine gastric adenocarcinoma and leiomyosarcoma: a retrospective study of 21 cases (1986-1999) and literature review.', *Journal of the American Animal Hospital Association*, 38(2), pp. 157–64. doi: 10.5326/0380157.

Takebe, N., Miele, L., Harris, P. J., Jeong, W., Bando, H., Yang, S. X., Ivy, S. P., Kahn, M., Yang, S. X. and Ivy, S. P. (2015) 'Targeting Notch, Hedgehog, and Wnt Pathways in cancer stem cells: clinical update', *Nat Rev Clin Oncol*, 12(8), pp. 445–464. doi: 10.1038/nrclinonc.2015.61.

Thrall, D. E. (2011) 'Proceedings of the 36th World Small Animal Veterinary Congress WSAVA', *Proceedings of the 36th World Small Animal Veterinary Congress*, pp. 244–246.

Tian F, Wang Y, Seiler M, Hu Z. Functional characterization of breast cancer using

pathway profiles. *BMC Medical Genomics*. 2014;7:45. doi:10.1186/1755-8794-7-45.

Trifonidou, M. a., Kirpensteijn, J. and Robben, J. H. (1998) 'A Retrospective Evaluation of 51 Dogs with Insulinoma', *Veterinary Quarterly*, 20(sup1), pp. S114–S115. doi: 10.1080/01652176.1998.10807459.

Tsuchitani, M., Sato, J. and Kokoshima, H. (2016) 'A comparison of the anatomical structure of the pancreas in experimental animals', pp. 147–154. doi: 10.1293/tox.2016-0016.

Vaidakis, D., Karoubalis, J., Pappa, T., Piaditis, G. and Zografos, G. N. (2010) 'Pancreatic insulinoma : current issues and trends', *Hepatobiliary pancreas Dis Int*, 9(3), pp. 234-241.

Vandamme, T., Peeters, M., Dogan, F., Pauwels, P., Van Assche, E., Beyens, M., Mortier, G., Vandeweyer, G., de Herder, W., Van Camp, G., Hofland, L. J. and de Beeck, K. O. (2015) 'Whole-exome characterization of pancreatic neuroendocrine tumor cell lines BON-1 and QGP-1', *Journal of Molecular Endocrinology*, 54(2), pp. 137–147. doi: 10.1530/JME-14-0304.

Vargas, A., Zeisser-Labouèbe, M., Lange, N., Gurny, R. and Delie, F. (2007) 'The chick embryo and its chorioallantoic membrane (CAM) for the in vivo evaluation of drug delivery systems', *Advanced Drug Delivery Reviews*, 59(11), pp. 1162–1176. doi: 10.1016/j.addr.2007.04.019.

Venkatesan, V., Gopurappilly, R., Goteti, S. K., Dorisetty, R. K. and Bhonde, R. R. (2011) 'Pancreatic progenitors: The shortest route to restore islet cell mass', *Islets*, 3(February 2015), pp. 295–301. doi: 10.4161/isl.3.6.17704.

Vinik, A., Feliberti, E., Perry, RP. (2017) 'Insulinomas'.*MDText.com.*

Vortmeyer, A. O., Huang, S., Lubensky, I. and Zhuang, Z. (2004) 'Non-islet origin of pancreatic islet cell tumors.', *The Journal of clinical endocrinology and metabolism*, 89(4), pp. 1934–8. doi: 10.1210/jc.2003-031575.

Wang, H., Chen, Y., Fernandez-Del Castillo, C., Yilmaz, O. and Deshpande, V. (2013) 'Heterogeneity in signaling pathways of gastroenteropancreatic neuroendocrine tumors: a critical look at notch signaling pathway.', *Modern pathology : an official journal of the United States and Canadian Academy of Pathology, Inc*. Nature Publishing Group, 26(1), pp. 139–47. doi: 10.1038/modpathol.2012.143.

Wang, H., Wang, S., Hu, J., Kong, Y., Chen, S., Li, L. and Li, L. (2009) 'Oct4 is expressed in Nestin-positive cells as a marker for pancreatic endocrine progenitor', *Histochemistry and Cell Biology*, 131(5), pp. 553–563. doi: 10.1007/s00418-009-0560-x.

Wang, M., Ma, X., Wang, J., Wang, L. and Wang, Y. (2014) 'Pretreatment with the γ-secretase inhibitor DAPT sensitizes drug-resistant ovarian cancer cells to

cisplatin by downregulation of Notch signaling', *International Journal of Oncology*, 44(4), pp. 1401–1409. doi: 10.3892/ijo.2014.2301.

Wang, T., Shigdar, S., Gantier, M. P., Hou, Y., Wang, L., Li, Y., Al Shamaileh, H., Yin, W., Zhou, S.-F., Zhao, X. and Duan, W. (2015) 'Cancer stem cell targeted therapy: progress amid controversies', *Oncotarget*, 6(42), pp. 44191–44206. doi: 10.18632/oncotarget.6176.

Wang, X. C., Xu, S. Y., Wu, X. Y., Song, H. D., Mao, Y. F., Fan, H. Y., Yu, F., Mou, B., Gu, Y. Y., Xu, L. Q., Zhou, X. O., Chen, Z., Chen, J. L. and Hu, R. M. (2004) 'Gene expression profiling in human insulinoma tissue: Genes involved in the insulin secretion pathway and cloning of novel full-length cDNAs', *Endocrine-Related Cancer*, 11(2), pp. 295–303. doi: 10.1677/erc.0.0110295.

Wang, Y., Lanzoni, G., Carpino, G., Cui, C., J, D.-B., E, W., Cardinale, V. and Al., E. (2013) 'Biliary Tree Stem Cells, Precursors to Pancreatic Committed Progenitors: Evidence for Possible Life-long Pancreatic Organogenesis', 31(9), pp. 1966–1979. doi: 10.1002/stem.

Wang, Z. (2011) 'Targeting notch to eradicate pancreatic cancer stem cells for cancer therapy', *Anticancer Res.*, pp. 1105–1113. doi: 31/4/1105 [pii].

Wang, Z., Ahmad, A., Li, Y., Azmi, A. S., Miele, L. and Sarkar, F. H. (2011) 'Targeting notch to eradicate pancreatic cancer stem cells for cancer therapy', *Anticancer Research*, 31(4), pp. 1105–1113. doi: 31/4/1105 [pii].

Wang, Z., Li, Y., Kong, D., Banerjee, S., Ahmad, A., Azmi, A. S., Ali, S., Abbruzzese, J. L., Gallick, G. E. and Sarkarr, F. H. (2009) 'Acquisition of epithelial-mesenchymal transition phenotype of gemcitabine-resistant pancreatic cancer cells is linked with activation of the notch signaling pathway', *Cancer Research*, 69(6), pp. 2400–2407. doi: 10.1158/0008-5472.CAN-08-4312.

Wei Wang, Subhasree Nag, Xu Zhang, Ming-Hai Wang, Hui Wang, Jianwei Zhou, and R. Z. (2016) 'Ribosomal Proteins and Human Diseases: Pathogenesis, Molecular Mechanisms, and Therapeutic Implications', *Med Res Rev*, 35(2), pp. 225–285. doi: 10.1002/med.21327.

Williams AJ, Coates PJ, Lowe DG, McLean C, Gale EA. 1992. Immunohistochemical investigation of insulinomas for islet amyloid polypeptide and insulin: evidence for differential synthesis and storage. *Histopathology* 21(3):215-23.

Wilson, H., Huelsmeyer, M., Chun, R., Young, K. M., Friedrichs, K. and Argyle, D. J. (2008) 'Isolation and characterisation of cancer stem cells from canine osteosarcoma.', *Veterinary journal (London, England : 1997)*, 175(1), pp. 69–75. doi: 10.1016/j.tvjl.2007.07.025.

Wooldridge, J.D., Freeman, E.C. 1999. Outcome of surgical versus medical treatment of dogs with beta cell neoplasia: 39 cases (1990-1997). J Am Vet Med Assoc 215: 226-230.

Wong, G. W., Knowles, G. C., Mak, T. W., Ferrando, A. A. and Zúñiga-Pflücker, J. C. (2012) 'HES1 opposes a PTEN-dependent check on survival, differentiation, and proliferation of TCRβ-selected mouse thymocytes', *Blood*, 120(7), pp. 1439–1448. doi: 10.1182/blood-2011-12-395319.

Wouters, E. G. H., Buishand, F. O., Kik, M. and Kirpensteijn, J. (2011) 'Use of a bipolar vessel-sealing device in resection of canine insulinoma.', *The Journal of small animal practice*, 52(3), pp. 139–45. doi: 10.1111/j.1748-5827.2011.01040.

Xia, B., Zhan, X. R., Yi, R. and Yang, B. (2009) 'Can pancreatic duct-derived progenitors be a source of islet regeneration?', *Biochemical and Biophysical Research Communications*. Elsevier Inc., 383(4), pp. 383–385. doi: 10.1016/j.bbrc.2009.03.114.

Xu, P., Zhang, A., Jiang, R., Qiu, M., Kang, C., Jia, Z., Wang, G., Han, L., Fan, X. and Pu, P. (2013) 'The Different Role of Notch1 and Notch2 in Astrocytic Gliomas', *PLoS ONE*, 8(1), pp. 1–9. doi: 10.1371/journal.pone.0053654.

Xu, Z., Tang, J., Xie, H., Du, Y., Huang, L., Yu, P. and Cheng, X. (2015) '5-Fluorouracil Chemotherapy of Gastric Cancer Generates Residual Cells with Properties of Cancer Stem Cells', 11(3), pp. 284–294. doi: 10.7150/ijbs.10248.

Yamada, Y. (2003) 'Plasma concentrations of 5-fluorouracil and F- b -alanine following oral administration of S-1 , a dihydropyrimidine dehydrogenase inhibitory fluoropyrimidine , as compared with protracted venous infusion of 5-fluorouracil', *British journal of cancer*, 89, pp. 816–820. doi: 10.1038/sj.bjc.6601224.

Yanagihara, K., Tanaka, H., Takigahira, M., Ino, Y., Yamaguchi, Y., Toge, T., Sugano, K. and Hirohashi, S. (2004) 'Establishment of two cell lines from human gastric scirrhous carcinoma that possess the potential to metastasize spontaneously in nude mice', *Cancer Science*, 95(7), pp. 575–582. doi: 10.1111/j.1349-7006.2004.tb02489.

Yang, W., Yoshigoe, K., Qin, X., Liu, J. S., Yang, J. Y., Niemierko, A., Deng, Y., Liu, Y., Dunker, A. K., Chen, Z., Wang, L., Xu, D., Arabnia, H. R. and Tong, W. (2014) 'Identification of genes and pathways involved in kidney renal clear cell carcinoma', *BMC Bioinformatics*. BioMed Central Ltd, 15(Suppl 17), p. S2. doi: 10.1186/1471-2105-15-S17-S2.

Yang, Y.-C., Wang, S.-W., Hung, H.-Y., Chang, C.-C., Wu, I.-C., Huang, Y.-L., Lin, T.-M., Tsai, J.-L., Chen, A., Kuo, F.-C., Wang, W.-M. and Wu, D.-C. (2007) 'Isolation and characterization of human gastric cell lines with stem cell

phenotypes.', *Journal of gastroenterology and hepatology*, 22, pp. 1460–1468. doi: 10.1111/j.1440-1746.2007.05031.

Yoon, S., Kim, S. and Nam, D. (2016) 'Improving Gene-Set Enrichment Analysis of RNA-Seq Data with Small Replicates', pp. 1–16. doi: 10.1371/journal.pone.0165919.

Yu, R. (2016) 'Animal models of spontaneous pancreatic neuroendocrine tumors', *Molecular and Cellular Endocrinology*. Elsevier Ireland Ltd, 421, pp. 60–67. doi: 10.1016/j.mce.2015.08.004.

Zeng, Z., Que, T., Zhang, J. and Hu, Y. (2014) 'A study exploring critical pathways in clear cell renal cell carcinoma', pp. 121–130. doi: 10.3892/etm.2013.1392.

Zhan, H. X., Cong, L., Zhao, Y. P., Zhang, T. P., Chen, G., Zhou, L. and Guo, J. C. (2012) 'Activated mTOR/P70S6K signaling pathway is involved in insulinoma tumorigenesis', *Journal of Surgical Oncology*, 106(8), pp. 972–980. doi: 10.1002/jso.23176.

Zhang M, Lykke-Andersen S, Zhu B, et al Characterising cis-regulatory variation in the transcriptome of histologically normal and tumour-derived pancreatic tissues Gut Published Online First: 20 June 2017. doi: 10.1136/gutjnl-2016-313146

Zhang, J., Francois, R., Iyer, R., Seshadri, M., Zajac-Kaye, M. and Hochwald, S. N. (2013) 'Current understanding of the molecular biology of pancreatic neuroendocrine tumors', *Journal of the National Cancer Institute*, 105(14), pp. 1005–1017. doi: 10.1093/jnci/djt135.

Zhao J, Moch AF, Scheidweiler AF, Baer AA, Schaffer AA, Speel EJ, Roth J, Heitz PU, Komminoth P 2001 Genomic imbalances in the progression of endocrine pancreatic tumors. *Genes Chromosomes Cancer* 32 364-372.

Zhao, J. (2017) 'Cancer stem cells and chemoresistance: the smartest survives the raid', pp. 145–158. doi: 10.1016/j.pharmthera.2016.02.008.Cancer.

Zhao, Z.-L., Zhang, L., Huang, C.-F., Ma, S.-R., Bu, L.-L., Liu, J.-F., Yu, G.-T., Liu, B., Gutkind, J. S., Kulkarni, A. B., Zhang, W.-F. and Sun, Z.-J. (2016) 'NOTCH1 inhibition enhances the efficacy of conventional chemotherapeutic agents by targeting head neck cancer stem cell', *Scientific Reports*. Nature Publishing Group, 6(October 2015), p. 24704. doi: 10.1038/srep24704.

Zhu, Z., Zhang, X., Guo, H. et al. *Mol Cell Biochem* (2015) 400: 287. https://doi.org/10.1007/s11010-014-2285-y

Zhu, J., Thakolwiboon, S., Liu, X., Zhang, M. and Lubman, D. M. (2014) 'Overexpression of CD90 (Thy-1) in Pancreatic Adenocarcinoma Present in the Tumor Microenvironment', *PLoS ONE*, 9, p. e115507. doi: 10.1371/journal.pone.0115507.

Zhu, L.-M., Tang, L., Qiao, X.-W., Wolin, E., Nissen, N. N., Dhall, D., Chen, J., Shen, L., Chi, Y., Yuan, Y.-Z., Ben, Q.-W., Lv, B., Zhou, Y.-R., Bai, C.-M., Chen, J., Song, Y.-L., Song, T.-T., Lu, C.-M., Yu, R. and Chen, Y.-J. (2016) 'Differences and Similarities in the Clinicopathological Features of Pancreatic Neuroendocrine Tumors in China and the United States: A Multicenter Study.', *Medicine*, 95(7), p. e2836. doi: 10.1097/MD.0000000000002836.

Zhu, T. S., Costello, M. a., Talsma, C. E., Flack, C. G., Crowley, J. G., Hamm, L. L., He, X., Hervey-Jumper, S. L., Heth, J. a., Muraszko, K. M., DiMeco, F., Vescovi, A. L. and Fan, X. (2011) 'Endothelial cells create a stem cell niche in glioblastoma by providing NOTCH ligands that nurture self-renewal of cancer stem-like cells', *Cancer Research*, 71(18), pp. 6061–6072. doi: 10.1158/0008-5472.CAN-10-4269.

Zlobec, I., Steele, R., Michel, R. P., Compton, C. C., Lugli, A. and Jass, J. R. (2006) 'Scoring of p53, VEGF, Bcl-2 and APAF-1 immunohistochemistry and interobserver reliability in colorectal cancer', *Modern Pathology*, 19(9), pp. 1236–1242. doi: 10.1038/modpathol.3800642.

8 Appendix

8.1 Canine cell line validation

Specimen Description

Species: canine **Purchase Order #: RI23048**

Description: cells

Number of Specimens/Animals: 2

ID	Client ID	Cell Line	Specimen
1	Niels P17	canINS	newly isolated canine in
2	Niels P23	canINS	newly isolated canine in

Services/Tests Performed: CellCheck - canine (canine STR profile, interspecies contamination test, canine species PCR) (1-2)

Genetic evaluation for: Canine Species PCR, Canine STR Profile, Interspecies Contamination Test

CELL CHECK

Species-specific PCR Evaluation

Species	1	2
mouse	-	-
rat	-	-
human	-	-
Chinese hamster	-	-
African green monkey	-	-
other	canine	canine

Marker Analysis

Marker Name	1	2
	Sample Results	Sample Results
Canine 1	237, 273	237, 273
Canine 17	267	267
Canine 2	256, 272	256, 272
Canine 3	174, 239	174, 239
Canine 16	164	164
Canine 4	116, 120	116, 120
Canine 5	123	123
Canine 6	150, 154	150, 154
Canine 13	287, 291	287, 291
Canine 7	159, 167	159, 167
Canine 14	188	188
Canine 19	155, 161	155, 161
Canine 8	252	252
Canine 15	196	196
Sex	X, Y	X, Y

Continue next page

Sample ID	Remarks
1	The sample was confirmed to be of canine origin and no mammalian interspecies contamination was detected. A genetic profile was generated for the sample by using a panel of STR markers for genotyping. This data is presented in the table as allele sizes in bp. A genetic profile has not been established for this cell line. However, both samples 1 and 2 have the same identical genetic profile. The profile generated for these samples can be used for comparison of samples in the future and should be included as a reference profile in publications.

Sample ID	Remarks
2	The sample was confirmed to be of canine origin and no mammalian interspecies contamination was detected. A genetic profile was generated for the sample by using a panel of STR markers for genotyping. This data is presented in the table as allele sizes in bp. A genetic profile has not been established for this cell line. However, both samples 1 and 2 have the same identical genetic profile. The profile generated for these samples can be used for comparison of samples in the future and should be included as a reference profile in publications.

Figure 8.1 Canine cell line validation using Short-tandem repeat (STR) analysis to confirm canine origin and test for interspecies contamination

8.2 Canine cell line characterisation

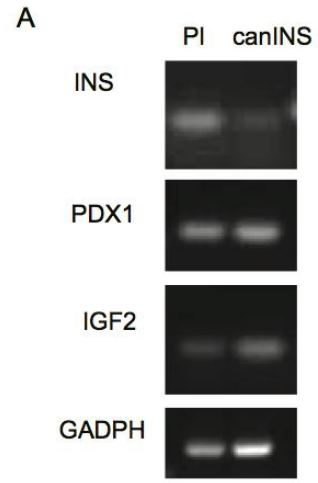

Figure 8.2 *canINS characterisation through RT-PCR. RT-PCR of neuroendocrine transcription factor (PDX1) and insulin related genes (INS and IGF2) using GADPH as a loading control comparing the primary insulinoma (PI) from which canINS was derived and the adherent canINS cell line.*

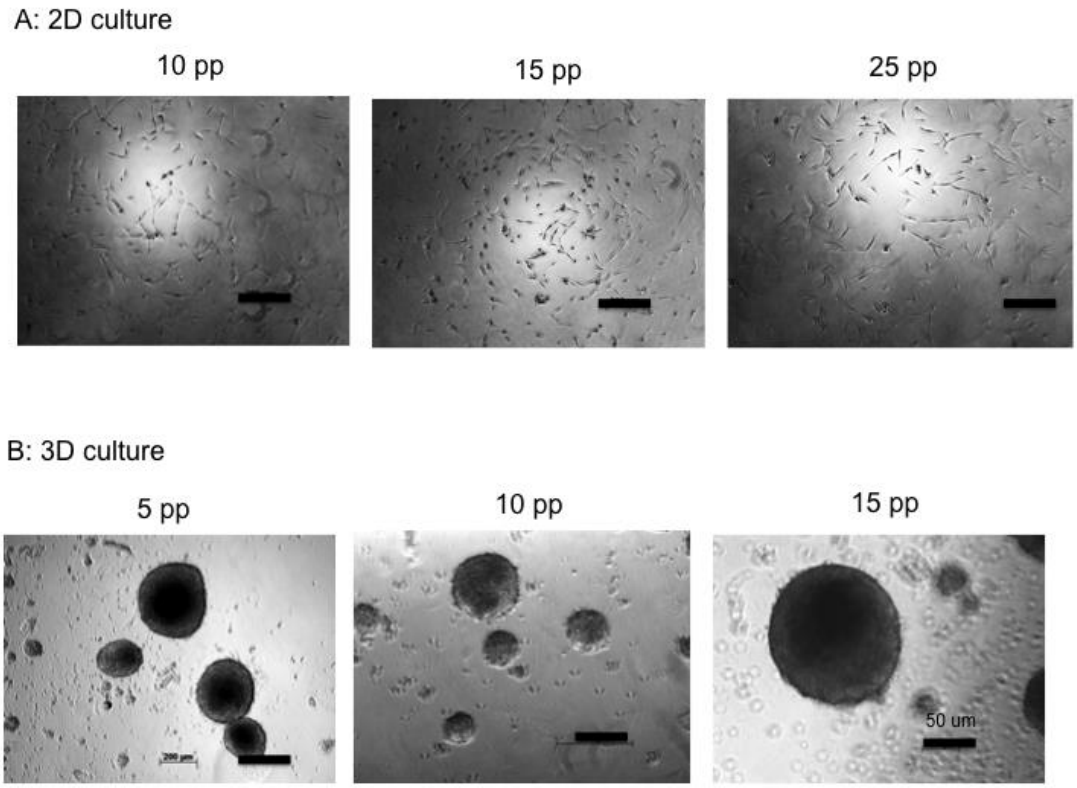

Figure 8.3 *Representative pictures of different passages of canINS in adherent (A) and sphere (B) culture. Scale bar= 200 µm (unless otherwise indicated).*

8.3 RNA-sequencing data quality analysis

Figure 8.4 RNA quality check of canine samples using RNA integrity number

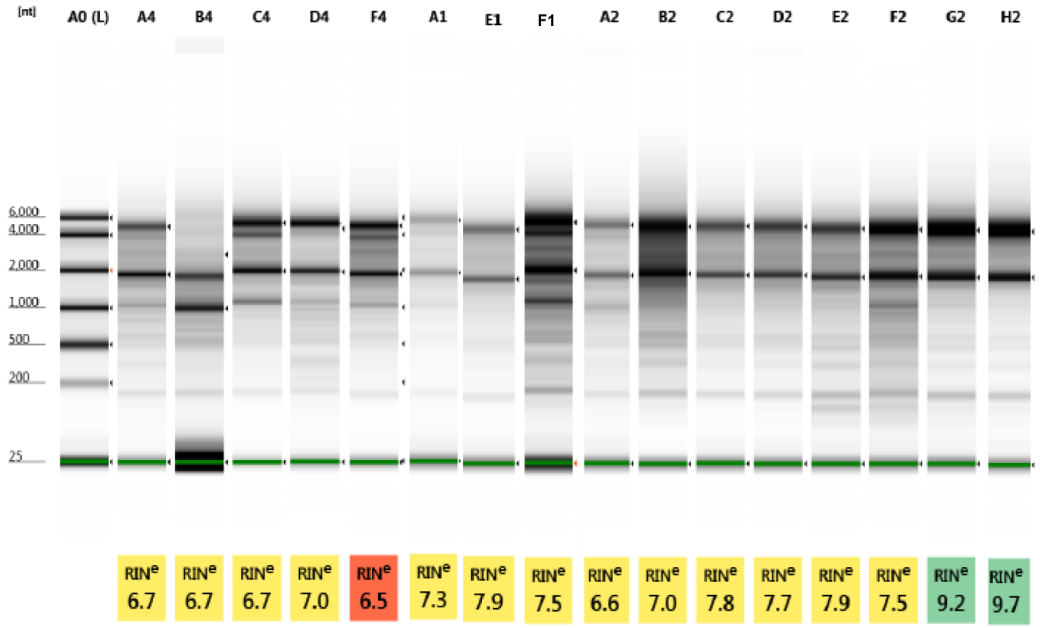

Well	RIN	28S/18S (Area)	Conc(ng/ µl)	Sample name
A0	-	-	97.5	Ladder
A4	6.7	0.9	217	BEN
B4	6.7	0.3	100	N17
C4	6.7	1.1	445	D35
D4	7.0	1.2	258	B13
F4	6.5	1.2	275	H30
A1	7.3	1.0	100	W36
E1	7.9	1.5	130	P3B
F1	7.5	1.0	168	SmM
A2	6.6	1.1	144	SnM
B2	7.0	1.5	490	NP4
C2	7.8	1.7	185	NP1
D2	7.7	1.6	225	NP2
E2	7.9	1.5	240	NP3
F2	7.5	1.8	386	LN1
G2	9.2	2.3	354	LN3
H2	9.7	2.6	318	LN2

8.4 Differential gene expression of RNA-sequencing data

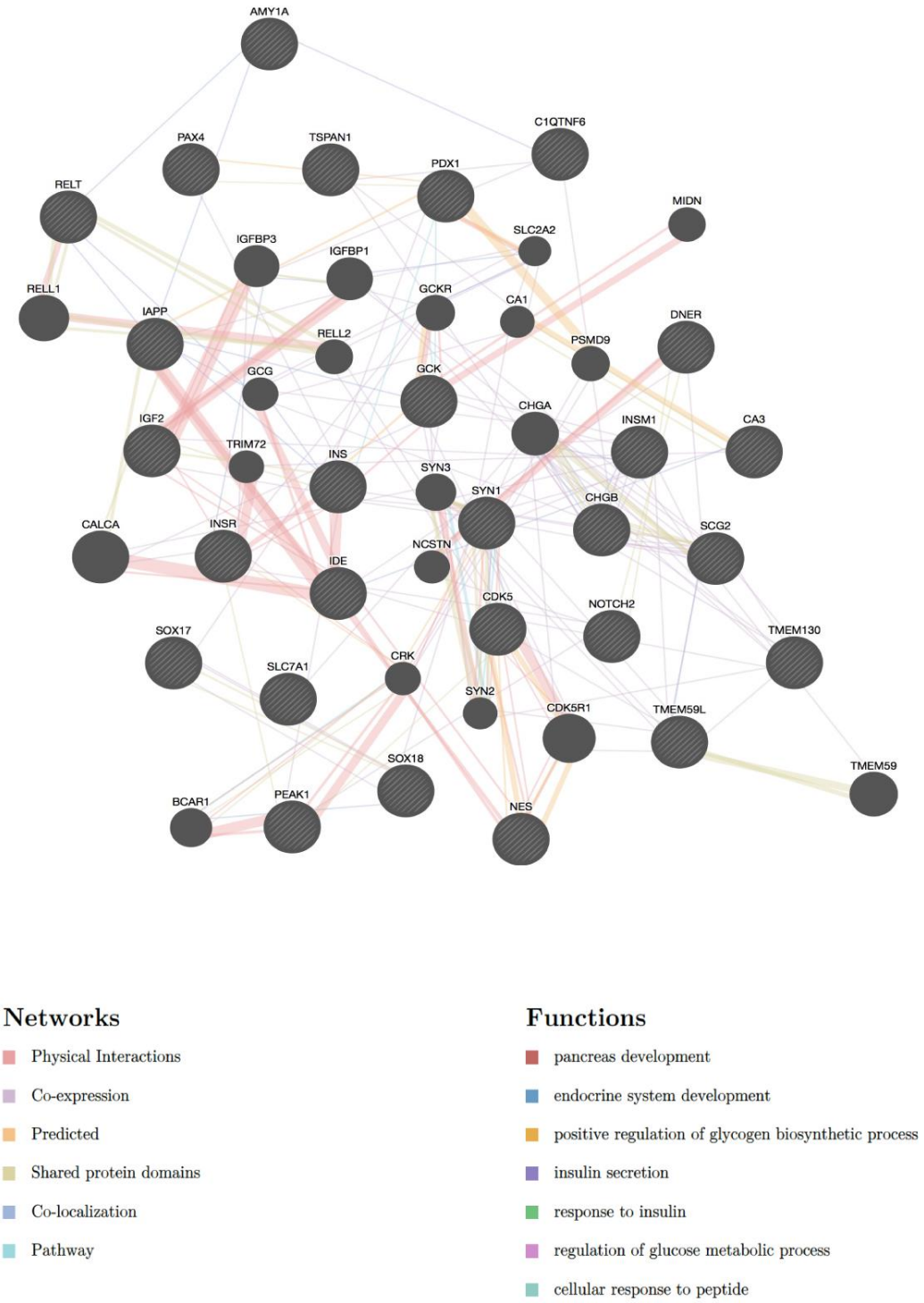

Figure 8.5 Genes networks interactions and functions of the top differentially expressed genes comparing normal pancreas vs primary insulinomas. Graphs made using genemania.com.

Table 8.1 Annotated differentially expressed genes in primary canine insulinomas compared to normal canine pancreatic tissues. FC, fold change; CPM, count per millions; FDR, false discovery rate[4]

GeneID	logFC	logCPM	P-Value	FDR	Description
ENSCAFG00000018810	-3.26059	2.710309	5.43E-11	5.95E-07	MKL/myocardin-like 2 [Source:HGNC Symbol;Acc:HGNC:29819]
ENSCAFG00000032335	5.987148	4.299956	7.38E-11	5.95E-07	Uncharacterized protein [Source:UniProtKB/TrEMBL;Acc:J9P9F2]
ENSCAFG00000020276	4.103535	4.414725	1.64E-10	8.84E-07	cysteine-rich, angiogenic inducer, 61 [Source:HGNC Symbol;Acc:HGNC:2654]
ENSCAFG00000025237	-7.63504	-0.86988	3.54E-10	1.30E-06	carbonic anhydrase III [Source:HGNC Symbol;Acc:HGNC:1374]
ENSCAFG00000018875	-3.33822	2.475732	4.58E-10	1.30E-06	hook microtubule-tethering protein 1 [Source:HGNC Symbol;Acc:HGNC:19884]
ENSCAFG00000015657	5.896898	6.408434	4.85E-10	1.30E-06	proprotein convertase subtilisin/kexin type 1 inhibitor [Source:HGNC Symbol;Acc:HGNC:17301]
ENSCAFG00000013945	6.615357	4.825368	7.22E-10	1.66E-06	complement component 1, q subcomponent-like 1 [Source:HGNC Symbol;Acc:HGNC:24182]
ENSCAFG00000006909	5.320692	3.164192	1.21E-09	2.44E-06	LIM domain only 1 [Source:HGNC Symbol;Acc:HGNC:6641]
ENSCAFG00000031298	-2.92763	2.631921	2.37E-09	3.92E-06	zinc finger with KRAB and SCAN domains 1 [Source:HGNC Symbol;Acc:HGNC:13101]
ENSCAFG00000029490	3.98087	3.425515	2.54E-09	3.92E-06	transmembrane p24 trafficking protein 9 [Source:HGNC Symbol;Acc:HGNC:24878]
ENSCAFG00000015244	4.954428	5.47062	2.77E-09	3.92E-06	protein tyrosine phosphatase, receptor type, N [Source:HGNC Symbol;Acc:HGNC:9676]
ENSCAFG00000001719	6.235457	3.750041	3.32E-09	3.92E-06	paired box 4 [Source:HGNC Symbol;Acc:HGNC:8618]

[4] *Continue from page 219-226*

GeneID	logFC	logCPM	P-Value	FDR	Description
ENSCAFG00000013222	4.767875	3.970888	3.39E-09	3.92E-06	myelin transcription factor 1 [Source:HGNC Symbol;Acc:HGNC:7622]
ENSCAFG00000005173	5.324881	4.467571	3.40E-09	3.92E-06	NK2 homeobox 2 [Source:HGNC Symbol;Acc:HGNC:7835]
ENSCAFG00000016052	5.504503	4.125219	5.11E-09	5.47E-06	solute carrier family 29 (equilibrative nucleoside transporter), member 4 [Source:HGNC Symbol;Acc:HGNC:23097]
ENSCAFG00000001254	4.676927	6.419811	5.43E-09	5.47E-06	early growth response 1 [Source:HGNC Symbol;Acc:HGNC:3238]
ENSCAFG00000025255	-3.09757	2.802967	6.10E-09	5.78E-06	pseudopodium-enriched atypical kinase 1 [Source:HGNC Symbol;Acc:HGNC:29431]
ENSCAFG00000025442	5.47718	4.802894	7.40E-09	6.63E-06	potassium voltage-gated channel subfamily H member 2 [Source:RefSeq peptide;Acc:NP_001003145]
ENSCAFG00000015146	5.590355	3.787805	7.87E-09	6.68E-06	synapsin I [Source:HGNC Symbol;Acc:HGNC:11494]
ENSCAFG00000028506	-7.63283	-0.61407	8.93E-09	6.88E-06	Alpha-amylase [Source:UniProtKB/TrEMBL;Acc:J9P0G7]
ENSCAFG00000015750	5.153271	3.302478	9.03E-09	6.88E-06	IQ motif and Sec7 domain 3 [Source:HGNC Symbol;Acc:HGNC:29193]
ENSCAFG00000002964	5.397304	2.443603	9.67E-09	6.88E-06	leucine rich repeat containing 4B [Source:HGNC Symbol;Acc:HGNC:25042]
ENSCAFG00000001423	5.387739	5.357894	9.90E-09	6.88E-06	copine V [Source:HGNC Symbol;Acc:HGNC:2318]
ENSCAFG00000001244	5.782502	4.936136	1.02E-08	6.88E-06	receptor accessory protein 2 [Source:HGNC Symbol;Acc:HGNC:17975]
ENSCAFG00000013663	5.324924	4.432561	1.10E-08	7.07E-06	guanine nucleotide binding protein (G protein), alpha z polypeptide [Source:HGNC Symbol;Acc:HGNC:4395]
ENSCAFG00000032227	4.428743	3.788197	1.14E-08	7.07E-06	olfactomedin 1 [Source:HGNC Symbol;Acc:HGNC:17187]
ENSCAFG00000008318	5.283127	4.616507	1.28E-08	7.67E-06	Uncharacterized protein [Source:UniProtKB/TrEMBL;Acc:J9P8N2]
ENSCAFG00000013851	-2.52668	4.246097	1.42E-08	8.15E-06	FYVE and coiled-coil domain containing 1 [Source:HGNC Symbol;Acc:HGNC:14673]
ENSCAFG00000010401	5.094083	3.490778	1.66E-08	8.82E-06	calcium binding protein 1 [Source:HGNC Symbol;Acc:HGNC:1384]

GeneID	logFC	logCPM	P-Value	FDR	Description
ENSCAFG00000030624	-3.40891	2.040184	1.71E-08	8.82E-06	CKLF-like MARVEL transmembrane domain containing 4 [Source:HGNC
ENSCAFG00000015455	-3.14754	3.283921	1.73E-08	8.82E-06	epithelial cell transforming 2 [Source:HGNC Symbol;Acc:HGNC:3155]
ENSCAFG00000016991	5.113856	5.226188	1.75E-08	8.82E-06	seizure related 6 homolog (mouse)-like 2 [Source:HGNC Symbol;Acc:HGNC:30844]
ENSCAFG00000011986	-5.28289	0.60902	1.89E-08	9.22E-06	perilipin 1 [Source:HGNC Symbol;Acc:HGNC:9076]
ENSCAFG00000001292	6.06448	3.739476	2.12E-08	1.01E-05	lymphocyte antigen 6 complex, locus H [Source:HGNC Symbol;Acc:HGNC:6728]
ENSCAFG00000019290	6.361058	3.855673	2.21E-08	1.02E-05	PDZ domain containing 4 [Source:HGNC Symbol;Acc:HGNC:21167]
ENSCAFG00000014197	5.402228	4.034561	2.64E-08	1.17E-05	RUN domain containing 3A [Source:HGNC Symbol;Acc:HGNC:16984]
ENSCAFG00000000272	-2.83921	3.614884	2.70E-08	1.17E-05	ARFGEF family member 3 [Source:HGNC Symbol;Acc:HGNC:21213]
ENSCAFG00000018423	-3.45153	0.899278	2.76E-08	1.17E-05	integrin subunit alpha 2 [Source:HGNC Symbol;Acc:HGNC:6137]
ENSCAFG00000012831	5.282994	2.857633	3.04E-08	1.23E-05	cornichon family AMPA receptor auxiliary protein 2 [Source:HGNC Symbol;Acc:HGNC:28744]
ENSCAFG00000028878	5.538705	4.185949	3.12E-08	1.23E-05	-
ENSCAFG00000002944	5.376577	3.584511	3.13E-08	1.23E-05	glucokinase (hexokinase 4) [Source:HGNC Symbol;Acc:HGNC:4195]
ENSCAFG00000007115	-2.6593	2.746762	3.63E-08	1.39E-05	Uncharacterized protein [Source:UniProtKB/TrEMBL;Acc:F1PKQ8]
ENSCAFG00000015328	5.467506	5.933879	3.76E-08	1.41E-05	transmembrane protein 130 [Source:HGNC Symbol;Acc:HGNC:25429]
ENSCAFG00000031922	4.734678	8.743398	3.91E-08	1.42E-05	glutathione peroxidase 3 [Source:HGNC Symbol;Acc:HGNC:4555]
ENSCAFG00000004315	5.738158	3.266964	3.97E-08	1.42E-05	synapse differentiation inducing 1 [Source:HGNC Symbol;Acc:HGNC:15885]
ENSCAFG00000000930	-2.77524	3.644007	4.10E-08	1.44E-05	AF4/FMR2 family member 4 [Source:HGNC Symbol;Acc:HGNC:17869]
ENSCAFG00000016657	5.351262	5.003235	5.25E-08	1.80E-05	cadherin related family member 2 [Source:HGNC Symbol;Acc:HGNC:18231]
ENSCAFG00000004321	5.468252	5.17912	5.95E-08	1.97E-05	tetraspanin 1 [Source:HGNC Symbol;Acc:HGNC:20657]
ENSCAFG00000006722	-2.44386	2.342876	6.07E-08	1.97E-05	membrane associated guanylate kinase, WW and PDZ domain containing 1

GeneID	logFC	logCPM	P-Value	FDR	Description
					[Source:HGNC Symbol;Acc:HGNC:946]
ENSCAFG00000009739	5.829201	2.380679	6.24E-08	1.97E-05	nerve growth factor (beta polypeptide) [Source:HGNC Symbol;Acc:HGNC:7808]
ENSCAFG00000006915	3.120668	3.693428	6.39E-08	1.98E-05	myotubularin related protein 7 [Source:HGNC Symbol;Acc:HGNC:7454]
ENSCAFG00000002613	5.927436	4.717845	6.68E-08	2.00E-05	synaptotagmin 5 [Source:HGNC Symbol;Acc:HGNC:11513]
ENSCAFG00000009428	5.112308	3.627949	6.71E-08	2.00E-05	cyclin and CBS domain divalent metal cation transport mediator 1 [Source:HGNC Symbol;Acc:HGNC:102]
ENSCAFG00000014687	4.890872	5.262421	6.88E-08	2.02E-05	transmembrane protein 59 like [Source:HGNC Symbol;Acc:HGNC:13237]
ENSCAFG00000004583	7.926904	1.858479	7.11E-08	2.05E-05	RAB37, member RAS oncogene family [Source:HGNC Symbol;Acc:HGNC:30268]
ENSCAFG00000012005	5.949764	1.216195	7.49E-08	2.12E-05	prolactin releasing hormone receptor [Source:HGNC Symbol;Acc:HGNC:4464]
ENSCAFG00000006660	-3.24531	4.226864	7.80E-08	2.16E-05	solute carrier family 7 (cationic amino acid transporter, y+ system), member 1 [Source:HGNC Symbol;Acc:HGNC:11057]
ENSCAFG00000028604	5.777008	5.1772	7.89E-08	2.16E-05	V-set and transmembrane domain containing 2 like [Source:HGNC Symbol;Acc:HGNC:16096]
ENSCAFG00000014996	6.002361	1.261288	8.11E-08	2.16E-05	cyclin-dependent kinase 5, regulatory subunit 2 (p39) [Source:HGNC Symbol;Acc:HGNC:1776]
ENSCAFG00000012987	5.255455	4.836488	8.19E-08	2.16E-05	potassium channel, voltage gated eag related subfamily H, member 6 [Source:HGNC Symbol;Acc:HGNC:18862]
ENSCAFG00000009820	-4.61177	0.611095	8.51E-08	2.21E-05	nitric oxide synthase 1 [Source:HGNC Symbol;Acc:HGNC:7872]
ENSCAFG00000004385	5.569835	4.287522	9.07E-08	2.32E-05	otoferlin [Source:HGNC Symbol;Acc:HGNC:8515]
ENSCAFG00000010382	4.679916	3.484436	9.45E-08	2.35E-05	amyloid beta (A4) precursor protein-binding, family A, member 2 [Source:HGNC Symbol;Acc:HGNC:579]
ENSCAFG00000019968	9.656531	0.889422	9.63E-08	2.35E-05	solute carrier family 38 member 8 [Source:HGNC Symbol;Acc:HGNC:32434]

GeneID	logFC	logCPM	P-Value	FDR	Description
ENSCAFG00000014627	-6.55084	3.236627	9.71E-08	2.35E-05	Elongation factor 1-alpha [Source:UniProtKB/TrEMBL;Acc:F2Z4P4]
ENSCAFG00000016186	4.596511	9.513824	9.97E-08	2.35E-05	secretogranin II [Source:HGNC Symbol;Acc:HGNC:10575]
ENSCAFG00000032120	5.404698	3.694562	1.00E-07	2.35E-05	C1q and tumor necrosis factor related protein 6 [Source:HGNC Symbol;Acc:HGNC:14343]
ENSCAFG00000018170	-2.62326	4.362235	1.00E-07	2.35E-05	insulin receptor [Source:HGNC Symbol;Acc:HGNC:6091]
ENSCAFG00000017133	5.303563	1.927711	1.08E-07	2.49E-05	-
ENSCAFG00000010559	4.973056	6.819662	1.11E-07	2.49E-05	secretagogin, EF-hand calcium binding protein [Source:HGNC Symbol;Acc:HGNC:16941]
ENSCAFG00000010175	4.644821	3.690634	1.11E-07	2.49E-05	cadherin 22, type 2 [Source:HGNC Symbol;Acc:HGNC:13251]
ENSCAFG00000004865	3.891504	3.299405	1.14E-07	2.52E-05	SWI/SNF related, matrix associated, actin dependent regulator of chromatin, subfamily d, member 3 [Source:HGNC Symbol;Acc:HGNC:11108]
ENSCAFG00000012810	5.620443	1.269393	1.15E-07	2.52E-05	transmembrane protein 151A [Source:HGNC Symbol;Acc:HGNC:28497]
ENSCAFG00000010872	4.84071	1.941841	1.18E-07	2.55E-05	adhesion G protein-coupled receptor B2 [Source:HGNC Symbol;Acc:HGNC:944]
ENSCAFG00000012794	5.095502	5.58296	1.22E-07	2.59E-05	CUGBP, Elav-like family member 3 [Source:HGNC Symbol;Acc:HGNC:11967]
ENSCAFG00000005988	4.582952	8.188557	1.33E-07	2.79E-05	chromogranin B [Source:HGNC Symbol;Acc:HGNC:1930]
ENSCAFG00000019362	4.636094	5.659348	1.40E-07	2.89E-05	L1 cell adhesion molecule [Source:HGNC Symbol;Acc:HGNC:6470]
ENSCAFG00000009873	-3.02732	3.605554	1.47E-07	3.00E-05	mannosidase, alpha, class 1A, member 2 [Source:HGNC Symbol;Acc:HGNC:6822]
ENSCAFG00000015290	-2.95776	0.931148	1.53E-07	3.09E-05	SFT2 domain containing 2 [Source:HGNC Symbol;Acc:HGNC:25140]
ENSCAFG00000004443	4.9168	3.414682	1.56E-07	3.12E-05	FBJ murine osteosarcoma viral oncogene homolog B [Source:HGNC Symbol;Acc:HGNC:3797]
ENSCAFG00000019956	4.391637	3.34165	1.70E-07	3.34E-05	WAP four-disulfide core domain 1 [Source:HGNC Symbol;Acc:HGNC:15466]
ENSCAFG00000029592	4.386106	3.379539	1.90E-07	3.70E-05	lipoma HMGIC fusion partner-like 4 [Source:HGNC Symbol;Acc:HGNC:29568]

GeneID	logFC	logCPM	P-Value	FDR	Description
ENSCAFG00000018827	-2.62718	2.782322	1.94E-07	3.72E-05	excision repair cross-complementation group 4 [Source:HGNC
ENSCAFG00000005605	3.930913	3.111339	2.08E-07	3.87E-05	RELT tumor necrosis factor receptor [Source:HGNC Symbol;Acc:HGNC:13764]
ENSCAFG00000014882	4.528802	0.524189	2.08E-07	3.87E-05	growth differentiation factor 15 [Source:HGNC Symbol;Acc:HGNC:30142]
ENSCAFG00000014822	-2.52339	3.317045	2.09E-07	3.87E-05	SECIS binding protein 2-like [Source:HGNC Symbol;Acc:HGNC:28997]
ENSCAFG00000016405	3.797384	4.46976	2.13E-07	3.91E-05	transmembrane protein 132A [Source:HGNC Symbol;Acc:HGNC:31092]
ENSCAFG00000013694	-5.16554	0.693649	2.28E-07	4.12E-05	adiponectin, C1Q and collagen domain containing [Source:HGNC Symbol;Acc:HGNC:13633]
ENSCAFG00000020033	-4.18796	-1.11328	2.32E-07	4.12E-05	C-type lectin domain family 3 member A [Source:HGNC Symbol;Acc:HGNC:2052]
ENSCAFG00000000915	5.265739	4.704253	2.32E-07	4.12E-05	regulatory factor X6 [Source:HGNC Symbol;Acc:HGNC:21478]
ENSCAFG00000006944	-3.03063	2.83843	2.37E-07	4.13E-05	solute carrier family 7 (cationic amino acid transporter, y+ system), member 2 [Source:HGNC Symbol;Acc:HGNC:11060]
ENSCAFG00000029607	3.604868	3.690097	2.38E-07	4.13E-05	syntaxin binding protein 6 (amisyn) [Source:HGNC Symbol;Acc:HGNC:19666]
ENSCAFG00000028566	4.620689	3.217499	2.41E-07	4.14E-05	neurensin 1 [Source:HGNC Symbol;Acc:HGNC:17881]
ENSCAFG00000020398	-2.89941	1.948053	2.48E-07	4.20E-05	pyruvate dehyrogenase phosphatase catalytic subunit 2 [Source:HGNC Symbol;Acc:HGNC:30263]
ENSCAFG00000007029	4.855321	4.662147	2.54E-07	4.26E-05	Uncharacterized protein [Source:UniProtKB/TrEMBL;Acc:E2RC57]
ENSCAFG00000014603	4.684328	2.734413	2.59E-07	4.31E-05	tripartite motif containing 9 [Source:HGNC Symbol;Acc:HGNC:16288]
ENSCAFG00000019623	4.811981	4.120328	2.66E-07	4.38E-05	F-box and leucine-rich repeat protein 16 [Source:HGNC Symbol;Acc:HGNC:14150]
ENSCAFG00000016019	3.020809	4.03316	2.75E-07	4.47E-05	fatty acid desaturase 2 [Source:HGNC Symbol;Acc:HGNC:3575]
ENSCAFG00000006713	4.686065	7.391629	2.96E-07	4.77E-05	amyloid beta (A4) precursor-like protein 1 [Source:HGNC Symbol;Acc:HGNC:597]

GeneID	logFC	logCPM	P-Value	FDR	Description
ENSCAFG00000019574	5.181725	3.329141	3.05E-07	4.83E-05	acyl-CoA thioesterase 7 [Source:HGNC Symbol;Acc:HGNC:24157]
ENSCAFG00000010548	4.410438	5.522616	3.05E-07	4.83E-05	delta/notch like EGF repeat containing [Source:HGNC Symbol;Acc:HGNC:24456]
ENSCAFG00000031669	3.905592	2.513455	3.09E-07	4.84E-05	cannabinoid receptor interacting protein 1 [Source:HGNC Symbol;Acc:HGNC:24546]
ENSCAFG00000013037	4.684318	4.895024	3.20E-07	4.96E-05	guanylate cyclase 2C [Source:HGNC Symbol;Acc:HGNC:4688]
ENSCAFG00000014257	4.663591	3.574601	3.26E-07	5.01E-05	protein phosphatase 2 regulatory subunit B, gamma [Source:HGNC Symbol;Acc:HGNC:9306]
ENSCAFG00000005264	5.021629	2.616905	3.40E-07	5.17E-05	insulinoma associated 1 [Source:HGNC Symbol;Acc:HGNC:6090]
ENSCAFG00000001815	-4.47388	1.121664	3.88E-07	5.80E-05	guanine deaminase [Source:HGNC Symbol;Acc:HGNC:4212]
ENSCAFG00000014302	5.121032	2.394708	3.88E-07	5.80E-05	actin like 6B [Source:HGNC Symbol;Acc:HGNC:160]
ENSCAFG00000029950	5.168064	2.468404	4.07E-07	6.03E-05	protein kinase (cAMP-dependent, catalytic) inhibitor beta [Source:HGNC Symbol;Acc:HGNC:9018]
ENSCAFG00000002951	4.559632	3.189683	4.12E-07	6.04E-05	synaptosome associated protein 91kDa [Source:HGNC Symbol;Acc:HGNC:14986]
ENSCAFG00000014243	3.511697	3.267092	4.46E-07	6.48E-05	Uncharacterized protein [Source:UniProtKB/TrEMBL;Acc:H9GWE1]
ENSCAFG00000014639	3.338963	4.475065	4.54E-07	6.53E-05	complement component 1, q subcomponent, C chain [Source:HGNC Symbol;Acc:HGNC:1245]
ENSCAFG00000011742	3.770207	2.910382	4.70E-07	6.66E-05	pleckstrin homology domain containing O1 [Source:HGNC Symbol;Acc:HGNC:24310]
ENSCAFG00000014583	5.032874	2.428702	4.71E-07	6.66E-05	carboxypeptidase Z [Source:HGNC Symbol;Acc:HGNC:2333]
ENSCAFG00000018854	4.82356	2.686925	4.91E-07	6.87E-05	seizure related 6 homolog (mouse) [Source:HGNC Symbol;Acc:HGNC:15955]
ENSCAFG00000012442	-2.67246	2.580984	4.94E-07	6.87E-05	DEAD (Asp-Glu-Ala-Asp) box helicase 6 [Source:HGNC Symbol;Acc:HGNC:2747]

GeneID	logFC	logCPM	P-Value	FDR	Description
ENSCAFG00000010476	-3.19988	3.995097	5.17E-07	6.94E-05	notch 2 [Source:HGNC Symbol;Acc:HGNC:7882]
ENSCAFG00000005250	6.605866	3.784714	5.20E-07	6.94E-05	urocortin 3 [Source:HGNC Symbol;Acc:HGNC:17781]
ENSCAFG00000031973	3.115829	2.221049	5.21E-07	6.94E-05	Uncharacterized protein [Source:UniProtKB/TrEMBL;Acc:J9NTK9]

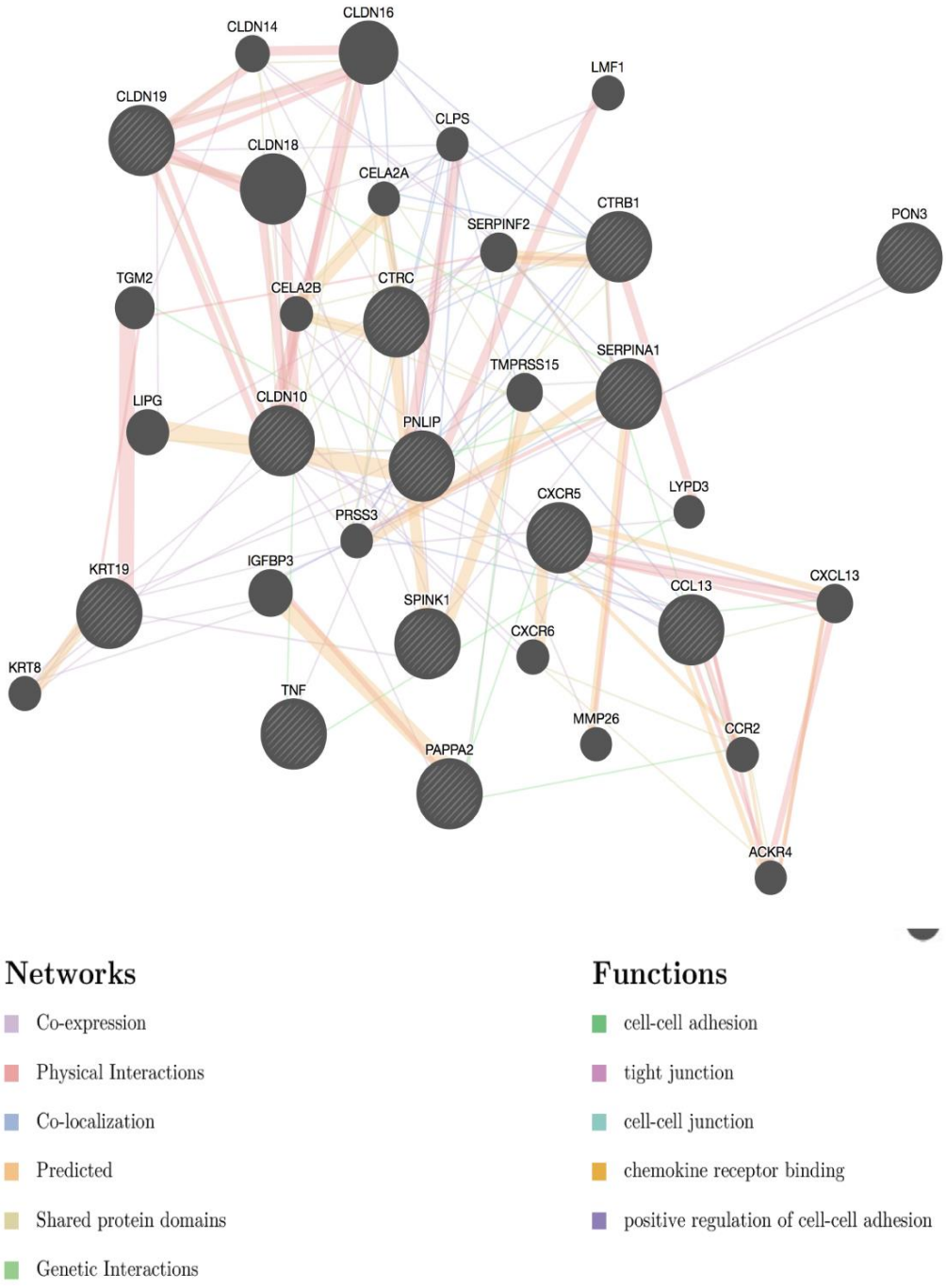

Figure 8.6 Genes networks interactions and functions of the top differentially expressed genes comparing normal pancreas vs primary insulinomas. Graphs made using genemania.com.

Table 8.2 Annotated differentially expressed genes in primary insulinoma against metastatic lymph nodes. FC, fold change; CPM, count per millions; FDR, false discovery rate.[5]

GeneID	logFC	logCPM	PValue	FDR	Description
ENSCAFG00000000090	5.413538	4.136216	4.47E-08	0.00074	melanocortin 4 receptor [Source:HGNC Symbol;Acc:HGNC:6932]
ENSCAFG00000002118	3.278324	5.750329	1.52E-07	0.001253	paraoxonase 3 [Source:HGNC Symbol;Acc:HGNC:9206]
ENSCAFG00000005293	6.312874	3.071982	5.10E-07	0.002811	SLIT and NTRK like family member 5 [Source:HGNC Symbol;Acc:HGNC:20295]
ENSCAFG00000008768	6.851048	0.794369	9.94E-07	0.004109	glutamate receptor, ionotropic, kainate 1 [Source:HGNC Symbol;Acc:HGNC:4579]
ENSCAFG00000014225	4.685339	8.663584	1.46E-06	0.004835	pappalysin 2 [Source:HGNC Symbol;Acc:HGNC:14615]
ENSCAFG00000013123	5.741419	0.096028	2.33E-06	0.005117	family with sequence similarity 196 member A [Source:HGNC Symbol;Acc:HGNC:33859]
ENSCAFG00000020380	4.127214	3.642315	2.69E-06	0.005117	adenylate kinase 5 [Source:HGNC Symbol;Acc:HGNC:365]
ENSCAFG00000018593	3.34194	2.521036	2.69E-06	0.005117	phosphatidylinositol-specific phospholipase C, X domain containing 3 [Source:HGNC Symbol;Acc:HGNC:31822]
ENSCAFG00000011356	3.302773	8.007952	3.41E-06	0.005117	von Willebrand factor A domain containing 5A [Source:HGNC Symbol;Acc:HGNC:6658]
ENSCAFG00000007775	2.963817	3.807721	3.64E-06	0.005117	nuclear receptor coactivator 2 [Source:HGNC Symbol;Acc:HGNC:7669]
ENSCAFG00000008867	-5.97914	4.005739	3.68E-06	0.005117	inter-alpha-trypsin inhibitor heavy chain 1 [Source:HGNC Symbol;Acc:HGNC:6166]
ENSCAFG00000003494	4.978143	1.432672	4.00E-06	0.005117	HECT, C2 and WW domain containing E3 ubiquitin protein ligase 1 [Source:HGNC Symbol;Acc:HGNC:22195]
ENSCAFG00000023437	-8.40857	4.737752	4.02E-06	0.005117	SEC14-like lipid binding 4 [Source:HGNC Symbol;Acc:HGNC:20627]

[5] *Continue page 228- 236*

GeneID	logFC	logCPM	PValue	FDR	Description
ENSCAFG00000005689	3.366323	3.815815	4.59E-06	0.005424	neuronal pentraxin I [Source:HGNC Symbol;Acc:HGNC:7952]
ENSCAFG00000000834	3.551235	5.440746	5.59E-06	0.005778	tumor necrosis factor receptor superfamily member 11b [Source:HGNC Symbol;Acc:HGNC:11909]
ENSCAFG00000018448	7.275648	4.189348	8.60E-06	0.008368	immunoglobulin heavy constant epsilon [Source:HGNC Symbol;Acc:HGNC:5522]
ENSCAFG00000009984	8.821599	0.795789	9.71E-06	0.008524	T-box, brain 1 [Source:HGNC Symbol;Acc:HGNC:11590]
ENSCAFG00000019160	8.024146	3.719553	9.88E-06	0.008524	Uncharacterized protein [Source:UniProtKB/TrEMBL;Acc:L7N0I5]
ENSCAFG00000010339	-8.31121	8.304282	1.08E-05	0.008524	transcobalamin 1 [Source:HGNC Symbol;Acc:HGNC:11652]
ENSCAFG00000010014	8.132274	0.155571	1.12E-05	0.008524	zona pellucida glycoprotein 4 [Source:HGNC Symbol;Acc:HGNC:15770]
ENSCAFG00000023580	5.618274	0.18747	1.16E-05	0.008524	-
ENSCAFG00000009850	5.187896	3.02403	1.19E-05	0.008524	dynein, axonemal, heavy chain 5 [Source:HGNC Symbol;Acc:HGNC:2950]
ENSCAFG00000004299	2.637691	4.71848	1.41E-05	0.009741	glutamate decarboxylase 2 [Source:HGNC Symbol;Acc:HGNC:4093]
ENSCAFG00000011587	-6.45235	3.783893	1.63E-05	0.010777	neuronal guanine nucleotide exchange factor [Source:HGNC Symbol;Acc:HGNC:7807]
ENSCAFG00000008126	-11.4968	9.152697	1.82E-05	0.011555	Uncharacterized protein [Source:UniProtKB/TrEMBL;Acc:F1PZN8]
ENSCAFG00000013221	5.94448	-0.22337	2.10E-05	0.012843	-
ENSCAFG00000002342	2.787659	4.981553	2.39E-05	0.012854	ets variant 1 [Source:HGNC Symbol;Acc:HGNC:3490]
ENSCAFG00000002540	-7.69326	5.71575	2.40E-05	0.012854	claudin 19 [Source:HGNC Symbol;Acc:HGNC:2040]
ENSCAFG00000009975	3.869341	2.941773	2.40E-05	0.012854	solute carrier family 2 (facilitated glucose transporter), member 13 [Source:HGNC Symbol;Acc:HGNC:15956]
ENSCAFG00000009258	4.222116	2.142936	2.50E-05	0.012854	cytohesin 1 interacting protein [Source:HGNC Symbol;Acc:HGNC:9506]
ENSCAFG00000005603	3.445453	3.535069	2.60E-05	0.012854	isthmin 1, angiogenesis inhibitor [Source:HGNC Symbol;Acc:HGNC:16213]
ENSCAFG00000017659	5.453793	4.512456	2.62E-05	0.012854	Uncharacterized protein [Source:UniProtKB/TrEMBL;Acc:E2RNE2]

GeneID	logFC	logCPM	PValue	FDR	Description
ENSCAFG00000008164	3.598028	0.685451	2.64E-05	0.012854	transmembrane protein 154 [Source:HGNC Symbol;Acc:HGNC:26489]
ENSCAFG00000009941	-6.09444	1.85253	4.03E-05	0.018493	stathmin domain containing 1 [Source:HGNC Symbol;Acc:HGNC:44668]
ENSCAFG00000000487	2.76762	9.685715	4.29E-05	0.019178	MHC class I DLA-88 precursor [Source:RefSeq peptide;Acc:NP_001014767]
ENSCAFG00000007008	3.069456	1.762053	4.50E-05	0.0196	RAB3C, member RAS oncogene family [Source:HGNC Symbol;Acc:HGNC:30269]
ENSCAFG00000016479	-3.59055	4.969102	4.88E-05	0.020668	transmembrane protein 184A [Source:HGNC Symbol;Acc:HGNC:28797]
ENSCAFG00000029145	6.409748	5.569631	5.17E-05	0.020668	prokineticin receptor 1 [Source:HGNC Symbol;Acc:HGNC:4524]
ENSCAFG00000009232	4.371116	6.030789	5.25E-05	0.020668	adhesion molecule with Ig-like domain 2 [Source:HGNC Symbol;Acc:HGNC:24073]
ENSCAFG00000016056	7.371578	0.001948	5.25E-05	0.020668	chromosome X open reading frame 67 [Source:HGNC Symbol;Acc:HGNC:33738]
ENSCAFG00000023899	7.285858	1.596778	5.40E-05	0.020703	carcinoembryonic antigen-related cell adhesion molecule 20 [Source:HGNC Symbol;Acc:HGNC:24879]
ENSCAFG00000018785	6.821707	3.162634	5.52E-05	0.020703	Rho GTPase activating protein 36 [Source:HGNC Symbol;Acc:HGNC:26388]
ENSCAFG00000011716	2.985608	1.788362	5.78E-05	0.020703	ubiquitin associated and SH3 domain containing B [Source:HGNCSymbol;Acc:HGNC:29884]
ENSCAFG00000014154	-3.04355	4.453639	5.94E-05	0.020703	Uncharacterized protein [Source:UniProtKB/TrEMBL;Acc:F1PRT9]
ENSCAFG00000001727	4.703709	1.120523	5.99E-05	0.020703	leucine rich repeat and Ig domain containing 2 [Source:HGNC Symbol;Acc:HGNC:21207]
ENSCAFG00000000681	4.015662	4.133856	6.01E-05	0.020703	fibrillin 2 [Source:HGNC Symbol;Acc:HGNC:3604]
ENSCAFG00000010858	3.265506	5.144436	6.41E-05	0.021508	limbic system-associated membrane protein [Source:HGNC Symbol;Acc:HGNC:6705]
ENSCAFG00000031149	3.298262	4.766274	6.50E-05	0.021508	lymphocyte transmembrane adaptor 1 [Source:HGNC Symbol;Acc:HGNC:26005]
ENSCAFG00000008130	-10.6671	7.837529	7.04E-05	0.02283	Uncharacterized protein [Source:UniProtKB/TrEMBL;Acc:F1PZN8]
ENSCAFG00000002905	-6.07418	1.034972	7.32E-05	0.023269	kallikrein related peptidase 4 [Source:HGNC Symbol;Acc:HGNC:6365]

GeneID	logFC	logCPM	PValue	FDR	Description
ENSCAFG00000000473	6.14522	-0.25471	7.49E-05	0.023385	thyrotropin-releasing hormone degrading enzyme [Source:HGNC
ENSCAFG00000008692	4.853102	3.465914	8.30E-05	0.02421	chemokine (C-X-C motif) ligand 13 [Source:HGNC Symbol;Acc:HGNC:10639]
ENSCAFG00000025531	5.298697	2.67068	8.31E-05	0.02421	contactin associated protein-like 2 [Source:HGNC Symbol;Acc:HGNC:13830]
ENSCAFG00000005583	5.754361	1.142792	8.39E-05	0.02421	glutamate receptor, metabotropic 7 [Source:HGNC Symbol;Acc:HGNC:4599]
ENSCAFG00000007728	2.449113	6.030118	8.49E-05	0.02421	solute carrier family 4, sodium bicarbonate cotransporter, member 8 [Source:HGNC Symbol;Acc:HGNC:11034]
ENSCAFG00000000492	4.627745	3.663675	8.65E-05	0.024258	Uncharacterized protein [Source:UniProtKB/TrEMBL;Acc:F1PE31]
ENSCAFG00000013988	6.096607	-1.52843	8.83E-05	0.024319	KIAA1024 [Source:HGNC Symbol;Acc:HGNC:29172]
ENSCAFG00000008467	3.155912	5.325941	8.97E-05	0.024319	EGF-like repeats and discoidin I-like domains 3 [Source:HGNC Symbol;Acc:HGNC:3173]
ENSCAFG00000029100	-9.6037	4.478581	9.44E-05	0.025188	ripply transcriptional repressor 1 [Source:HGNC Symbol;Acc:HGNC:25117]
ENSCAFG00000017080	-11.1816	2.825372	0.000101	0.026348	epsin 3 [Source:HGNC Symbol;Acc:HGNC:18235]
ENSCAFG00000017480	-9.34709	9.167655	0.000102	0.026348	aquaporin 8 [Source:HGNC Symbol;Acc:HGNC:642]
ENSCAFG00000002028	2.619021	5.140393	0.00011	0.027179	very low density lipoprotein receptor [Source:HGNC Symbol;Acc:HGNC:12698]
ENSCAFG00000002498	2.632324	2.811878	0.000112	0.027179	histone deacetylase 9 [Source:HGNC Symbol;Acc:HGNC:14065]
ENSCAFG00000010414	-8.39131	4.716021	0.000112	0.027179	glucagon [Source:HGNC Symbol;Acc:HGNC:4191]
ENSCAFG00000001927	6.496054	-2.10774	0.000112	0.027179	transmembrane protein 252 [Source:HGNC Symbol;Acc:HGNC:28537]
ENSCAFG00000023647	-8.38703	5.131435	0.000115	0.027504	keratin 19, type I [Source:HGNC Symbol;Acc:HGNC:6436]
ENSCAFG00000002095	7.871758	-1.12118	0.000116	0.027504	adhesion G protein-coupled receptor F4 [Source:HGNC Symbol;Acc:HGNC:19011]
ENSCAFG00000015429	-8.5549	10.44299	0.000124	0.028987	protein disulfide isomerase family A member 2 [Source:HGNC Symbol;Acc:HGNC:14180]
ENSCAFG00000005592	-8.81249	12.29635	0.000128	0.029456	syncollin [Source:HGNC Symbol;Acc:HGNC:18442]

GeneID	logFC	logCPM	PValue	FDR	Description
ENSCAFG00000000131	-6.09334	5.804107	0.000135	0.030577	glutaminase 2 [Source:HGNC Symbol;Acc:HGNC:29570]
ENSCAFG00000003703	2.412112	2.746102	0.000145	0.032055	SET domain containing (lysine methyltransferase) 7 [Source:HGNC Symbol;Acc:HGNC:30412]
ENSCAFG00000030890	4.990546	-0.19279	0.000148	0.032207	Uncharacterized protein [Source:UniProtKB/TrEMBL;Acc:J9P455]
ENSCAFG00000002402	3.94871	-0.35047	0.000154	0.032988	diacylglycerol kinase beta [Source:HGNC Symbol;Acc:HGNC:2850]
ENSCAFG00000018877	-7.26956	4.011299	0.00016	0.033077	natriuretic peptide receptor 3 [Source:HGNC Symbol;Acc:HGNC:7945]
ENSCAFG00000005057	-7.30316	5.274069	0.000162	0.033077	inter-alpha-trypsin inhibitor heavy chain 2 [Source:HGNC Symbol;Acc:HGNC:6167]
ENSCAFG00000012609	-9.12612	12.37093	0.000165	0.033077	CUB and zona pellucida-like domains 1 [Source:HGNC Symbol;Acc:HGNC:17937]
ENSCAFG00000007124	-9.12834	7.118399	0.000165	0.033077	FXYD domain containing ion transport regulator 3 [Source:HGNC Symbol;Acc:HGNC:4027]
ENSCAFG00000008874	2.196825	5.330629	0.000167	0.033077	hormonally up-regulated Neu-associated kinase [Source:HGNC Symbol;Acc:HGNC:13326]
ENSCAFG00000002914	-9.0375	11.92677	0.000168	0.033077	kallikrein-1 precursor [Source:RefSeq peptide;Acc:NP_001003262]
ENSCAFG00000010901	3.735649	2.441554	0.000172	0.033077	fatty acyl-CoA reductase 2 [Source:HGNC Symbol;Acc:HGNC:25531]
ENSCAFG00000016373	-8.00219	3.969844	0.000173	0.033077	arylacetamide deacetylase-like 4 [Source:HGNC Symbol;Acc:HGNC:32038]
ENSCAFG00000016301	-8.88686	16.30217	0.000174	0.033077	chymotrypsin C [Source:HGNC Symbol;Acc:HGNC:2523]
ENSCAFG00000029087	-7.49504	5.156802	0.000175	0.033077	GATA binding protein 4 [Source:HGNC Symbol;Acc:HGNC:4173]
ENSCAFG00000004446	2.102584	5.044488	0.000177	0.033077	transmembrane protein 43 [Source:HGNC Symbol;Acc:HGNC:28472]
ENSCAFG00000020084	-8.72137	16.10934	0.000178	0.033077	Chymotrypsinogen 2 Chymotrypsin 2 chain A Chymotrypsin 2 chain B Chymotrypsin 2 chain C [Source:UniProtKB/Swiss-Prot;Acc:P04813]
ENSCAFG00000019267	-9.32712	12.71248	0.000182	0.033444	deoxyribonuclease I [Source:HGNC Symbol;Acc:HGNC:2956]
ENSCAFG00000010263	-8.92863	14.32939	0.000187	0.0339	phospholipase A2 group IB [Source:HGNC Symbol;Acc:HGNC:9030]

GeneID	logFC	logCPM	PValue	FDR	Description
ENSCAFG00000014733	-8.84092	15.94977	0.000189	0.034024	Uncharacterized protein [Source:UniProtKB/TrEMBL;Acc:F1PI75]
ENSCAFG00000010348	-8.86952	4.227818	0.000195	0.034024	trefoil factor 3 [Source:HGNC Symbol;Acc:HGNC:11757]
ENSCAFG00000005458	-7.19894	5.754844	0.000195	0.034024	claudin 10 [Source:HGNC Symbol;Acc:HGNC:2033]
ENSCAFG00000014481	-8.7263	16.38149	0.000202	0.03415	Anionic trypsin [Source:UniProtKB/Swiss-Prot;Acc:P06872]
ENSCAFG00000012561	-9.85081	7.170177	0.000203	0.03415	deleted in malignant brain tumors 1 [Source:HGNC Symbol;Acc:HGNC:2926]
ENSCAFG00000020083	-9.5441	14.46867	0.000205	0.03415	Uncharacterized protein [Source:UniProtKB/TrEMBL;Acc:E2RSM7]
ENSCAFG00000025016	3.178023	0.657592	0.000205	0.03415	C-X-C motif chemokine [Source:UniProtKB/TrEMBL;Acc:F1PMC0]
ENSCAFG00000007893	-4.8334	4.213767	0.000206	0.03415	retinol binding protein 4 [Source:HGNC Symbol;Acc:HGNC:9922]
ENSCAFG00000003429	-8.94569	4.988933	0.000213	0.034841	cystic fibrosis transmembrane conductance regulator [Source:HGNC Symbol;Acc:HGNC:1884]
ENSCAFG00000016065	-4.43835	7.516535	0.000226	0.036621	60S ribosomal protein L6 [Source:UniProtKB/TrEMBL;Acc:F1Q424]
ENSCAFG00000015753	-10.3318	1.981585	0.000229	0.036759	surfactant protein D [Source:HGNC Symbol;Acc:HGNC:10803]
ENSCAFG00000011175	-5.71392	3.737615	0.000232	0.036836	Na+/K+ transporting ATPase interacting 1 [Source:HGNC Symbol;Acc:HGNC:25743]
ENSCAFG00000007686	3.765447	-0.12012	0.00024	0.03778	solute carrier organic anion transporter family member 5A1 [Source:HGNC Symbol;Acc:HGNC:19046]
ENSCAFG00000009670	-7.78503	5.876514	0.000245	0.038148	recombination signal binding protein for immunoglobulin kappa J region-like [Source:HGNC Symbol;Acc:HGNC:13761]
ENSCAFG00000024968	-8.64783	15.03396	0.00025	0.038414	carboxypeptidase A1 [Source:HGNC Symbol;Acc:HGNC:2296]
ENSCAFG00000000868	-3.58541	6.199531	0.000251	0.038414	SPARC related modular calcium binding 2 [Source:HGNC Symbol;Acc:HGNC:20323]
ENSCAFG00000009344	-4.09236	5.015874	0.000254	0.038474	solute carrier family 22 member 23 [Source:HGNC Symbol;Acc:HGNC:21106]

GeneID	logFC	logCPM	PValue	FDR	Description
ENSCAFG00000008893	-6.77198	0.808194	0.00026	0.038875	ventricular zone expressed PH domain containing 1 [Source:HGNC
ENSCAFG00000025473	-8.45197	15.23339	0.000263	0.038875	carboxypeptidase A4 [Source:HGNC Symbol;Acc:HGNC:15740]
ENSCAFG00000017615	2.631327	2.328871	0.000273	0.038875	ST8 alpha-N-acetyl-neuraminide alpha-2,8-sialyltransferase 5 [Source:HGNC Symbol;Acc:HGNC:17827]
ENSCAFG00000013291	-5.18413	6.23609	0.000274	0.038875	-
ENSCAFG00000019801	-5.68514	7.369966	0.000274	0.038875	Uncharacterized protein [Source:UniProtKB/TrEMBL;Acc:E2R5E9]
ENSCAFG00000003075	6.611216	2.93008	0.000278	0.038875	amphiregulin [Source:HGNC Symbol;Acc:HGNC:651]
ENSCAFG00000009696	-5.5737	6.616194	0.000278	0.038875	WAP four-disulfide core domain 2 [Source:HGNC Symbol;Acc:HGNC:15939]
ENSCAFG00000024988	-3.31959	3.184731	0.000279	0.038875	frizzled-related protein [Source:HGNC Symbol;Acc:HGNC:3959]
ENSCAFG00000017191	2.909902	2.014403	0.00028	0.038875	transmembrane p24 trafficking protein family member 8 [Source:HGNC Symbol;Acc:HGNC:18633]
ENSCAFG00000029139	5.060855	-0.73334	0.000285	0.038997	sodium channel, voltage gated, type XI alpha subunit [Source:HGNC Symbol;Acc:HGNC:10583]
ENSCAFG00000010325	-8.53467	9.712077	0.000285	0.038997	gastric intrinsic factor [Source:HGNC Symbol;Acc:HGNC:4268]
ENSCAFG00000015860	-8.53321	3.623894	0.000289	0.039138	secretoglobin, family 1A, member 1 (uteroglobin) [Source:HGNC Symbol;Acc:HGNC:12523]
ENSCAFG00000008226	-8.86108	15.05102	0.000291	0.039138	carboxypeptidase B precursor [Source:RefSeq peptide;Acc:NP_001003005]
ENSCAFG00000012892	-8.50389	8.42447	0.000295	0.039281	endoplasmic reticulum protein 27 [Source:HGNC Symbol;Acc:HGNC:26495]
ENSCAFG00000008319	3.333094	-0.32058	0.000301	0.039495	chondrolectin [Source:HGNC Symbol;Acc:HGNC:17807]
ENSCAFG00000031298	2.296518	3.02524	0.000305	0.039495	zinc finger with KRAB and SCAN domains 1 [Source:HGNC Symbol;Acc:HGNC:13101]
ENSCAFG00000010039	-9.28266	7.180269	0.000305	0.039495	3 beta-hydroxysteroid dehydrogenase/Delta 5-->4-isomerase [Source:RefSeq

GeneID	logFC	logCPM	PValue	FDR	Description
					peptide;Acc:NP_001010954]
ENSCAFG00000008670	2.212305	5.555275	0.000309	0.03965	protein tyrosine kinase 2 beta [Source:HGNC Symbol;Acc:HGNC:9612]
ENSCAFG00000009330	2.685463	2.939346	0.000323	0.041094	synaptic vesicle glycoprotein 2C [Source:HGNC Symbol;Acc:HGNC:30670]
ENSCAFG00000000587	-6.63255	3.095562	0.000331	0.041735	grainyhead-like transcription factor 2 [Source:HGNC Symbol;Acc:HGNC:2799]
ENSCAFG00000011852	-8.54384	15.71782	0.000343	0.04279	pancreatic lipase-related protein 1 [Source:HGNC Symbol;Acc:HGNC:9156]
ENSCAFG00000006647	-8.55149	11.03874	0.000344	0.04279	serine peptidase inhibitor, Kazal type 1 [Source:HGNC Symbol;Acc:HGNC:11244]
ENSCAFG00000014536	-8.809	9.225646	0.00035	0.043207	serpin peptidase inhibitor, clade I (pancpin), member 2 [Source:HGNC Symbol;Acc:HGNC:8945]
ENSCAFG00000010349	-8.1587	9.84284	0.000358	0.043816	trefoil factor 2 [Source:HGNC Symbol;Acc:HGNC:11756]
ENSCAFG00000003818	-8.8074	16.51734	0.000367	0.044113	Uncharacterized protein [Source:UniProtKB/TrEMBL;Acc:F1PCE8]
ENSCAFG00000019238	-4.53596	6.730212	0.000367	0.044113	matrix metallopeptidase 23B [Source:HGNC Symbol;Acc:HGNC:7171]
ENSCAFG00000023682	2.447999	1.860781	0.000368	0.044113	protocadherin gamma subfamily A, 1 [Source:HGNC Symbol;Acc:HGNC:8696]
ENSCAFG00000017061	7.040803	-1.71466	0.000385	0.045169	outer dense fiber of sperm tails 4 [Source:HGNC Symbol;Acc:HGNC:19056]
ENSCAFG00000028653	-10.1301	7.801111	0.000385	0.045169	Uncharacterized protein [Source:UniProtKB/TrEMBL;Acc:J9NST6]
ENSCAFG00000010375	-5.14177	1.117658	0.000386	0.045169	alpha 1,3-galactosyltransferase 2 [Source:HGNC Symbol;Acc:HGNC:30005]
ENSCAFG00000024895	5.662521	-1.66278	0.000392	0.045169	Olfactory receptor [Source:UniProtKB/TrEMBL;Acc:F1PTA0]
ENSCAFG00000018023	-8.53712	14.30157	0.000392	0.045169	glycoprotein 2 (zymogen granule membrane) [Source:HGNC Symbol;Acc:HGNC:4441]
ENSCAFG00000011446	2.319016	3.119531	0.000395	0.045169	ubiquitin specific peptidase 13 (isopeptidase T-3) [Source:HGNC Symbol;Acc:HGNC:12611]
ENSCAFG00000024062	-8.40878	9.066328	0.000396	0.045169	Uncharacterized protein [Source:UniProtKB/TrEMBL;Acc:F1PAB0]
ENSCAFG00000008018	-7.66115	5.93285	0.000402	0.04524	Uncharacterized protein [Source:UniProtKB/TrEMBL;Acc:E2R0T0]

GeneID	logFC	logCPM	PValue	FDR	Description
ENSCAFG00000005426	3.645683	5.652025	0.000402	0.04524	ribonuclease, RNase A family, 4 [Source:HGNC Symbol;Acc:HGNC:10047]
ENSCAFG00000002064	4.63158	1.203302	0.000408	0.045301	solute carrier family 5 (sodium/choline cotransporter), member 7 [Source:HGNC Symbol;Acc:HGNC:14025]
ENSCAFG00000008093	-5.41801	4.39659	0.000414	0.045334	4-hydroxyphenylpyruvate dioxygenase [Source:HGNC Symbol;Acc:HGNC:5147]
ENSCAFG00000023446	-6.36399	3.745458	0.000414	0.045334	fructose-bisphosphatase 2 [Source:HGNC Symbol;Acc:HGNC:3607]
ENSCAFG00000011815	-8.40678	15.69088	0.000424	0.046114	pancreatic lipase [Source:HGNC Symbol;Acc:HGNC:9155]
ENSCAFG00000020334	-8.86682	13.97005	0.000427	0.046186	chymotrypsin-like [Source:HGNC Symbol;Acc:HGNC:2524]
ENSCAFG00000015984	6.230282	-0.5904	0.000432	0.04639	A-kinase anchoring protein 4 [Source:HGNC Symbol;Acc:HGNC:374]
ENSCAFG00000003833	-2.64966	4.687933	0.000444	0.047369	syndecan 1 [Source:HGNC Symbol;Acc:HGNC:10658]
ENSCAFG00000017147	2.221196	4.250376	0.000448	0.047458	angel homolog 1 (Drosophila) [Source:HGNC Symbol;Acc:HGNC:19961]
ENSCAFG00000007862	-4.79146	6.154264	0.000451	0.047458	solute carrier family 43 (amino acid system L transporter), member 1 [Source:HGNC Symbol;Acc:HGNC:9225]
ENSCAFG00000018597	-5.46868	2.662824	0.000459	0.048028	laminin subunit alpha 1 [Source:HGNC Symbol;Acc:HGNC:6481]
ENSCAFG00000028559	-8.45186	4.229013	0.000464	0.048256	solute carrier family 25 member 45 [Source:HGNC Symbol;Acc:HGNC:27442]
ENSCAFG00000012675	-3.61044	4.566662	0.000477	0.049275	selenium binding protein 1 [Source:HGNC Symbol;Acc:HGNC:10719]
ENSCAFG00000009859	3.304718	-0.39781	0.000482	0.049389	GPRIN family member 3 [Source:HGNC Symbol;Acc:HGNC:27733]
ENSCAFG00000019872	-8.00404	15.55308	0.000484	0.049389	carboxyl ester lipase [Source:HGNC Symbol;Acc:HGNC:1848]
ENSCAFG00000013899	-6.06306	6.873638	0.000487	0.04941	Uncharacterized protein [Source:UniProtKB/TrEMBL;Acc:E2RTH3]

Table 8.3 Differentially expressed genes common within the three dataset. logFC, fold change[6]

GENE ID	GENE SYMBOL	GENE	ROLE	LOGFC		
				Normal pancreas vs Primary INS	**Normal Lymph nodes vs metastatic lymph nodes**	**Primary INS vs Metastatic lymph nodes**
ENSCAFG00000011356	VWA5A	von Willebrand factor A domain containing 5A	Glycoprotein involved in cell adhesion and migration often altered in a variety of cancers	3.13235	2.808187	8.007952
ENSCAFG00000002118	PON3	paraoxonase 3	Enzyme controlling cell death through apoptosis in response to DNA damage	3.057447	9.857268	5.750329
ENSCAFG00000000487	TAP2	MHC class I DLA-88 precursor	Involved in the presentation of foreign antigen to the immune system. Loss or mutation contributes to the evasion of cancer cell from the host immune system	2.662129	2.539064	9.685715
ENSCAFG00000004299	GAD3	glutamate decarboxylase 2	Enzyme that acts as major autoantigen in insulin-dependent	2.20579	10.10222	4.71848

[6] *Continue page 237-239*

GENE ID	GENE SYMBOL	GENE	ROLE	LOGFC		
			diabetes			
ENSCAFG00000000834	TNFRS11B	tumour necrosis factor receptor superfamily member 11b	Regulates osteoclast development and it has been related with poor prognosis factor in a variety of cancers	2.39948	5.312691	5.440746
ENSCAFG00000008692	CCL13	chemokine (C-X-C motif) ligand 13	Overexpressed and related to poor prognosis in breast and lung cancer	3.690534	-3.41308	3.465914
ENSCAFG00000007728	SCL4A8	solute carrier family 4, sodium bicarbonate cotransporter, member 8	Carrier protein involved in transport of glucose	1.602634	4.79368	6.030118
ENSCAFG00000000681	FB2	fibrillin 2	Extracellular matrix protein involved in tumour invasion. Involved in hypermethilation in pancreatic cancer	3.204135	3.92762	4.133856
ENSCAFG00000017147	ANGEL1	angel homolog 1 (Drosophila)	Highly expressed in normal pancreas	-1.29944	4.355296	4.250376
ENSCAFG00000010858	LSAMP	limbic system-associated membrane protein	It mediates neuronal growth and acts as a tumour suppressor. Deletion associated with more malignant prostate cancer and osteosarcoma	2.371685	5.308851	5.144436
ENSCAFG00000009232	AMIGO2	adhesion molecule with Ig-like domain 2	Leuchine-rich repeat containing cell adhesion molecule implicated overexpressed in gastric, thyroid and	2.224195	5.912331	6.030789

GENE ID	GENE SYMBOL	GENE	ROLE	LOGFC		
			pancreatic cancer			
ENSCAFG00000014225	PAPPA2	pappalysin 2	Inhibitory factor of insulin growth factor. Mutation in this gene cause insulin resistance particularly in pregnancy derived diabetes	1.753377	12.2249	8.663584

8.5 Functional analysis of RNA-sequencing data

Table 8.4 Gene ontology terms upregulated in primary insulinomas vs normal pancreas using gene set enrichment analysis[7]

NAME	DESCRIPTION	SIZE	FDR
GO:0031012	extracellular_matrix	158	0
GO:0005578	proteinaceous_extracellular_matrix	155	0
GO:0005581	collagen_trimer	44	2.91E-04
GO:0001558	regulation_of_cell_growth	30	2.18E-04
GO:0008201	heparin_binding	72	6.97E-04
GO:0005576	extracellular_region	424	5.81E-04
GO:0045597	positive_regulation_of_cell_differentiation	27	1.00E-03
GO:0005520	insulin-like_growth_factor_binding	17	0.001643
GO:0007601	visual_perception	49	0.00165
GO:0005125	cytokine_activity	93	0.002006
GO:0042102	positive_regulation_of_T_cell_proliferation	37	0.001903
GO:0005249	voltage-gated_potassium_channel_activity	51	0.001961
GO:0050840	extracellular_matrix_binding	21	0.001878
GO:0006813	potassium_ion_transport	79	0.002053
GO:0045595	regulation_of_cell_differentiation	25	0.002437

[7] *Continue page 239- 242*

NAME	DESCRIPTION	SIZE	FDR
GO:0034765	regulation_of_ion_transmembrane_transport	64	0.002989
GO:0031018	endocrine_pancreas_development	18	0.004143
GO:0071805	potassium_ion_transmembrane_transport	78	0.004637
GO:0005201	extracellular_matrix_structural_constituent	26	0.004895
GO:0006955	immune_response	157	0.005
GO:0043197	dendritic_spine	35	0.005135
GO:0043025	neuronal_cell_body	116	0.006244
GO:0042391	regulation_of_membrane_potential	55	0.00703
GO:0006816	calcium_ion_transport	75	0.008151
GO:0005244	voltage-gated_ion_channel_activity	62	0.007895
GO:0007269	neurotransmitter_secretion	18	0.008763
GO:0072562	blood_microparticle	64	0.009048
GO:0086091	regulation_of_heart_rate_by_cardiac_conduction	22	0.011053
GO:0035987	endodermal_cell_differentiation	25	0.010792
GO:0005267	potassium_channel_activity	39	0.010636
GO:0001540	beta-amyloid_binding	23	0.010601
GO:0005245	voltage-gated_calcium_channel_activity	29	0.010892
GO:0032024	positive_regulation_of_insulin_secretion	17	0.01088
GO:0050853	B_cell_receptor_signaling_pathway	26	0.011608
GO:0035249	synaptic_transmission,_glutamatergic	25	0.011552

NAME	DESCRIPTION	SIZE	FDR
GO:0030199	collagen_fibril_organization	30	0.01215
GO:0005216	ion_channel_activity	141	0.015884
GO:0008076	voltage-gated_potassium_channel_complex	54	0.015603
GO:0002376	immune_system_process	27	0.016381
GO:0030507	spectrin_binding	16	0.019292
GO:0030073	insulin_secretion	25	0.019713
GO:0008009	chemokine_activity	28	0.019595
GO:0005251	delayed_rectifier_potassium_channel_activity	24	0.020797
GO:0005178	integrin_binding	66	0.021452
GO:0051965	positive_regulation_of_synapse_assembly	47	0.022655
GO:0007268	synaptic_transmission	75	0.024499
GO:1903561	extracellular_vesicle	42	0.025033
GO:0003341	cilium_movement	15	0.024529
GO:0007612	learning	32	0.027483
GO:0007267	cell-cell_signaling	47	0.027073
GO:0010951	negative_regulation_of_endopeptidase_activity	80	0.032177
GO:2000352	negative_regulation_of_endothelial_cell_apoptotic_process	19	0.033195
GO:0034220	ion_transmembrane_transport	125	0.032847
GO:0035235	ionotropic_glutamate_receptor_signaling_pathway	17	0.041853
GO:0044297	cell_body	36	0.041438

NAME	DESCRIPTION	SIZE	FDR
GO:0048786	presynaptic_active_zone	15	0.041007
GO:1902042	negative_regulation_of_extrinsic_apoptotic_signaling_pathway_via_death_domain_receptors	19	0.047548
GO:0071310	cellular_response_to_organic_substance	18	0.046743
GO:0042056	chemoattractant_activity	19	0.048779
GO:0070588	calcium_ion_transmembrane_transport	84	0.04937

Table 8.5 Gene ontology terms downregulated in primary insulinomas vs normal pancreas using gene set enrichment analysis[8]

NAME	DESCRIPTION	SIZE	FDR
GO:0022627	cytosolic_small_ribosomal_subunit	29	0.0
GO:0022625	cytosolic_large_ribosomal_subunit	26	0.0021156834
GO:0006412	translation	247	0.0018979316
GO:0003735	structural_constituent_of_ribosome	194	0.0017787857
GO:0018024	histone-lysine_N-methyltransferase_activity	24	0.0019956175
GO:0005840	ribosome	197	0.0016630146
GO:0006414	translational_elongation	34	0.0049810847
GO:0006606	protein_import_into_nucleus	28	0.009734071
GO:0034968	histone_lysine_methylation	21	0.008965263
GO:0047485	protein_N-terminus_binding	60	0.009387202
GO:0006888	ER_to_Golgi_vesicle-mediated_transport	45	0.009992128
GO:0030433	ER-associated_ubiquitin-dependent_protein_catabolic_process	48	0.012185925
GO:0003746	translation_elongation_factor_activity	32	0.011248546
GO:0010494	cytoplasmic_stress_granule	25	0.014950822
GO:0030529	intracellular_ribonucleoprotein_complex	174	0.01601557
GO:0051568	histone_H3-K4_methylation	16	0.030657513
GO:0008536	Ran_GTPase_binding	19	0.02910957

[8] *Continue next page*

NAME	DESCRIPTION	SIZE	FDR
GO:0032922	circadian_regulation_of_gene_expression	39	0.03574508
GO:0006730	one-carbon_metabolic_process	25	0.03484931
GO:0005801	cis-Golgi_network	29	0.03317578
GO:0017148	negative_regulation_of_translation	33	0.041525565
GO:0045727	positive_regulation_of_translation	28	0.040887456
GO:0016627	oxidoreductase_activity,_acting_on_the_CH-CH_group_of_donors	25	0.03947905
GO:0016573	histone_acetylation	27	0.04306576
GO:0006446	regulation_of_translational_initiation	22	0.042669903
GO:0070301	cellular_response_to_hydrogen_peroxide	25	0.049455997
GO:0003730	mRNA_3'-UTR_binding	20	0.049979594

Table 8.6 Pathways upregulated in primary insulinomas vs normal pancreas using Reactome tool[9]

NAME	DESCRIPTION	SIZE	FDR
R-CFA-1442490	Collagen degradation	45	0
R-CFA-1650814	Collagen biosynthesis and modifying enzymes	59	0
R-CFA-1474228	Degradation of the extracellular matrix	83	0
R-CFA-1296071	Potassium Channels	77	0
R-CFA-1474290	Collagen formation	71	0
R-CFA-112316	Neuronal System	231	2.81E-04
R-CFA-166658	Complement cascade	42	7.13E-04
R-CFA-2022090	Assembly of collagen fibrils and other multimeric structures	38	7.31E-04
R-CFA-1474244	Extracellular matrix organization	216	8.34E-04
R-CFA-419037	NCAM1 interactions	20	8.30E-04
R-CFA-1296072	Voltage gated Potassium channels	32	0.001128
R-CFA-166663	Initial triggering of complement	23	0.001101
R-CFA-198933	Regulation of gene expression in neuroendocrine committed (NEUROG3+) progenitor cells	65	0.001272
R-CFA-216083	Integrin cell surface interactions	77	0.00283
R-CFA-375276	Peptide ligand-binding receptors	105	0.003519
R-CFA-3000178	ECM proteoglycans	40	0.00871
R-CFA-194223	Regulation of beta cell development	16	0.012661
R-CFA-373076	Class A/1 (Rhodopsin-like receptors)	170	0.013647

[9] *Continue next page*

NAME	DESCRIPTION	SIZE	FDR
R-CFA-500792	GPCR ligand binding	216	0.023978
R-CFA-112315	Transmission across Chemical Synapses	161	0.026287
R-CFA-2129379	Molecules associated with elastic fibres	29	0.026925
R-CFA-70171	Glycolysis	22	0.028065
R-CFA-166786	Creation of C4 and C2 activators	16	0.027523
R-CFA-1566948	Elastic fibre formation	33	0.028165
R-CFA-418594	G alpha signalling events	91	0.038687
R-CFA-5576892	Phase_0 rapid depolarisation	26	0.039231
R-CFA-5576894	Phase_1 inactivation of fast Na+ channels	20	0.040212
R-CFA-112314	Neurotransmitter Receptor Binding And Downstream Transmission In The Postsynaptic Cell	108	0.042135
R-CFA-975634	Retinoid metabolism and transport	31	0.043184
R-CFA-6806667	Metabolism of fat-soluble vitamins	39	0.042293
R-CFA-977606	Regulation of Complement cascade	21	0.046695

Table 8.7 Pathways downregulated in primary insulinoma compared to normal pancreatic tissues using Reactome tool

NAME	DESCRIPTION	SIZE	FDR
R-CFA-72766	Translation	62	0
R-CFA-72702	Ribosomal scanning and start codon recognition	47	0
R-CFA-72649	Translation initiation complex formation	46	0
R-CFA-72662	Activation of the mRNA upon binding of the cap-binding complex and eIFs, and subsequent binding to 43S	47	0
R-CFA-156827	L13a-mediated translational silencing of Ceruloplasmin expression	46	3.77E-04
R-CFA-532668	N-glycan trimming in the ER and Calnexin/Calreticulin cycle	17	6.35E-04
R-CFA-70895	Branched-chain amino acid catabolism	22	0.001809
R-CFA-72695	Formation of the ternary complex, and subsequently, the 43S complex	39	0.001975
R-CFA-72737	Cap-dependent Translation Initiation	53	0.002719
R-CFA-72613	Eukaryotic Translation Initiation	53	0.002447
R-CFA-901042	Calnexin/calreticulin cycle	15	0.003483
R-CFA-6811440	Retrograde transport at the Trans-Golgi-Network	41	0.006645
R-CFA-204174	Regulation of pyruvate dehydrogenase (PDH) complex	16	0.0243
R-CFA-1227986	Signaling by ERBB2	37	0.024519
R-CFA-2173793	Transcriptional activity of SMAD2/SMAD3:SMAD4 heterotrimer	40	0.031826
R-CFA-2173795	Downregulation of SMAD2/3:SMAD4 transcriptional activity	23	0.045277

Table 8.8 Gene ontology terms downregulated in metastatic lymph nodes vs primary insulinomas using gene set enrichment analysis

NAME	DESCRIPTION	SIZE	FDR
GO:0003735	structural_constituent_of_ribosome	200	0.0
GO:0005840	ribosome	203	0.0
GO:0006412	translation	253	0.0
GO:0072562	blood_microparticle	64	0.0017276717
GO:0004252	serine-type_endopeptidase_activity	100	0.0013821374
GO:0008236	serine-type_peptidase_activity	88	0.0025729418
GO:0030529	intracellular_ribonucleoprotein_complex	177	0.0027126358
GO:0006414	translational_elongation	34	0.032809116

Table 8.9 Pathways upregulated in metastatic lymph nodes compared to primary insulinomas using Reactome tool

NAME	DESCRIPTION	SIZE	FDR
R-CFA-392451	G_beta:gamma_signalling_through_PI3Kgamma	26	0.033549

Table 8.10 Pathways downregulated in metastatic lymph nodes compared to primary insulinomas using Reactome tool

NAME	DESCRIPTION	SIZE	FDR
R-CFA-156590	Glutathione conjugation	25	0.013401
R-CFA-196741	Cobalamin (Cbl, vitamin B12) transport and metabolism	20	0.031193
R-CFA-72766	Translation	63	0.027515
R-CFA-5368287	Mitochondrial translation	79	0.027888
R-CFA-72695	Formation of the ternary complex and the 43S complex	40	0.033168
R-CFA-5419276	Mitochondrial translation termination	78	0.028773
R-CFA-72613	Eukaryotic Translation Initiation	54	0.034266
R-CFA-70614	Amino acid synthesis and interconversion (transamination)	24	0.034897
R-CFA-72737	Cap-dependent Translation Initiation	54	0.038949
R-CFA-5389840	Mitochondrial translation elongation	76	0.035154
R-CFA-156827	L13a-mediated translational silencing of Ceruloplasmin expression	47	0.036565
R-CFA-72662	Activation of the mRNA upon binding of the cap-binding complex and eIFs, and subsequent binding to 43S	48	0.038595
R-CFA-71291	Metabolism of amino acids and derivatives	207	0.041431
R-CFA-72649	Translation initiation complex formation	47	0.049302

8.6 Human and canine primers for qRTPCR

Table 8.11 Human primers sequences for qRTPCR (Chiron *et al.*, 2012; Gao *et al.*, 2014; Deng *et al.*, 2015; Eskandani, Abdolalizadeh and Hamishehkar, 2015; Irshad *et al.*, 2015; Seyedi *et al.*, 2015; Sukowati *et al.*, 2015) [10]

Gene	Forward sequence	Reverse sequence	Product size (bp)
OCT4	GAGAACCGAGTGAGAGGCAACC	CATAGTCGCTGCTTGATCGCTTG	186
INS	TTCTTCTACACACCCAAGAC	CTAGTTGCAGTAGTTCTCCA	192
SOX2	AACCCCAAGATGCACAACTC	GCTTAGCCTCGTCGATGAAC	158
SOX9	CCCTTCGTGGAGGAGGCGGA	CCGGAGGAGGAGTGTGGCGA	198
NANOG	GCCTGTGA TTTGTGGGCCTGA	GTGGAAGAA TCAGGGCTGTCCTG	135
PDX1	CAGCACTCCACCTTGGGACC	TCCCCGCTGTGTGTGTTAGGG	101
ISL1	GA TCAAA TGCGCCAAGTGCAG	CAGCGGAAACACTCGA TGTGA	93
PA	CTTTGTGGATAACCATGACAATCAA	CAACTGCCATTTTATACAGCCTAG	95
PNLIP	TTGCGTGTGGAACCTGACG	TCTTTTCCTGCTACTGCTCCCAGC	83
GHR	CCATTGCCCTCAACTGGACTT	AATATCTGCATTGCGTGGTGC	95

[10] *Continue page 251-253*

Gene	Forward sequence	Reverse sequence	Product size (bp)
LIFR	GAAAACTGTAAAGCATTACA	AGAGTCTGGAGACACTAA	243
EGFR	GGAGAACTGCCAGAAACTGACC	GCCTGCAGCACACTGGTTG	106
NOTCH1	CCGTCATCTCCGACTTCATCT	GTGTCTCCTCCCTGTTGTTCTG	468
NOTCH2	GCTGATGCTGCCAAGCGT	CCGGGGAAGACGATCCAT	474
NOTCH3	CTGGCGAGACTGCTTTGC	CGACTGTGCCGCTTTGAG	661
NOTCH4	CGGCCTCTGAAGAACAGAAC	ATCTCCACCTCACACCACTG-3′	472
HEY1	GCCGAGATCCTGCAGATGA	GCTGGGAAGCGTAGTTGTTG	223
JAG1	CGGCCTCTGAAGAACAGAAC	TCACCAAGCAACAGA TCCAA	82
JAG2	AGGTGGAGACGGTTGTTAC	TTGCACTGGTAGAGCACGTC	231
HES1	ACGTGCGAGGGCGTTAATAC	ATTGATCTGGGTCATGCAGTTG	75
CD90	CGCTCTCCTGCTAACAGTCTTGC	CCCCCACAGTGCCAAAGAGC	185
CD24	AAACAACAACTGGAACTTCAAGTAACT	GGTGGTGGCATTAGTTGGATTT	83
CD34	CTGATACCGAATTGTGACTC	TTGGGCGTAAGAGATGTC	255

Gene	Forward sequence	Reverse sequence	Product size (bp)
CD133	TGGATGCAGAACTTGACAACGT	ATACCTGCTACGACAGTCGTGGT	350
VIMENTIN	AACTTCTCAGCA TCACGA TGAC	TTGTAGGAGTGTCGGTTGTTAAG	62
SNAIL1	TCTGAGTGGGTCTGGAGGTG	CTCTAGGCCCTGGCTGCTAC	109
GADPH	CAAGATCATCAGCAATGCCT	CAGGGATGATGTTCTGGAGAG	194
HPRT	ATAAGCCAGACTTTGTTGGA	CTCAACTTGAACTCTCATCTTAGG	156

Table 8.12 Canine primers sequences for qRTPCR (Michishita *et al.*, 2011; Hodgkiss-Geere *et al.*, 2012; Boerkamp *et al.*, 2013; Buishand *et al.*, 2013; Dailey *et al.*, 2013; Kruitwagen *et al.*, 2014; Schotanus *et al.*, 2014; van Rijn *et al.*, 2014; Lu *et al.*, 2015)[11]

Gene	Forward sequence	Reverse sequence	Product size (bp)
OCT4	CTCTGCAGCCAATCAACCACAA	GGAGAGGGGGATGAGAAGTACAAT	237
INS	TCAAGCAGATCACTGTCC	GGTGTTGGTTCACAAAGG	89
IGF2	CTTCTGGAGACCTACTGTGC	CTGCTTCCAGGTGTCGTATTG	128
SOX2	AACCCCAAGATGCACAACTC	CGGGGCCGGTATTTATAATC	289
SOX9	CCAACGCCATCTTCAAGG	GGAGTGCACCTCGCTCAT	71
NANOG	CTATAGAGGAGAGCACAGTGAAG	GTTCGGATCTACTTTAGAGTGAGG	160
PDX1	TCCCGTGGATGAAGTCTACC	CGTGGCCTCGAGATGTATTT	150
ISL1	GGTTTCTCCGGATTTGGAAT	CACGAAGTCGTTCTTGCTGA	164
PA	CTTTGTGGATAACCATGACAATCAA	CAACTGCCATTTTATACAGCCTAG	208
PNLIP	TGTGTGGACTGGAAGAGTGGC	ACAAACTGGGCATCGCTGG	271
GHR	GCGCATCCCAGAGTCTACA	ACCATGACGAACCCCATCT	115

[11] *Continue page 254-256*

Gene	Forward sequence	Reverse sequence	Product size (bp)
LIFR	ACTGGAGTTGGACCTCAGAC	CTGAGAATCAGGTGACCAAG	129
EGFR	CTGGAGCATTCGGCA	TGGCTTTGGGAGACG	93
NOTCH1	CATCATCAATGGCTGCAAGGG	TCATTCTCACACGTGGCACC	126
NOTCH2	TCGGGATAGCTATGAGCCCT	GGCATGTTGCTTTCCCCAAC	188
NOTCH3	TCTGCCAGAGTTCCGTGGTG	ATGGGGTACAAGGGCTGCTG	117
NOTCH4	GGAAGGGAGCCAGGGACCAACACA	TCAGGGCCACAGCGGGACAAATC	96
HEY1	ACCTGAAAATGCTGCACACG	GCTGGGAGGCGTAGTTGTTA	195
JAG1	GGGCAACACCTTCAATCTCAAG	CATTACTGGAATCCCACGCTTC	122
JAG2	GGGTACGTGCGTGGGC	CACCGTTGTAGCAAGGCAG	109
HES1	CATCCAAGCCTATCATGGAGA	GTTCCGGAGGTGCTTCACT	163
CD90	CTGTGCTCAGAGACAAACTG	TTAGCCAACTCAGAGAAAGTAGG	185
CD24	GCTCCTACCCACGCAGATTT	ATCACGAAGAGACTGGCTGT	153

Gene	Forward sequence	Reverse sequence	Product size (bp)
CD34	TGACACCCCAAGTACCATCA	GGCTCCTTCTCACACAGCAC	162
CD133	CTGGGGCTGCTCTTTGTGAT	AGGCCCCATTTTTCTTCTGTC	115
VIMENTIN	GGAGCAGCAGAACAAGATCC	AGACGTGCCAAAGAAGCATT	282
SNAIL1	CCCAAGCCCAGCCGATGAG	CTTGGCCACGGAGAGCCC	200
GADPH	TGTCCCCACCCCCAATGTATC	CTCCGATGCCTGCTTCACTACCTT	100
RPS5	TCACTGGTGAGAACCCCCT	CCTGATTCACACGGCGTAG	141

8.7 Flow Cytometry

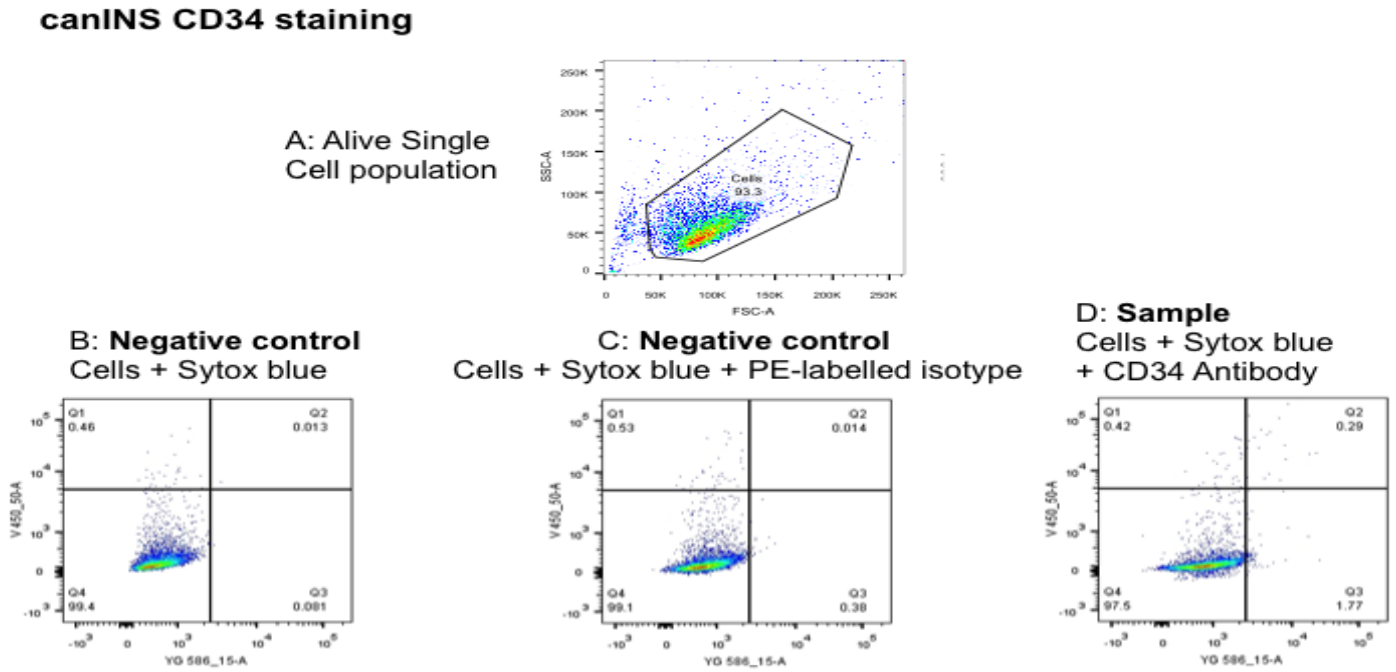

Figure 8.7 Flow cytometry for CD34 in the canine adherent insulinoma cell line. The relation between side scatter (SSC) and forward scatter (FSC) is used to identify the proportion of alive single cells (A). This experiment has been performed using two negative controls: cells + dead cell discriminator (Sytox blue),B, and cell + PE-labelled isotype and dead cell discriminator, C. canINS shows almost 2% of CD34+ population (D).

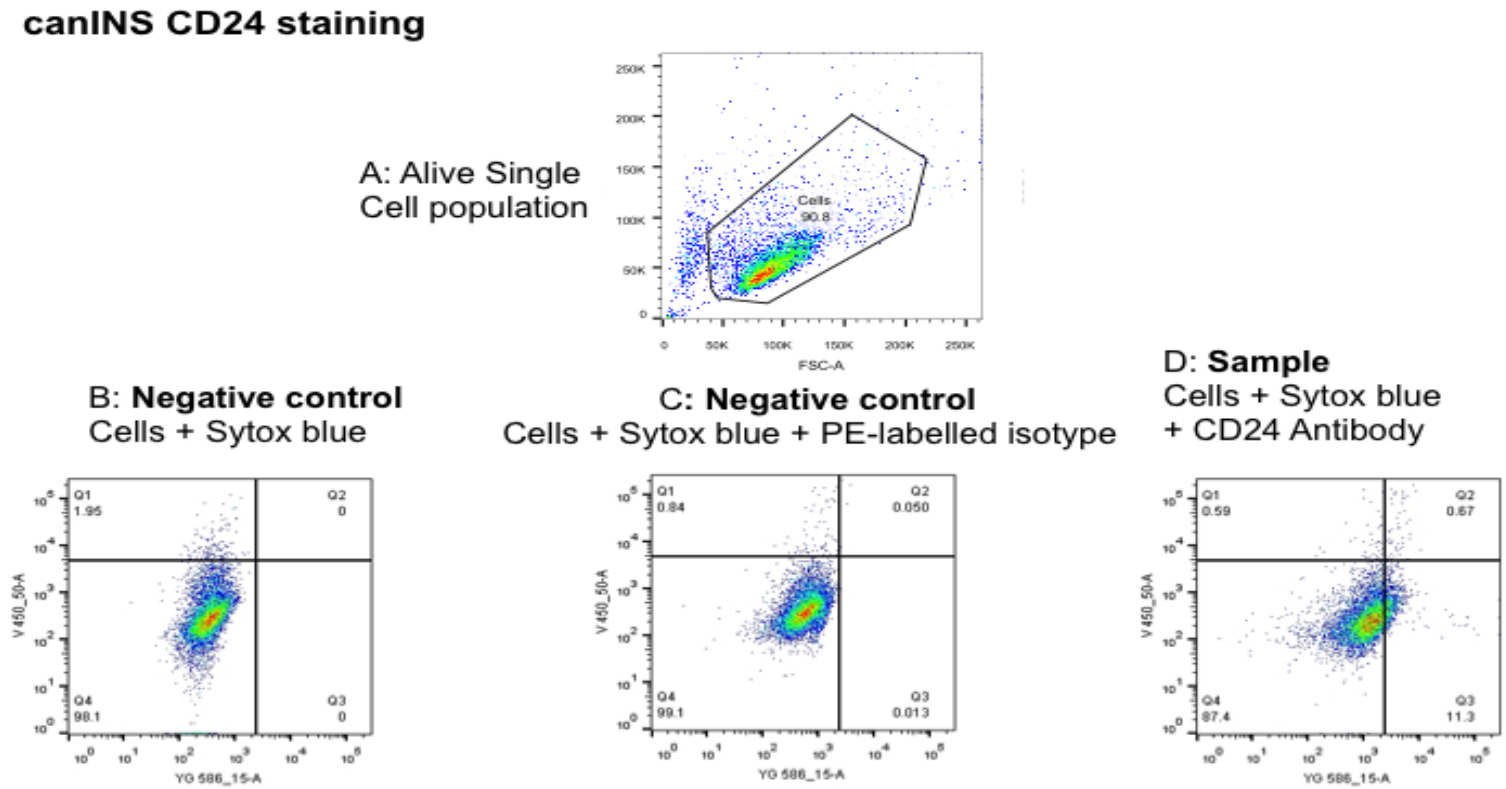

Figure 8.8 Flow cytometry for CD24 in the canine adherent insulinoma cell line. The relation between side scatter (SSC) and forward scatter (FSC) is used to identify the proportion of alive single cells (A). This experiment has been performed using two negative controls: cells + dead cell discriminator (Sytox blue),B, and cell + PE-labelled isotype and dead cell discriminator, C. canINS shows almost 11% of CD24+ population (D).

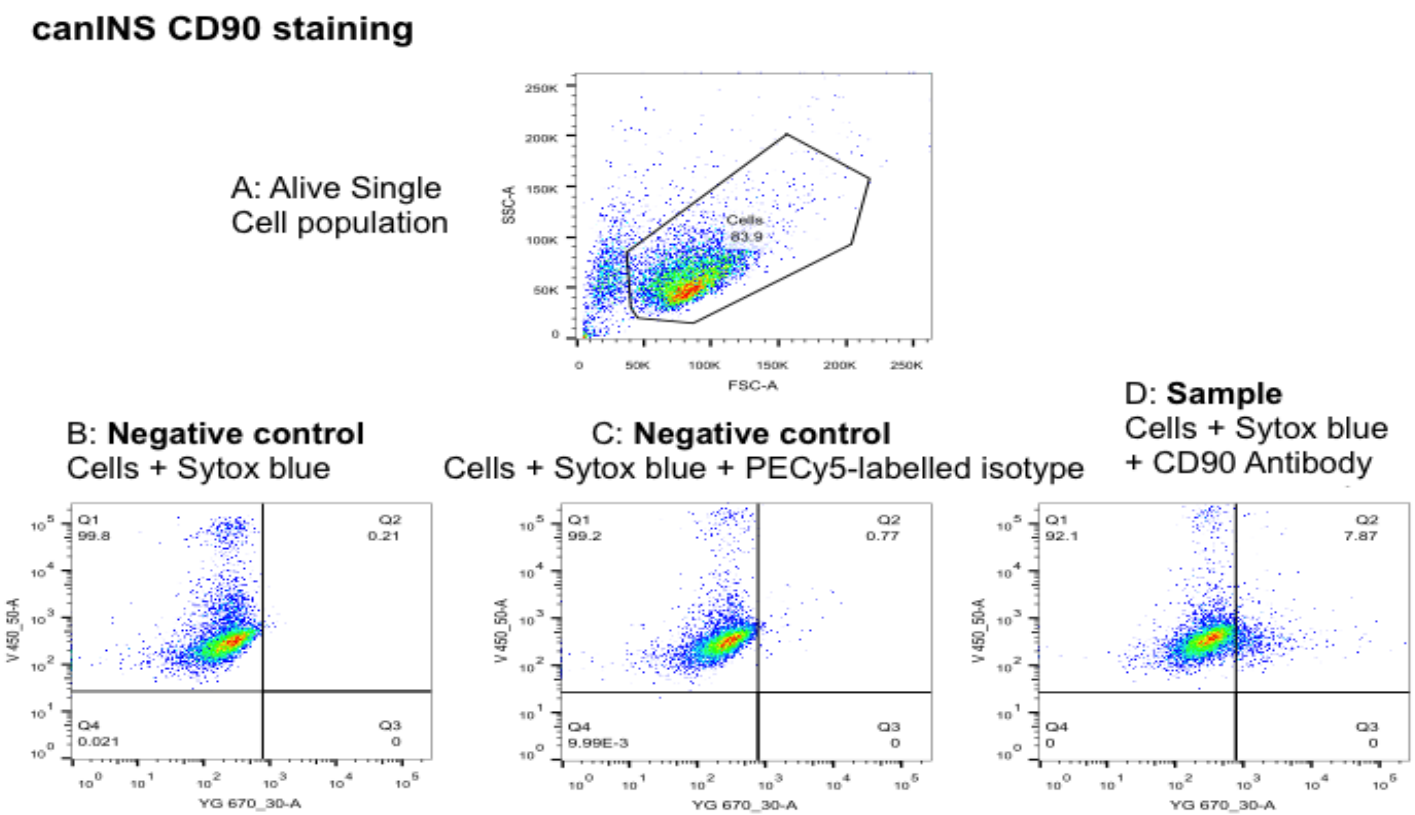

Figure 8.9 Flow cytometry for CD90 in the canine adherent insulinoma cell line. The relation between side scatter (SSC) and forward scatter (FSC) is used to identify the proportion of alive single cells (A). This experiment has been performed using two negative controls: cells + dead cell discriminator (Sytox blue),B, and cell + PECy5-labelled isotype and dead cell discriminator, C. canINS shows about 8% of CD90+ population (D).

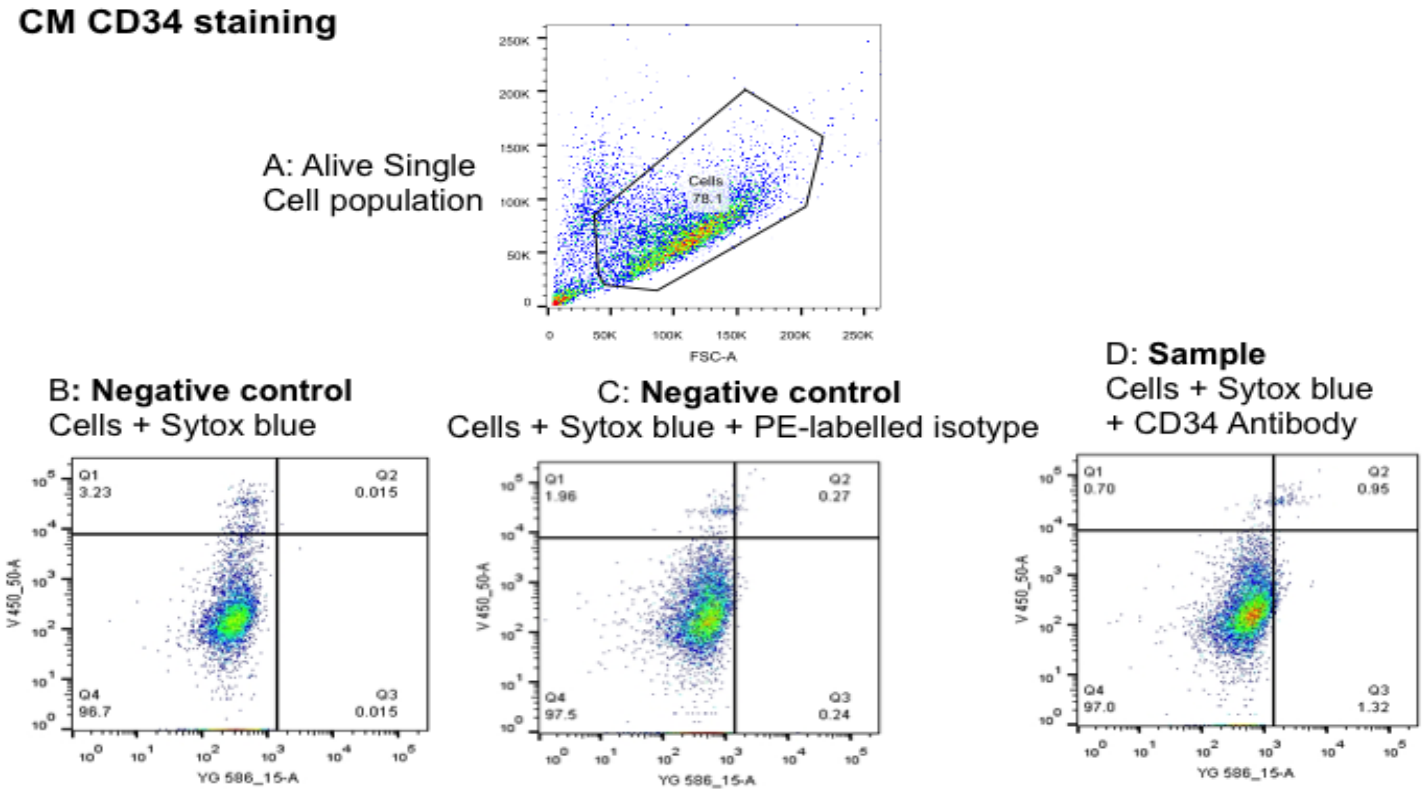

Figure 8.10 Flow cytometry for CD34 in the human adherent insulinoma cell line. The relation between side scatter (SSC) and forward scatter (FSC) is used to identify the proportion of alive single cells (A). This experiment has been performed using two negative controls: cells + dead cell discriminator (Sytox blue),B, and cell + PE-labelled isotype and dead cell discriminator, C.). CM shows almost 2% of CD34+ population (D).

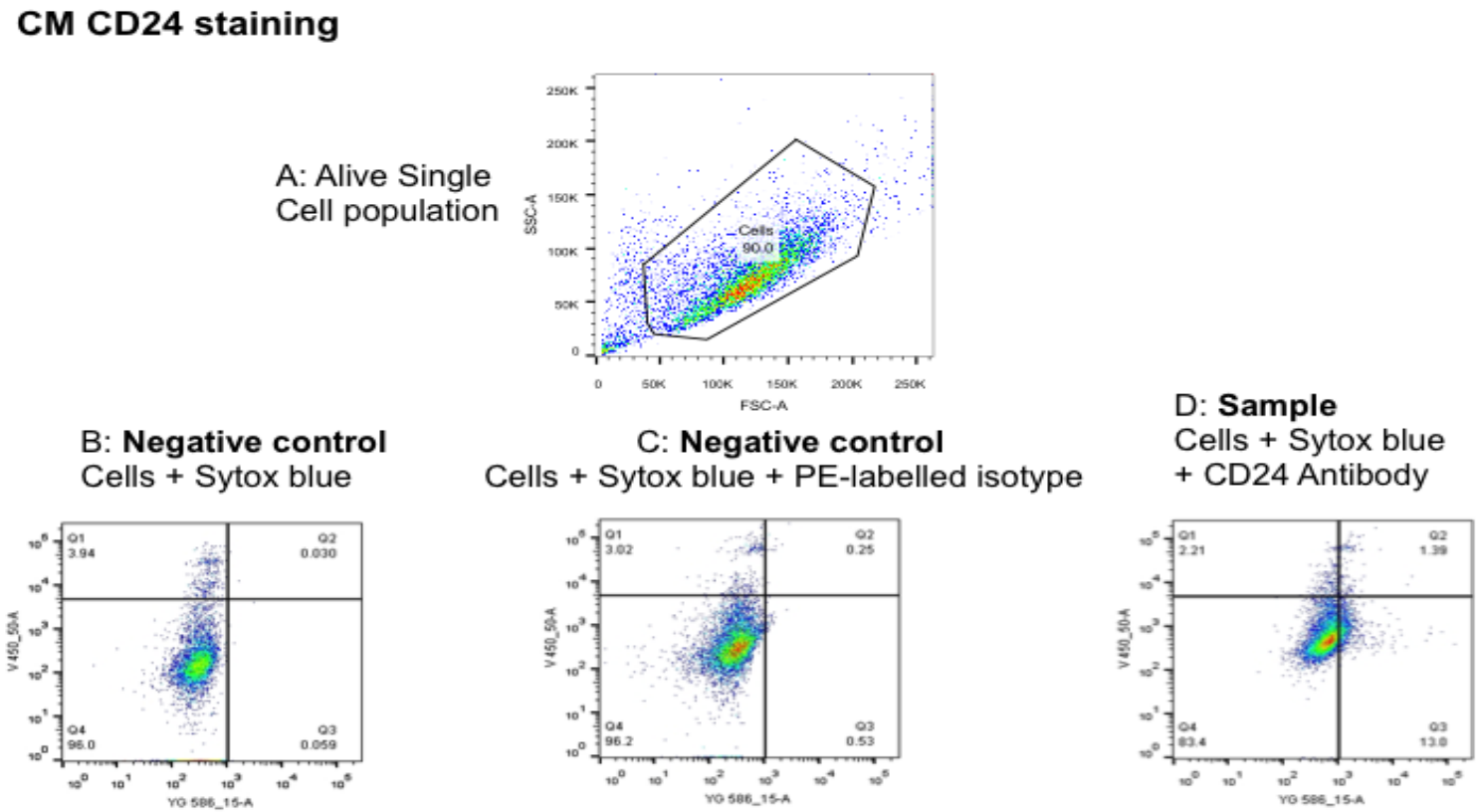

Figure 8.11 Flow cytometry for CD24 in the human adherent insulinoma cell line. The relation between side scatter (SSC) and forward scatter (FSC) is used to identify the proportion of alive single cells (A). This experiment has been performed using two negative controls: cells + dead cell discriminator (Sytox blue),B, and cell + PE-labelled isotype and dead cell discriminator, C. CM shows about 14% of CD24+ population (D).

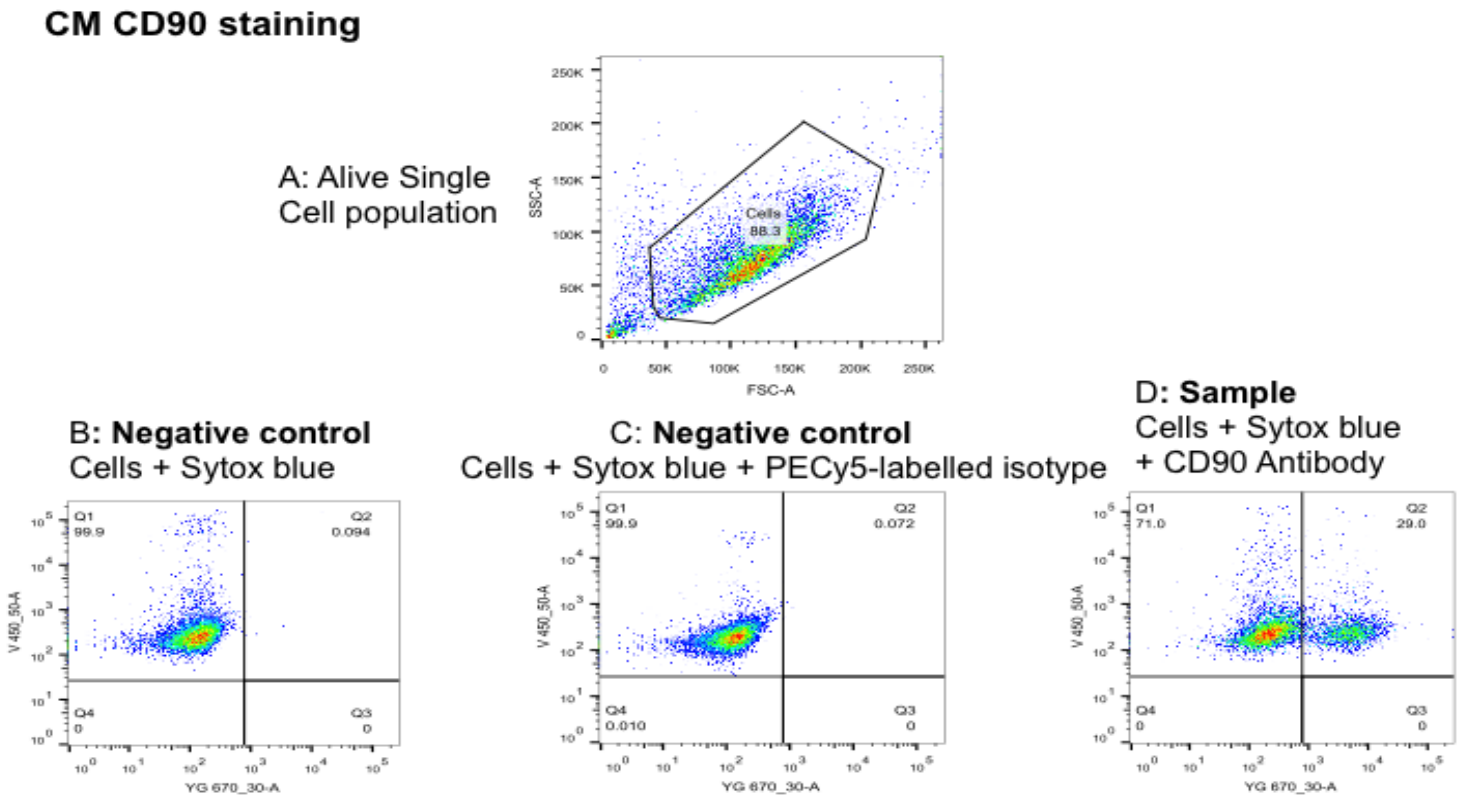

Figure 8.12 Flow cytometry for CD90 in the human adherent insulinoma cell line. The relation between side scatter (SSC) and forward scatter (FSC) is used to identify the proportion of alive single cells (A). This experiment has been performed using two negative controls: cells + dead cell discriminator (Sytox blue),B, and cell + PECy5-labelled isotype and dead cell discriminator, C. canINS shows about 29% of CD90+ population (D).

A **canINS NOTCH2 Extracellular staining**

Alive Single Cell population

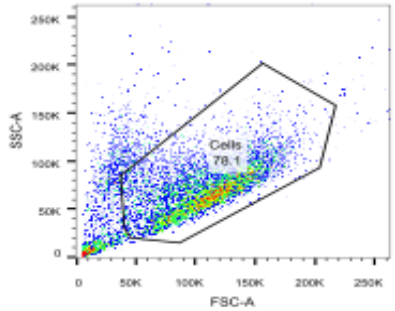

Negative control
Cells + Zombie violet

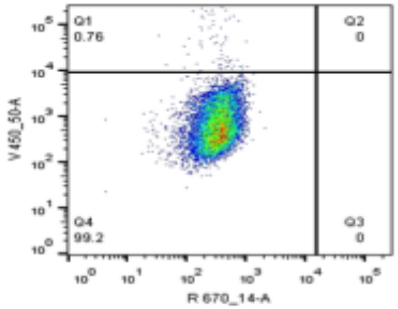

Negative control
Cells+ Zombie violet + secondary antibody Alexa 647conjugate

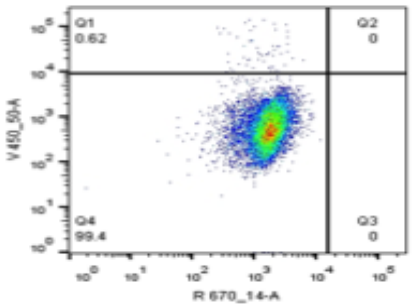

Negative control
Cells+ Zombie violet + isotype + secondary antibody alexa 647conjugate

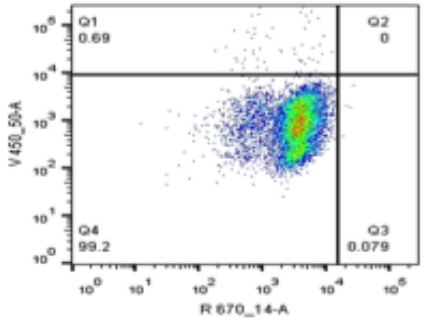

Sample
Cells + Zombie Violet + NOTCH2 primary antibody + secondary antibody alexa 647 conjugate

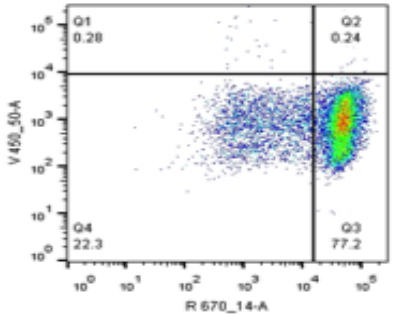

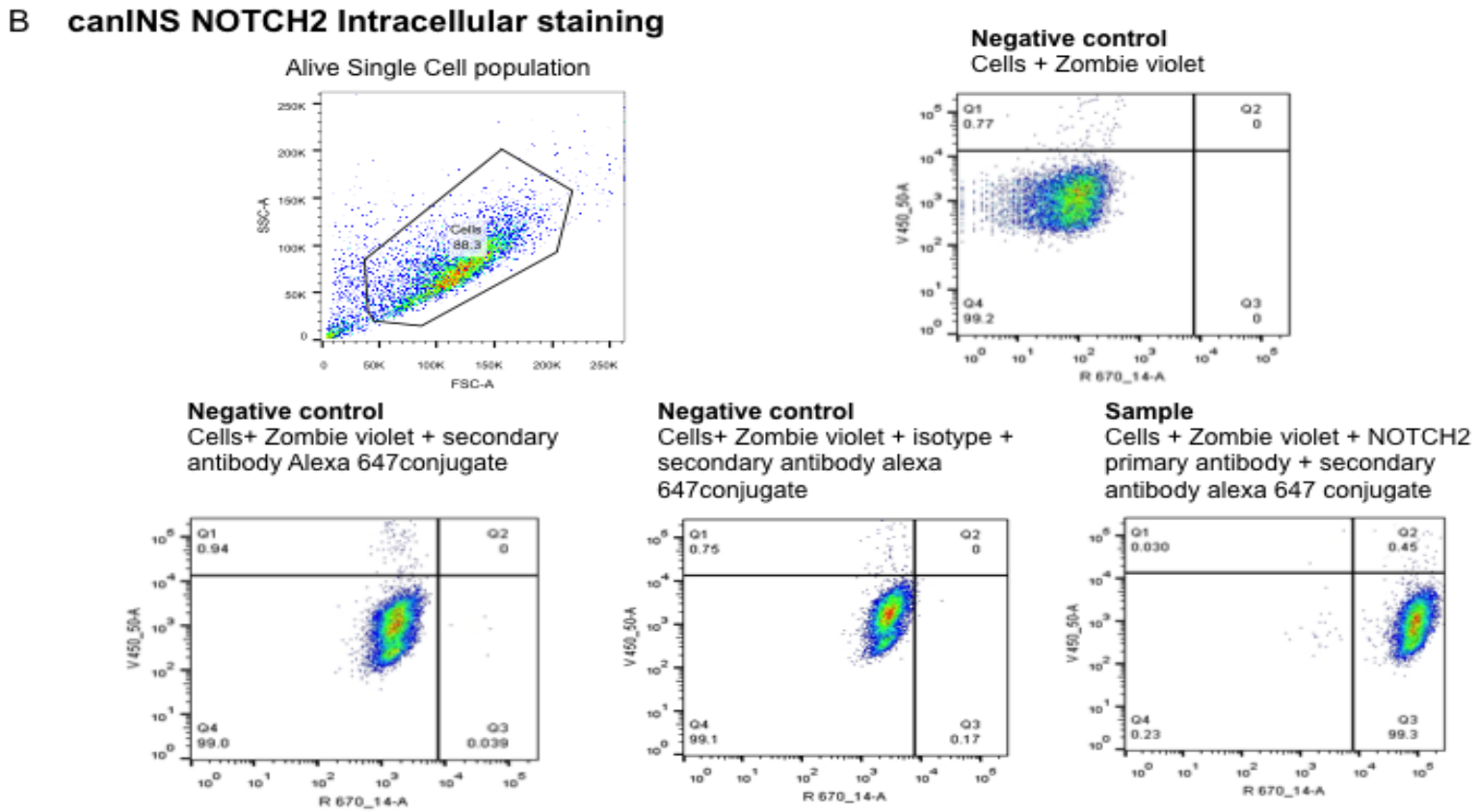

Figure 8.13 Flow cytometry for NOTCH2 in the canine adherent insulinoma cell line at the extracellular (A) and intracellular (B) level. The relation between side scatter (SSC) and forward scatter (FSC) is used to identify the proportion of alive single cells. This experiment has been performed using three negative controls: cells + dead cell discriminator (Zombie violet; cell + secondary antibody Alexa 647 conjuugate + Zombie

Violet; and cells + Zombie violet + isotype +secondary antibody. canINS shows about 77% of NOTCH2+ population at extracellular level (A) and 99% at intracellular level (B).

A **CM NOTCH2 Extracellular staining**

Alive Single Cell population

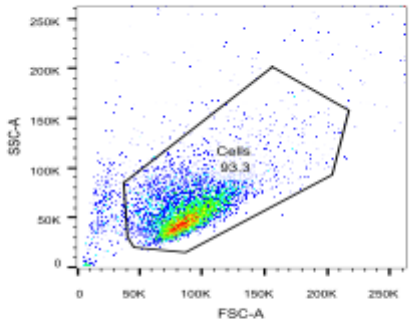

Negative control
Cells + Zombie violet

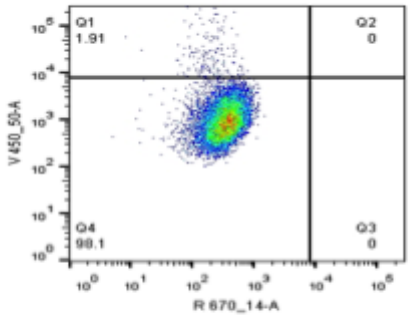

Negative control
Cells+ Zombie violet + secondary antibody Alexa 647conjugate

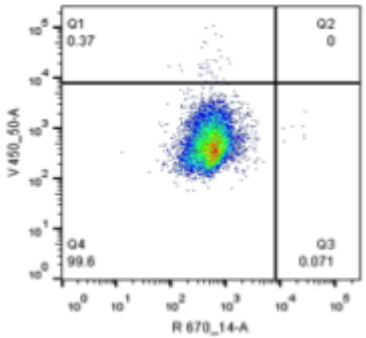

Negative control
Cells+ Zombie violet + isotype + secondary antibody alexa 647conjugate

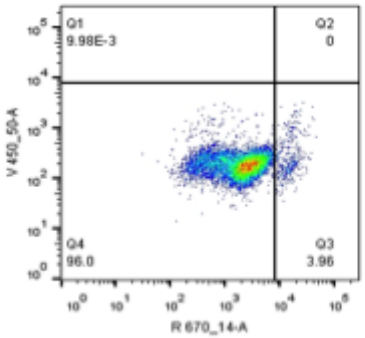

Sample
Cells + Zombie violet + NOTCH2 primary antibody + secondary antibody alexa 647 conjugate

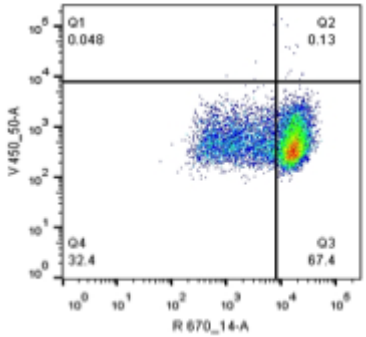

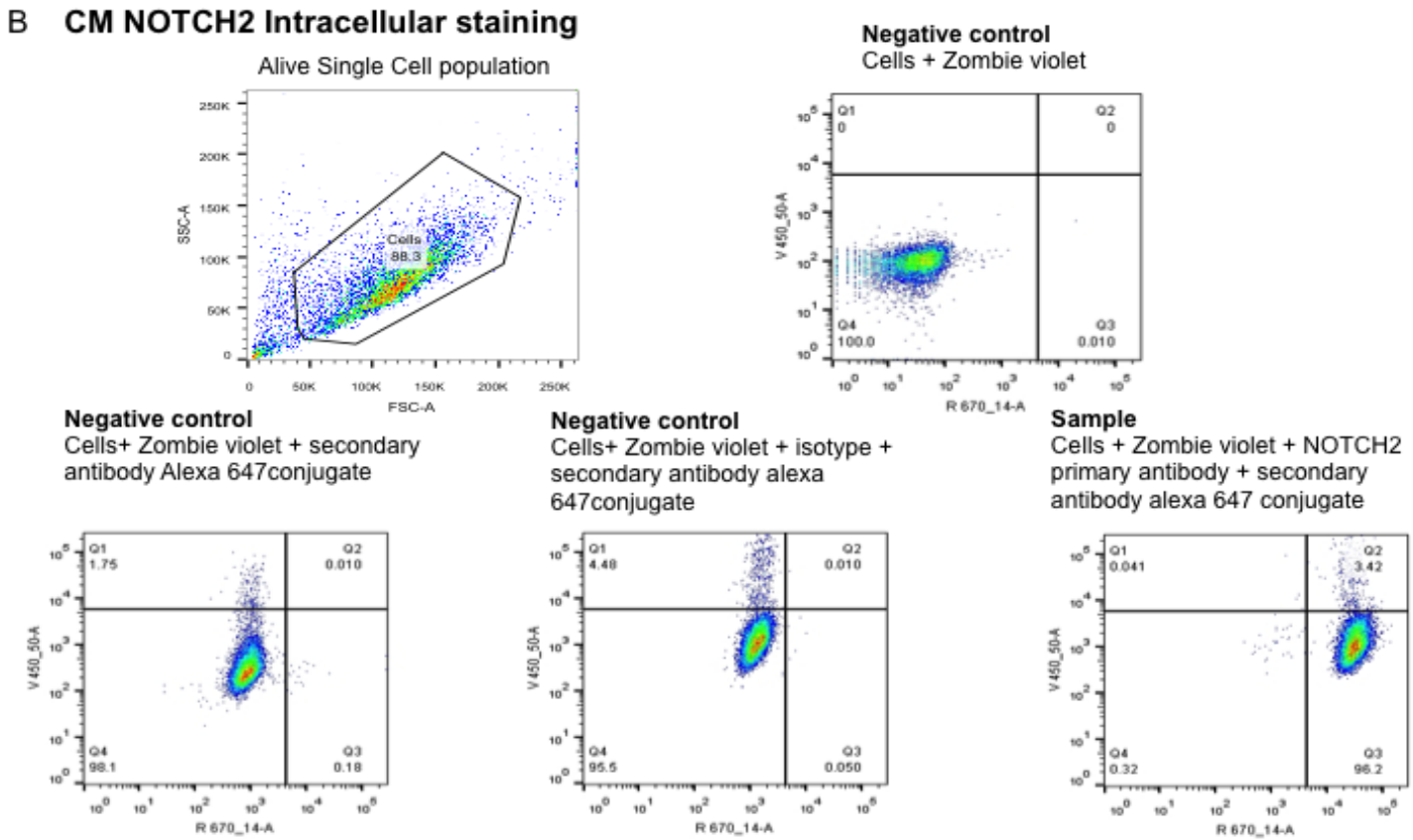

Figure 8.14 Flow cytometry for NOTCH2 in the human adherent insulinoma cell line at the extracellular (A) and intracellular (B) level. The relation between side scatter (SSC) and forward scatter (FSC) is used to identify the proportion of alive single cells (A). This experiment has been performed using three negative controls: cells + dead cell discriminator (Zombie violet); cell + secondary antibody Alexa 647 conjuugate + Zombie

Violet; and cells + Zombie violet + isotype +secondary antibody. CM shows about 67% of NOTCH2+ population at extracellular level (A) and 96% at intracellular level (B).

8.8 Fluorescent-activated cell sorting

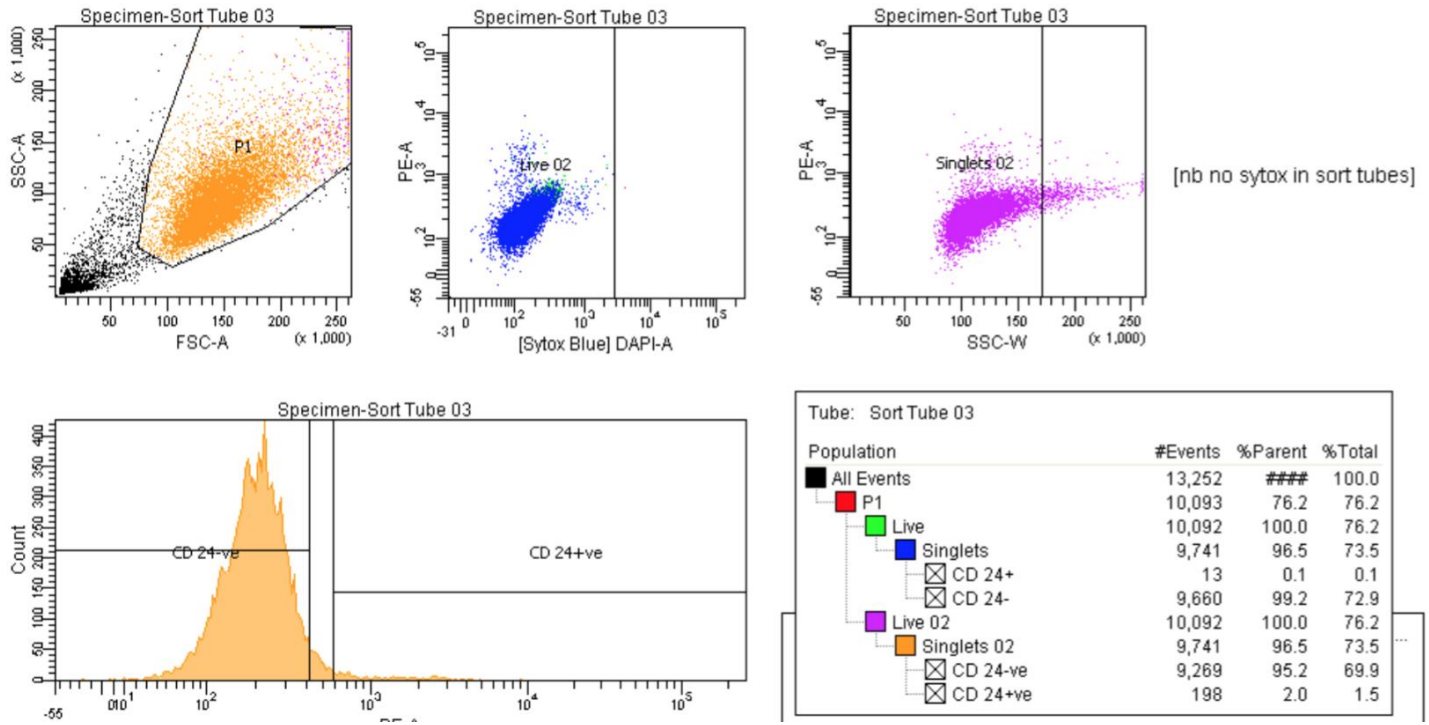

Figure 8.15 Fluorescence-activated cell sorting (FACS) of canine adherent insulinoma cell line. Tables show settings for CD24 PE labelled antibody. Results were analysed with FACS DIVA software (version 6.1.3) showing that 1.5% of the canine insulinoma cells were CD24 positive.

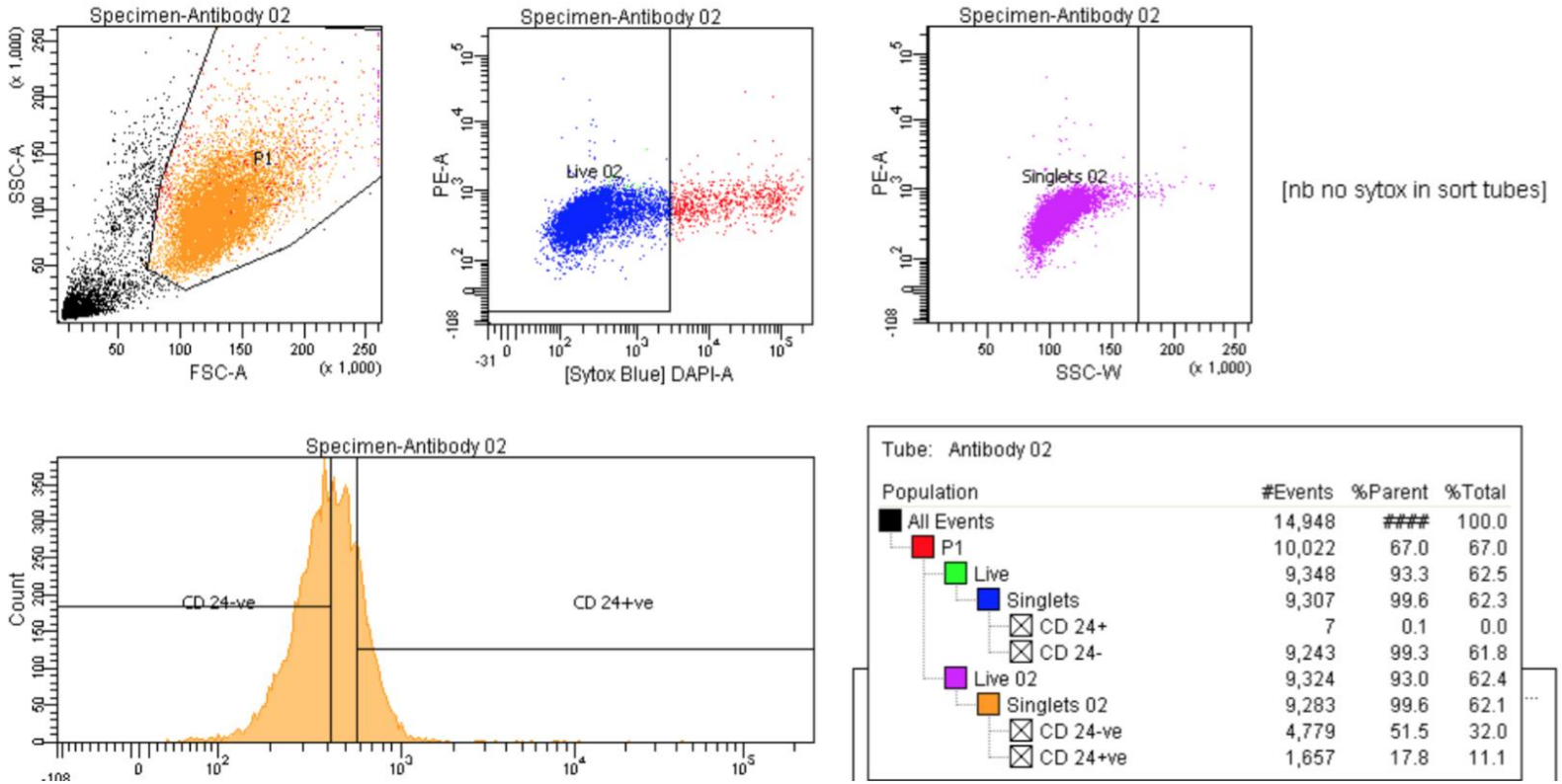

Figure 8.16 Fluorescence-activated cell sorting (FACS) of human adherent insulinoma cell line. Tables show settings for CD24 PE labelled antibody. Results were analysed with FACS DIVA software (version 6.1.3) showing that 11.1% of the human insulinoma cells were CD24 positive.

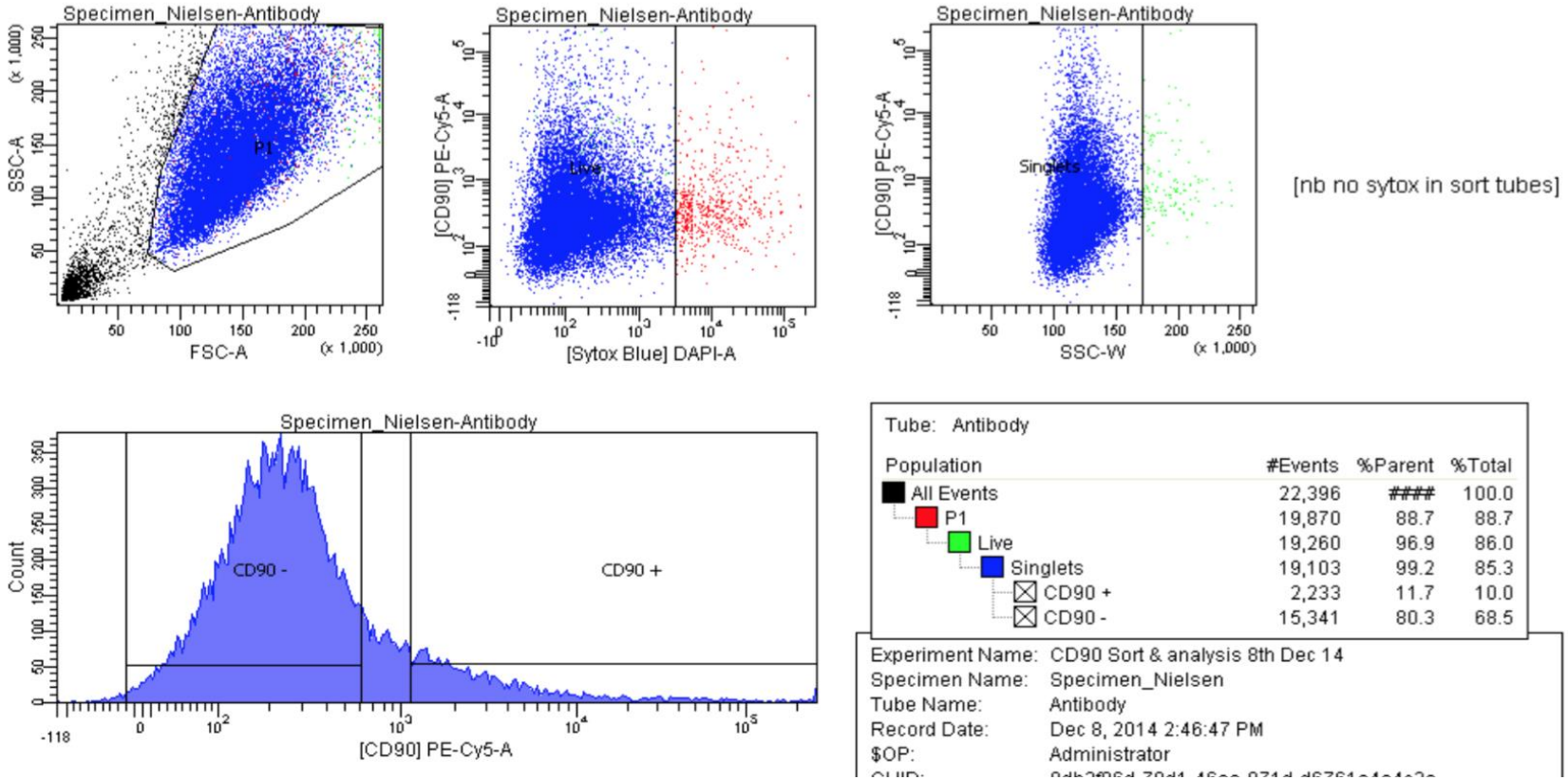

Figure 8.17 Fluorescence-activated cell sorting (FACS) of canine adherent insulinoma cell line. Tables show settings for CD90 PE-Cy5 labelled antibody. Results were analysed with FACS DIVA software (version 6.1.3) showing that 10% of the canine insulinoma cells were CD90 positive.

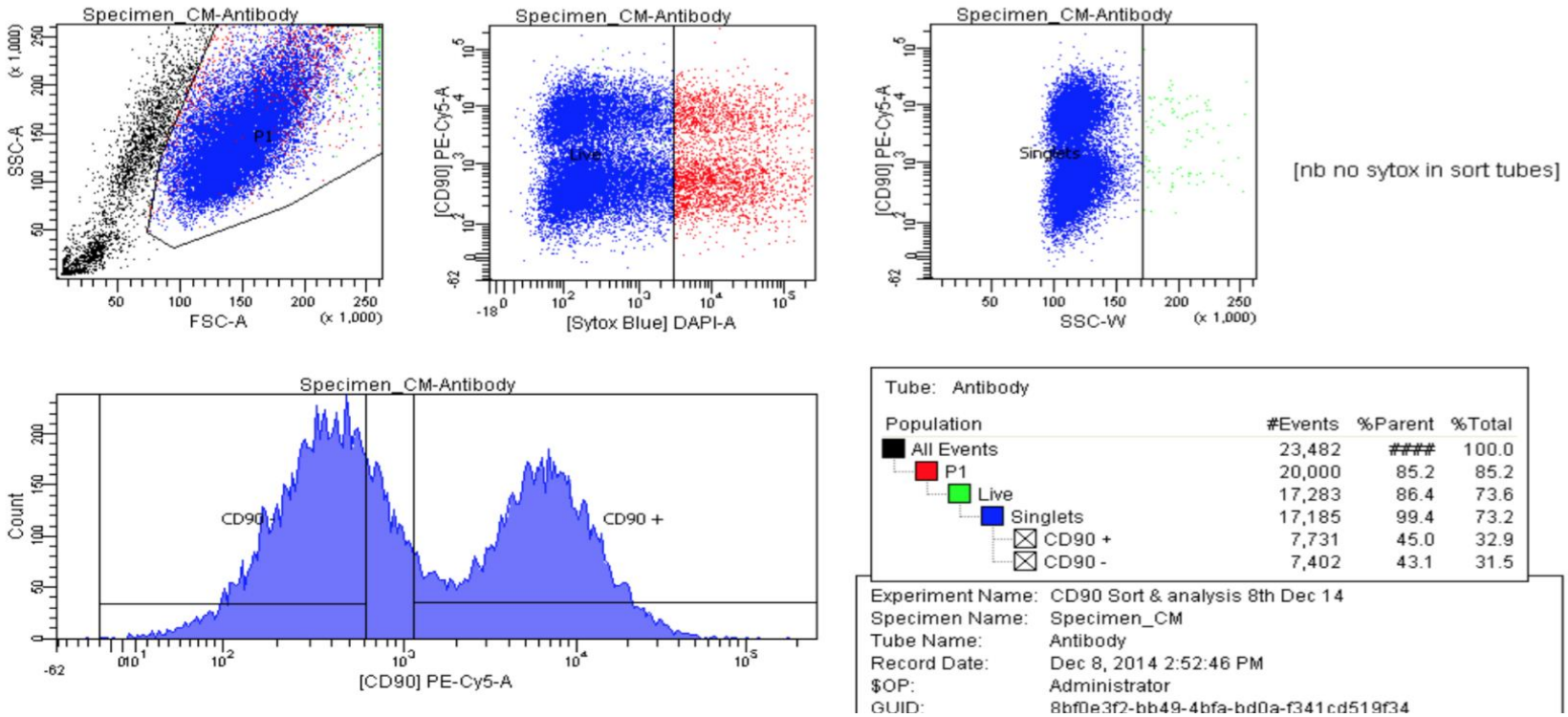

Figure 8.18 Fluorescence-activated cell sorting (FACS) of human adherent insulinoma cell line. Tables show settings for CD90 PE-Cy5 labelled antibody. Results were analysed with FACS DIVA software (version 6.1.3) showing that 32 % of the human insulinoma cells were CD90 positive.

8.9 qRTPCR data

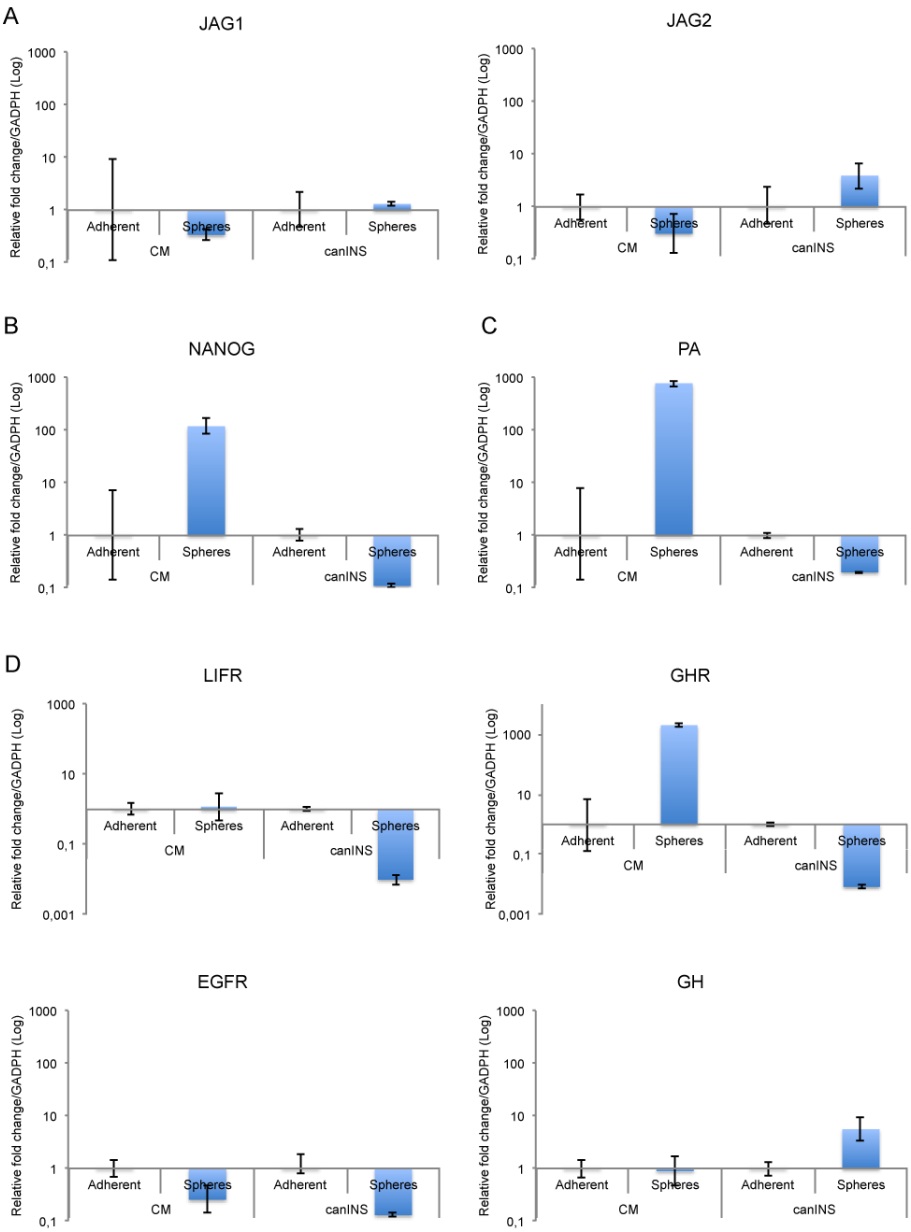

Figure 8.19 qRT-PCR of self-renewal pathway (A), stem cell (B), pancreatic markers and growth factor and growth factor receptor (D) related genes comparing CM and canINS in both adherent and sphere culturing conditions. The P-values represent the comparison with a stated hypothesis (values >1) using one samples t-test. *P-values <0.05 were considered statistically significant.